CHALMERS

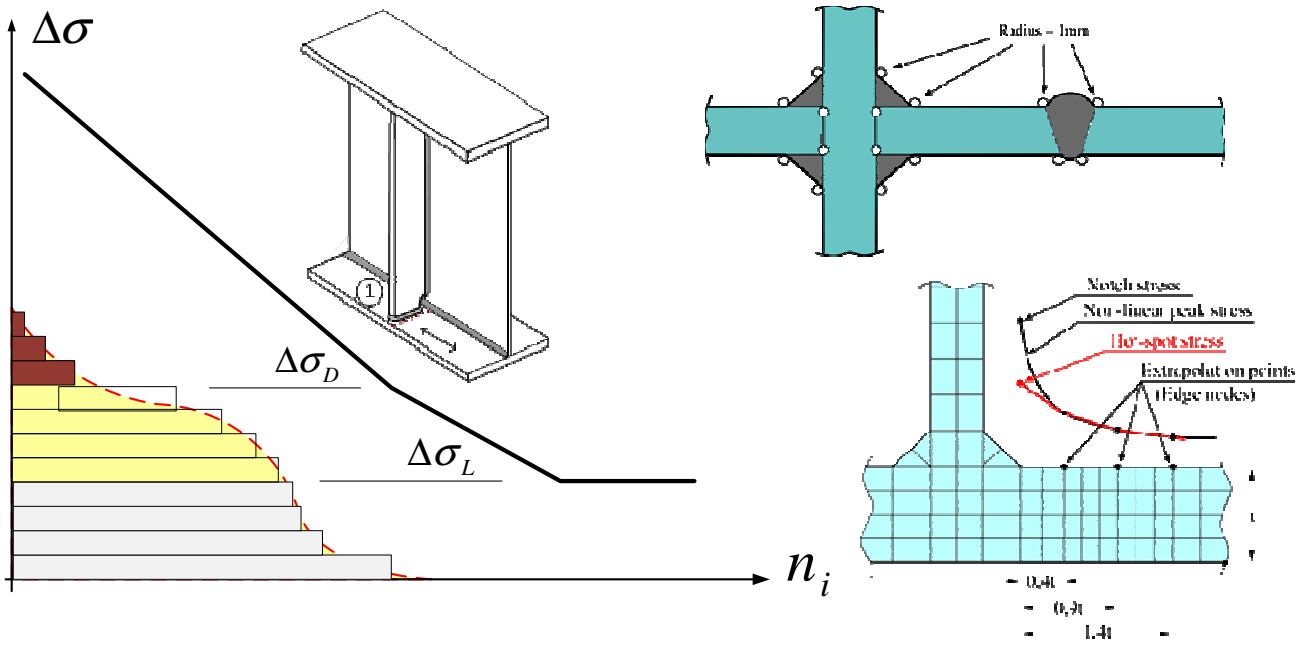

Fatigue design of steel and composite bridges

MOHAMMAD AL-EMRANI
MUSTAFA AYGÜL

Department of Civil and Environmental Engineering
Division of Structural Engineering
Steel and Timber Structures
CHALMERS UNIVERSITY OF TECHNOLOGY
Göteborg, Sweden 2014
Report 2014:10

REPORT 2014:10

Error! Reference source not found.

MOHAMMAD AL-EMRANI

Department of Civil and Environmental Engineering
Division of Structural Engineering
Steel and Timber Structures

CHALMERS UNIVERSITY OF TECHNOLOGY

Göteborg, Sweden 2014

Fatigue design of steel and composite bridges

MOHAMMAD AL-EMRANI

Chalmers tekniska högskola 2014:

ISSN 1652-9162
Department of Civil and Environmental Engineering
Division of Structural Engineering
STEEL AND TIMBER STRUCTURES
Chalmers University of Technology
SE-412 96 Göteborg
Sweden
Telephone: + 46 (0)31-772 1000

Chalmers Reproservice, Göteborg, Sweden 2014

Preface

This report has been produced within the research project "Methods for the fatigue design of steel and composite bridges" which was funded by the Swedish Road Administration, Trafikverket. The authors would like to express their gratitude to the following persons who have followed up and supported the work in the project and contributed with valuable comments and suggestions to this report:

Lahja Rydberg-Forssbeck	Trafikverket
Robert Hällmark	Trafikverket
Kurt Palmqvist	Trafikverket

In addition, parts of the recommendations and guidelines presented in this report where based on previous extensive research in the field of fatigue of welded connections conducted within other research projects and in various master's thesis projects. The authors are most thankful for the contributions of the following colleagues to the work:

Mohsen Heshmati	Chalmers
Farshid Zamiri	Chalmers / EPFL-Switzerland

Göteborg, November 2014

Mohammad Al-Emrani & Mustafa Aygul

CONTENTS

List of notations

$\Delta\sigma$	direct stress range
$\Delta\sigma_m$	mean stress range
$\Delta\sigma_C$, $\Delta\tau_C$	reference stress value of the fatigue strength at 2 million cycles
$\Delta\sigma_D$	reference stress value of the fatigue strength at 5 million cycles
$\Delta\sigma_L$, $\Delta\tau_D$	reference stress value of the fatigue strength at cut-off limit
$\Delta\sigma_{LM}$	stress range calculated from load model
$\Delta\sigma_{FLM}$	stress range calculated from fatigue load model
$\Delta\sigma_E$, $\Delta\tau_E$	equivalent constant amplitude stress range related to cycles
$\Delta\sigma_{E,2}$, $\Delta\tau_{E,2}$	equivalent constant stress range at 2 million stress cycles
σ_{hss}	structural hot spot stress
$\sigma_\perp$	stress perpendicular to the weld toe
σ_1	first principal stress
σ_2	second principal stress
σ_{str}	structural/geometric stress
σ_{ens}	effective notch stress
σ_{max}	maximum applied stress
σ_{min}	minimum applied stress
σ_{nom}	nominal stress
σ_{str}	structural stress
σ_m	membrane stress
σ_b	bending stress
σ_{nlp}	non-linear peak stress
τ_{xy}	shear stress in x-y direction
γ_{Ff}	partial factor for equivalent constant amplitude stress ranges
γ_{Mf}	partial factor for fatigue strength
Φ_2	dynamic factor
λ_i	damage equivalent factors
k_s	thickness correlation factor
k_m	misalignment correlation factor
F	normal force
M	bending moment
ΔM	bending moment range

m	slope of fatigue strength curve
N	number of stress cycles
R	stress ratio
t	plate thickness
D	Damage accumulation factor
LM	Load Model
FLM	Fatigue Load Model
AADT	Annual Average Daily Traffic
UDL	Uniformly Distributed Load
CEN	the European Committee for Standardization
ULS	Ultimate Limit State
SLS	Serviceability Limit State
FLS	Fatigue Limit State
ALS	Accidental Limit State
CAFL	Constant Amplitude Fatigue Loading
VAFL	Variable Amplitude Fatigue Loading
LDF	Load Distribution Factor

1 Introduction

This document is essentially meant to cover aspects related to the fatigue design and analysis of welded steel and steel-concrete composite bridges. It has been the intention of the authors to – wherever is judged necessary and feasible – present and highlight the background of various aspects in the fatigue design.

Fatigue load models are treated in Chapter 2 for both road and railway bridges. Focus has been on the fatigue load models which are to be used with the simplified λ-method as well as the damage accumulation method. Both methods are covered in more details in Chapter 3. Worked examples on the application of these two methods in conjunction with the nominal-stress approach are given in Chapter 4.

Recommendations and guidelines for the fatigue design and analysis with local approaches are given in Chapter 5 for the hot-spot stress method and Chapter 6 for the effective notch-stress method.

Even if the hot-spot stress method is included in the Eurocode as an alternative to the conventional nominal stress method, no rules, recommendations or guidelines are today provided as to how this method should be applied. Chapters 4 & 5 are aimed at giving basic and general background information on the application of local approaches that often are suitable to use in conjunction with Finite Element Analysis.

1.1 Eurocodes for bridge design

The recommendations and guidelines given in this document for the fatigue design and analysis of steel and composite bridges are primarily based on the current rules and regulations in relevant parts of the Eurocodes.

The different parts of the Eurocodes dealing with the design of steel bridges and steel parts of composite bridges are listed in Figure 1-1 and describe below.

EN 1090 - Execution of steel structures

EN 1090 includes the general conditions and requirements for the execution of steel structures. The execution of steel structures is covered to the quality of the construction materials and products that should be used. Special requirements of seismic design are not covered by *EN 1090*.

EN 1990:2002 – Basis of structural design

The general principles and rules for the design and production works of structures, structural safety, serviceability and durability are presented in *EN 1990:2002*, which is intended to be used together with the other Eurocode parts. During bridge design stage when calculating the loads on structures, the partial factors to be used for load combinations are presented in this part of the Eurocode.

EN 1991-2:2003 - Actions on structures – Part 2: Traffic loads on bridges

Traffic loads on bridges to be used for different design limit states are defined in *EN 1991* in part 2. The code provides imposed loads for different proportions of the various types of standardised vehicles/trains according to the type of bridges and traffics. *EN 1991-2:2003* is also intended to be used together with *EN 1990* and *EN 1991* to *EN 1999*.

EN 1993-1-9:2005 - Design of Steel Structures – Part 1 – 9: Fatigue

EN 1993-1-9:2005 presents general requirements and methods for the fatigue assessment of steel structures and their components. This part of the Eurocode is applicable to all grades of structural steels (including stainless steels) with suitable corrosion protection and maintenance during the required life time. This means that the structures subjected only to mildly corrosive environments, such as normal atmospheric conditions, are covered by the *EN 1993-1-9:2005*. The effect of seawater corrosion and also the effect of the high temperature (> 150 °C) are not covered.

EN 1993-2:2006 - Design of Steel Structures – Part 2: Steel Bridges

EN 1993-2:2006 consists of requirements and design rules for steel bridges and steel parts of composite bridges. In this part of the Eurocode, the recommended load models for the design limit states and methods given in *EN 1991-2:2003* are presented. Also damage equivalence factor λ and the partial factors for fatigue verifications are given. It is worth mentioning here that the design of composite bridges is covered in *EN 1994-2*.

EN 1994-2:2005 consists of requirements and design rules for concrete parts of composite bridges. In this part of the Eurocode, the recommended design methods for the design limit states and methods given in *EN 1991-2:2003* are presented. Also shear connections between the concrete and steel parts and their interaction effects are given.

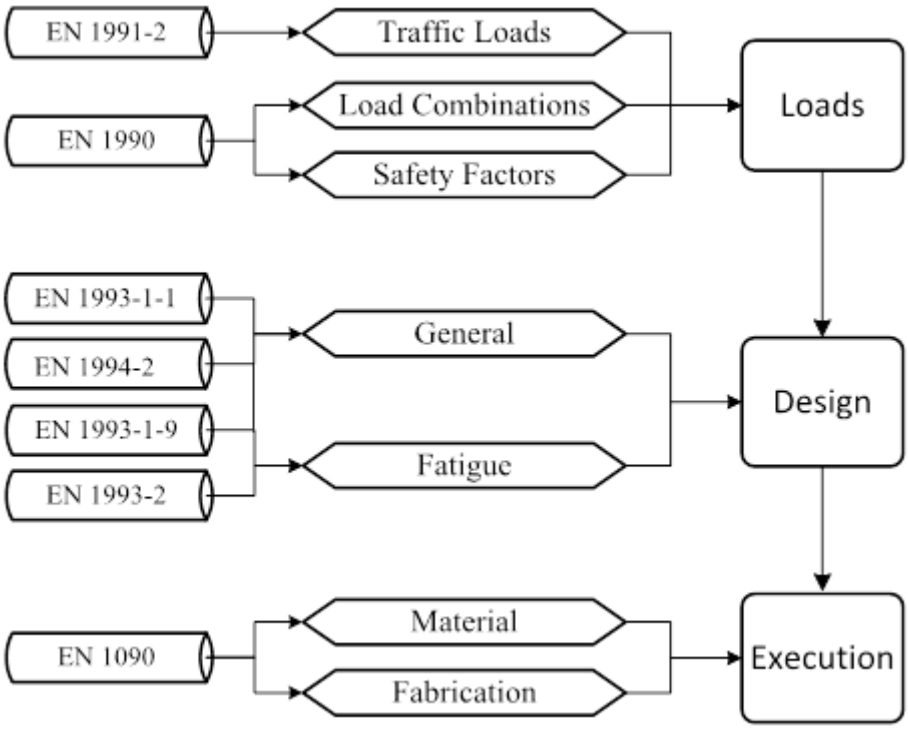

Figure 1-1 The Eurocode parts used in bridge design and execution

1.2 Application areas and limitations

The applicability of the fatigue design recommendations and guidelines given in this document is limited by the scopes and limitations of the various relevant parts in the Eurocode.

1.2.1 Material

The range of structural steel grades used in steel bridges is given in Table 3.1 in *EN 1993-1-1:2005.* The code also recommends that for material properties and geometrical data to be used in design of steel bridges the relevant ENs, ETA or ETA product standard should be complied. Higher structural steel grades (> S700) are however listed in *EN 1993-1-12:2007*.

1.2.2 Temperature

It is well-known that material properties are dependent on the temperature. The effect of temperature on the fatigue strength of a detail should be checked due to fact that the temperature effect for example with a very low temperature can change the crack growth rate which can in turn change the fatigue strength of structural steels.

With a high temperature, the fatigue strength of structural steel might be reduced because of the increased plastic deformation which can lead to increased fatigue damage accumulation [1]. However, temperatures above 150 ℃ are not considered in *EN 1993-1-1:2005* when computing the fatigue strength of structural steels. Instead, high temperature above 150 ℃ should be considered as the temperature induced damage or additional load in form of temperature following recommendations given in *EN 1991-1-1:2005* when computing the reduced fatigue strength.

1.2.3 Corrosion

Fatigue strength of materials can be affected by the environment which can influence both the crack initiation and crack growth phase of fatigue cracks. Corrosion can reduce the fatigue life of a structure by introducing surface flaws which can be considered as local stress raisers that may cause high stress concentrations. Therefore, structural steels should be protected against corrosion.

2 Fatigue load models in Eurocode

Load effects generated by traffic loads on bridges are generally very complex. Not only are the stress ranges generated by these loads of variable amplitudes, but also other parameters that might affect the fatigue performance of bridge details such as the mean stress values and the sequence of loading cycles are rather stochastic.

In order to treat such complex loading situations there is a need to represent the "real" traffic loads in term of one or more **equivalent load models**. Expressed in term of load effects (i.e. stresses and deformation) the variable amplitude stress ranges generated by real traffic loads on bridges should be represented as one or more equivalent constant amplitude stress ranges, which are easier to treat in a design situation. In doing so, the fatigue damage generated by these equivalent load models should be equivalent to that caused by the real traffic load on bridges. The fatigue load models in *EN 1990 and EN 1991-2* were derived on the basis of these principles.

In principle, the procedure used to derive the fatigue load models in Eurocode (illustrated graphically in Figure 2.1) is as follows:

1. Selection of typical bridges for simulating bridge responses to traffic flow
2. Selection of typical structural details for fatigue analysis along with their fatigue resistance curves
3. Using measured traffic data and the influence line for each studied detail, perform a simulation of bridge response to obtain the stress history relevant for fatigue design of the detail
4. Employing an appropriate cycle counting method to transform the stress history into a stress histogram with a number of constant amplitude stress ranges.
5. Applying damage accumulation rule (Palmgren-Miner rule) to obtain an equivalent stress range $\Delta\sigma_E$, causing the same damage factor as the stress histogram generated in the traffic simulation.
6. Deriving damage-equivalent fatigue load models, which generate a comparable damage to that caused by $\Delta\sigma_E$.

It goes without saying that an accurate determination of fatigue load models for both road and railway bridges requires an appropriate selection of the geometry of the load model vehicles, its axle loads, axel spacing as well as the composition of traffic and its dynamic effects. All these factors have been considered in the derivation of traffic load models for bridges in Eurocode. A detailed description of how traffic load models for road bridges was performed can be found in [3].

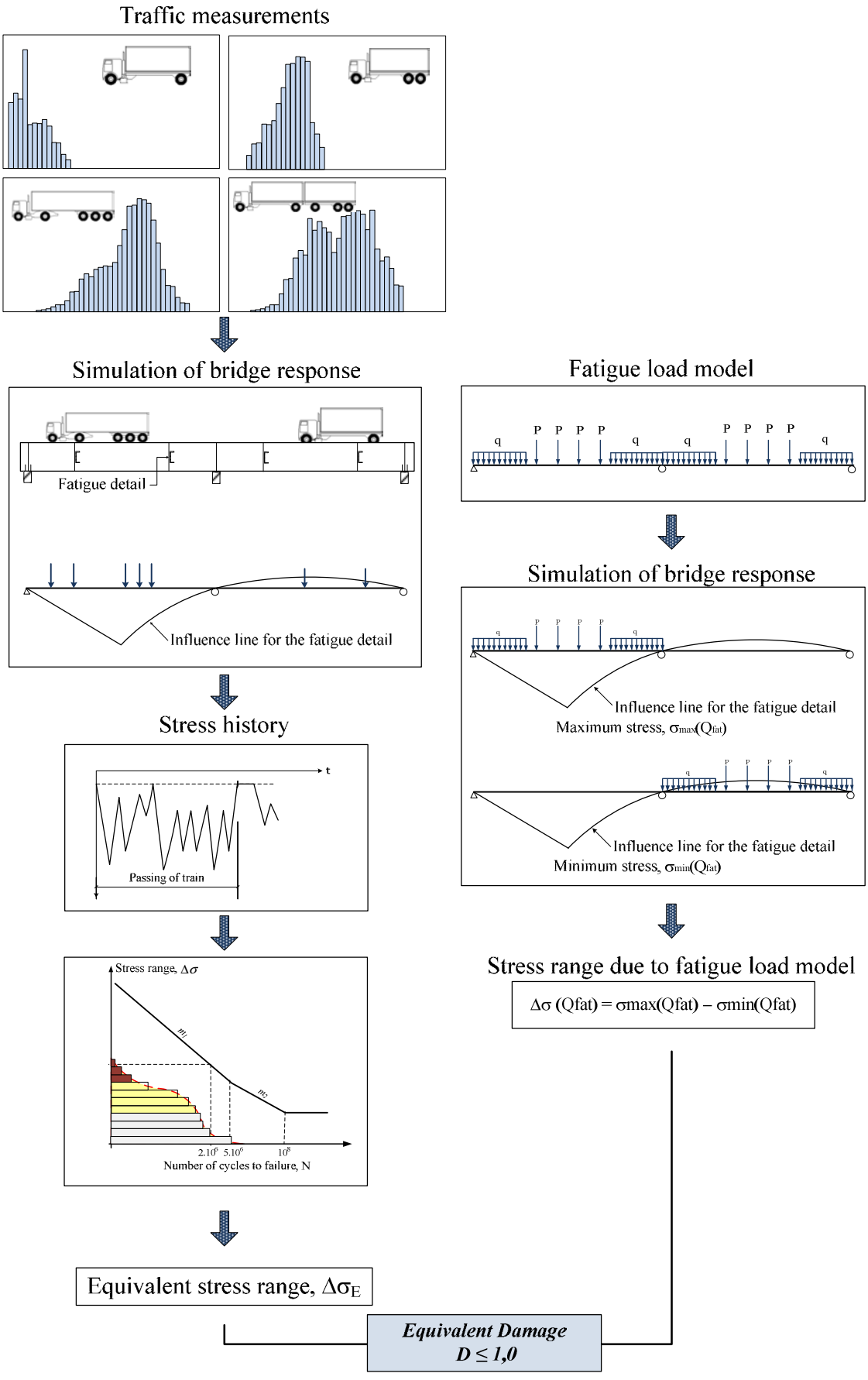

Figure 2-1 The principles for the derivation of fatigue load models in the Eurocode

2.1 Fatigue load models for road bridges

The fatigue load models for road bridges recommended in *EN 1991-2:2003* were derived according to the procedure presented in the previous section. In *EN 1991-2:2003*, there are totally five recommended fatigue load models to reflect the actual load conditions accurately when designing road bridges against fatigue. These fatigue load models have been defined and calibrated based on a wide range of European traffic data measurements in which the traffic measured during the two measurement periods, the years 1977 – 1982 and 1984 – 1988. These measurements recorded on various types of roads and bridges in different European countries [3]. Figure 2-2 shows an example from these traffic measurements presented as percentage of vehicle type.

	1	2	3	4	5	6	7	8	9	10
Location	Caronte	Montlhery	Autreville	Haagsche Schouw	Rheden	Limburger Bahn	Forth	Manchester	Rio Verde	Auxerre
Land	F	F	F	NL	NL	D	GB	GB	I	F
Measured	(2)	(2)	(2)	(2)	(2)	(2)	(1)	(1)	(1)	(2)
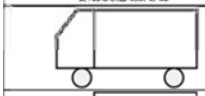	49,2	57,2	39,2	80,3	52,1	41,3	89,1	94,1	58,1	22,7
	4,8	4,3*	3,5*	4,4*	6,1*	3,1	1,9	1,1	2,0	1,3
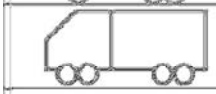	-	-	-	-	-	-	1,0	-	-	-
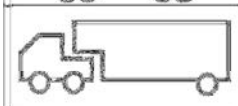	17,8	8,4	12,5	3,1	4,1	4,1	2,3	0,6	3,6	
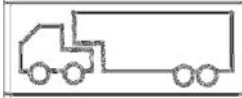	22,6*	18,1*	28,5	4,6*	11,8	5,5	5,6*	3,7*	3,3	65,2
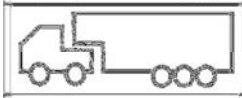	-	0,8*	8,2	1,1	6,9*	5,4*	-	-	10,8	-
	-	5,0	-	0,3	1,2	2,7*	-	-	-	-
	-	-	-	0,5	1,2*	-	-	-	-	-
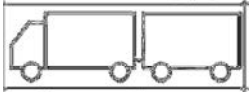	3,4	5,7	3,7*	3,6	7,6	13,8	-	-	1,9	-
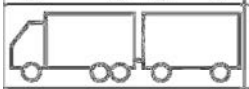	"	"	"	0,3	1,4	6,9	"	"	"	10,8
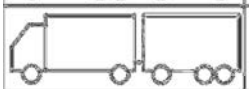	1,1	-		2,3	0,7	3,8	16,2	-	-	2,6
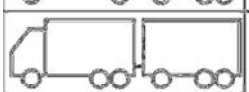	0,4	"	"	"	"	"	"	"	4,2	"
Various	0,6	0,5	2,1	1,4	5,2	1,0	0,1	0,5	16,8*	-

*Decisive for vehicle loads, 1) All vehicles, 2) Only lorries

Figure 2-2 Percentage of the types of vehicles [3]

The Auxerre traffic has been chosen as the basis for the derivation of the load models for road bridges in *EN 1991-2:2003*. The Auxerre traffic displays neither the largest axle loads nor the longest measurement. However, it has the largest frequency of large axle loads which is an essential factor to derive a characteristic design load for fatigue design of bridges. Another reason for choosing the Auxerre traffic as a common "European traffic" is that the extrapolation method used to determine characteristic values needed a sample of uniform traffic, which was provided by this traffic composition.

All in all, five different load models are proposed in *EN 1991-2:2003* for road traffic. The choice of appropriate load model depends on the fatigue verification method used in design. In addition, the use of a specific load model might lead to conservative results in a specific case, while another load model might be more appropriate in a specific situation. In the following sections, a more detailed description of each load model is presented and comments are made on the application of these load models when appropriate.

2.1.1 Fatigue load model 1, FLM1

Fatigue load model 1 (FLM 1) is intended to be used to check an "infinite fatigue design" situation, i.e. to check whether the fatigue life of the bridge may be considered infinite. This load model generates a "constant amplitude" stress range which is the algebraic difference between the minimum and maximum stress obtained from positioning the load model in the corresponding tow positions.

FLM 1 is directly derived from the characteristic load model 1 (LM 1) used in the ULS design by multiplying the concentrated axle loads (Q_{ik}) by 0.7 and the weight density of the uniformly distributed loads (q_{ik}, q_{rk}) by 0.3. Thus, FLM 1 is composed of both concentrated and uniformly distributed loads. Fatigue verification with FLM 1 is performed by comparing the stress range generated by this model to the Constant Amplitude Fatigue limit (CAFL). Therefore fatigue design using FLM 1 will yield a very heavy structure.

The characteristic LM 1 is composed of double-axle concentrated loads (called the Tandem System) applied in conjunction with a uniformly distributed load (UDL). This load model was developed using measured traffic data on the motorway (A6) Paris-Lyon near Auxerre. The vehicle geometry and the axle loads are specified in *EN 1991-2:2003* and reproduced in Figure 2-3 which is recommended for bridges with span length less than 200m. As shown in this figure, the amount of uniformly distributed load applied on bridge lanes including remaining area is the same except for lane number 1, in which a higher fatigue load is recommended. Recommendations for load models for bridges with larger span (≥ 200m) are given in *TRVK Bro 11:085*.

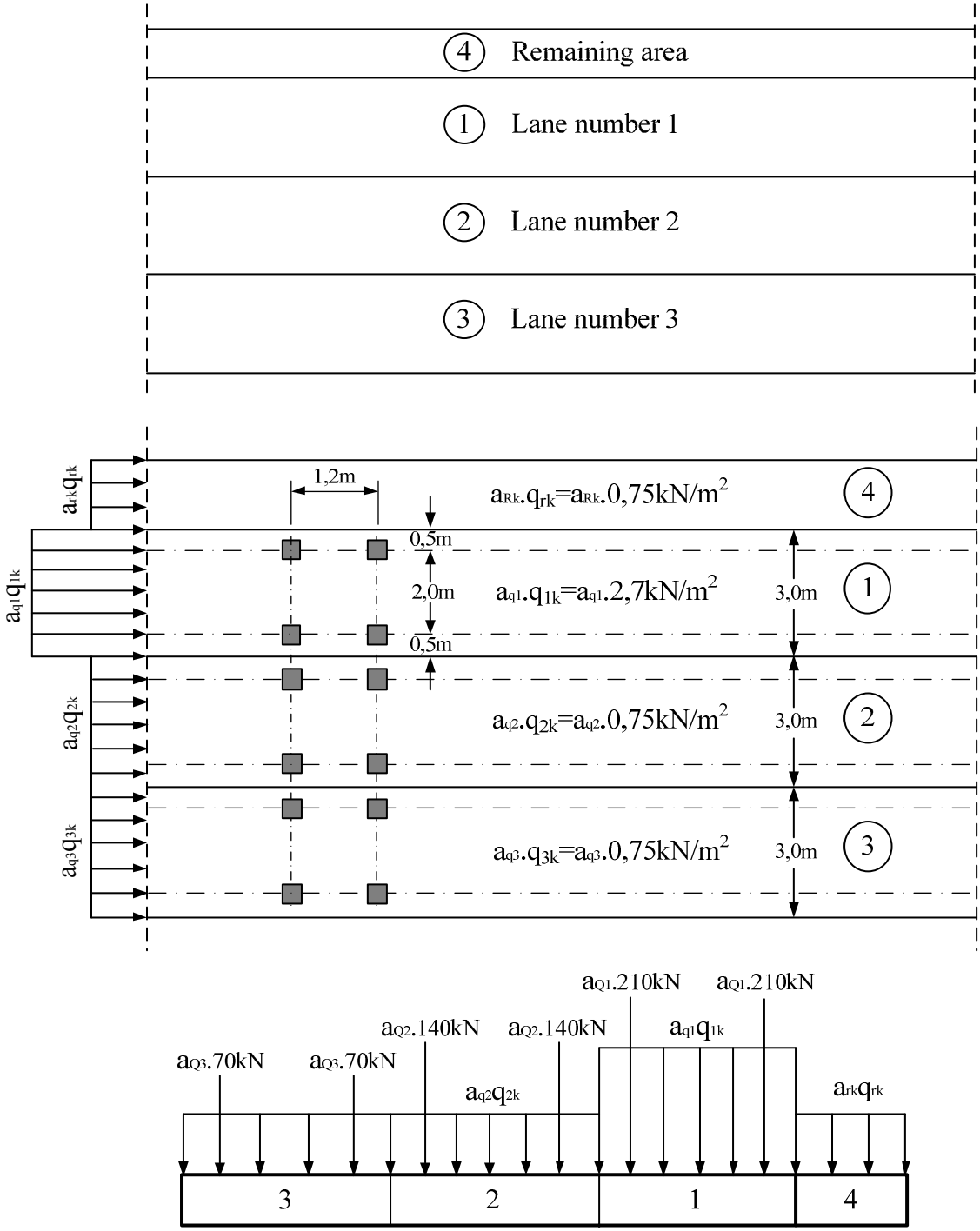

Figure 2-3 Fatigue load model 1 according to EN 1991-2:2003

2.1.2 Fatigue load model 2, FLM2

Fatigue load model 2 (FLM2) is defined as a set of frequent lorries in Table 4.6 of *EN 1991-2:2003*. In this table, the set of frequent vehicles is composed of five standard lorries, which represent the most common lorries in Europe. Each lorry is presented with its specific arrangement of axle spacing, axle loads and wheel types for the frequent loading. The loads in fatigue load model 2 and the set of standard lorries was established using the measured traffic data on motorway (A6) Paris-Lyon at Auxerre [4].

Notes on the application of FLM1 and FLM2

- *Similar to FLM 1, Fatigue load model 2 is intended to be used of determining the maximum and minimum stresses when designing for an unlimited fatigue life. The stress range generated by each lorry should be compared to the CAFL in the fatigue verification.*

- *FLM 2 is intended to be used in situations where the presence of more than one vehicle over the bridge can be neglected. This is the situation for bridge details with short influence lines, e.g. local bending effects in orthotropic steel bridge decks. The fatigue verification should therefore be performed for each vehicle in the traffic set as – dependent on the length of influence line for the particular detail – an axle load, a bogie axle or an entire vehicle may cause a loading cycle. Thus for such situations, FLM 2 deliver more accurate results than FLM 1.*

- *Fatigue verification applying FLM 1 and FLM 2 is performed by checking that the stress range (the algebraic difference between the maximum and minimum stress) for the detail and load effect under consideration does not exceed the CAFL. This exerts a limitation on the application of these two load models as for some details, such as welded details loaded in shear, a constant amplitude fatigue limit is not defined in the code.*

2.1.3 Fatigue load model 3, FLM 3

Fatigue Load Model 3 (FLM 3) is composed of a single vehicle with four axles of 120kN each (the total weight of the vehicle is thus 480kN). The vehicle geometry and the axle loads are specified in *EN 1991-2:2003* and reproduced in Figure 2-4.

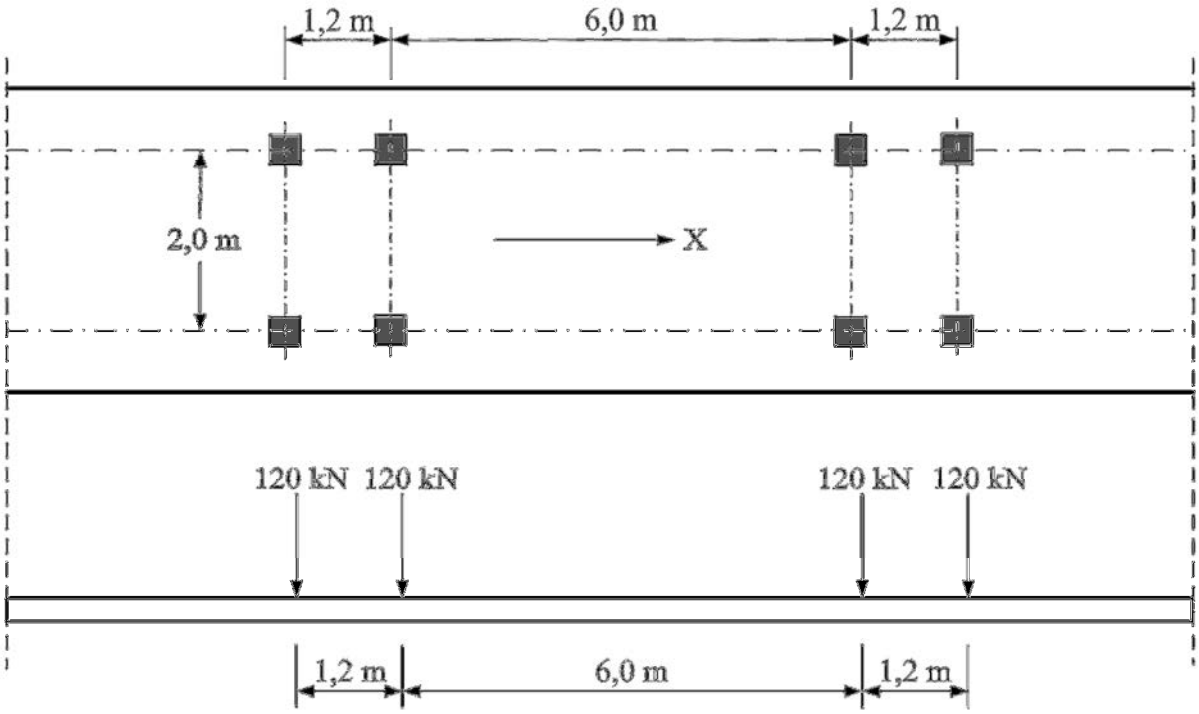

Figure 2-4 Fatigue load model 3 according to EN 1991-2:2003

Similar to FLM 1 and FLM 2, FLM 3 was also derived using the measured traffic data on the motorway Paris-Lyon at Auxerre [5]. The total weight of the vehicle in FLM3 is slightly higher than the measured total weight in the Auxerre traffic, which was 469kN. On the other hand, the single axle load of 120kN in FLM 3 is lower than the measured maximum axel load which was 131kN.

FLM 3 is used to verify the fatigue life of the investigated details by calculating the maximum and minimum stresses resulting from the longitudinal and transversal location of the load model. The model is thus intended to be used with the simplified λ–method, i.e. to verify that the computed stress range is equal to or less than the fatigue strength of the investigated detail. The model is sufficiently accurate for road bridges with spans longer than 10 m, but has an inclination to yield conservative results for shorter spans [6].

In general, when performing fatigue verification with FLM 3, the model vehicle should be positioned along the centre of the notional traffic lane. Some bridge details experience, however, local load effects and are therefore sensitive to the location of the wheel load in the transverse direction of the bridge (details in orthotropic bridge decks, for example). For such situations, *EN 1991-2:2003, 4.6.1(5)* directs the designer to use a statistical distribution of the location of FLM3 within the traffic lane.

FLM 3 was compared with the reference traffic to verify the accuracy of the model [7]. This comparison was also performed in order to check the accuracy of the field application, i.e. the accuracy of the load model in various sections using the influence lines. This comparison considering the slope of 3 is shown in Figure 2-5.

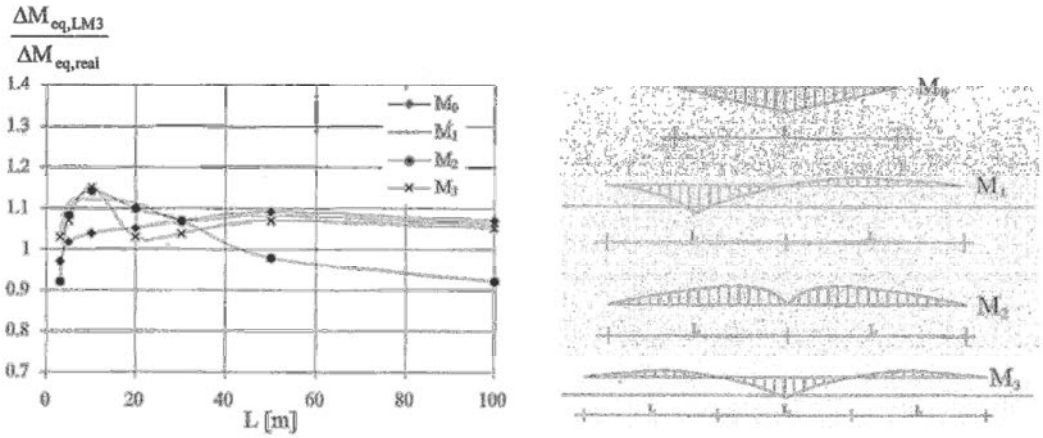

Figure 2-5 Comparison of the fatigue load model 3 with the reference traffic [7]

where

$\Delta M_{eq,FLM3}$: The equivalent stress range produced by the fatigue load model

$\Delta M_{eq,real}$: The equivalent range of moment obtained from the measured traffic data from Auxerre traffic

As seen in Figure 2-5, the code recommended fatigue load model yields results on the safe side (i.e. ratios > 1,0) except for moment over intermediate supports in continuous beams (M_2) for span lengths larger than 40,0 m. To overcome this problem, FLM 3 has been modified by considering a second similar vehicle but with a reduced axel load of 36kN. This second vehicle follows the main FLM3 vehicle with a minimum distance (centre to centre) of 40m on the same lane. This correction for influence line, M_2 was again compared with the reference traffic data as shown in Figure 2-6. FLM 3 using an additional vehicle with the reduced axle loads represents more correct response for the calibration of the traffic load.

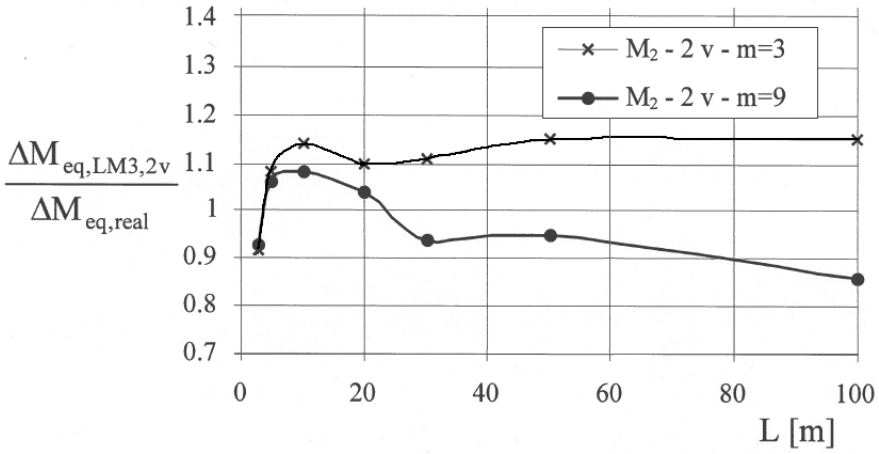

Figure 2-6 Comparison of the modified fatigue load model 3 [7]

2.1.4 Fatigue load model 4, FLM 4

Fatigue load model 4 (FLM 4) is a set of 5 different lorries with different geometry and axle load, which are intended to simulate the effects of "real" heavy traffic loads on road bridges, see Table 2-1. The properties of the lorries in FLM4 are consistent with the most common heavy vehicles on European roadways and are assumed to be

representative for standard lorries in Europe. *EN 1991-2:2003* provides also the properties of each lorry by the number of axles and spacing represented with an equivalent load for each axle. Different traffic types are accounted for by defining different composition of lorries as percentage of the heavy traffic volume. For the application of fatigue load model 4 on road bridges, a definition of the total annual number of lorries crossing the road bridge (N_{obs}) has also been defined by the code.

The lorry composition and properties recommended for FLM 4 is the same set of lorries recommended for FLM 2. Only the characteristic axle loads corresponding to the average loads are reduced. To check the accuracy of this load model with respected to the reference traffic data (the Auxerre traffic), a comparison was performed in [7] and the results are shown in Figure 2-7 (M_0 to M_3 are defined in Figure 2-5). As seen in this figure, the result for short influence lines is consistent with those from the reference traffic data. This means that this load model yields very precise evaluation of the fatigue resistance for short span bridges.

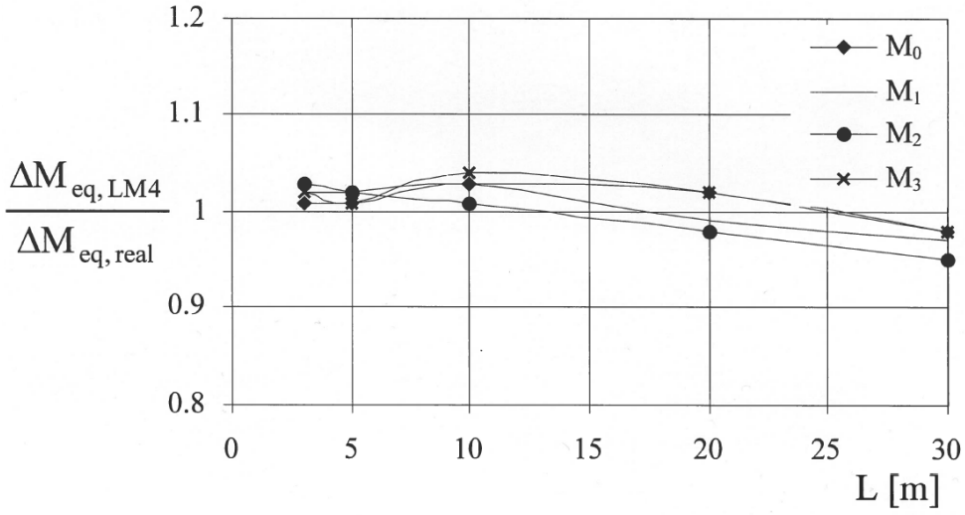

Figure 2-7 Comparison of FLM 3 with the reference traffic [7]

Table 2-1 Set of equivalent lorries specified in EN 1991-2:2003

Vehicle type				***Traffic type***		
				Lorry percentage		
Lorry	***Axle spacing [m]***	***Equivalent axle loads [kN]***	***Wheel type****	***Long distance***	***Medium distance***	***Local traffic***
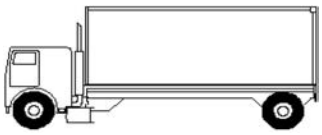	4,5	70 130	A B	20,0	40,0	20,0
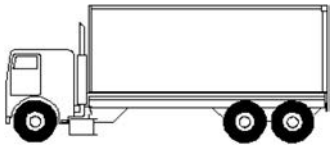	4,20 1,30	70 120 120	A B B	5,0	10,0	5,0
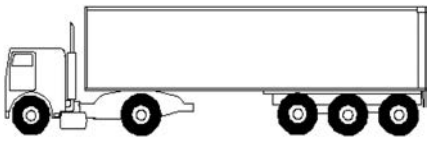	3,20 5,20 1,30 1,30	70 150 90 90 90	A B C C C	50,0	30,0	5,0
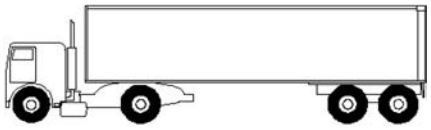	3,40 6,00 1,80	70 140 90 90	A B B B	15,0	15,0	5,0
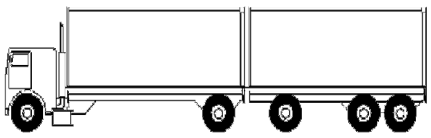	4,80 3,60 4,40 1,30	70 130 90 80 80	A B C C C	10,0	5,0	5,0

* The type and size of wheels is given in *Table 4.8 in EN 1991-2:2003*

FLM 4 is mainly intended to be used in the time-history analysis in association with a cycle counting procedure to assemble stress cycle ranges[1] when assessing the fatigue life of the structure. In other words, FLM 4 is recommended to be used with the cumulative damage assessment concept.

[1] To obtain a resultant stress histogram by assembling a stress history from each lorry passage

Notes to the use of FLM3 and FLM4

- *Since both FLM 3 and FLM 4 are meant to be used for fatigue verification with finite fatigue life (i.e. for a specific design life), the number of cycles needs to be specified somehow (observe that this was not needed for FLM 1 & FLM 2 as they are meant to verify that the fatigue life of the bridge is infinite). For road bridges, the number of cycles is expressed in EN 1991-2:2003 as a "traffic category". Four traffic categories are proposed in EN 1991-2:2003, each with information about the number of slow lanes and the number of heavy vehicles – observed or estimated – per year and per slow lane, N_{obs}.*

- *With slow lane it is meant traffic lanes used predominantly by heavy vehicles*

  - *With heavy vehicles it is meant lorries with a gross weight higher than 100kN*

  - *N_{obs} for each traffic category are a nationally determined parameter. The indicative figures for N_{obs} in EN 1991-2:2003, 4.6.1(3) for different traffic categories are replaced in TRVK Bro 11:085 by the values given in B.3.2.1.3 which is reproduced in the Table below (observe that the values in the Table below should be doubled for road bridges with single lane). Annual average daily traffic, abbreviated AADT (ÅDT in Swedish), is a mean value that refers to the daily traffic volume of a highway for a year.*

  - *For AADT bigger than 24000 (Category X in the table), a certain investigation of the prerequisites for the fatigue design should be performed.*

Table 2-2 Traffic category according to TRVK Bro 11:2003

Traffic category	***AADT heavy traffic (ÅDT)***
X	24000 <
1	6000 < AADT ≤ 24000
2	1500 < AADT ≤ 6000
3	600 < AADT ≤ 1500
4	≤ 600

- *FLM4 requires in addition the definition of a "traffic type", see Table 2-2. TRVK Bro 11:085 specifies that the traffic type on Swedish roads should be taken as "regional".*

- *For bridges with more than one lane, AADT heavy traffic is reduced by a factor of 0.9 due to the distribution of the heavy traffic into other lanes.*

- *Except for the additional vehicle that might need to be considered in FLM 3 (for moment over intermediate supports in continuous bridges), each vehicle in FLM 3 and FLM 4 should cross the bridge "alone", i.e. in the absence of any other traffic vehicles.*

- *As shown in Figure 2-6 and Figure 2-7, the comparisons show that FLM 3 yield sufficiently accurate results for bridges with higher span length (≥ 20 m) while FLM 4 represents the load effect accurately for bridges with shorter span (≤ 20 m).*

2.1.5 Fatigue load model 5, FLM 5

Fatigue load model 5 (FLM 5) is based on recorded road traffic and a direct application of measured traffic data. This load model is intended to be used to accurately verify the fatigue strength of cable-stayed or suspended bridges, other complex and important bridges or bridges with "unusual" traffic. Fatigue verification

with FLM 5 requires traffic measurement data, an extrapolation of this data in time and a rather sophisticated statistical analysis. *EN 1991-2:2003* provides additional information in this respect in its Annex B.

2.1.6 Summary

The fatigue load models recommended in *EN 1991-2:2003* for road bridges are based on reference influence surfaces for different types of bridge structures, i.e. simply supported and continuous bridges for span length between 3m and 200 m [7]. These load models can be divided in two main groups depending on the required fatigue life. The first group is used to verify infinite fatigue life. This group contains of FLM 1 and FLM 2. The second group of the fatigue load models is aimed for performing fatigue assessing for given fatigue design life using the damage accumulation method based on Palmgren-Miner rule or the damage equivalent concept, also called simplified λ-coefficient method. In this group, FLM 3 is applied when performing the damage equivalent concept and FLM 4 when performing the cumulative damage concept. The grouping of the fatigue load models for road bridges are compiled in Figure 2-8 below.

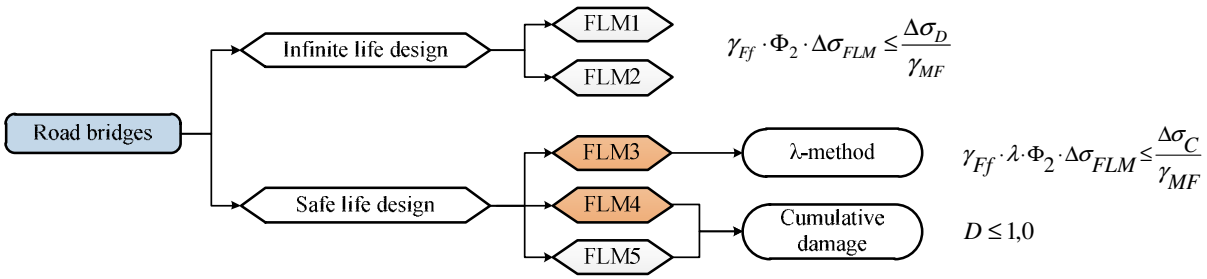

Figure 2-8 Fatigue load models for road bridges according to EN 1991-2:2003

2.2 Fatigue load models for railway bridges

The fatigue load models recommended in *EN 1991-2:2003* were derived to represent the effect of railway traffic loads on the European railways network. These load models have been calibrated using railway traffic data from UIC (the International Union of Railways) and ERRI (the European Rail Research Institute) [8].

In addition, the load models for railway bridges given in *EN 1991-2:2003* are only applicable to standard and wide track gauge mainline networks *[EN 1991-2:2003,6.1(3)]*. In other words, these models are not applicable for other type of railway tracks such as:

- Narrow-gauge railways
- Tramways and other light railways
- Preservation railways
- Rack and pinion railways
- Funicular railways

The dynamic factors Φ_2 and Φ_3 accounting for the influence of the train speed, the structure rigidity and the track quality are also applied to the fatigue load models, even though these factors were originally derived for extreme loading cases and indented to be used for static assessments of bridge members [6]. These dynamic

factors are only valid for train speeds up to 200 km/h. For higher train speeds, special dynamic analysis is required for the fatigue verification in order to more accurately account for additional load effects generated by dynamic effects, such as vibration and resonance.

Unlike the situation for road bridges, fatigue assessment of railway bridges has to be performed according to the "safe life design" principle. Fatigue usually governs the design of railway bridges, and an "infinite life design" approach would result in an extreme and uneconomic design. The λ-coefficient method as well as the cumulative damage method can be used in fatigue verification of railway bridges. Different load models are assigned in EN 1991-2 to be applied in conjunction with each of these methods. These load models are described below.

2.2.1 Fatigue load models for the λ-coefficient method

The fatigue load model to be used for the verification of the fatigue strength of railway bridges when using the damage equivalent concept is derived from load model 71 excluding the ultimate strength design adjustment factor, (α=1.0). In addition to FLM71, load models SW/0 and SW/2 should be used in conjuction with fatigue design of continuous railway bridges with standard and heavy rail traffic respectively. In railway bridges with multiple tracks, fatigue loads should be applied to a maximum of two tracks in the most unfavourable positions for the investigated detail.

2.2.1.1 Fatigue load model 71, FLM 71

The load arrangements and the characteristic values for LM 71 are given *EN 1991-2:2003,6.3.2* and reproduced in Figure 2-9. There is no limit for the length of the uniformly distributed load. Thus, LM 71 has to be applied to the track or each of the tracks to obtain the maximum effects (internal forces) by positioning the concentrated loads in the most unfavourable position with reference to the studied detail with the uniformly distributed load extended as much as needed to reflect the maximum effects of the train traffic.

The characteristic value of LM71 should be used in the fatigue verification, excluding any ULS adjustment factor, α.

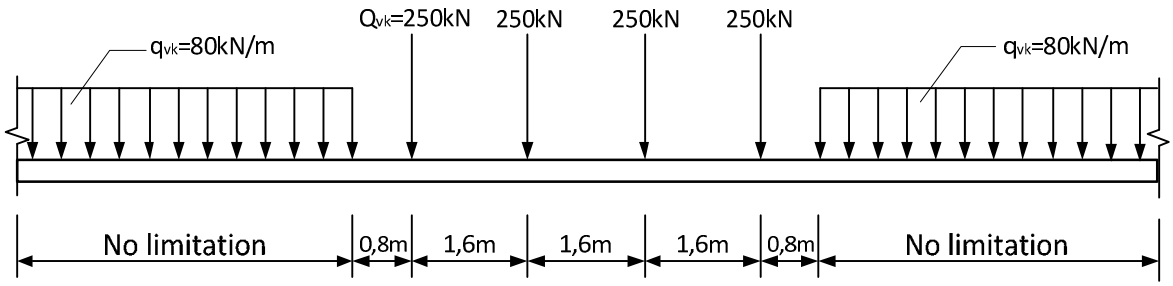

Figure 2-9 Load model 71 defined in EN 1991-2:2003

2.2.1.2 Fatigue load model SW/0 and SW/2

As an alternative to FLM71 load models SW/0 and SW/2 (for heavy traffic) can be used. These two load models are in general appropriate for continuous bridges or

bridge beams. The load arrangement and the characteristic values recommended in *EN 1991-2:2003* for these two load models are shown in Figure 2-10 and Figure 2-11.

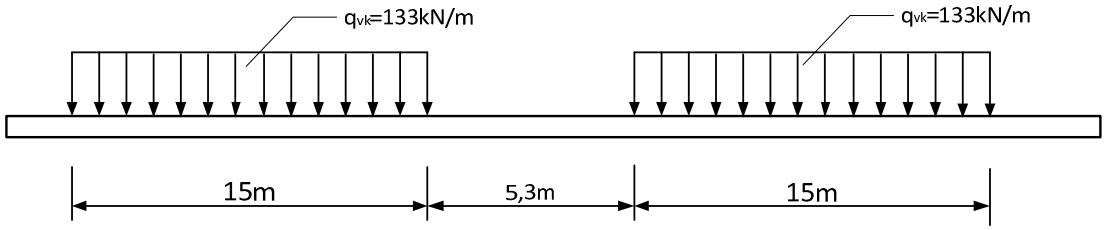

Figure 2-10 Load model SW/0 defined in EN 1991-2:2003

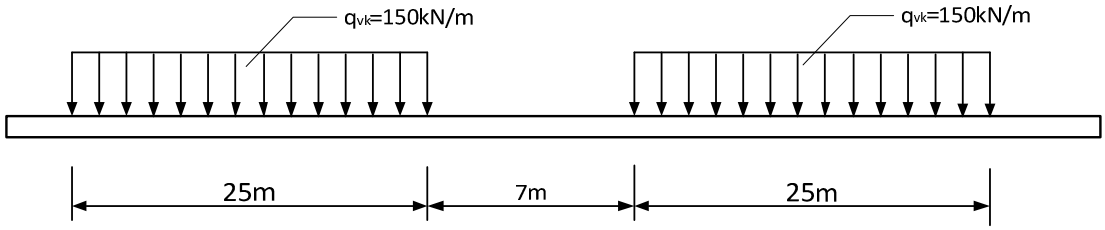

Figure 2-11 Load model SW/2 defined in EN 1991-2:2003

2.2.2 Fatigue load models for the cumulative damage method

According to *EN 1991-2:2003*, the fatigue design stress spectra used in the cumulative damage assessment procedure should be calculated on the basis of the so called "traffic mixes". A traffic mix is a set of train load models each composed of several wagons with predefined axel loads and axel spacing. Depending on the daily traffic on the network, one of three predefined mixes can be selected. These are: "standard traffic mix", "heavy traffic mix" and "light traffic mix". The composition of each traffic mix is defined in *Annex D of 1991-2:2003* along with standard train types. In addition to the traffic mix, a traffic volume per year has to be defined. The standard traffic mixes in Eurocode are all based on a traffic volume of 25 million tonnes per year.

2.2.2.1 Fatigue load "Standard traffic mix"

The fatigue load of "Standard traffic mix" is composed of 8 different train types with a total number of 67 train passages per day. This traffic mix contains both passenger train types including high speed trains and freight train types. The axle loads of the trains are varying from 70kN to 225kN. Standard traffic mix recommended in *EN 1991-2:2003* is shown in Table 2-3.

Table 2-3 Fatigue load model "Standard traffic mix" according to the Eurocode

Train type	***Number of trains [per day]***	***Mass of train [tonnes]***	***Traffic volume [10^6 tonnes/year]***
1	12	663	2,90
2	12	530	2,32
3	5	940	1,72
4	5	510	0,93
5	7	2160	5,52
6	12	1431	6,27
7	8	1035	3,02
8	6	1035	2,27
	67		**24,95**

2.2.2.2 Fatigue load "Heavy traffic mix"

The fatigue load model of "heavy traffic mix" consists of 4 standardized trains with a total number of 51 of train crossing over the bridge per day. This traffic mix is meant to represent only standardized types of freight trains. The axle loads of the trains are up to 250kN. The "Standard traffic mix" given in *EN 1991-2:2003* is reproduced here in Table 2-4.

Table 2-4 Fatigue load model "heavy traffic mix" according to the Eurocode

Train type	***Number of trains [per day]***	***Mass of train [tonnes]***	***Traffic volume x 10^6 [tonnes/year]***
5	6	2160	4,73
6	13	4131	6,79
11	16	1135	6,63
12	16	1135	6,63

	51		**24,78**

2.2.2.3 Fatigue load "Light traffic mix"

The composition of the fatigue loads for "Light traffic mix" contains 4 standardised train types with a total number of 67 trains per day. This traffic mix is meant to represent a mix of both passenger trains and freight trains. The axle loads of the trains vary between 110kN and 225kN. The recommended composition for this traffic mix in *EN 1991-2.2003* is shown in Table 2-5.

Table 2-5 Fatigue load model "Light traffic mix" according to the Eurocode

Train type	***Number of trains [per day]***	***Mass of train [tonnes]***	***Traffic volumex10^6 [tonnes/year]***
1	10	663	2,4
2	5	530	1,0
5	2	2160	1,4
9	190	296	20,5
	67		**25,3**

2.2.2.4 Train models suggested in TRVK Bro 11:085

Paragraphs (3) and (7) in *EN 1991-2:2003, 6.9* allows for different traffic mixes other than those given in Annex D to be defined by the authorities in each nation in order to better represent the rail traffic on individual projects. In *TRVK Bro 11:085, B.3.2.1.4*, three different train models are specified for fatigue verification of railway bridges with the damage accumulation method. This is done on the basis of the value of the multiplier α which is defined in *EN 1991-2:2003, 6.3.2(3)*.

Bridges that are designed with α = 1.33.
The following traffic mix shown in Table 2-6 should be used:

Table 2-6 Traffic mix med axial load ≤ 25tonne according to TRVK Bro 11:085

Train type	***No. of trains [day]***	***Total mass [tonnes]***	***Traffic volume [tonnes/year]***
1	12	663	$2{,}90 \cdot 10^6$
2	12	530	$2{,}32 \cdot 10^6$
3	5	940	$1{,}72 \cdot 10^6$
4	5	510	$0{,}93 \cdot 10^6$

5	7	2160	$5{,}52 \cdot 10^6$
6	12	1431	$6{,}27 \cdot 10^6$
11	7	1135	$2{,}91 \cdot 10^6$
12	6	1135	$2{,}49 \cdot 10^6$
	66		***$25{,}06 \cdot 10^6$***

Bridges that are designed with α = 1,60.

For this case, train load model 13S should be used. This model is composed of 68 wagons per train, each with a mass of 124 tonnes, see Figure 2-12. The number of trains per day is set to 10 in *TRVK Bro 11:085, B.3.2.1.4 (v)* and the total traffic volume per year is $34.70 \cdot 10^6$ tonnes. The train is assumed to cross the bridge with a maximum velocity of 60 km/h.

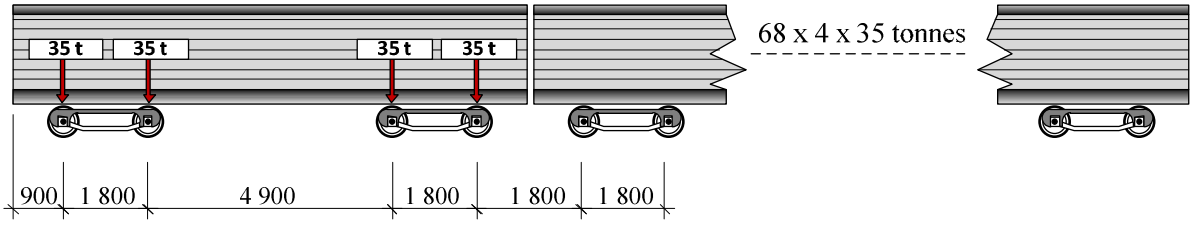

Figure 2-12 Train load model 13S and axle loads according to TRVK Bro 11:085

2.2.3 Summary

The load models for the fatigue verification of railway bridges in Eurocode can be categorised into two main groups depending on the fatigue assessment methods. The first group is meant to be used for fatigue verification using the simplified λ-coefficient method. This group contains fatigue load model 71 (FLM 71), fatigue load model SW/0 (FLM SW/0) and fatigue load model SW/0 (FLM SW/2). The second group of load models is meant to be used when the fatigue verification is to be performed using the damage accumulation concept based on Palmgren-Miner rule. This group contains different traffic mixes which are defined in *EN 1991-2* and which can be modified by the national annex.

Figure 2.11 Fatigue design procedure of railway bridges

3 Fatigue design methods

Eurocode allows for the application of two principal methods for the fatigue design of bridges: The equivalent damage method, also known as the **λ-coefficient method**, and the more general **cumulative damage method**. The background and the application of these two methods are presented in this chapter. The two methods are also demonstrated (and to some degree compared) in two worked examples in Chapter 4.

3.1 The concept of Equivalent Stress Range

As was mentioned in the previous Chapter, load effects generated by traffic loads on bridges are generally very complex. The stress ranges generated by these loads are usually of variable amplitudes which are relatively difficult to treat in design situations. There is, therefore, a need to represent the fatigue load effects caused by the "actual" variable amplitude loading in term of an **equivalent constant amplitude load effects**.

The treatment of such complex fatigue loading situation is usually treated in the following principle steps:

1. Transformation of the variable amplitude loading into a representative constant amplitude loading. This is usually done by some kind of **cyclic counting** method.
2. Using the new set of representative constant amplitude loading to perform the fatigue design or analysis. This is done either:
   - directly, by applying the **Palmgren-Miner damage accumulation rule,** or
   - by using the **equivalent stress range concept**.

The rules concerned with the fatigue design of bridges in Eurocode allow for the application of any of these two methods. The simplified λ-method in Eurocode is an adaption of the general equivalent stress range concept corrected by various λ-factors, while a direct application of the Palmgren-Miner rule can alternatively be used. As was discussed in the previous chapter, Specific fatigue load models have been derived and implemented in Eurocode for each of these two methods.

The principles of the damage accumulation rule (Palmgren-Miner) are presented in more details in Section 3.3 of this Chapter. In principle, a structural steel detail subjected to a given stress histogram will fail in fatigue when the damage factor D reaches a specific value. In EN 1993-1-9, the value of the damage factor, D was set to unity. Thus:

$$D = \sum_i D_i = \sum_i \frac{n_i}{N_i} \qquad \text{Eq. 3-1}$$

with

$$N_i = N_C \cdot \left(\frac{\Delta\sigma_C / \gamma_{Mf}}{\gamma_{Ff} \cdot \Delta\sigma_i} \right)^m \qquad \text{Eq. 3-2}$$

and n_i being the total number of loading cycles in the stress histogram.

The fatigue damage caused by a number of loading blocks with constant amplitude loading can also be represented by an ***equivalent stress range.*** The definition ***of equivalent stress range*** is that constant amplitude stress range which if applied with the same total number of loading cycles of the variable stress range ($\sum n_i$) would cause the same total damage as the variable amplitude loading block.

If one, for simplicity, assumes an S-N curve with a constant slope of 3, an expression for the equivalent stress range can be derived as follows in Eq. 3-3 for any load spectrum:

$$\Delta\sigma_E = \left[\frac{\sum_{i=1}^{n} n_i \times \Delta\sigma_i^m}{\sum_{i=1}^{n} n_i} \right]^{\frac{1}{m}} \qquad \text{Eq. 3-3}$$

In Eurocode, fatigue verification based on the simplified λ-method adopts an equivalent stress concept, where the stresses obtained from relevant load models in *EN 1991-2:2003* are modified with various λ-factors in order to be expressed as an equivalent stress range at 2 million cycles, $\Delta\sigma_{E,2}$. This transformation from $\Delta\sigma_E$ to $\Delta\sigma_{E,2}$ can be easily obtained from:

$$\frac{\Delta\sigma_{E,2}^m}{2\cdot 10^6} = \frac{\Delta\sigma_E{}^m}{N} \qquad \text{Eq. 3-4}$$

giving

$$\Delta\sigma_{E,2} = \Delta\sigma_E \left(\frac{N}{2\cdot 10^6} \right)^{1/m} \qquad \text{Eq. 3-5}$$

Doing so, the fatigue verification is reduced to a direct comparison between the equivalent stress range at 2 million cycles and the fatigue class (or fatigue strength) of the detail, i.e.

$$\Delta\sigma_{E,2} \le \Delta\sigma_C \qquad \text{Eq. 3-6}$$

with all partial factors being omitted for simplicity

3.2 Fatigue design with the λ-coefficient method

The λ-coefficient method is a conventional simplified fatigue assessment method, which is based on comparing an equivalent stress range with the studied detail category. The basic idea with this method is that the fatigue damage caused by the stress range spectrum is associated with an equivalent stress range $\Delta\sigma_E$ or an equivalent stress range at 2 million stress cycles, $\Delta\sigma_{E,2}$. The latter is – per definition – the fatigue strength. The method is derived originally for railway bridges, but applies also for road bridges. The purpose of this method is to convert fatigue verifications using λ–coefficients into a conventional fatigue resistance control, i.e. stress range check.

The conventional fatigue resistance control is on the basis of conditioning a lower or equal maximum stress range to the detail capacity stress range. The maximum stress range is the stress obtained from the fatigue load models which were originally derived to be used with this method, refer back to Figure 2.1 and the associated discussion in Chapter 2.

The fatigue verification is expressed as:

$$\lambda_{Ff} \cdot \lambda \cdot \Phi_2 \cdot \Delta\sigma_{FLM} \leq \frac{\Delta\sigma_C}{\lambda_{\max}} \qquad \text{Eq. 3-7}$$

where

γ_{Ff} is the partial safety factor for fatigue loading

γ_{Mf} is the partial safety factor for fatigue resistance

λ is the fatigue damage equivalent factor related to 2.10^6 cycles

Φ_2 is the dynamic factor

$\Delta\sigma_{FLM}$ is the stress range due to the fatigue load model

$\Delta\sigma_C$ is the reference stress range value of the fatigue strength

The λ-coefficient is obtained considering four different λ-coefficients as following:

$$\lambda = \lambda_1 \cdot \lambda_2 \cdot \lambda_3 \cdot \lambda_4 \leq \lambda_{\max} \qquad \textit{Eq. 3-8}$$

where

λ_1 is the span factor taking into account the length of the span and the structure type

λ_2 is the volume factor taking into account the traffic volume

λ_3 is the time factor taking into account the design life of the bridge

λ_4 is the lane factor taking into account the traffic on more than one lane

λ_{max} is the maximum damage equivalent factor taking into account the fatigue limit

The λ factors are in more detail described in the following sections.

Figure 3.1 presents an overview of the application of the λ-coefficient method with the relevant parts of Eurocode involved in the fatigue verification with this method.

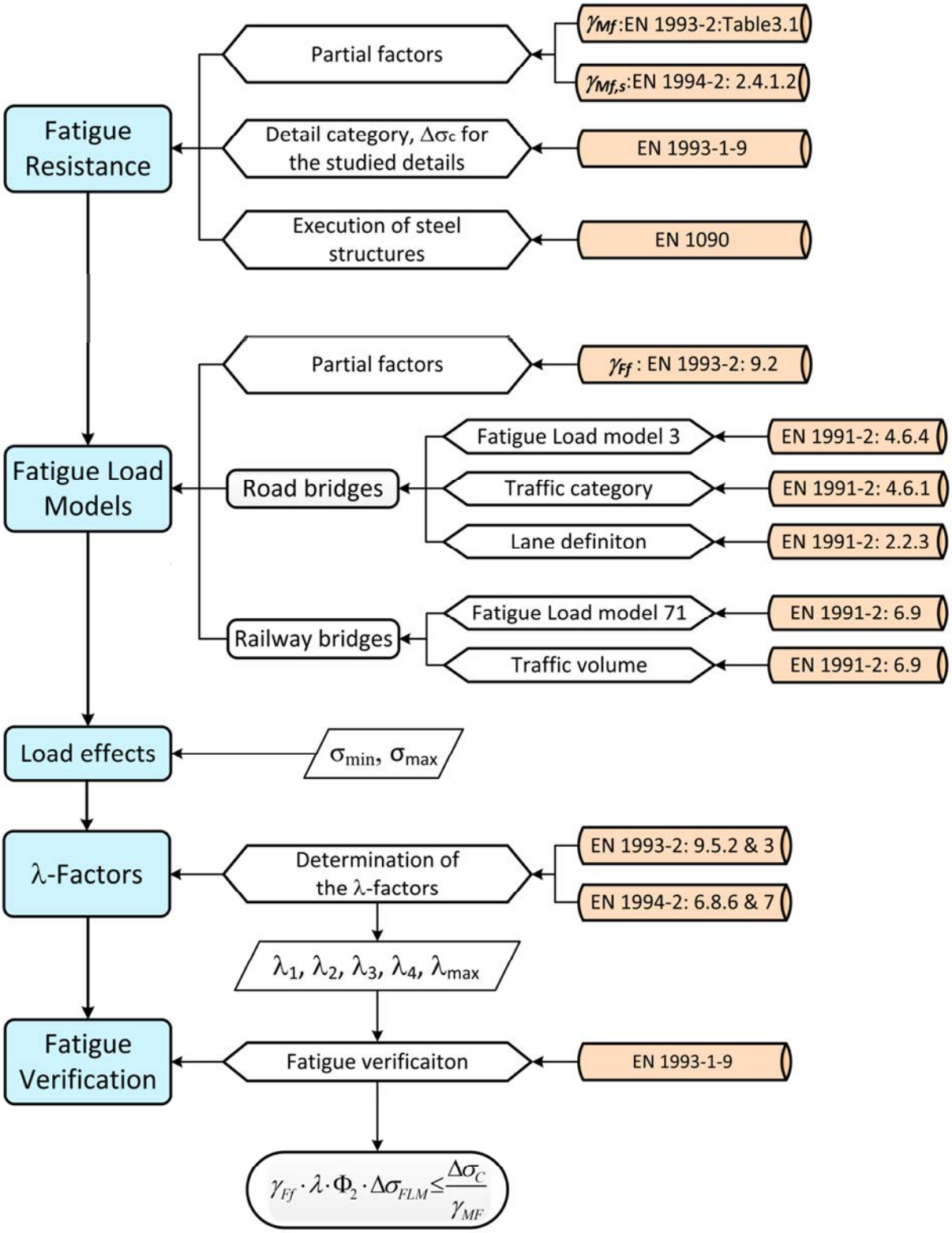

Figure 3.1 Overview of the application of the λ–coefficient method

3.2.1 Factor λ_1

The factor λ_1 takes into account the effect of span length in conjunction with the position of the loads at which the load response has maximum value, i.e. by using influence lines/areas. *EN 1993-2:2003* defines the mid-span and support section over bridge spans to be able to examine the critical influence lines/areas when determining the λ_1 factor. The code defined locations to be used for determining the critical length of the influence lines for moments and shear for a continuous span is shown in Figure 3-1. The definition for other locations for both moments and shear is also given in *Section 9.5 in EN 1993-2:2006*.

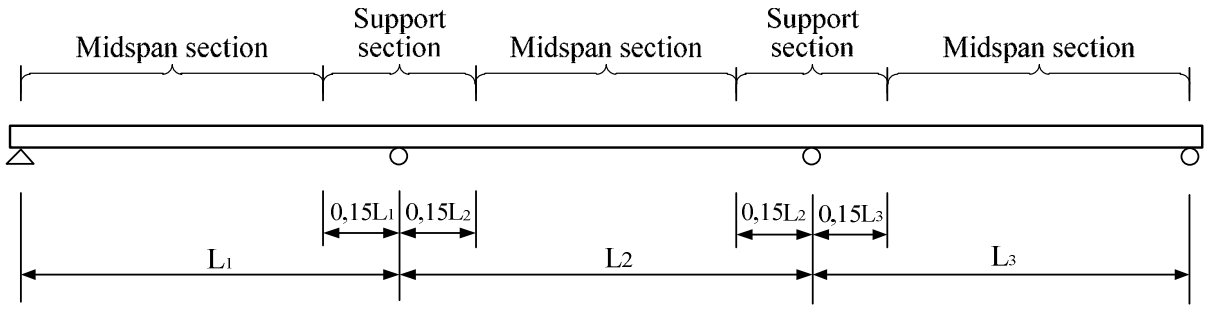

Figure 3-1 Location of mid-span or support section [9]

Figure 3-3 shows a simple example to illustrate the calculation of the critical influence length for different sections in a continuous bridge girder.

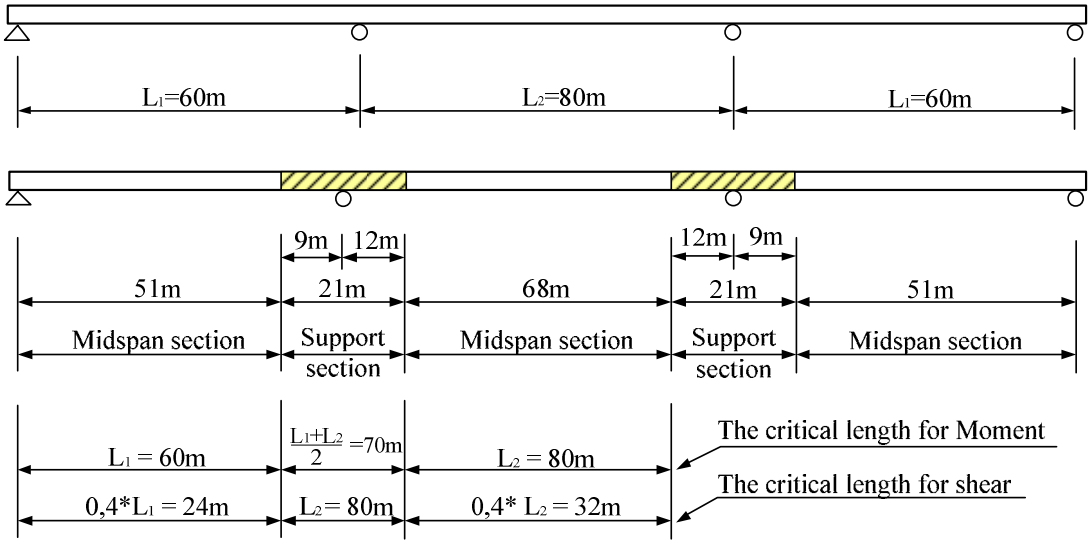

Figure 3-2 Critical lengths to be used for the determination of the factor λ_1

The recommended λ_1 values to be used in bridge design for road and railway bridges are given in the Eurocode. As stated earlier, the damage equivalent factor λ_1 for both road and railway bridges is depended on the span length. The factor λ_1 values recommended in the code are plotted in Figure 3-3 for both road and railway bridges. When determining the λ_1 factor for road bridges two different curves are used depending on the location of the detail under consideration (mid-span region or support region). For railway bridges the λ_1 factor depends on the traffic mix as defined in Table 9.3 and Table 9.4 of *EN 1993-2:2006*.

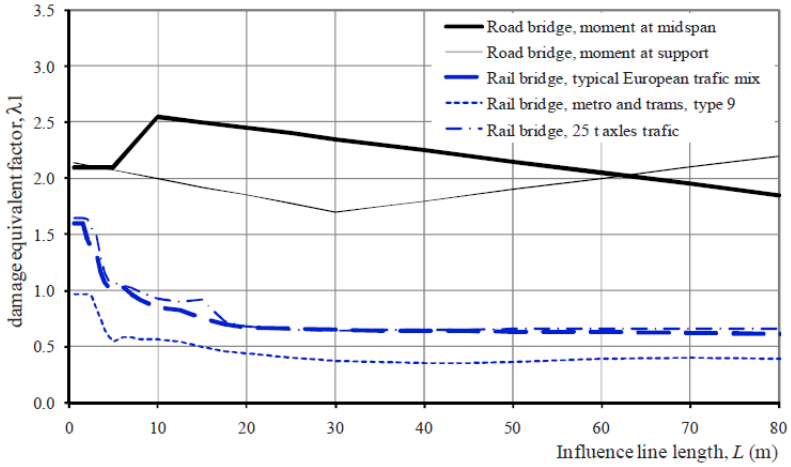

Figure 3-3 The factor λ_1 for road and railway bridges as a function of the critical influence line length [10]

It is worth remarking that *EN 1991-2:2003* states that "the National Annex may give the relevant values for the factor λ_1". *TRVK Bro 11:085* has therefore a different recommendation when determining the λ_1 factor for railway bridges; these are treated in Section 3.2.1.2

3.2.1.1 Factor λ_1 for road bridges

The λ_1 factor for road bridges is defined for the details subjected to stresses from FLM 3 and for the bridge span lengths from 10m to 80m. In case of road bridges with longer span it is accepted that a linear extrapolation can be performed to obtain the λ_1 value. This procedure may also be applied to road bridges with shorter span than 10m for the bending moments over the support. However, in case of moment at mid span the extrapolated λ_1 value (see Figure 3-3) may give conservative result.

The major factors when determining the λ_1 factor are the location of the studied detail to take into account the effect of the length of the influence line/area and the type of the load effect acting on this detail; bending moment or shear force. A summary of the rules in *EN 1993-2: 2006, 9.5.2* when determining the λ_1 factor for road bridges is given in Table 3-1.

Table 3-1 Damage equivalent factor λ_1 for road bridge details

Studied region	***Length of the span, [m]***	***λ_1 - factor***	***Remarks***
At mid-span side	$10 \le L \le 80$	$2{,}55 - 0{,}7 \cdot \frac{L-10}{70}$	--
At intermediate support	$10 \le L \le 30$	$2{,}0 - 0{,}3 \cdot \frac{L-10}{20}$	$L=L_1+L_2$
At intermediate support	$30 \le L \le 80$	$1{,}70 + 0{,}5 \cdot \frac{L-30}{50}$	$L=L_1+L_2$

3.2.1.2 Factor λ_1 for railway bridges

The λ_1 factor for railway bridges is defined for the details subjected to stresses from the fatigue load model 71, SW/0 or SW/2 and for bridge span lengths up to 100m.

In Eurocode *EN 1993-2.2006 (EN 1993-2:2006, 9.5.3 Table 9.3 and Table 9.4)*, the λ_1 factor values for different lengths are given. Some of these values have been modified by *TRVK Bro 11:085*. This modification is made for bridges with heavy traffic and span lengths shorter than 10 m. In these cases the λ_1 factors decrease linearly with increased span length. The recommended value at L=0 is 1,65 or 1,46 and at L=10m is 1,0. Both values given in *EN 1993-2:2006* and in *TRVK Bro 11:085* are graphically reproduced in Figure 3-4.

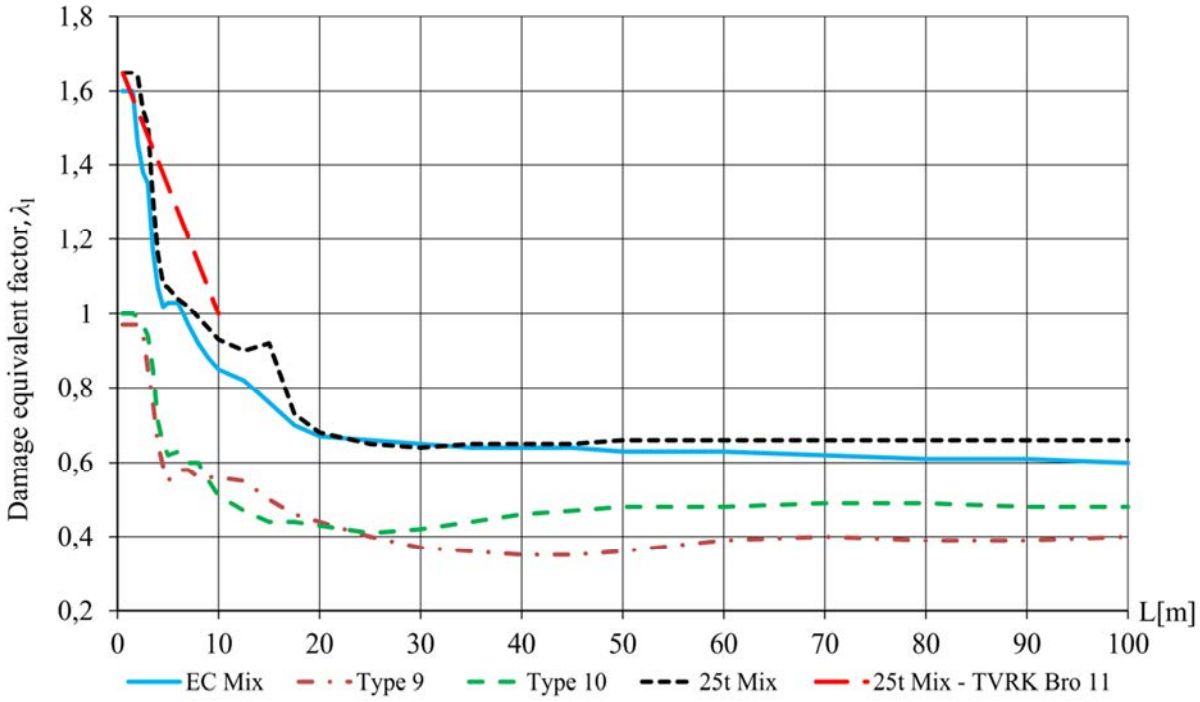

Figure 3-4 Damage equivalent factor λ_1 for railway bridges

3.2.2 Factor λ_2

The factor λ_2 is a coefficient that takes into account of the annual traffic flow and the traffic composition on the actual bridge. For road bridges, the value of λ_2 obtains through a calibration of the actual traffic to the reference traffic (the Auxerre traffic). In bridge design, the number of heavy vehicles per year and per slow lane for road bridges (N_{obs}) and the amount of freight transported per track and per year for railway bridges should be specified by a competent authority.

3.2.2.1 Factor λ_2 for road bridges

According to *EN 1993-2:2006*, the factor λ_2 considering the actual bridge traffic flow and composition should be calculated as following:

$$\lambda_2 = \frac{Q_{ml}}{Q_0} \cdot \left(\frac{N_{Obs}}{N_0} \right)^{1/m} \qquad \textit{Eq. 3-9}$$

where

Q_{ml} is the average gross weight (kN) of the lorries in the slow lane

Q_0 is the equivalent weight (kN) of the reference traffic

N_0 is the annual number of lorries for the reference traffic

N_{Obs} is the annual number of lorries in the slow lane

m is the slope of S-N curve; the largest m value in case of bilinear curve

The average gross weight of the lorries in the slow lane can be calculated by the following formula:

$$Q_{ml} = \left(\frac{\sum n_i \cdot Q_i^m}{\sum n_i} \right)^{1/m} \qquad \text{Eq. 3-10}$$

where

n_i is the number of lorries of gross weight Q_i in the slow lane

Q_i is the gross weight of the lorry "i" in the slow lane

m is the slope of S-N curve; the largest m value in case of bilinear curve

As stated earlier *EN 1993-2:2006* is using the Auxerre traffic as the reference traffic data and recommends therefore using $N_0=0.5\text{x}10^6$ and $Q_0=480$kN when calculating the λ_2 factor (for this specific case the factor λ_2 is equal to 1.0). Based on these two reference values, the factor λ_2 for any Q_{ml} and N_{Obs} can be obtained from Table 9.1 of *EN 1993-2:2006*, which is reproduced in Table 3-2 (m=5). *TRVK Bro 11:085* recommends using $Q_{m1}=410$kN for regional traffic and $Q_{m1}=445$kN for long distance traffic. The λ_2 factors for these recommended values are also added in Table 3-2 below.

Table 3-2 Recommended λ_2 factors for given values of Q_{ml} and N_{Obs}

Q_{ml}	N_{Obs}							
	$0{,}25x10^6$	$0{,}50x10^6$	$0{,}75x10^6$	$1{,}00x10^6$	$1{,}25x10^6$	$1{,}50x10^6$	$1{,}75x10^6$	$2{,}00x10^6$
200	0,362	0,417	0,452	0,479	0,500	0,519	0,535	0,550
300	0,544	0,625	0,678	0,712	0,751	0,779	0,803	0,825
400	0,725	0,833	0,904	0,957	1,001	1,038	1,071	1,100
410	0,744	0,854	0,926	0,981	1,026	1,064	1,097	1,127
445	0,807	0,927	1,005	1,065	1,114	1,155	1,191	1,223
500	0,907	1,042	1,130	1,197	1,251	1,298	1,338	1,374
600	1,088	1,250	1,356	1,436	1,501	1,557	1,606	1,649

3.2.2.2 Factor λ_2 for railway bridges

The factor λ_2 values for railway bridges recommended to be used are presented in Table 3-3 given in *EN 1993-2:2006, 9.5.3(6)*. Here, the amount of freight transported over the bridge per year is used as parameter.

Table 3-3 The λ_2 factors for the design life of road and railway bridges

Traffic per year [10^6 tonnes/track]	***5***	***10***	***15***	***20***	***25***	***30***	***35***	***40***	***50***
λ2	0,72	0,83	0,90	0,96	1,00	1,04	1,07	1,10	1,15

3.2.3 Factor λ_3

The λ_3 factor considers the design life of the bridge and according to *EN 1993-2:2006*, this factor used for both road and railway bridges should be calculated as following:

$$\lambda_3 = \left(\frac{t_{Ld}}{100}\right)^{1/m} \qquad \textit{Eq. 3-11}$$

The λ–coefficient method in Eurocode and the corresponding fatigue load models were derived based on a reference design life of 100 years. The λ_3 factors give the possibility of modifying the design life in years as given in Table 3-4 (m=5) in *EN 1993-2:2006, 9.5.2(3) and 9.5.3(6)* [11].

Table 3-4 the λ_3 factors for the design life of road and railway bridges

Design life in years	***50***	***60***	***70***	***80***	***90***	***100***	***120***
λ3	0,871	0,903	0,931	0,956	0,979	1,00	1,037

3.2.4 Factor λ_4

3.2.4.1 Factor λ_4 for road bridges

The factor λ_4 considers the vehicles interactions and accounts the multilane effect. In other words, the λ_4 factor takes into account of interactions between lorries simultaneously loading on several lanes defined in the design (multilane effect) and should be according to *EN 1993-2:2006* calculated using the following formula:

$$\lambda_4 = \sqrt[m]{\sum_{j=1}^{k} \frac{N_j}{N_1} \cdot \left(\frac{\eta_j \cdot Q_{mj}}{\eta_1 \cdot Q_1} \right)^m} \qquad \textit{Eq. 3-12}$$

$$\lambda_4 = \left[1 + \frac{N_2}{N_1} \cdot \left(\frac{\eta_2 \cdot Q_{m2}}{\eta_1 \cdot Q_{m1}} \right)^m + \frac{N_3}{N_1} \cdot \left(\frac{\eta_3 \cdot Q_{m2}}{\eta_1 \cdot Q_{m1}} \right)^m + ...+ \frac{N_k}{N_1} \cdot \left(\frac{\eta_k \cdot Q_{mk}}{\eta_1 \cdot Q_{m1}} \right)^m \right]^{1/m} \qquad \textit{Eq. 3-13}$$

where

k is the number of lanes with heavy traffic

N_j is the number of lorries per year in lane j

Q_{mj} is the average gross weight of the lorries in lane j

η_j is the influence line for the international force that produces the stress range

m is the slope of S-N curve; the largest m value in case of bilinear curve

This expression shows that the factor λ_4 is equal to 1,0 when considering a single bridge lane.

3.2.4.2 Factor λ_4 for railway bridges

For railway bridges with two tracks, the factor λ_4 taking into account the second track's effect on the first track should be calculated the following formula:

$$\lambda_4 = \left(n + (1-n) \cdot \left[a^5 + (1-a)^5 \right] \right)^{1/5} \qquad \textit{Eq. 3-14}$$

where

a $\Delta\sigma_1/\Delta\sigma_{1+2}$

$\Delta\sigma_1$ is the stress range at the section in interest produced by FLM 71 on the first track

$\Delta\sigma_{1+2}$ is the stress range at the same section produced by FLM 71 on both tracks

n is the percentage of traffic

As seen in this expression, the stress range obtained from the first track will be divided by the stress range which is obtained by adding the stress from both tracks. This means that the factor λ_4 will always be smaller than 1,0. This is the major difference between the factor λ_4 for railway bridges and the factor λ_4 for road bridges.

3.2.5 Factor λ_{max}

The final λ factor is obtained by multiplying the above mentioned individual λ–factors. An upper limit value has also to be considered defined. This is made through the factor λ_{max} which mainly takes into account the fatigue limit of the detail under consideration. The limitation of the damage equivalent factor value for railway bridges is based on the load model which gives an upper bound value while this factor for road bridges is on the same basis as the simulations for the λ_1 factor.

3.2.5.1 Factor λ_{max} for road bridges

The λ_{max} factor for road bridges for the span lengths from 10m to 80m is defined only for the sections subjected to the fatigue stresses caused by bending moment. This is clear as the S-N curves for shear effects do not have a defined constant amplitude fatigue limit. However, when using the λ-equivalence concept FLM 3 does not generate an upper limit value to establish a suitable λ_{max} value. The limiting λ value is therefore established by simulating the road traffic. Similar to the λ_1 factor given in *EN 1993-2:2006*, the maximum λ values are depended on the length of the bridge span and also the location of the detail under consideration. *EN 1993-2:2006* presents therefore two graphs to determine the λ_{max} factor which are shown in Figure 3-5.

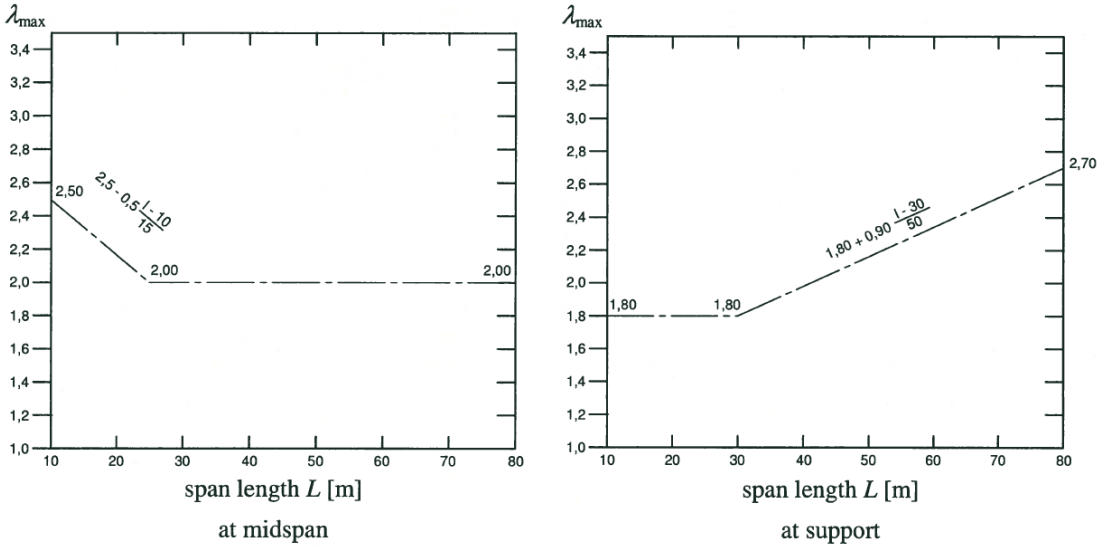

Figure 3-5 λ_{max} factor for road bridge sections subjected to bending stresses

3.2.5.2 Factor λ_{max} for railway bridges

According to *EN 1993-2:2006* the value of λ should not exceed the factor λ_{max}, which is specified as 1.4 for railway bridges with span up to 100m. The determination of the factor λ_{max} is based on the stress range spectrum produced by the fatigue load model which was obtained from the Auxerre traffic data, see Figure 3-6 [3]. The data used for determining this factor was the flowing traffic since congested traffic gave higher maximum stress range which in turn resulted in higher the factor λ_{max}. The fatigue load model used for railway bridges generates an upper limit value in term of the maximum stress range which is bound by the constant amplitude fatigue loading (CAFL), $\Delta\sigma_D$ as shown in Figure 3-6.

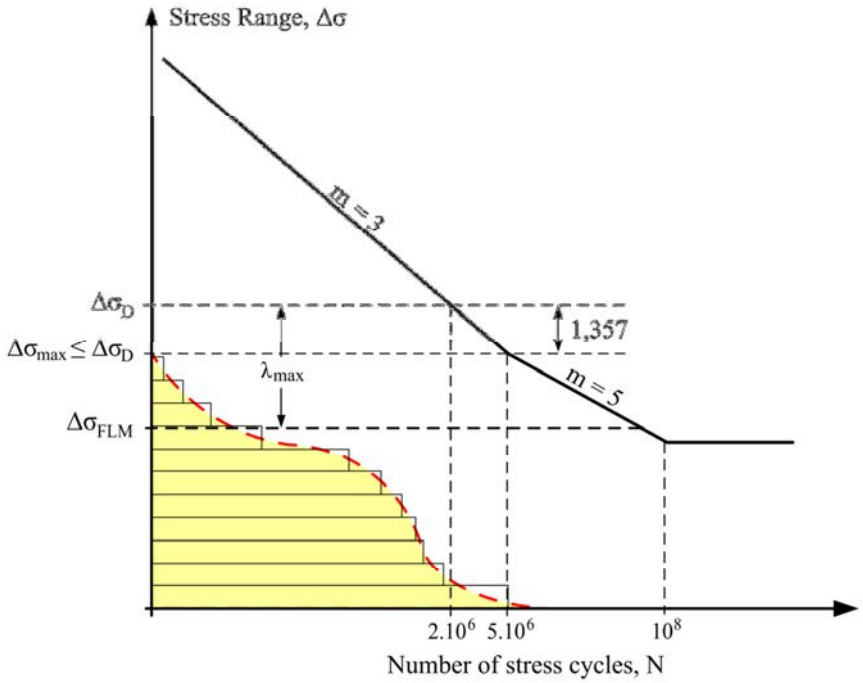

Figure 3-6 Determination of the factor λ_{max} [3]

According to the definition of the fatigue damage equivalent concept, the equivalent fatigue stress range generated by the fatigue load model should be equal to or less than the fatigue strength of the detail category related to 2.10^6 stress cycles. This is basis of the limitation of the λ factor which can be determined using *Eq. 3-15* and *Eq. 3-16* as following;

$$\lambda_{\max} \cdot \Delta\sigma_{FLM} \le \Delta\sigma_C \qquad \textit{Eq. 3-15}$$

$$\lambda_{\max} = \left(\frac{\Delta\sigma_C}{\Delta\sigma_D}\right) \cdot \frac{\Delta\sigma_{\max}}{\Delta\sigma_{FLM}} \qquad \textit{Eq. 3-16}$$

where $\left(\frac{\Delta\sigma_C}{\Delta\sigma_D}\right) = \left(\frac{5}{2}\right)^{1/3}$

$$\lambda_{\max} = 1{,}357 \cdot \frac{\Delta\sigma_{\max}}{\Delta\sigma_{FLM}} \qquad \textit{Eq. 3-17}$$

3.3 Fatigue design with the Damage Accumulation Method

Load effects generated by traffic loads on bridges are generally very complex. Not only are the stress ranges generated by these loads of variable amplitudes, but also other parameters that might affect the fatigue performance of bridge details such as the mean stress values and the sequence of loading cycles are rather stochastic.

In order to treat such complex loading situations there is a need to represent the fatigue load effects caused by the "actual" variable amplitude loading in term of equivalent **constant amplitude loading**. In other words, a complex loading situation such as the one shown in Figure 3-8 should be represented as one or more equivalent constant amplitude loads, so that the latter will cause equivalent **fatigue damage** as the real loading history. Two steps are needed:

Transformation of the variable amplitude loading into a representative constant amplitude loading, this is usually done by some kind of **cyclic counting** method.

Using the new set of representative constant amplitude loading to perform the fatigue design or analysis, this is done either:

- directly, by applying the **Palmgren-Miner damage accumulation rule,** or
- by using the **equivalent stress range concept**

The rules concerned with the fatigue design of bridges in Eurocode allow for the application of any of these two methods. The simplified λ-method in Eurocode is an adaption of the general equivalent stress range concept corrected by various λ-factors, while a direct application of the Palmgren-Miner rule can alternatively be used for both railway and road bridges.

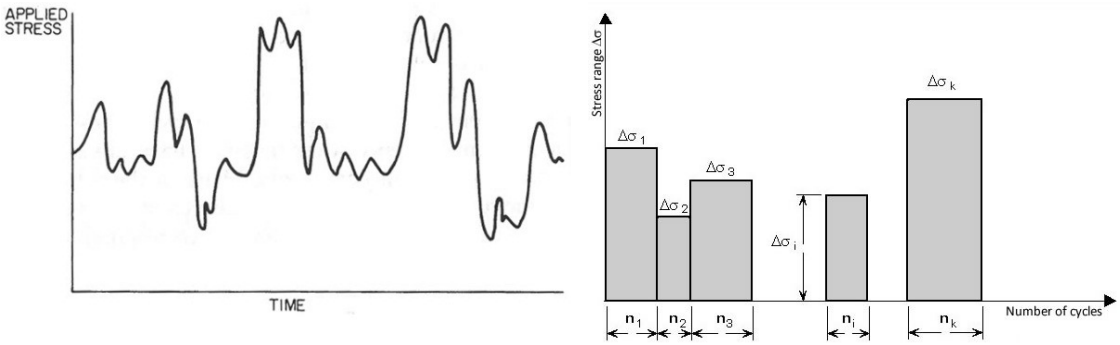

Figure 3-7 An example of variable amplitude loading and stress histogram resulting from the application of cyclic counting method.

The most common cycle counting methods are the "**rain flow**" and the "**reservoir**" stress counting methods. In general, these two methods do not lead to exactly the same result. However, in terms of fatigue damage both counting procedures give very close results, especially for "long" stress histories.

A detailed description of the principle of these counting methods is beyond the scope of this document. The principles of the Palmgren-Miner damage rule and the concept of equivalent stress range are however introduced below.

3.4 Palmgren-Miner damage accumulation

As known, an S-N curve represents the relation between the stress range $\Delta\sigma$ (or $\Delta\tau$) in a specific detail and the total number of cycles to failure, N. In other words, a specific detail with a certain fatigue strength (represented by an S-N curve) will fail after N cycles of a stress range $\Delta\sigma$. At failure, the fatigue life is consumed and the total fatigue damage in the detail would then be 100%, or $D = 1,0$. If the same detail is now loaded with a number of stress cycles $n < N$ at the same stress range, the fatigue damage accumulated in the detail would then be:

$$D = \frac{n}{N} \qquad \textit{Eq. 3-18}$$

giving:

$$D = 1,0 \quad when \quad n = N$$

$$D < 1,0 \quad when \quad n < N$$

With this in mind, if the detail is subjected to a number i of loading blocks each with a constant amplitude stresses $\Delta\sigma_i$ which is repeated n_i number of times, then the total fatigue damage accumulated in the detail would be the sum of the damage caused by the individual loading blocks:

$$D = \sum_i D_i = \sum_i \frac{n_i}{N_i} \qquad \textit{Eq. 3-19}$$

The following example demonstrates the principles of damage accumulation: A structural detail with a detail category 36 is subjected to a stress spectrum with two stress blocks; each with a stress range $\Delta\sigma_i$ and a corresponding number of cycles n_i. To check the fatigue life of the detail, the damage accumulated through each stress block should be calculated. The number of cycles which would cause failure at each stress range $\Delta\sigma_i$ can be directly calculated from *Eq. 3-20*:

$$N_i = 5.10^6 \left(\frac{\Delta\sigma_D / \gamma_{Mf}}{\lambda_{Ff} \cdot \Delta\sigma_i} \right)^m \qquad \textit{Eq. 3-20}$$

where m is taken as 3 or 5 depending on the level of stress. The results are shown in the table below, with γ_{Ff} and γ_{Mf} taken as 1,0.

Table 3-5 Calculation of damage accumulation

$\Delta\sigma_i$ [MPa]	n_i	N_i	$D_i = \frac{n_i}{N_i}$
53,3	350 000	616 595	0,57
43,3	430 000	1 150 054	0,37
	780 000		0,94

3.5 The application of Equivalent Stress Range

As stated earlier, the fatigue damage caused by a number of loading blocks with constant amplitude loading can be represented by an ***equivalent stress range*** **which is defined as** constant amplitude stress range which if applied with the same total number of loading cycles of the variable stress range would cause the same total damage as the variable amplitude loading block.

If one, for simplicity, assumes an S-N curve with a constant slope of 3, an expression for the equivalent stress range can be derived as follows for any load spectrum:

The damage caused by each loading block in the loading spectrum is

$$D_i = \frac{n_i}{N_i} \qquad \textit{Eq. 3-21}$$

and the total damage is:

$$D = \sum_i D_i \qquad \textit{Eq. 3-22}$$

For a design curve with a constant slope m=3 the total number of cycles to cause failure N_i at a specific stress range $\Delta\sigma_i$ can be expressed as (partial factors are omitted for clarity):

$$N_i = 5 \cdot 10^6 \cdot \left(\frac{\Delta\sigma_D / \gamma_{Mf}}{\gamma_{Ff} \cdot \Delta\sigma_i} \right)^3 \qquad \textit{Eq. 3-23}$$

Eq. 3-23 can also be writes as ($\Delta\sigma_C$ is the stress at 2 million stress cycles):

$$N_i = 2 \cdot 10^6 \cdot \left(\frac{\Delta\sigma_C / \gamma_{Mf}}{\gamma_{Ff} \cdot \Delta\sigma_i} \right)^3 \qquad \textit{Eq. 3-24}$$

Thus,

$$D = \frac{\sum_{i=1}^{n} n_i \cdot \Delta\sigma_i^3}{5 \cdot 10^6 \cdot \Delta\sigma_D^3} \qquad \textit{Eq. 3-25}$$

Per definition, the equivalent stress range $\Delta\sigma_E$ will cause the same damage D after the same total number of cycles, i.e.

$$D_E = \frac{\sum_{i=1}^{n} n_i}{N} = \frac{\Delta\sigma_E^3}{5 \cdot 10^6 \cdot \Delta\sigma_D^3} \cdot \sum_{i=1}^{n} n_i \qquad \textit{Eq. 3-26}$$

Therefore:

$$\Delta\sigma_E = \left[\frac{\sum_{i=1}^{n} n_i \cdot \Delta\sigma_i^3}{\sum_{i=1}^{n} n_i} \right]^{\frac{1}{3}} \qquad \textit{Eq. 3-27}$$

Referring back to the simple example in the previous page, a direct application of the expression above will yield an equivalent stress,

$$\Delta\sigma_{eq} = 48{,}3 \text{ MPa}$$

which will give a total number to failure:

$$N = 5.10^6 \left(\frac{26{,}53/1}{1 \cdot 48{,}3} \right)^3 = 828591$$

i.e. the almost same total number of loading cycles in the stress histogram.

In a more general case, a histogram is composed of several stress blocks with different stress ranges. When calculating the total fatigue damage, *D*, consideration should be given to where – in relation to the S-N curve – each stress block is positioned. Of course, all stress ranges below the cut-off limit are assumed not to contribute to the fatigue damage and can thus be neglected. In addition, with a tri-linear S-N curve, the slope of the S-N curve should also be considered. Thus, the total damage in this general case – again omitting the partial factors – is:

$$D = \sum_{\Delta\sigma_i > \Delta\sigma_D} \frac{n_i \Delta\sigma_i^3}{2\times10^6 \times \Delta\sigma_D^3} + \sum_{\Delta\sigma_D > \Delta\sigma_i > \Delta\sigma_L} \frac{n_i \Delta\sigma_i^5}{5\times10^6 \times \Delta\sigma_D^5} \qquad \textit{Eq.} \text{ 3-28}$$

which can also be expressed in term of equivalent stress:

$$\Delta\sigma_E = \left(\frac{\sum n_i \Delta\sigma_i{}^{m_i} + \sum n_j \Delta\sigma_j{}^{m_i} \left(\Delta\sigma_j / \Delta\sigma_D\right)^{m_j - m_i}}{\sum n_i + \sum n_j} \right)^{1/m_i} \qquad \textit{Eq. 3-29}$$

here,

i	is the index of stress ranges with a magnitude higher than $\Delta\sigma_D$ and their corresponding stress cycles,
j	is the index of stress ranges with a magnitude lower than $\Delta\sigma_D$ and their corresponding stress cycles.
m_i	is the slope of the tri-linear S-N relation above the knee-point $\Delta\sigma_D$, $m_i = 3$ for structural steel details.
m_j	is the slope of the tri-linear S-N relation below the knee-point $\Delta\sigma_D$, $m_j = 5$ for structural steel details.

Calculation of the total fatigue damage for any stress histogram is illustrated in Figure 3-8.

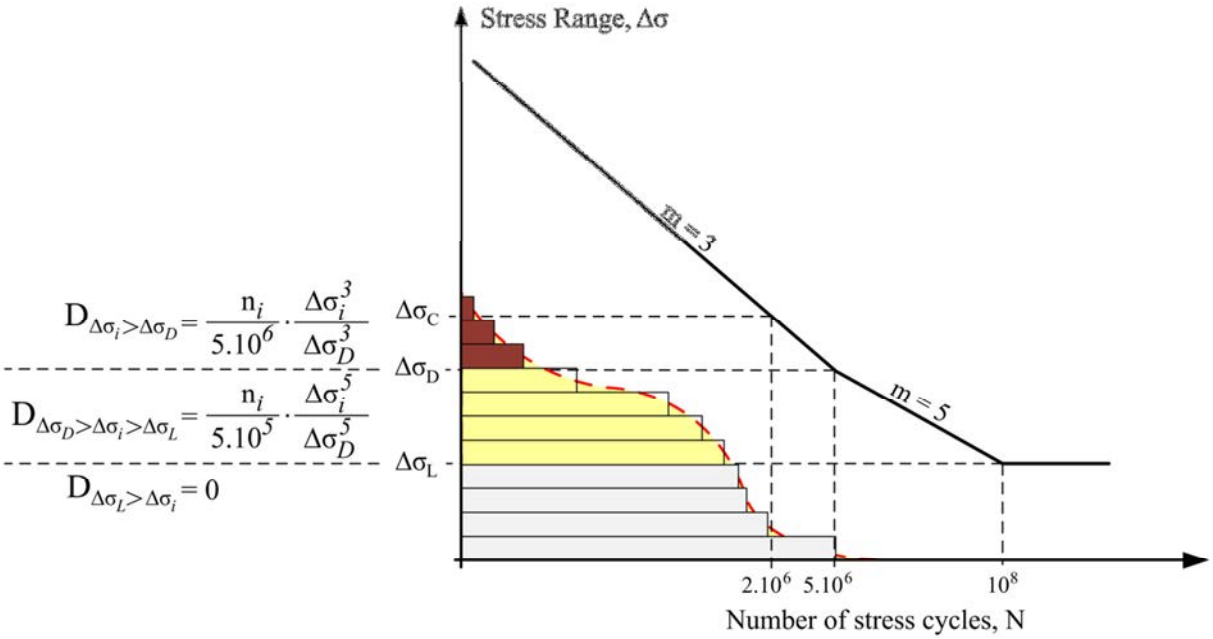

Figure 3-8 Fatigue damage calculation with a given stress histogram

The equivalent stress range $\Delta\sigma_E$ depends only on the fatigue load spectrum and the slope constant m. In other words, knowing $\Delta\sigma_E$ makes it easy to choose directly a detail category which will have an adequate fatigue resistance.

In Eurocode, fatigue verification based on the simplified λ-method adopts an equivalent stress concept, where the stresses obtained from relevant load models in *EN 1991-2:2003* are modified with various λ-factors in order to be expressed as an equivalent stress range at 2 million cycles, $\Delta\sigma_{E,2}$. This transformation from $\Delta\sigma_E$ to $\Delta\sigma_{E,2}$ can be easily obtained from:

$$\frac{\Delta\sigma_{E2}^m}{2\cdot 10^6} = \frac{\Delta\sigma_E{}^m}{N} \qquad \textit{Eq. 3-30}$$

giving

$$\Delta\sigma_{E,2} = \Delta\sigma_E \left(\frac{N}{2\cdot 10^6}\right)^{1/m} \qquad \textit{Eq. 3-31}$$

Doing so, the fatigue verification is reduced to a direct comparison between the equivalent stress range at 2 million cycles and the fatigue class (or fatigue strength) of the detail, i.e.

$$\Delta\sigma_{E,2} \le \Delta\sigma_C \qquad \textit{Eq. 3-32}$$

Also here with all partial factors are being omitted for simplicity.

It should be noted, of course, that fatigue verification formats both with the Palmgren-Miner summation and the equivalent stress range concept are equivalent in terms of damage and will yield effectively the same results.

Comment:

- *As the fatigue damage factor, D, and the equivalent stress, $\Delta\sigma_E$ or $\Delta\sigma_{E,2}$ are obtained using the relevant influence lines for load effects and representative load models, there is no need for any corrections factors, such as those used in the simplified λ-method.*

3.6 The application of the damage accumulation method

Annex A in *EN 1993-1-9:2005* gives information on the application of the damage accumulation method in the fatigue design of steel structures. What concerns bridges the use of damage accumulation method is suggested in two cases:

1. When actual traffic data is available. This is covered in Annex B of *EN 1991-2:2003* and will not be treated in this document

2. Along with the traffic load models derived for this purpose. These are LM4 for road bridges (*EN 1991-2:2003, 4.6.5*) and train types 1 to 12 in Annex D of *EN 1991-2:2003* of Eurocode

For both road and railway bridges, the traffic load models to be used with the damage accumulation method are intended to reflect the real "heavy" traffic on European road and railway networks. The variation in traffic intensity and vehicle (or train) types on individual bridges is covered by defining different "traffic types" or "traffic mixes" for road and railway traffic respectively. These are also a subject for adaption and modification by the countries through their national annexes.

In the following, the traffic load models proposed in *EN 1991-2:2005* for fatigue verification with the cumulative damage concept will be shortly introduced. A summary of the main steps involved in the application of this method is then made. The method is also demonstrated in two worked examples, one for road bridge and one railway bridge.

3.7 Application to road bridges

The traffic load model to be used with fatigue verification of road bridges according to the damage accumulation method is load model LM4. This model is composed of 5 standard lorries which are assumed to simulate the effects of real road traffic on the bridge. The definition of each lorry is given by the number of axles, the load on each axle as well as the axle spacing which are reproduced in Table 3-6 and Table 3-7. The number of heavy vehicles, N_{obs} per year and per slow lane (observed or estimated) applies also for fatigue verification with the damage accumulation method. Indicative figures for N_{obs} and the recommended values for different traffic categories are given in *EN 1991-2:2003 4.6.1(3)*.

Table 3-6 Set of equivalent lorries for fatigue load model 4

	Lorry			*Traffic Type and its percentage of Nobs*			
		Axle spacing (m)	*Equivalent axle loads (kN)*	*Long distance*	*Medium distance*	*Local traffic*	*Wheel type*
1	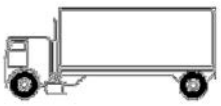	4,50	70 130	20	40	80	A B
2		4,50 1,30	70 120 120	5	10	5	A B B
3	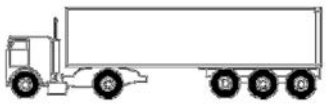	3,20 5,20 1,30 1,30	70 150 90 90 90	50	30	5	A B C C C
4		3,40 6,00 1,80	70 140 90 90	15	15	5	A B B B
5		4,80 3,60 4,40 1,30	70 130 90 80 80	10	5	5	A B C C C

Table 3-7 Set of equivalent lorries for fatigue load model 4

Wheel/axle type	***Geometrical properties***
A	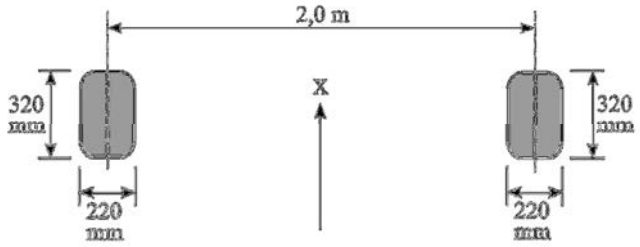
B	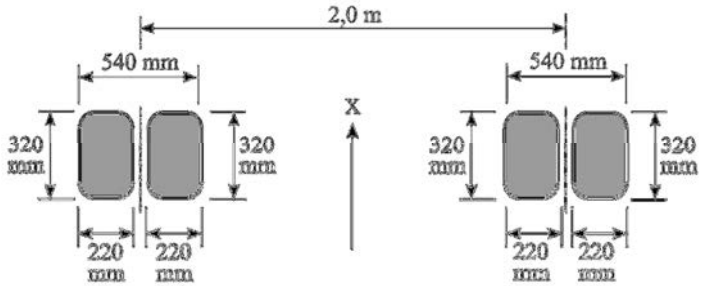
C	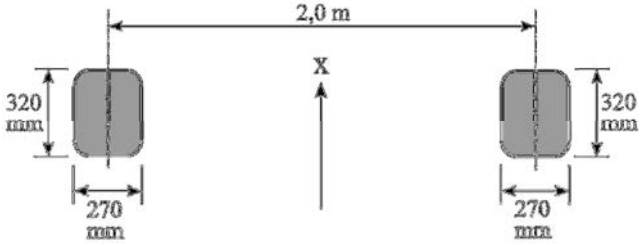

For Swedish roadways, these values are substituted in *TRVK Bro 11:085* by the values given in B.3.2.1.3 (h), which is reproduced in Table 3-8. The traffic parameter N_{obs} for the traffic categories (the number maximum gross vehicle weight more than 100kN per year per slow lane) in this recommendation is replaced with annual average daily traffic, AADT which is a mean value of the daily heavy traffic volume for a roadway. The traffic type is assumed to be "regional distance". Observe that the recommended values in this table are given for road bridges with simple lane. In case of more than one traffic direction, the values in Table 3-8 should be reduced by a factor of 0,9 due to the traffic distribution on other lanes.

TRVK Bro 11:085 recommends a certain investigation of the prerequisites for the fatigue design should be performed for AADT bigger than 24000 (Category X in the table below).

Table 3-8 Traffic category according to TRVK Bro 11

Traffic category	***AADT heavy traffic (ÅDT)***
X	24 000 < AADT
1	6 000 < AADT ≤ 24 000
2	1 500 < AADT ≤ 6 000

3	600 < AADT ≤ 1 500
4	AADT ≤ 600

The fatigue verification procedure should be performed – for those details that are determinant for the fatigue performance of the bridge – according to the following steps:

1. Establish the bridge specific data for fatigue verification. Besides the design life of the bridge this includes:
    a. the "traffic category" with the associated number of heavy lorries in the slow lane, N_{obs} *[EN 1991-2:2003, 4.6.1(3)1]*,
    b. the "traffic type" with the associated percentage of lorries, Table 4.7 in *EN 1991-2:2003*.
2. For the detail in hand, obtain the influence line for relevant load effects (shear or bending stresses).
3. By passing the load model over the influence line, establish the time history response (i.e. stress vs. time, or time step)
4. Construct the stress histogram by mean of a cycle-counting method. For simple cases, such as for simply-supported road bridges, the stress histogram can be easily obtained with hand calculations, see example 4.1 in Section 4.
5. Select an appropriate fatigue category and establish the corresponding S-N curve ($\Delta\sigma_C$ at $2\cdot10^6$ cycles, $\Delta\sigma_D$ at $5\cdot10^6$ cycles and $\Delta\sigma_L$ at $100\cdot10^6$ cycles)
6. Use the stress histogram either to:
    a. Calculate a total damage

$$D_i = \frac{n_i}{5\cdot10^6}\cdot\left(\frac{\gamma_{Ff}\cdot\gamma_{Mf}\cdot\Delta\sigma_i}{\Delta\sigma_D}\right)^3 \quad \text{if} \quad \gamma_{Ff}\Delta\sigma_i \geq \frac{\Delta\sigma_D}{\gamma_{Mf}} \qquad \text{Eq. 3-33}$$

$$D_i = \frac{n_i}{5\cdot10^6}\cdot\left(\frac{\gamma_{Ff}\cdot\gamma_{Mf}\cdot\Delta\sigma_i}{\Delta\sigma_D}\right)^5 \quad \text{if} \quad \frac{\Delta\sigma_L}{\gamma_{Mf}} \leq \gamma_{Ff}\Delta\sigma_i < \frac{\Delta\sigma_D}{\gamma_{Mf}} \qquad \text{Eq. 3-34}$$

    and verify that

$$D = \sum_i D_i \leq 1{,}0 \qquad \textit{Eq. 3-35}$$

    b. Calculate the equivalent stress at $2\cdot10^6$ cycles

$$\Delta\sigma_E = \left(\frac{\sum n_i \left(\gamma_{Ff} \Delta\sigma_i\right)^3 + \sum n_j \left(\gamma_{Ff} \Delta\sigma_j\right)^3 \left(\frac{\gamma_{Ff}\gamma_{Mf}\Delta\sigma_j}{\Delta\sigma_D} \right)^2}{\sum n_i + \sum n_j} \right)^{1/3} \qquad \textit{Eq. 3-36}$$

$$\Delta\sigma_{E,2} = \Delta\sigma_E \left(\frac{N}{2 \cdot 10^6} \right)^{1/3} \qquad \textit{Eq. 3-37}$$

and verify that:

$$\frac{\Delta\sigma_{E,2} \cdot \gamma_{Ff} \cdot \gamma_{Mf}}{\Delta\sigma_C} \leq 1{,}0 \qquad \textit{Eq. 3-38}$$

The procedure is illustrated in Figure 3-10 below.

Notes to the application of the cumulative damage method

- *Even though it is not explicitly mentioned in EN 1993-1-9:2005, it follows from the definition of the CAFL, that if all stress ranges in a stress histogram (variable amplitude loading) are below the CAFL, no fatigue damage should be expected to take place; i.e. the fatigue life will be infinite!*

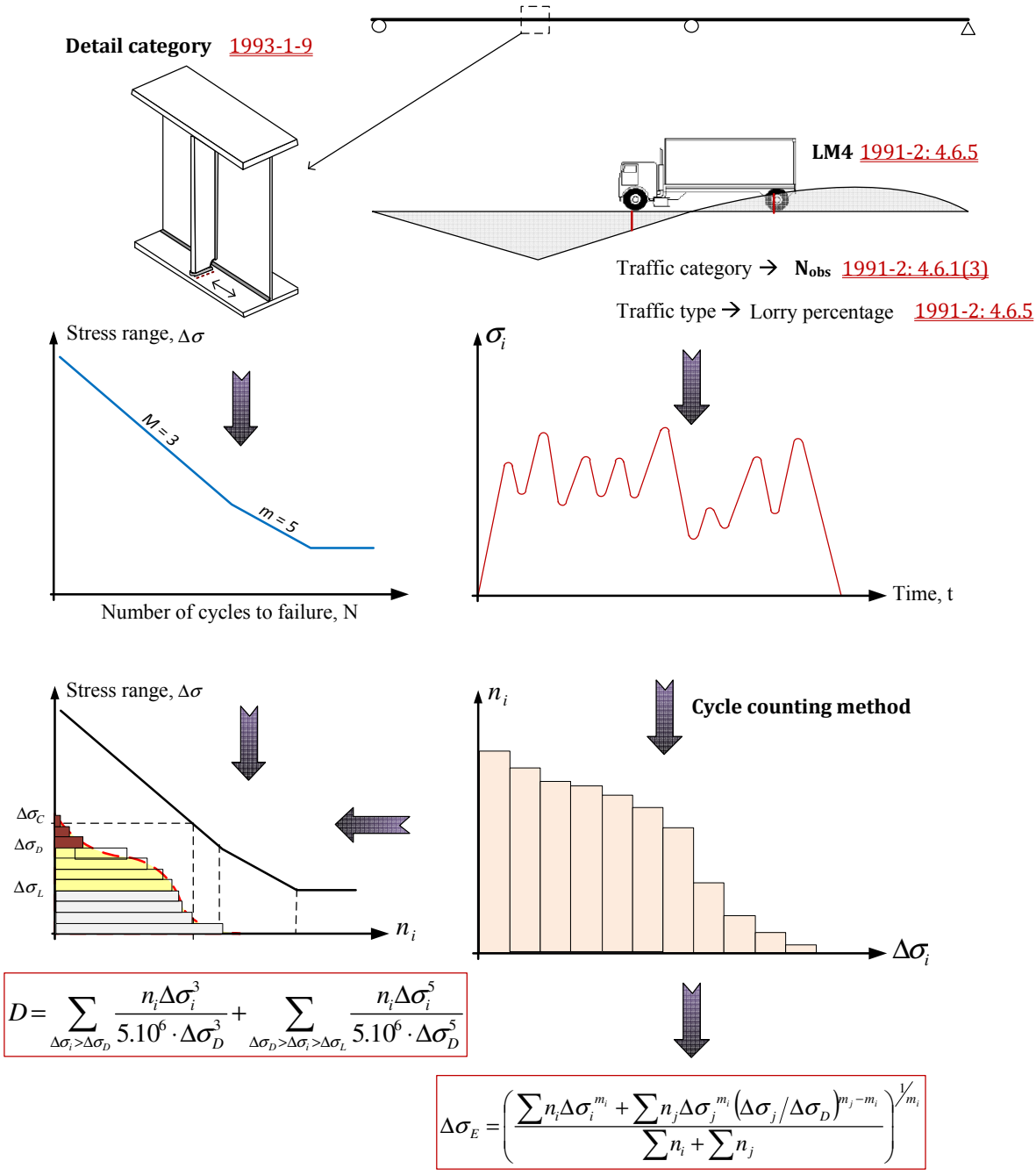

Figure 3-10 The application steps of cumulative damage method

3.8 Application for railway bridges

The verification of the fatigue performance of railway bridges follows the same procedure described above for road bridges. Two main differences can be identified; both are related to the traffic load:

1. A total tonnage per track and year is used instead of the total number of trains per track and year. An indicative value of 25 tonnes per year and per track is suggested in *EN 1991-2:2003, 6.9(4)*.

2. Three different "traffic mixes" are provided to reflect the real traffic type on the bridge. These are composed of sets of trains selected from totally 12 train models which are provided in Annex D of *EN 1991-2:2003*.

Paragraphs (3) and (7) in *EN 1991-2:2003, 6.9* allows for different traffic mixes other than those given in Annex D to be defined to better represent the rail traffic on individual projects. In *TRVK Bro 11:085, B.3.2.1.4 (v)* two different train models are specified for fatigue verification of railway bridges with the damage accumulation method. This is achieved on the basis of the value of the multiplier α which is defined in *EN 1991-2:2003, 6.3.2(3)*.

1. ***Bridges that are designed with α = 1,33***. The following traffic mix as shown in Table 3-9 should be used:

Table 3-9 Traffic mix with axial load ≤ 25tonnes according to TRVK Bro 11:085

Train type	***No. of trains per day***	***Total mass*** *[ton]*	***Traffic volume*** *[ton/year]*
1	12	663	$2{,}90 \cdot 10^6$
2	12	530	$2{,}32 \cdot 10^6$
3	5	940	$1{,}72 \cdot 10^6$
4	5	510	$0{,}93 \cdot 10^6$
5	7	2160	$5{,}52 \cdot 10^6$
6	12	1431	$6{,}27 \cdot 10^6$
11	7	1135	$2{,}91 \cdot 10^6$
12	6	1135	$2{,}49 \cdot 10^6$
	66		**$25{,}06 \cdot 10^6$**

2. ***Bridges that are designed with α = 1,60***

For this case, train load model 13S should be used, see Figure 3-9. This model is composed of 68 wagons per train, each with a mass of 140 tonnes. The number of trains per day is set to 10 in *TRVK Bro 11:085 B.3.4.1.4 (v)* and the total traffic volume per year is $34{,}70 \cdot 10^6$ tonnes. The train is assumed to cross the bridge with a maximum velocity of 60 km/h.

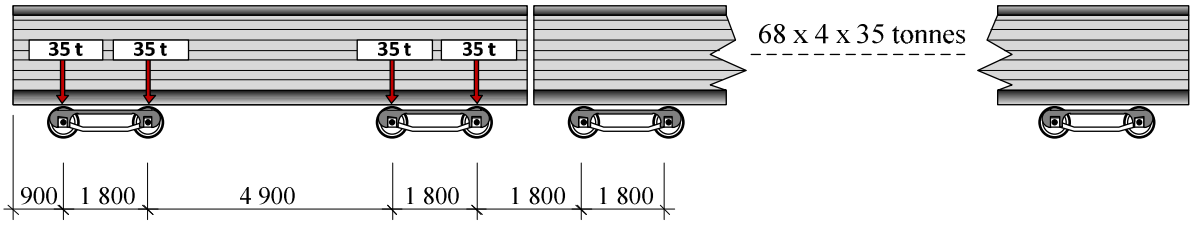

Figure 3-9 Train load model 13S and axle loads according to TRVK Bro 11:085

Fatigue verification of railway bridges with the damage accumulation method follows the same procedure described in the previous section for road bridges. The application of the traffic mix associated with $\boldsymbol{\alpha = 1{,}33}$ is a bit lengthy and might need to be implemented in a computer program. For load model 13S, it is still feasible to perform the calculations in a rather simple way (the axel distances and the axle weights are constant throughout the entire train.

4 Worked examples

4.1 Fatigue design of a road Bridge

A verification of the fatigue life of a road bridge is treated in this example. The verification is made with reference to three different structural details for the sake of demonstration. Both the simplified λ-method and the damage accumulation method are demonstrated. An elevation of the bridge is shown in Figure 4-1 and Figure 4-2 shows the cross-section of the composite bridge.

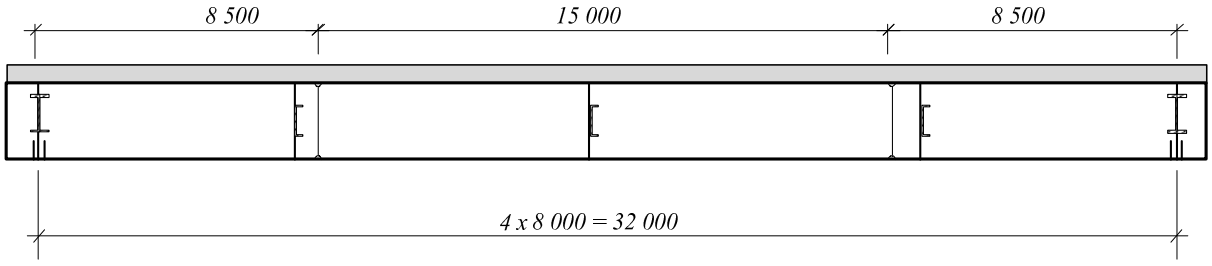

Figure 4-1 Elevation of the road bridge [mm]

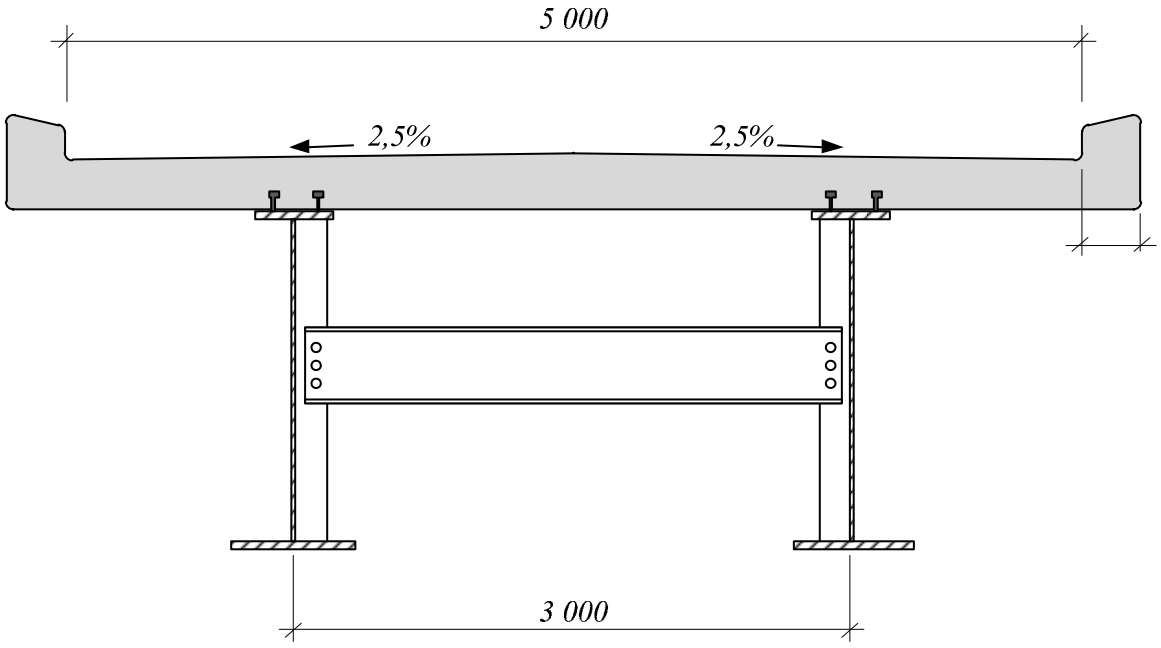

Figure 4-2 Cross-section of the road bridge [mm]

4.1.1 General description

The road bridge in this worked example is a composite steel-concrete bridge with a single span of 32,0 m. The bridge is assumed to be straight in the horizontal plan, with a constant total depth along the entire span. The two steel girders are joined by diaphragms at each L/4. The intermediate diaphragms are made of channel profiles, while the end cross-beams are made with I-sections.

4.1.2 Concrete deck

The concrete deck is 5,0 m wide, excluding the concrete edge beams. The average depth of the concrete deck is assumed to be 270 mm. Composite action between the concrete deck and the steel girders is achieved by means of two rows of shear studs welded to the top flange of each girder. The deck is made with normal concrete of class C35/45, thus:

f_{ck} = 35 MPa (Characteristic compressive strength)

f_{ctm} = 3,2 MPa (Mean value of axial tensile strength)

E_{cm} = 34 GPa (Secant modulus of elasticity)

4.1.2.1 Steel girders

The twin steel girders are identical. Each girder is made of three segments (9,0 m + 15 m + 9,0 m) which are assembled on site by welding. At the locations of the two field splices a change in the dimensions of the steel beam cross-section is also made in order to optimize the use of steel in the intermediate 15 m long segments of the beams.

Butt welds are used to connect the upper flange to the web as well as between the vertical stiffeners and the upper flanges. 5 mm fillet welds are used for the connections at the bottom side of the girders, see Figure 4-3. The welded shear studs are made of ϕ22mm.

Steel grade S355 is used throughout the entire bridge.

The dimensions of the steel cross-sections for all three segments are given in Table 4-1.

Table 4-1 Dimensions of the steel girders in different regions of the bridge

Segment	b_{ft} *[mm]*	t_{ft} *[mm]*	b_{fb} *[mm]*	t_{fb} *[mm]*	h_w *[mm]*	t_w *[mm]*	***H*** *[mm]*
1 & 3	500	20	700	25	1315	13	1360
2	500	25	700	30	1305	13	1360

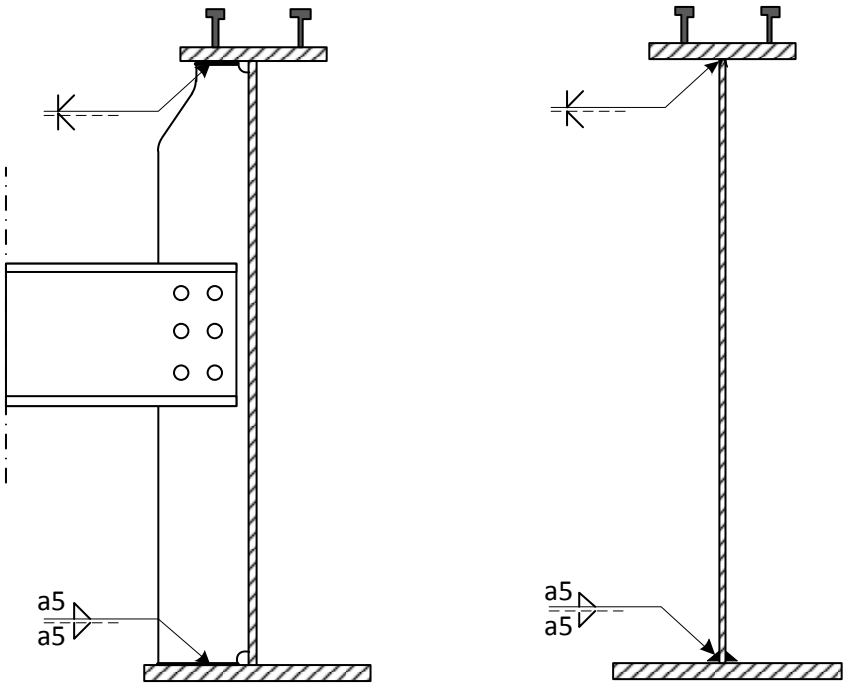

Figure 4-3 Details of the welds in the steel girders

4.1.2.2 Bridge specific traffic data

The following bridge specific data has been provided by the road authorities:

- Design life = 80 years
- The safe life assessment method should be used for bridges *[TRVFS 2011:12]* with high consequence of failure.
- Partial factors for fatigue:

  γ_{Ff} = 1,0 *EN 1993-2:2003, 9.2*

  $\gamma_{Mf,s}$ = 1,0 For shear studs *[EN 1994-2:2005, 2.4.1.2(6)]*, *[TRVFS 2011:12]*

  γ_{Mf} = 1,35 Otherwise *[EN 1993-1-9:2005, Table 3.1]*

- Traffic category 4[2] "Local roads with low flow rates of lorries" is used for the design of the bridge. Thus, the total number of heavy lorries in the slow lane, N_{obs} is estimated to 50 000; i.e. medium flow rate of lorries *[EN 1991-2:2003, 4.6.1(3)]*
- For fatigue design using the simplified λ-method:

  → The average gross weight of the lorries in the slow lane Q_{MI} is set to 410kN
- For fatigue design using the damage accumulation method

  → The category "local traffic" is used *[EN 1991-2:2003, Table 4.7]*

[2] Observe that TRVK Bro 11:085 specifies in B.3.4 (h) modified values for N_{obs} (AADT) for different traffic categories and that traffic type "regional" should be used.

4.1.2.3 Bridge Cross-section properties for fatigue verification

The following has been verified with reference to relevant Eurocode parts:

- Compression flange is in cross-section class 2 (observe that if the requirements for shear studs spacing in *EN 1994-2:2005, 6.6.5.5* are fulfilled, the compressed steel flange can be assumed to be fully supported by the concrete deck, which makes this check superficial).
- No reduction of the web due to normal stress buckling is relevant.
- A check of the effective width of the concrete deck shows that the effective deck with is 2450 mm (b_{eff} = 2450 mm).

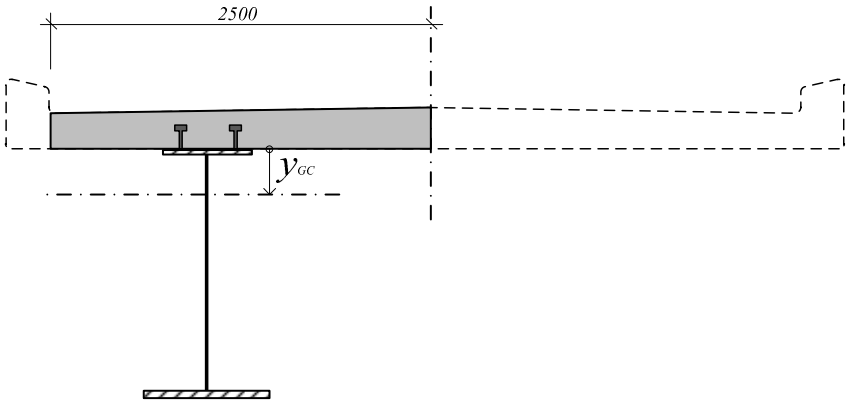

Figure 4-4 Bridge cross-section adopted in calculating the relevant cross-section properties for fatigue verification

In the calculation of the cross-section properties for the composite section, the concrete deck is transformed into an equivalent steel area with its centre of gravity located at the centre of gravity of the concrete deck. Due to symmetry, only half the bridge in the transversal direction as shown in Figure 4-4 is considered.

Table 4-2 Cross-section properties for fatigue verification

Segment	I_{steel} [mm^4]	I_{tot} [mm^4]	A_{tot} [mm^2]	y_{GC} [mm]	W_{top} [mm^3]	W_{bot} [mm^3]
1&3	$1{,}398\cdot10^{10}$	$4{,}158\cdot10^{10}$	$1{,}513\cdot10^{5}$	138	$-1{,}020\cdot10^{8}$	$3{,}403\cdot10^{7}$
2	$1{,}643\cdot10^{10}$	$4{,}643\cdot10^{10}$	$1{,}555\cdot10^{5}$	162	$-1{,}074\cdot10^{8}$	$3{,}876\cdot10^{7}$

4.1.2.4 Definition of bridge lanes and calculation of the load distribution factor

The total carriageway width of the bridge (distance between edge beams) is 5,0 m. Thus there is only one notional lane with a width of 3,0 m and a remaining area which is 2,0 m wide *[EN 1991-2:2003, 4.2.3 and 4.2.4]*.

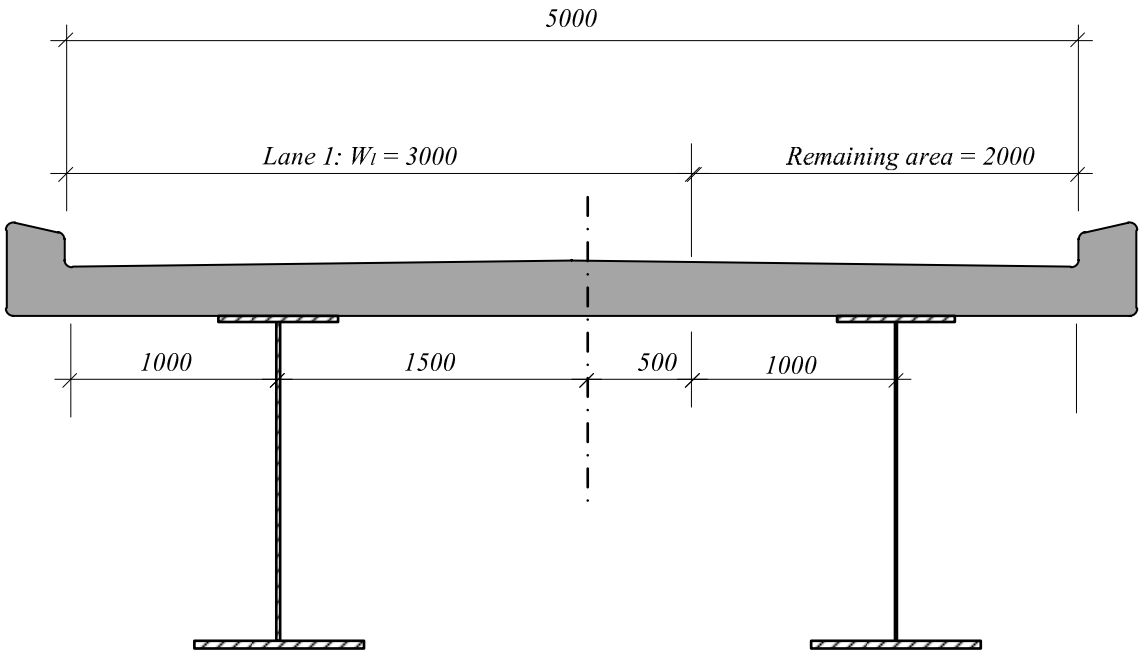

Figure 4-5 Definition of bridge lane and remaining area [mm]

In the transversal direction, the fatigue load model is placed centrally in the slow lane *[EN 1991-2:2003, 4.6.1(4)]*.

The load distribution factor (LDF) for the load arrangement is:

$$LDF = 0{,}5 + \frac{e}{c} = 0{,}5 + \frac{1000}{3000} = 0{,}833$$

Observe that the LDF calculated herein is valid for calculation of the load effects with both FLM 3 and FLM 4 as the distance between wheels in axles is the same for both load models, i.e. 2.0 m.

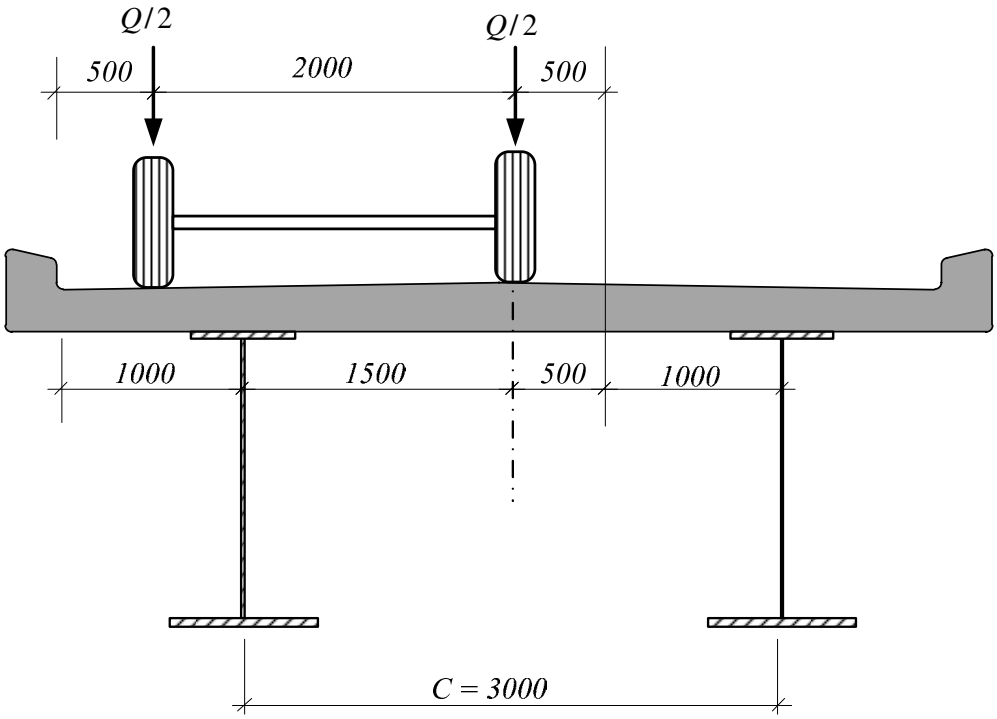

Figure 4-6 Position of FLM 3 in the transversal direction of the bridge [mm]

4.1.3 Fatigue verification using the simplified λ-method

For the sake of this example, the fatigue verification is made with reference to three different details only:

Detail 1: The connection of the vertical stiffener to the lower flange of the main girders at mid-span, i.e. x = 16 000 mm.

Detail 2: The rat-hole detail at the girder splice at x = 8 500 mm.

Detail 3: The shear studs at the supports, i.e. x = 0 mm.

Description of these three details with the relevant information for fatigue resistance is given in Figure 4-7.

Detail	[MPa]		[MPa]
1	$\Delta\sigma_c = 80$	m=3	$\Delta\sigma_D = 59$
2	$\Delta\sigma_c = 71$	m=3	$\Delta\sigma_D = 52$
3	$\Delta\tau_c = 90$	m=8	

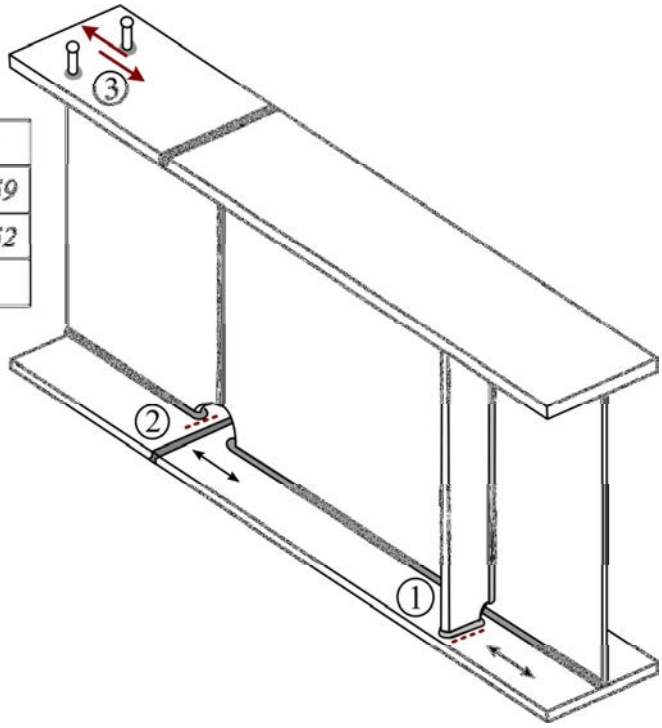

Figure 4-7 Fatigue details considered in this example for fatigue verification

4.1.3.1 Traffic fatigue load model

The traffic load model for fatigue verification of road bridges with the simplified λ-method is given is FLM3 *[EN 1991-2:2003 4.6.4]*. The model consists of a single vehicle with 4 axles each with a total load of 120 kN. The vehicle is assumed to move in the middle of the slow lane of the bridge. According to *EN 1991-2:2003*, a second vehicle with a reduced axel load of 36 kN may also need to be considered in order to better model fatigue effects over intermediate supports in continuous bridges. The distance between the centres of the two vehicles should not be taken less than 40. This makes a consideration of this vehicle irrelevant for this bridge.

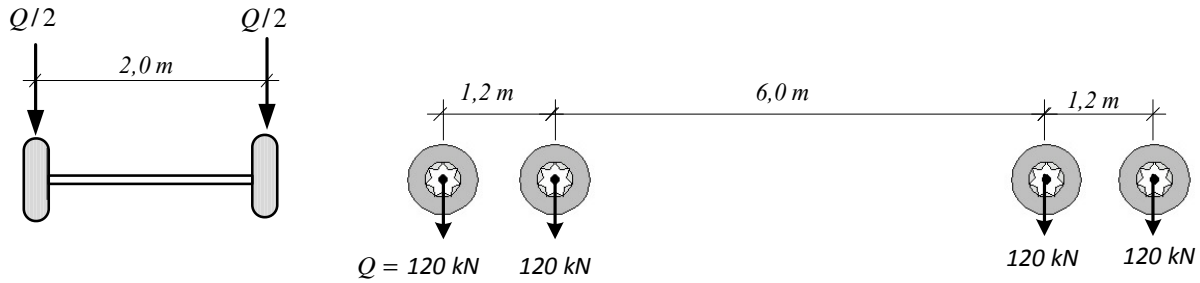

Figure 4-8 Fatigue load model 3 (FLM 3)

4.1.3.2 Determination of load effects

For the first two details considered here (Details 1 & 2) the relevant load effect for the fatigue check is the normal stresses from bending at the top of the bottom flange. For check of the shear studs close to the supports, the influence line for shear at x = 0 m is used. In all cases, the load effects are obtained from moving FLM 3 along the relevant influence line.

For Detail 1 @ x = 16,0 m

$$\Delta M = 120kN \cdot 0{,}833 * (\sum \eta)$$

$$\Delta M = 2480kNm$$

For Detail 2 @ x = 8,5 m

$$\Delta M = 120kN \cdot 0{,}833 * (\sum \eta)$$

$$\Delta M = 2050kNm$$

For Detail 3 @ x = 0,0 m

$$\Delta V = 120kN \cdot 0{,}833 * (\sum \eta)$$

$$\Delta V = 345kN$$

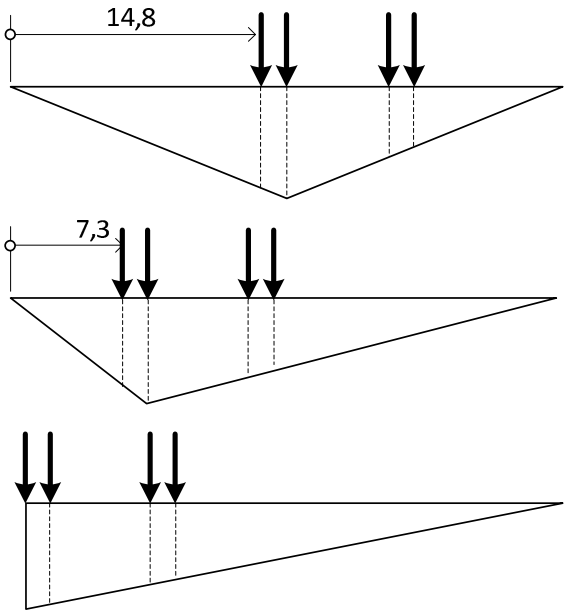

Figure 4-9 Influence lines and sectional forces for fatigue verification of the studied details

In term of stresses, the load effects are:

$\Delta\sigma_{p1}$ = 62,4 MPa calculated at the top surface of the lower flange @ x = 16,0 m

$\Delta\sigma_{p2}$ = 59,0 MPa calculated at the top surface of the lower flange @ x = 8,5 m

$\Delta\tau$ = 80 MPa

$\Delta\tau$ in shear studs is calculated based on a nominal stud diameter of 22 mm and assuming 2x4 studs/m on each flange.

4.1.3.3 Determination of the λ-factors

The λ-factors for Detail 1 and Detail 2 are similar.

For the structural steel details in a composite road bridge with a span up to 80 m, the λ-factors can be obtained from *EN 1993-2:2006, 9.5.2*.

$$\lambda = \lambda_1 \times \lambda_2 \times \lambda_3 \times \lambda_4 \leq \lambda_{max} \qquad \textit{Eq. 4-1}$$

The value of λ_{max} which takes into account the existence of the fatigue limit can be obtained *9.5.2 (8) in EN 1993-2:2006*.

For moment in midspan λ_{max} = 2,00

For determining λ_1, the critical length of the influence line needs to be determined. *Section 9.5.2 (2) in EN 1993-2:2006* should be applied. For a simply-supported bridge, the critical length of the influence line is equal to the span length (L = 32m), for both moment and shear action at midspan and near the supports.

$$\lambda_1 = 2{,}55 - 0{,}7\frac{L-10}{70} = 2{,}33$$

The average gross weight of the lorries in the slow lane Q_{M1} and the total number of heavy lorries in the slow lane, N_{obs} where defined in the project specifications:

$$Q_{M1} = 410kN$$

$$N_{obs} = 50 \cdot 10^3$$

With the reference values as given in [EN 1993-2:2006, 9.5.2 (3)]:

$$Q_0 = 480kN$$

$$N_0 = 500 \cdot 10^3$$

Thus the factor for traffic volume is:

$$\lambda_2 = \frac{Q_{M1}}{Q_0}\left(\frac{N_{obs}}{N_0}\right)^{\frac{1}{5}} = 0{,}539$$

The design life of the bridge is 80 years which gives a correction factor:

$\lambda_3 = \left(\frac{80}{100}\right)^{\frac{1}{5}} = 0{,}956$, which is according to [EN 1993-2:2006, 9.5.2 (5)].

The bridge has only one traffic lane, thus:

$$\lambda_4 = 1{,}0$$

The total λ-factors with reference to Detail 1 and Detail 2 becomes

$$\lambda_4 = 2{,}33 \cdot 0{,}539 \cdot 0{,}956 \cdot 1{,}0 = 1{,}201$$

Which is less than $\lambda_{max} = 2{,}0$

Fatigue verification of shear studs (Detail 3) is treated in EN 1994-2:2005. The verification condition reads:

$$\gamma_{Ff} \cdot \Delta\tau_{E,2} \leq \frac{\Delta\tau_c}{\gamma_{Mf,s}} \qquad \textit{Eq. 4-2}$$

where,

$$\Delta\tau_{E,2} = \lambda_v \cdot \Delta\tau, \quad \Delta\tau_c = 90MPa$$

and

$$\lambda_v = \lambda_{v,1} \times \lambda_{v,2} \times \lambda_{v,3} \times \lambda_{v,4} \qquad \textit{Eq. 4-3}$$

For road bridges with spans up to 100 m, $\lambda_{v,1}$ should be taken as 1.55 [EN 1994-2:2005, 6.8.6.1(4)].

The other factors, $\lambda_{v,2}$ to $\lambda_{v,4}$ are obtained from EN 1993-2:2006. However, the fatigue strength curve (S-N curve) for shear studs loaded in shear has a slope of 1:8 (i.e. m = 8) and thus the λ-factors for shear studs need to be corrected with reference to that. That is made by replacing the exponent 1/5 with 1/8 in the expressions for λ_{v2} to λ_{v4}.

Therefore:

$$\lambda_{v,2} = \frac{Q_{M1}}{Q_0}\left(\frac{N_{obs}}{N_0}\right)^{\frac{1}{8}} \quad \rightarrow \quad \lambda_{v,2} = \frac{410}{480}\left(\frac{0{,}05}{0{,}5}\right)^{\frac{1}{8}} = 0{,}641$$

$$\lambda_{v,3} = \left(\frac{80}{100}\right)^{\frac{1}{8}} = 0{,}973$$

$$\lambda_{v,3} = 1{,}0$$

$$\lambda_v = 1{,}550 \cdot 0{,}641 \cdot 0{,}973 \cdot 1{,}0 = 0{,}967$$

The dynamic amplification factor is included in the fatigue load model FLM 3, therefore $\phi_2 = 1{,}0$.

4.1.3.4 Fatigue verification

For each detail, the fatigue verification can now be performed by comparing the equivalent stress range at 2 million cycles ($\Delta\sigma_{E,2}$ or $\Delta\tau_{E,2}$) with the fatigue strength of each detail accounting for relevant partial factor for fatigue resistance (γ_{Mf}).

In addition to the fatigue check in this format, a damage accumulation factor can also be derived for example from *A.6 in EN 1993-1-9:2005*. The damage factor can be expressed as:

$$D = \left(\frac{\gamma_{Ff} \cdot \Delta\sigma_{E,2}}{\Delta\sigma_D / \gamma_{Mf}}\right)^3 \qquad \textit{Eq. 4-4}$$

For Detail 1:

$$\Delta\sigma_{E,2} = \lambda \cdot \phi_2 \cdot \Delta\sigma_p = 74{,}9 MPa$$

The corresponding fatigue resistance at 2 million cycles (i.e. the fatigue strength):

$$\Delta\sigma_C = 80 MPa$$

And the verification reads:

$$\frac{\gamma_{Ff} \cdot \gamma_{Mf} \cdot \Delta\sigma_{E,2}}{\Delta\sigma_C} = 1{,}264 > 1{,}0$$

and the corresponding damage factor is:

$$D = \left(\frac{\gamma_{Ff} \cdot \gamma_{Mf} \cdot \Delta\sigma_{E,2}}{\Delta\sigma_C}\right)^3 = 2{,}02 > 1{,}0$$

For Detail 2:

$$\Delta\sigma_{E,2} = \lambda \cdot \phi_2 \cdot \Delta\sigma_p = 71{,}5 MPa$$

and

$$\Delta\sigma_C = 71 MPa$$

And the verification reads:

$$\frac{\gamma_{Ff} \cdot \gamma_{Mf} \cdot \Delta\sigma_{E,2}}{\Delta\sigma_C} = 1{,}359 > 1{,}0$$

With a corresponding damage factor:

$$D = \left(\frac{\gamma_{Ff} \cdot \gamma_{Mf} \cdot \Delta\sigma_{E,2}}{\Delta\sigma_C} \right)^3 = 2{,}512$$

Detail 3:

The shear stress range in each stud is $\Delta\tau = 80$ MPa (see 4.2 above), thus:

$$\Delta\tau_{E,2} = \lambda_v \cdot \Delta\tau \qquad \Delta\tau_{E,2} = 0{,}967 \times 80 = 77{,}4 MPa$$

With $\gamma_{Mf,s} = 1{,}0$ as recommended in *TRVFS 2011:12*, the verification reads:

$$1{,}0 \cdot 77{,}4 \leq \frac{90}{1{,}0}$$

which is satisfied. The required number of shear studs with reference to fatigue may be calculated as:

$$n_{studs} = \frac{90}{77{,}4} \cdot 8 = 10$$

Observe that the number of shear studs close to the supports of simply-supported bridge is usually determined by the requirements in the ULS, while the fatigue verification governs by the number of shear studs in mid-span region.

4.1.4 Fatigue verification using the Damage Accumulation method

Eurocode allows for fatigue verification of road and railway bridges to be performed using the cumulative damage method. For this purpose, EN 1991-2 provides load models for both road bridges *(EN 1991-2:2003, 4.6.5)* and railway bridges *(EN 1991-2:2003, D.3)*. For the purpose of illustration, the method is applied here to verify the fatigue strength of Detail 1.

For road bridges, fatigue load model 4 (FLM 4) should be used for calculating the total fatigue damage accumulated through the design service life of the bridge. This fatigue load model is composed of 5 different vehicles (lorries) which are meant to represent the real traffic composition on road bridges in a more accurate way. Detailed information about the composition of FLM4 can be found in Table 4.7 in *EN 1991-2:2003*.

Verification of the fatigue strength of Detail 1 in this example is performed according to the following steps:

1. Relevant data for the fatigue strength of the detail is established

2. The stress history is determined by moving each vehicle in FLM 4 individually along the bridge, in the centre of the traffic lane (thus, the load effects need to be modified with relevant LDF, see Section 4.1.2.4 in this example).

3. The stress histogram is constructed using appropriate method (for example the reservoir method).

4. The damage caused by individual blocks in the stress histogram is calculated (accounting for the slope of the S-N curve) and all damage components are summed to obtain a total damage.

5. Verification is made by checking the condition $D_{tot} \leq 1{,}0$.

In this simple example (a simply supported bridge) the stress history from each lorry passage and the resultant stress histogram are obtained by hand calculations.

4.1.4.1 Fatigue strength curve

The fatigue strength curve for Detail 1 is shown in Figure 4-10. Detail Category 80 applies as given for Detail 7 in *EN 1993-1-9:2005, Table 8.4* assuming that the thickness of the vertical stiffener with the fillet welds on each side is less than 50 mm. Thus:

$\Delta\sigma_c$=80,0 MPa

$\Delta\sigma_D$=59,0 MPa

$\Delta\sigma_L$=32,0 MPa

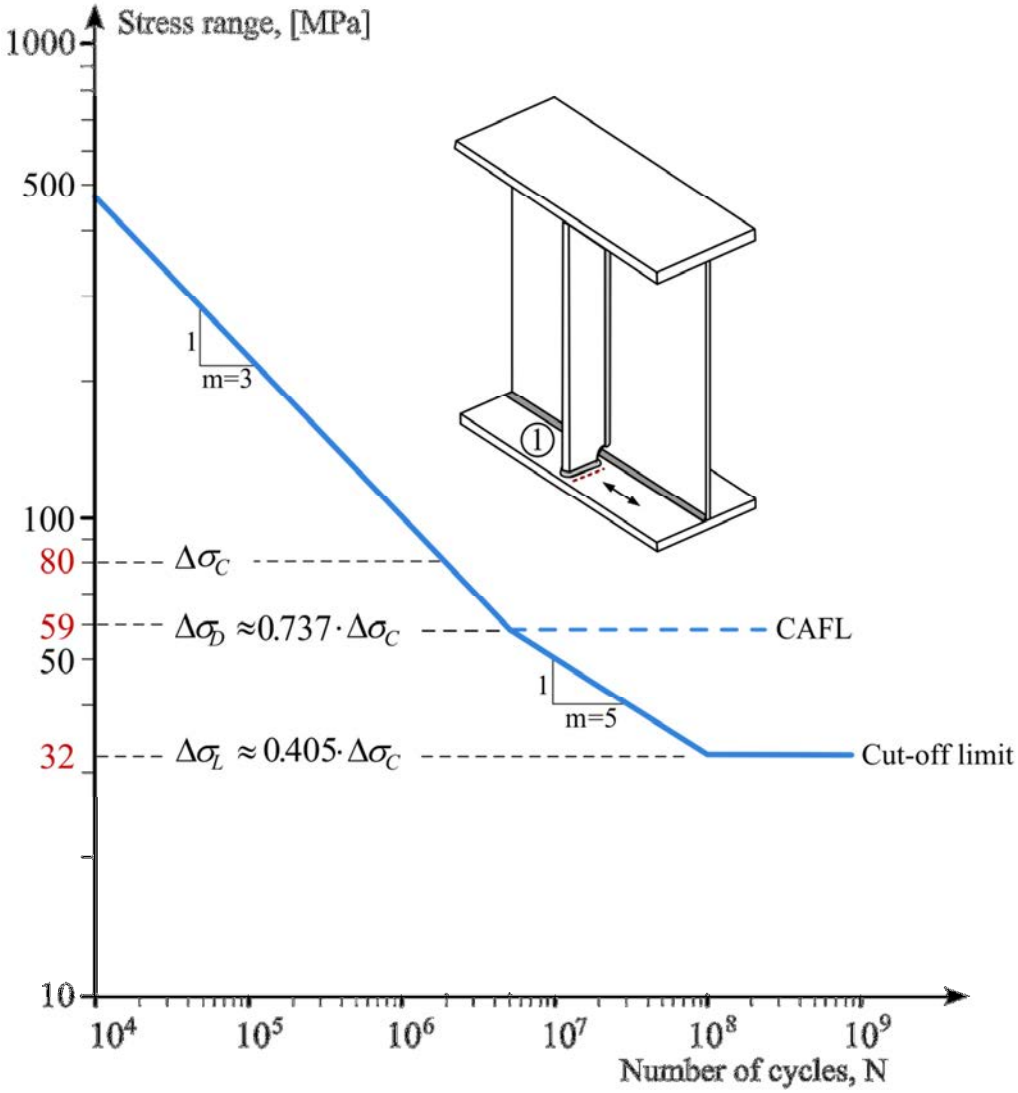

Figure 4-10 Fatigue resistance data for Detail 1

4.1.4.2 Bridge response, stress history and stress histogram

In this simple example (a simply supported bridge) the stress history from each lorry passage is obtained with hand calculations by moving each lorry over the influence line for moment in bridge mid-span. The results are summarized in Table 4-3.

Obviously, vehicle 3 (total weight of 490 kN) causes the maximum moment variation followed by vehicle 5 and 4. After modifying the bending moments in with reference to the load distribution in the transversal direction of the bridge (LDF in Section 4.1.2.4 of this example), the stress range at Detail 1 can be calculated for each vehicle type.

Table 4-3 Moment response at bridge mid-span due to FLM4

Lorry	*Response, Moment [kNm]*
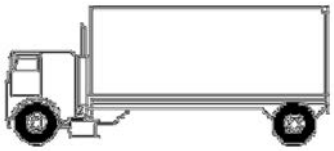 *1*	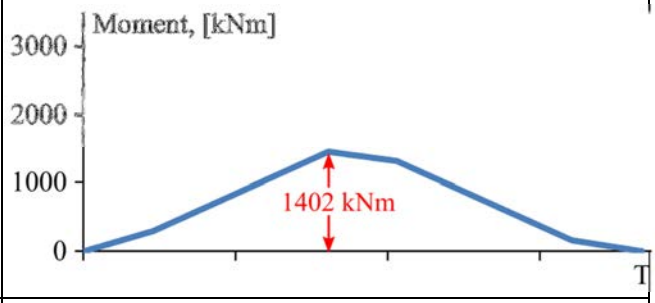
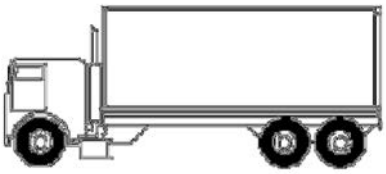 *2*	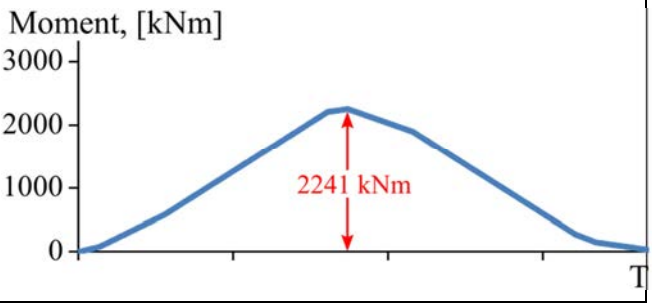
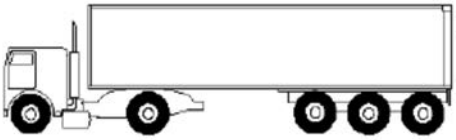 *3*	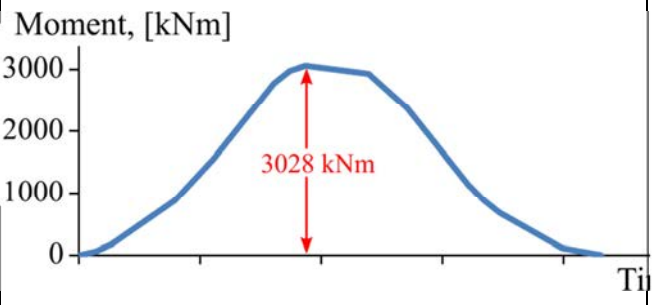
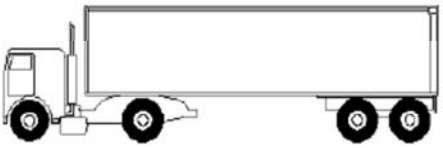 *4*	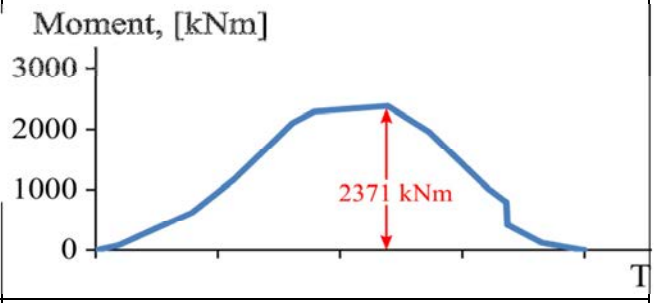
 *5*	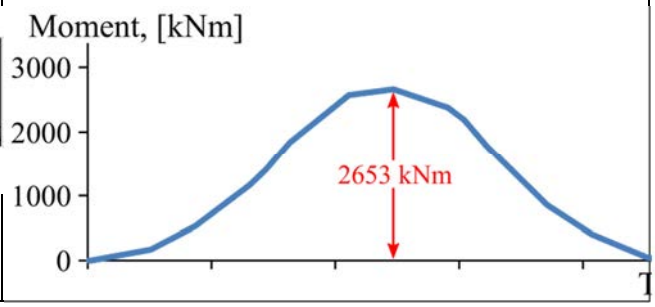

The final composition of the stress histogram (Stress range – Number of cycles) will depend on the percentage of each vehicle or lorry which in turn is determined based on the "traffic category".

In this example, traffic category 4 "local roads with low flow rates of lorries" is assumed. Thus:

N_{obs} = 50 000 *[EN 1991-2:2003, 4.6.1(3)]*

The percentage of each lorry in N_{obs} is obtained from Table 4.7 in *EN 1991-2:2003* for "local traffic". The result is summarized in Table 4-4.

Table 4-4 The number of cycles during the design life of the bridge assuming traffic category 4, "local roads with low flow rates of lorries"

Lorry	***%***	***n_i/year***	***n_i in 80 years***
1	80	$40 \cdot 10^3$	$3{,}2 \cdot 10^6$
2	5	$2{,}5 \cdot 10^3$	$0{,}2 \cdot 10^6$
3	5	$2{,}5 \cdot 10^3$	$0{,}2 \cdot 10^6$
4	5	$2{,}5 \cdot 10^3$	$0{,}2 \cdot 10^6$
5	5	$2{,}5 \cdot 10^3$	$0{,}2 \cdot 10^6$
Sum	***100***	***$50 \cdot 10^3$***	***$4{,}0 \cdot 10^6$***

The results of the damage accumulation calculations are shown in Table 4-5.

Comment:

- *As one block in the histogram exceeds:*

$$\frac{\Delta\sigma_D}{\gamma_{Mf}} = \frac{59}{1{,}35} = 43{,}7MPa$$

- *The constant amplitude fatigue Limit "disappears" and is replaced by the cut-off limit, $\Delta\sigma_L$.*

- *None of the stress blocks in the histogram is below the cut-off limit reduced with the partial factor for resistance; i.e.*

$$\frac{\Delta\sigma_L}{\gamma_{Mf}} = \frac{32}{1{,}35} = 23{,}7MPa$$

- *Thus all stress blocks contribute to the total damage, however according to their position in relation to:*

$$\frac{\Delta\sigma_D}{\gamma_{Mf}} = \frac{59}{1{,}35} = 43{,}7MPa$$

The number of cycles to failure, N_i is calculated from:

$$N_i = 5 \cdot 10^6 \left(\frac{\Delta\sigma_D / \gamma_{Mf}}{\Delta\sigma_p \gamma_{Ff}} \right)^m$$

Where m = 3 or 5.

Table 4-5 Fatigue damage calculations using "Local traffic" composition

Lorry	***ΔMi*** *[kNm]*	***Δσi*** *[MPa]*	***m***	***Ni*** *[Cycles]*	***ni*** *[Cycles]*	***Di***
1	1193	30	5	$3{,}27 \cdot 10^7$	$3{,}2 \cdot 10^6$	0,097
2	1867	47	3	$4{,}02 \cdot 10^6$	$0{,}2 \cdot 10^6$	0,050
3	2522	63,5	3	$1{,}63 \cdot 10^6$	$0{,}2 \cdot 10^6$	0,123
4	1976	49,7	3	$3{,}39 \cdot 10^6$	$0{,}2 \cdot 10^6$	0,059
5	2210	55,6	3	$2{,}42 \cdot 10^6$	$0{,}2 \cdot 10^6$	0,083
					$4 \cdot 10^6$	**0,412**

With a design life of 80 years the total damage is calculated to 0,412, which is much less than unity. The theoretical design life of the bridge with reference to the fatigue strength of Detail 1 is about 195 years when traffic category 4 is assumed.

Comment:

- *It is apparent that using the damage accumulation method – which is a bit more time requiring – yield results which are more "accurate". Indeed, the load composition in FLM4 is more realistic with reference to real*

traffic on road bridges and representing this composition with one heavy load model (FLM3) will yield results on the safe side.

For the sake of comparison, the damage calculations are made in Table 4-6 for traffic type "medium distance", see *EN 1991-2:2003, 4.6.5*.

Table 4-6 Fatigue damage calculations using "Medium distance"

Lorry	ΔM_i	$\Delta\sigma_i$	***m***	N_i	**%**	n_i	D_i
1	1193	30	5	$3{,}27\cdot10^7$	40	$1{,}6\cdot10^6$	0,049
2	1867	47	3	$4{,}02\cdot10^6$	10	$0{,}4\cdot10^6$	0,100
3	2522	63,5	3	$1{,}63\cdot10^6$	30	$1{,}2\cdot10^6$	0,736
4	1976	49,7	3	$3{,}39\cdot10^6$	15	$0{,}6\cdot10^6$	0,177
5	2210	55,6	3	$2{,}42\cdot10^6$	5	$0{,}2\cdot10^6$	0,083
					100	***$4{,}0\cdot10^6$***	***1,145***

With 80 years, the total damage 1,145 which is larger than unity. The theoretical design life of the bridge with reference to the fatigue strength of Detail 1 is then about 70 years.

Comment:

- *The damage accumulation can also be expressed in term of equivalent stress.*

$$\Delta\sigma_E = \left(\frac{\sum n_i \left(\gamma_{Ff}\Delta\sigma_i\right)^3 + \sum n_j \left(\gamma_{Ff}\Delta\sigma_j\right)^3 \left(\frac{\gamma_{Ff}\gamma_{Mf}\Delta\sigma_j}{\Delta\sigma_D} \right)^2}{\sum n_i + \sum n_j} \right)^{1/3}$$

- *Which here gives:*

$$\Delta\sigma_E = 35{,}012\,MPa$$

- *The number of cycles to failure at this stress range is*

$$N_E = 5 \cdot 10^6 \cdot \left(\frac{\frac{\Delta\sigma_D}{\gamma_{Mf}}}{\gamma_{Ff} \cdot \Delta\sigma_E} \right)^3 = 9705 \cdot 10^6 \, Cycles$$

- *And the total damage becomes:*

$$D = \frac{\sum_i n_i}{N_E} = 0{,}412$$

- *Which is the same damage sum obtained in Table 4-5 above.*

Comment:

- *A fatigue verification following the same format used in the simplified λ-method can be derived from the damage accumulation calculations:*

- *With: $\Delta\sigma_{E=}$35,012MPa*

$$\Delta\sigma_{E,2} = \Delta\sigma_E \cdot \left(\frac{\sum_i n_i}{2 \cdot 10^6} \right)^3 = 44{,}112 \, MPa$$

- *And the verification reads*

$$\frac{\gamma_{Mf} \cdot \gamma_{Ff} \cdot \Delta\sigma_{E,2}}{\Delta\sigma_C} = 0{,}744 < 1{,}0 \; Satisfied$$

- *Again this yields the same damage factor, D:*

$$D = \left(\frac{\gamma_{Mf} \cdot \gamma_{Ff} \cdot \Delta\sigma_{E,2}}{\Delta\sigma_C} \right)^3 = 0{,}412$$

4.2 Worked example – fatigue design of a railway bridge

This example covers the verification of the fatigue limit state for a railway bridge. The verification is made with reference to three different structural details for the sake of demonstration. Both the simplified λ-method and the damage accumulation method are demonstrated.

4.2.1 Description of the bridge

The railway bridge is a steel bridge with a single span of 20,0 m. The bridge girder is delivered to the construction site in two segments which are 8,5 m and 12,5 m long. These two segments are assembled on site by welding, see Figure 4-11. The cross-section of the bridge is composed of two steel girders with a common upper flange forming together an open hat-shaped profile. The cross-section dimensions are kept constant along the entire span. The two steel girders are joined by U-shaped diaphragms at each L/4, which are bolted to welded vertical stiffeners, see Figure 4-12.

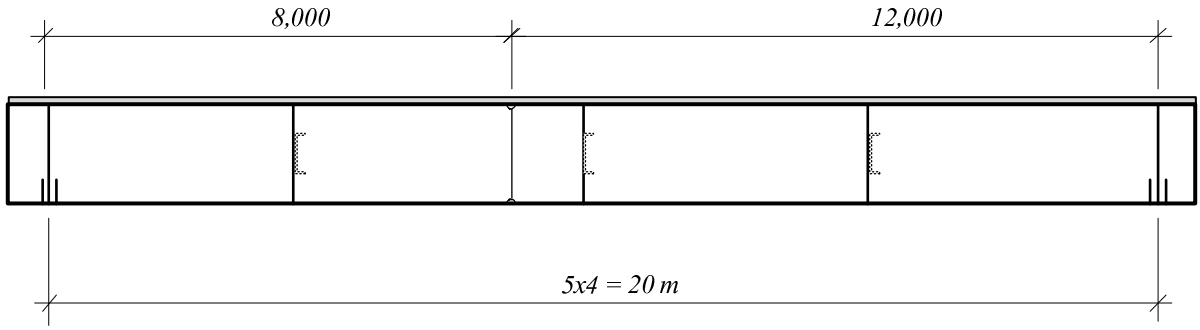

Figure 4-11 Elevation of the railway bridge

Butt welds are used to connect the upper flange to the web as well as for the connection between the vertical stiffeners and the upper flanges. 5 mm fillet welds are used for the connections at the bottom side of the girders. The steel grade used for all load-carrying parts in the bridge is S355. The dimensions of the steel cross-section are given in Figure 4-12 and the relevant cross-section properties for the fatigue verification are listed in Table 4-7.

Table 4-7 Cross-section constants used in fatigue verification

I [mm^4]	A [mm^2]	y_{GC} [mm]	W_{top} [mm^3]	W_{bot} [mm^3]	S_{bot} [mm^3]
$7{,}531 \cdot 10^{10}$	$1{,}626 \cdot 10^{5}$	627	$-1{,}202 \cdot 10^{8}$	$8{,}623 \cdot 10^{7}$	$5{,}031 \cdot 10^{7}$

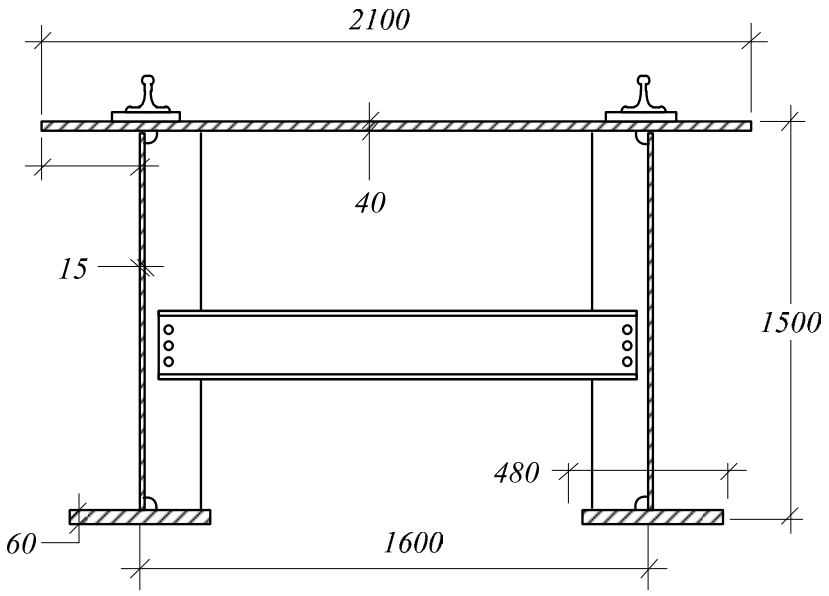

Figure 4-12 Cross-section of the bridge

4.2.2 Bridge specific traffic data

The following bridge specific data has been adopted in this example:

- Design life = 120 years
- The safe life assessment method should be used for bridges *[BFS 2011:10]* with high consequence of failure.

  ➔ Partial factors for fatigue

  γ_{Ff} = 1,0 1993-2: 9.2

  γ_{Mf} = 1,35 Otherwise [*1993-1-9:2005, Table 3.1*]
- Rail traffic with 25 t axels is used for fatigue verification [*1993-2:2006, 9.5.*3].
- The traffic per year is specified to 25 million tonnes per track
- Carefully maintained track is assumed

4.2.3 Fatigue verification using the simplified λ-method

For the sake of this example, the fatigue verification is made with reference to three different details only:

Detail 1: The connection of the vertical stiffener to the lower flange of the main girders at mid-span, i.e. x = 10,0 m.

Detail 2: The rat-hole detail at the girder splice @ x = 8,0 m.

Detail 3: Connection of welded stiffener to girder web @ x = 5,0 m.

Description of these three details with the relevant information for fatigue resistance is given in Figure 4-13 and Table 4-8.

Table 4-8 Fatigue resistance data for the three structural details chosen for fatigue verification

Detail	***Design stress***	$\Delta\sigma_c$ ***[MPa]***	$\Delta\sigma_D$ ***[MPa]***	$\Delta\sigma_L$ ***[MPa]***
1	Normal stress in flange	80	59	32
2	Normal stress in flange	71	52	29
3	Principle stress in the web	80	59	32

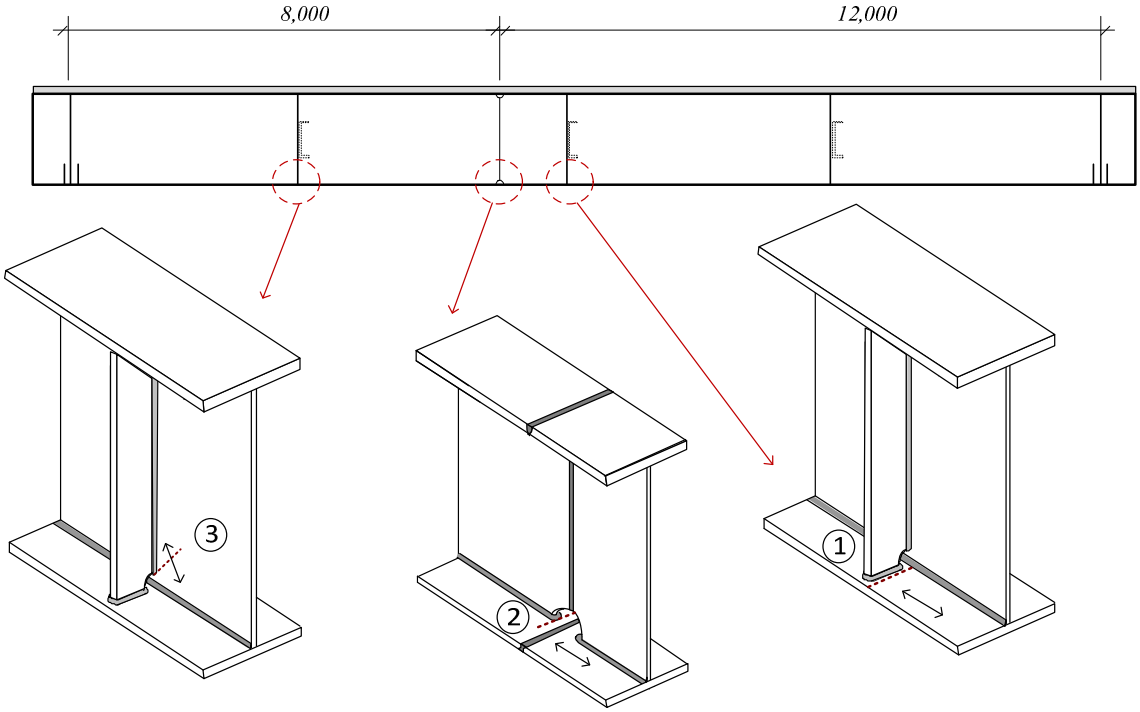

Figure 4-13 The details selected for fatigue verification

4.2.3.1 Train load model and load effects

The traffic load model for fatigue verification of railway bridges is LM71 in *EN 1991-2: 2003, 6.9*, see Figure 4-14.

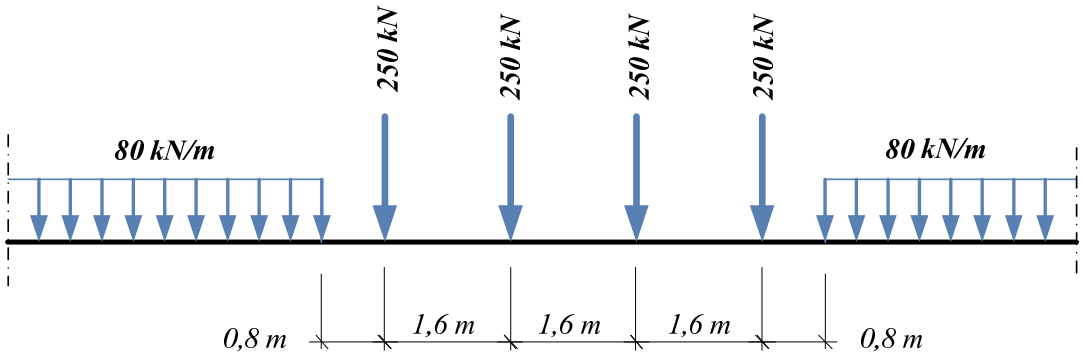

Figure 4-14 Traffic load model LM71

Relevant load effects for fatigue verification of each detail are obtained by placing LM71 in the most unfavourable position. Normally this is easily obtained from various computer programs. In this simple example, and for the sake of demonstration, hand calculations are used to obtain the stress ranges for fatigue verification. The results – in term of sectional forces – are given in Figure 4-15.

In term of stresses at relevant check points, the load effects are:

$\Delta\sigma_{p1}$ = 65,88 MPa calculated at the top surface of the lower flange @ x = 10,0 m

$\Delta\sigma_{p2}$ = 67,72 MPa calculated at the top surface of the lower flange @ x = 8,0 m

$\Delta\sigma_{p3}$ = 46,85 MPa calculated at the bottom termination of the weld connecting the vertical stiffener to the girder web @ x = 5,0 m

$\Delta\tau_{p3}$ = 17,80 MPa calculated at the bottom termination of the weld connecting the vertical stiffener to the girder web @ x = 5,0 m

$\Delta\sigma_{p3}$ and $\Delta\tau_{p3}$ should be combined to give the principal stress at the actual location, thus:

$$\Delta\sigma_{principal} = \frac{\Delta\sigma_{p3}}{2} + \sqrt{\left(\frac{\Delta\sigma_{p3}}{2}\right)^2 + \Delta\tau_{p3}^{\,2}} = 52{,}85 MPa$$

*For **Detail 1** @ x = 10,0 m*

$$\Delta M = 6100 kNm$$

*For **Detail 2** @ x = 8,5 m*

$$\Delta M = 5900 kNm$$

*For **Detail 3** @ x = 5,0 m*

$$\Delta M = 4622 kNm$$

*For **Detail 3** @ x = 5,0 m*

$$\Delta V = 800 kN$$

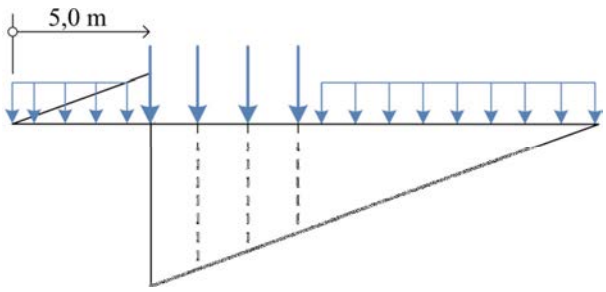

Figure 4-15 Influence lines and load positions giving the sectional forces relevant for fatigue verification of the selected three details

4.2.3.2 Determination of the λ-factors

For the structural steel details in a steel railway bridge, the λ-factors can be obtained from *EN 1993-2:2006, 9.5.3*.

$$\lambda = \lambda_1 \times \lambda_2 \times \lambda_3 \times \lambda_4 \leq \lambda_{max} \qquad \textit{Eq. 4-5}$$

The value of λ_{max} which takes into account the existence of the fatigue limit is defined in *9.5.3 (9) in EN 1993-2*.

$\lambda_{max} = 1{,}4$.

For determining λ_1, the critical length of the influence line needs to be determined. Section 9.5.3 (4) in *EN 1993-2.2006* should be applied. For a simply-supported

bridge, the critical length of the influence line is equal to the span length, for both moment and shear action at midspan and near the supports.

For the simply-supported bridge with *L = 20,0* m and adopting "Rail traffic with 25 t axles":

$\lambda_1 = 0{,}68$ *[EN 1993-2:2006, 9.5.3 (3)]*

The traffic per year was specified to 25 million tonnes per track, which gives:

$\lambda_2 = 1{,}0$ *[EN 1993-2: 2006, 9.5.3 (5)]*

Adopting a design life of 120 years:

$\lambda_3 = 1{,}04$ *[EN 1993-2: 2006, 9.5.3 (6)]*

With one track in the bridge, thus:

$\lambda_4 = 1{,}0$ *[EN 1993-2: 2006, 9.5.3 (7)]*

Finally:

$$\lambda = 0{,}68 \cdot 1{,}0 \cdot 1{,}04 \cdot 1{,}0 = 0{,}707 \leq \lambda_{\max} = 1{,}4$$

For railway bridges a dynamic amplification factor should be included in the fatigue verification, *[EN 1991-2: 2003, 6.4.5.2 and D.2]*.

For a carefully maintained track:

$$\phi_2 = \frac{1{,}44}{\sqrt{L_\phi} - 0{,}2} + 0{,}82 = 1{,}157$$

where

L_Φ is the determinant length of the bridge, which for the simply-supported bridge at hand is equal to the theoretical bridge span, L *[EN 1991-2:2003, Table 6.2]*.

The value of Φ_2 should fulfil the limits below, which is satisfied.

$(1{,}0 \leq \phi_2 \leq 1{,}67)$

4.2.3.3 Fatigue verification

For each detail, the fatigue verification can now be performed by comparing the equivalent stress range at 2 million cycles ($\Delta\sigma_{E,2}$ or $\Delta\tau_{E,2}$) with the fatigue strength of each detail accounting for relevant partial factor for fatigue resistance (γ_{Mf}).

In addition to the fatigue check in this format, a damage accumulation factor can also be derived for example from *A.6 in EN 1993-1-9:2005*. The damage factor can be expressed as:

$$D_{eq} = \left(\frac{\gamma_{Mf} \cdot \gamma_{Ff} \cdot \Delta\sigma_{E,2}}{\Delta\sigma_C} \right)^3 \qquad \text{Eq. 4-6}$$

For ***Detail 1***

$\Delta\sigma_{p1} = 65{,}88 MPa$

$\Delta\sigma_{E,2} = 0{,}707 \cdot 1{,}157 \cdot 65{,}88 = 53{,}9 MPa$

The fatigue verification reads:

$$\frac{\gamma_{Ff} \cdot \Delta\sigma_{E,2}}{\Delta\sigma_C / \gamma_{Mf}} = \frac{1{,}35 \cdot 53{,}9}{80/1{,}0} = 0{,}91 \leq 1{,}0$$

In term of equivalent damage, the result is:

$$D_{eq} = \left(\frac{1{,}0 \cdot 1{,}35 \cdot 53{,}9}{80} \right)^3 = 0{,}753$$

Following the same principles, the other two details are treated. The results are summarized in Table 4-9.

Table 4-9 Results from fatigue verification of the selected details according to the λ-method

Detail	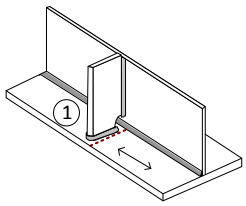	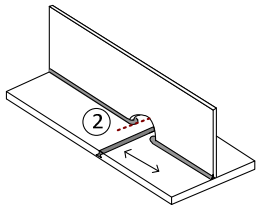	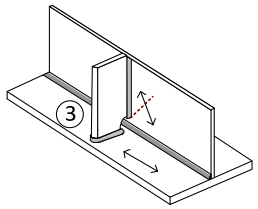
$\Delta\sigma_{E,2}$	53,9	52,1	43,25
$\Delta\sigma_c$	80	71	80
λ-verification	0,91	0,99	0,73
D_{eq}	0,753	0,974	0,389

4.3 Fatigue verification using the Damage Accumulation method

Eurocode allows for fatigue verification of road and railway bridges to be performed using the cumulative damage method. For this purpose, *EN 1991-2:2003* provides the relevant load models for railway bridges in Annex D.3. For the purpose of illustration, the method is applied here to verify the fatigue strength of the selected

three details. The calculations are shown in more details for Detail 1, while the results are summarized for the other two details.

4.3.1 Traffic load models

The traffic mix which is relevant for the bridge in this example (heavy traffic mix with 25 t axles) is found in Table D.2 in *Annex D.3 of EN 1991-2:2003*. This traffic mix is composed of the 4 different train models as given in Table 4-10. For axle loads, axle configurations and other information related to each train model, refer to Annex D.3 of *EN 1991-2:2003*.

Table 4-10 Train types, mass and frequency for D2 composition in Annex D.3 of EN 1991-2:2003

Train type	***Number of train*** *[per day]*	***Train mass*** *[t]*	***Traffic volume x10^6*** *[year]*
5	6	2160	4,73
6	13	1431	6,79
11	16	1135	6,63
12	16	1135	6,63

Verification of the fatigue strength is performed according to the following steps:

1. The stress history for each detail is determined by moving each train model individually over the influence line for the relevant load effect which governs the fatigue life of the detail.

2. A stress histogram is constructed using the Rain-flow counting method including all 4 train models with their number of occurrence per day.

3. The damage caused by individual stress blocks in the stress histogram is calculated (accounting for the slope of the S-N curve) and all damage components are summed to obtain a total damage.

4. Verification is made by checking the condition $D_{tot} \leq 1{,}0$.

In this simple example the stress history from each train passage and the resultant stress histogram are obtained by means of a computer program made in MATLAB.

4.3.2 Bridge response to train load models

Detail 1 is located in the middle of the bridge span. The relevant stress range is the normal stress from bending at the upper face of the bottom flange. In Figure 4-16, the time response of the bridge with reference to Detail 1 is shown for the passage of each

train model in the studied composition. The results from the damage accumulation calculations are listed in Table 4-11.

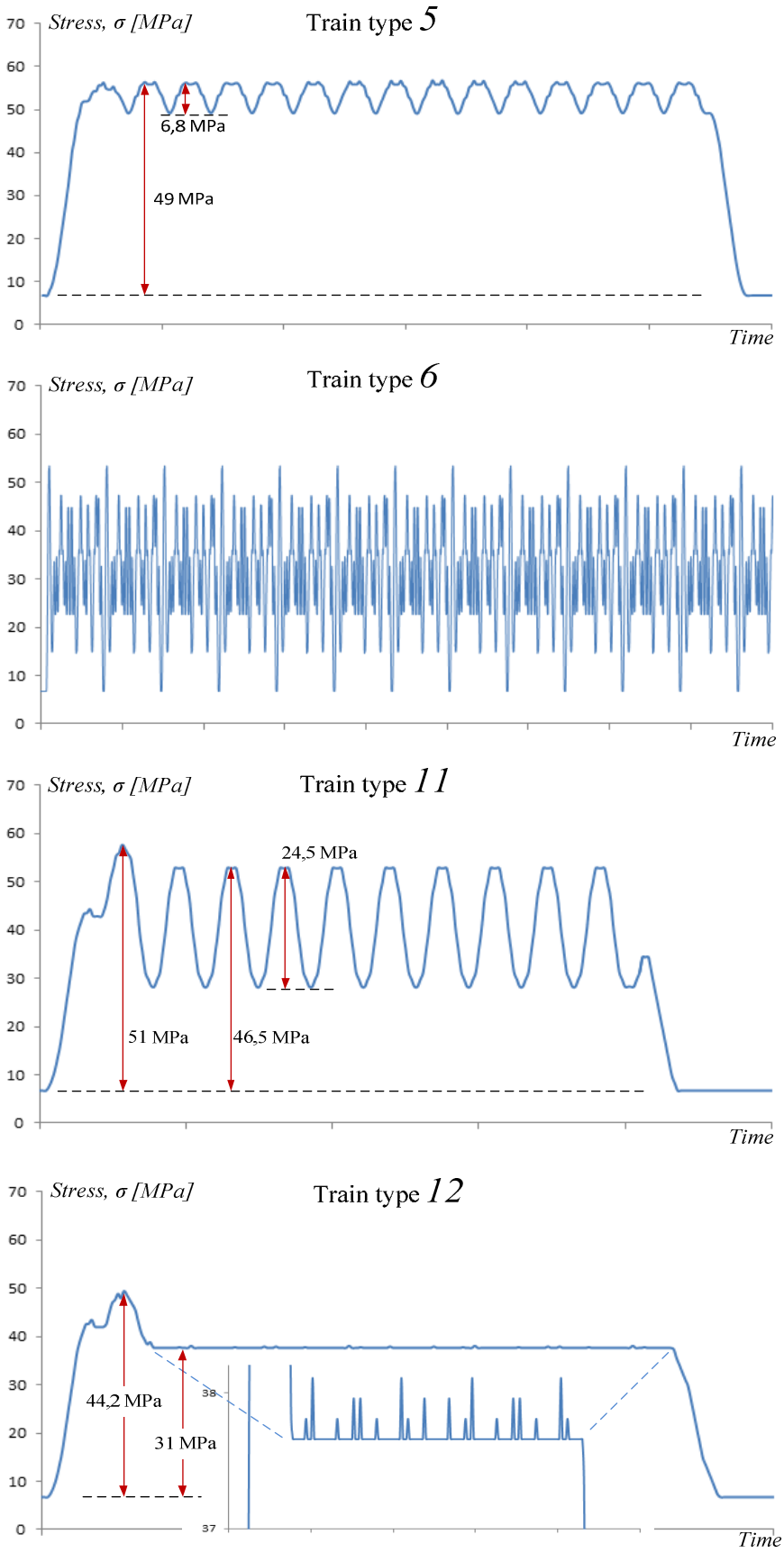

Figure 4-16 The time response of the bridge with reference to the normal stress from bending at Detail 1

Comment:

- *A closer look at the response of Detail 1 indicates that train load models 11 and 6 should stand for the larger portion of the fatigue damage. Train load models 5 and 12 cause essentially one loading cycle per train damage. This is also confirmed by the results in Table 4-11.*

- *The results – in term of total damage - from the simplified λ-method and from the damage accumulation method are very close. As expected, the damage accumulation method gives somewhat lower damage compared to the λ-method, except for Detail 2, where the damage from the λ-method is about 7% lower than that obtained from the damage accumulation method. The results are still very close which indicates that the fatigue load models in the two different methods are well calibrated against each other's.*

Table 4-11 Fatigue damage for Detail 1 calculated for each individual train model per 120 years. The equivalent damage according to the simplified λ-method is also given for comparison

Detail	D_{LM5}	D_{LM6}	D_{LM11}	D_{LM12}	D_{tot}	D_{λ}
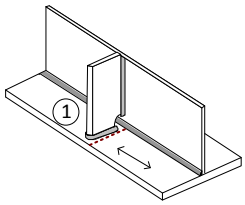	0,0795	0,2195	0,2951	0,1261	***0,72***	***0,753***
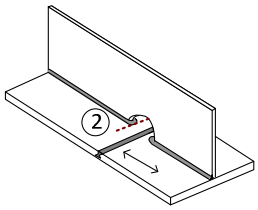	0,1076	0,3690	0,4099	0,1653	***1,05***	***0,975***

	0,0395	0,0994	0,1081	0,0346	***0,28***	***0,389***

Figure 4-17 shows the histogram obtained for Detail 1 (bending stresses) as a result of the adopted train composition. Apparently, the majority of the stress ranges in the histogram are below the cut-off limit for the studied detail category, reduced by the partial factor for fatigue resistance, γ_{Mf}. The stress blocks in the histogram, which actually contribute to the fatigue damage (shown in red) are all below $\Delta\sigma_D/\gamma_{Ff}$ so that a slope of 1:5 applies in damage calculations.

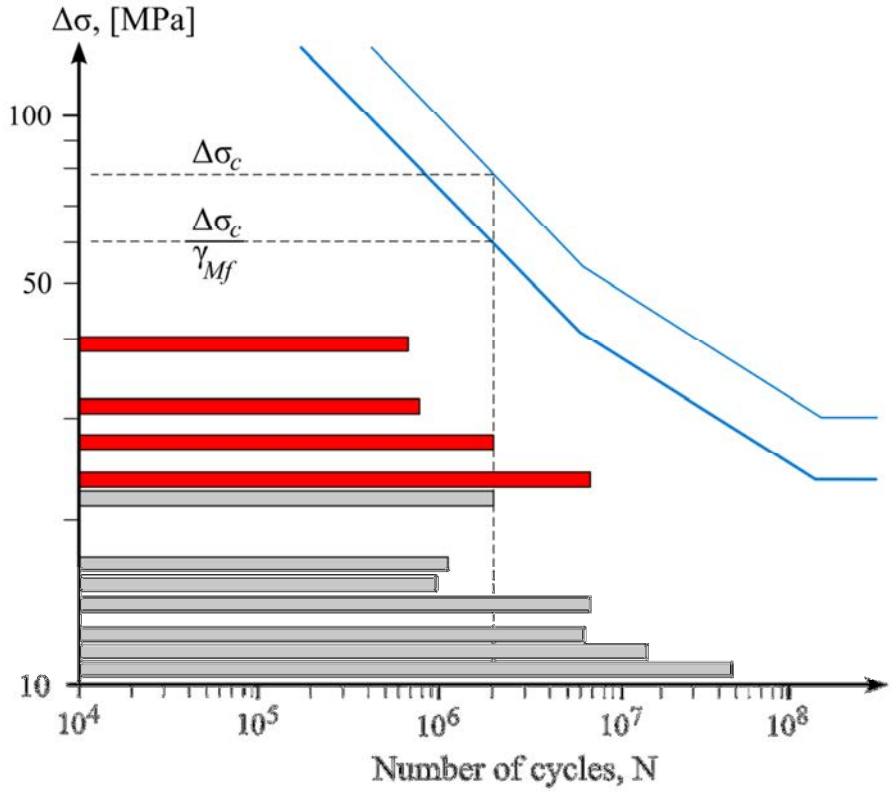

Figure 4-17 The stress histogram along with the S-N curve relevant for Detail 1

Comment: *TRVK Bro 11:085* specifies in Table B.3.4.1.5 train compositions which differ from those defined in *EN 1991-2:2003* for railway traffic, see Section 3.8. Three alternative models are given:

1. ***Bridges that are designed with α = 1,33***. The traffic mix shown in Table 4-12 should be used:

Table 4-12 Traffic mix med axial load ≤ 25tonne according to TRVK Bro 11

Train type	***Number of trains per day***	***Total mass*** *[ton]*	***Traffic volume*** *[ton/year]*
1	12	663	$2{,}90 \cdot 10^6$
2	12	530	$2{,}32 \cdot 10^6$
3	5	940	$1{,}72 \cdot 10^6$
4	5	510	$0{,}93 \cdot 10^6$
5	7	2160	$5{,}52 \cdot 10^6$
6	12	1431	$6{,}27 \cdot 10^6$
11	7	1135	$2{,}91 \cdot 10^6$
12	6	1135	$2{,}49 \cdot 10^6$
	66		***$25{,}06 \cdot 10^6$***

2. ***Bridges that are designed with α = 1,60***

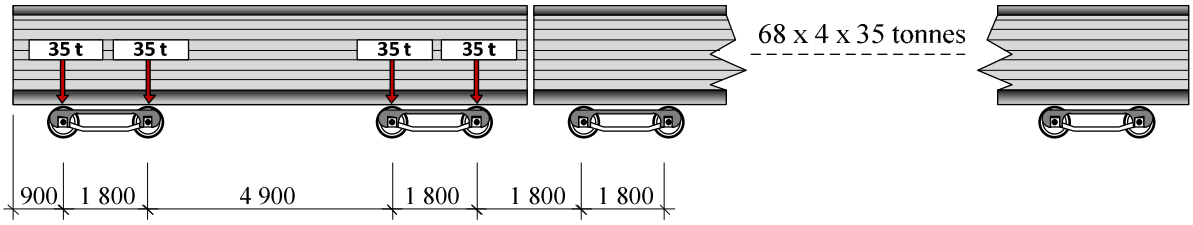

Figure 4-18 Train load model 13S and axle loads according to TRVK Bro 11:085

For this case, train load model 13S should be used. This model is composed of 68 wagons per train, each with a mass of 140 tonnes, see Figure 4-18. The number of trains per day is set to 10 in *TRVK Bro 11:085* and the total traffic volume per year is $34{,}70 \cdot 10^6$ tonnes. The train is assumed to cross the bridge with a maximum velocity of 60 km/h.

In Table 4-13, the damage accumulation calculations have been performed with the traffic mix given in *TRVK Bro 11:085*. As expected the results are very similar to those obtained previously in Table 3.15.

Table 4-13 Damage calculation with the traffic mix given in TRVK Bro 11:085

Detail	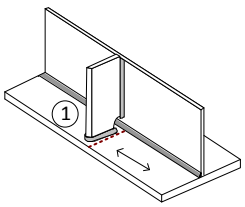	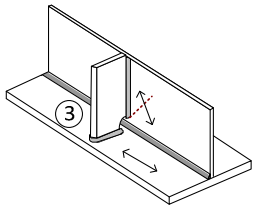	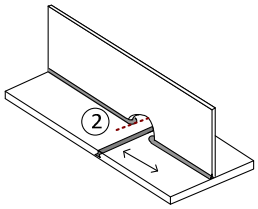
D_{LM1}	0,1203	0,1568	0,0489
D_{LM2}	0,0200	0,0337	0,0091
D_{LM3}	0,0428	0,0752	0,0036
D_{LM4}	0,0158	0,0278	0,0047
D_{LM5}	0,0928	0,1255	0,0461
D_{LM6}	0,2026	0,3407	0,0917
D_{LM11}	0,1291	0,1793	0,0473
D_{LM12}	0,0473	0,0620	0,0130
D_{tot}	0,670	1,000	0,260
D_{λ}	0,753	0,975	0,389

On the other hand, damage calculation with train model 13S gives very low damage factor for Detail 1. Owing to the arrangement of the axles in this load model, there will be one loading cycle per train passage over the bridge, see Figure 4-19.

The total number of cycles during the 120 year design life of the bridge is thus:

n = 10 x 356 x 120 = 427 200 cycles

with a moment range of 6 050 kNm corresponding to a stress range of 65,3 MPa for the detail studies.

The total number of loading cycles causing failure of the detail is:

$$N = 5 \cdot 10^6 \left(\frac{\Delta\sigma_D / \gamma_{Mf}}{\Delta\sigma_p \, \gamma_{Ff}} \right)^m = 1\,500\,000$$

and the total damage for this detail is:

D = 0,285

This is much lower than *D = 0,670* previously calculated for the traffic mix.

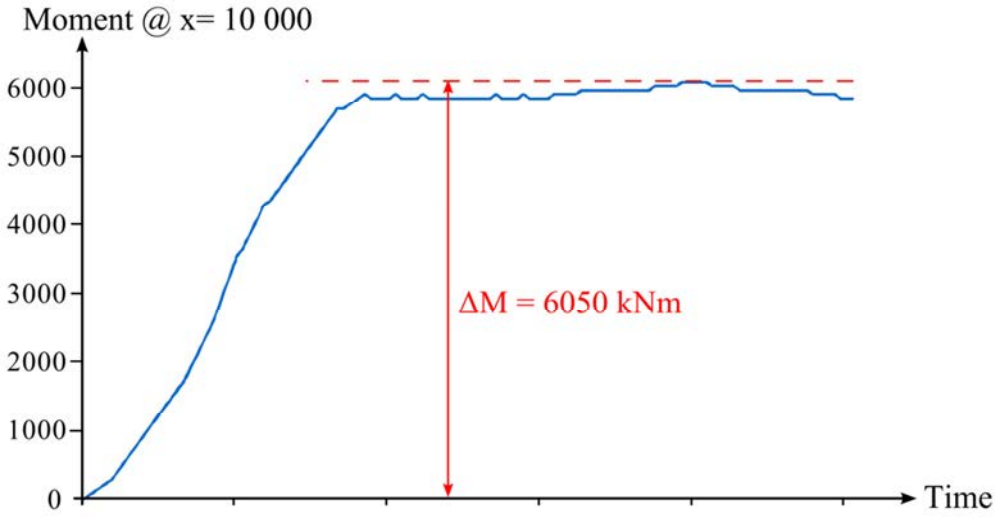

Figure 4-19 The response of the bridge with reference to Detail 1 and train load model 13S. Train model position giving maximum load effect at the studied detail is also shown

5 Fatigue design using the structural hot-spot stress method

5.1 Introduction

The structural hot-spot stress method has been developed to enable evaluating the fatigue strength of welded structures in cases where the nominal stress is hard to estimate because of geometric and/or loading complexities. This method has been used in the fatigue design of pressure vessels and welded tubular structures since 1960s. The method was later on transferred to non-tubular welded joints in ships and FPSOs (Floating Production, Storage and Offloading units) [12-14] and has finally become a codified procedure for evaluating the fatigue life of welded structures. The philosophy of the structural hot-spot stress method is base the fatigue verification on the structural/geometric stress at the point of crack initiation (usually a weld toe), the so called hot-spot points[3]. The calculated stress will, thus, include the geometrical stress concentrations generated by the geometry of the detail, as well as any local load redistribution effects, such as those caused by shear lag or warping.

The major advantage of the structural hot-spot stress approach is that the "global" stress raising effects caused by the geometry of the detail are implicitly taken into account in the stress calculations. One consequence of this is that the number of *S–N* curves needed for fatigue evaluation with the structural hot-spot stress method is substantially reduced, which is another advantage of this method.

An illustrative example that explains the principle difference between the conventional nominal stress method and the structural hot-spot method is shown in Figure 5-1. While six different detail categories are needed to describe the fatigue strength of a simple non-load carrying attachment, based on different geometrical parameters, only one fatigue category is needed when the structural hot-spot stress method is applied. The effect of the stress concentration caused by the geometry of the detail is – in the case of the structural hot-spot stress method – accounted for on the load-effect side, while in the nominal stress method this effect is covered on the resistance side (by assigning different fatigue categories).

[3] These points also called reference points, i.e. the critical points in the vicinity of the weld toe; the hot-spots points.

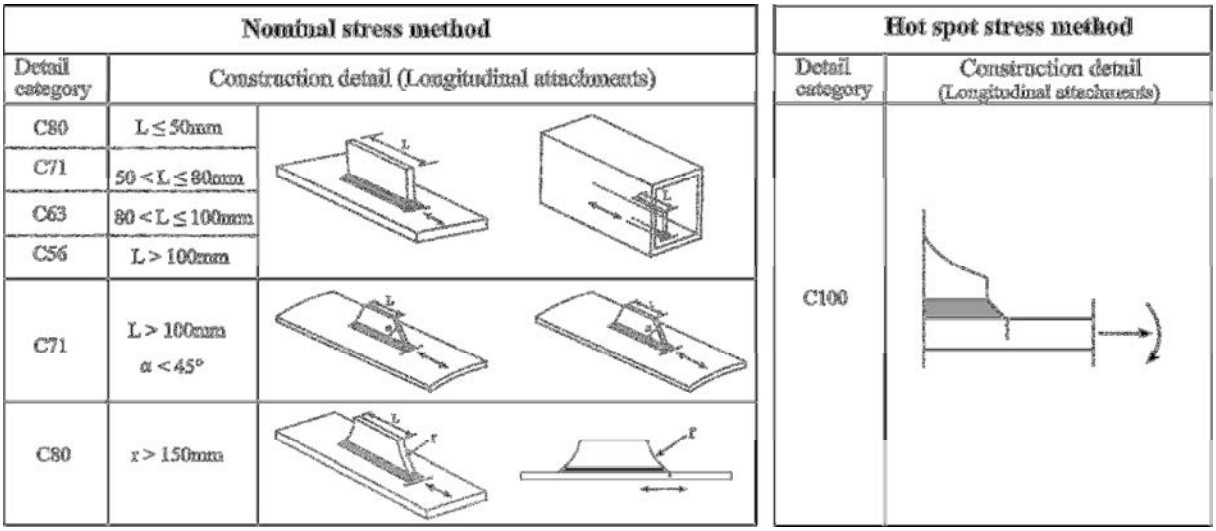

Figure 5-1 Fatigue class recommendations based on the nominal and the structural hot-spot stress methods acc. to EN 1993-1-9:2005

The benefit of the structural hot-spot stress method (and any other method which gives more accurate estimation of load effects) is clearly seen in complex details and in details with complex load situations. On a more global level, load effects such as shear lag effects, normal stresses due to torsion and warping and flange curling might be substantial and are often hard to estimate in real complex structures. Even more difficult to estimate and capture are local stress concentrations that result from local flexibilities and abrupt change in stiffness (Figure 5-2 (a) and (b)) and details with local force transfer such as the detail shown in Figure 5-3 (c).

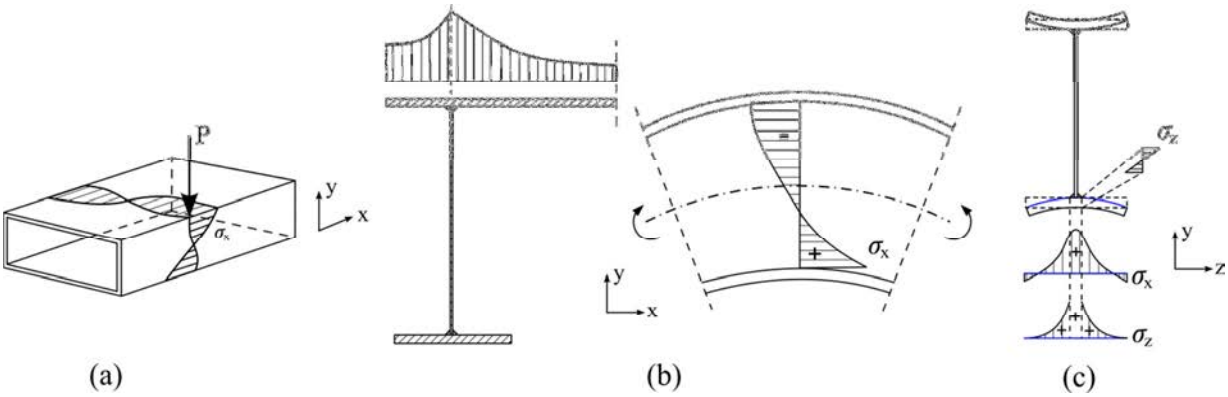

Figure 5-2 Global: a) Warping effects; b) shear-lag effects; c) Curvature and flange curling effects

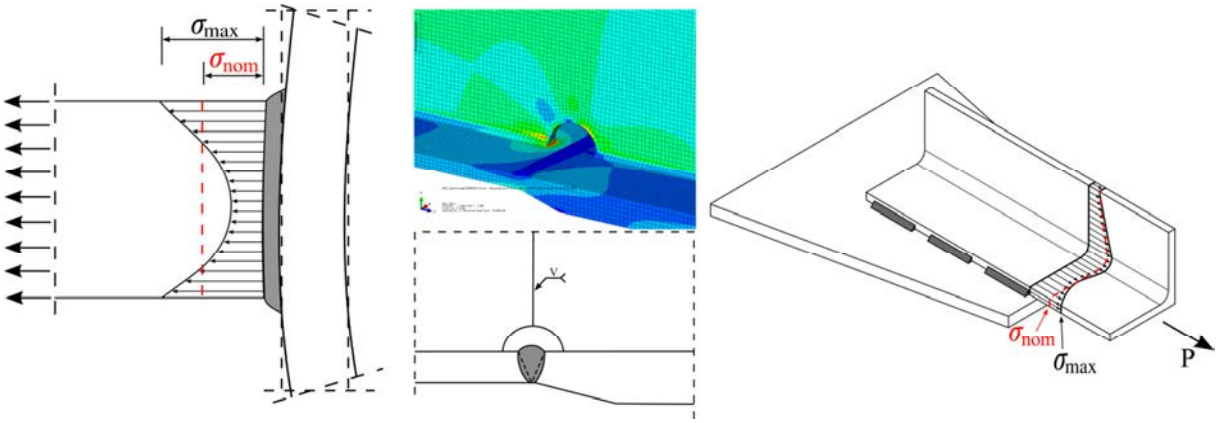

Figure 5-3 Local: a) flexibility/local deformation; b) local force transfer; c) local flange bending at thickness transition.

The structural hot-spot stress is usually derived from finite element models of the structure or the structural element or detail under consideration. Therefore, both global and local stress affects, such as those mentioned above are directly and accurately accounted for in the calculation of load effects. These effects might be substantial even in elements with relatively simple geometry and – for fatigue loaded structures – might be determinant for the fatigue performance of the structure. An illustrative example is shown in Figure 5-4. The welded I-shaped bridge hanger suffered fatigue cracking derived by the "secondary" stresses in the hanger web and flanges. The stresses – which were generated by the change in cross-section depth close to the hanger connection – are rather hard to predict with conventional hand-calculations, but are easy to capture and account for in FE-analysis.

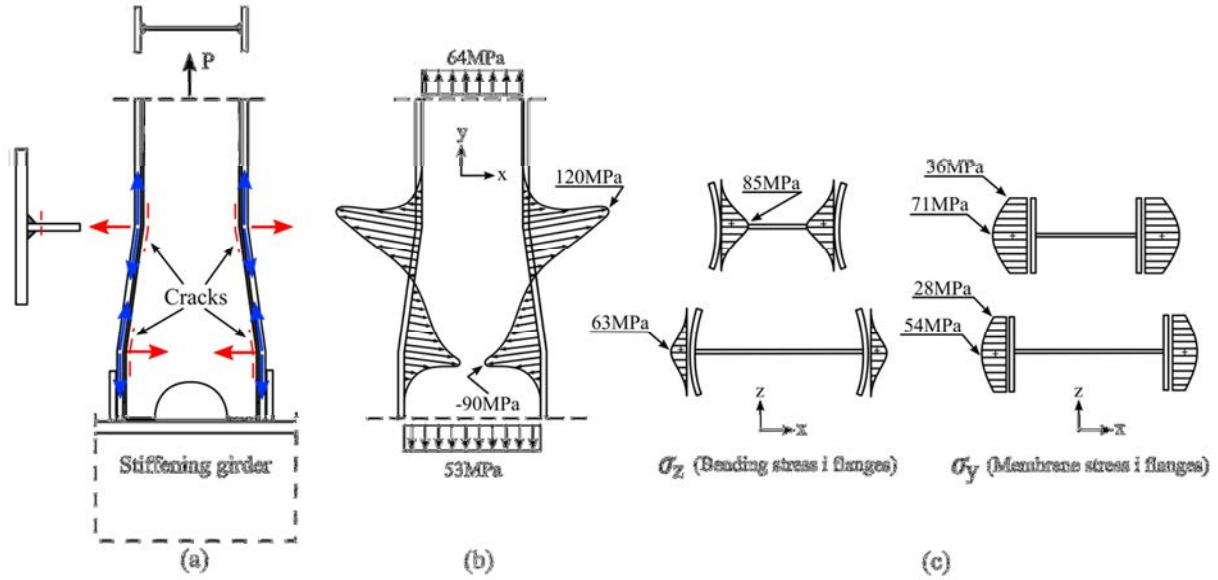

Figure 5-4 Example of fatigue cracks in bridge hanger due to unforeseen or overlooked load effects: a) Cracks locations, b) principle stress in the plane of the web, c) bending stresses in the flanges due to flange curling effects [15]

5.2 Principles of the structural hot-spot stress method

The **fatigue strength** of any welded detail is, basically, a function of three main parameters:

1. The stress concentration effects caused by detail geometry, also called geometric discontinuities
2. The local stress raising effects caused by the shape and dimensions of the weld and the surrounding region
3. Local weld defects such as undercuts, porosities, lack of fusion and similar

When fatigue verification is performed with the conventional nominal stress method, all these parameters are accounted for on the fatigue strength side, i.e. in the process of selection of a suitable S-N curve. Thus, as was mentioned in connection to Figure 5-1 above, the same structural detail can be assigned different S-N curves based on the parameter (or parameters) that govern the fatigue strength of that detail. Only nominal stresses are therefore needed in the fatigue verification.

On the contrary, the stress range used in fatigue design with the structural hot-spot stress method already includes the stress raising effects, emanating from geometrical discontinuities and/or caused by complex loading conditions (point 1 above). Including the stress raising sources in the design stress calculations leads to the main advantage of the structural hot-spot stress method for welded structures. The S-N curves to be used with this method need only to cover the local stress raiser effects and the local weld defects in different welded details, which require only a few S-N curves. However, local stress effects due to the weld itself (point 2 above), are excluded in the derivation of the hot-spot stress and need to be accounted for on fatigue resistance side.

Figure 5-5 shows a simple detail with the stress distribution in front of the weld toe at the location of anticipated crack initiation. The stress in the main plate at this location is composed of: 1) nominal membrane stress; 2) bending stress caused by the geometry of the detail; and 3) a non-linear stress part caused by the weld shape and local weld geometry. Following the definition of the hot-spot stress, excluding the non-linear local stress results in a combination of membrane and bending stresses which together give the hot-spot stress in the detail.

It is worth pointing out again here, that if the hot-spot stress in the detail shown in Figure 6-5 is obtained from a finite element analysis, the effects of all essential geometric parameters on the stress in the detail are directly and more accurately accounted for (width of main plate, shape, length and thickness of attachment, etc.).

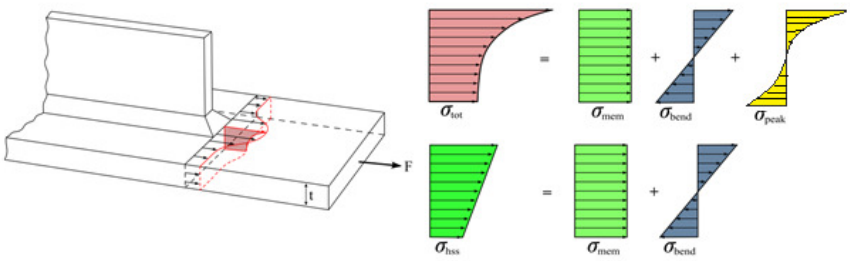

Figure 5-5 Stress distribution in front of weld toe and definition of the structural hot-spot stress

The calculation of the structural hot-spot stress should be performed assuming linear elastic material behaviour. Since the structural hot-spot stress – per definition – is to be calculated at the point of crack initiation (i.e. at weld toe), the method meets the problem of stress singularity at these sharp points. The "correct" theoretical value of the stress at the weld toe is infinity. It is with reference to this problem various stress linearization techniques are proposed to exclude the non-linear stress component close to the weld toe. These techniques are discussed in more details in the next section.

5.3 Structural hot-spot stress determination in welded details

Figure 6-6 shows a "generic" welded detail. For the sake of determining the structural hot-spot stress, one should distinguish between two types of "hot-spots", Type "a" and Type "b". The main difference between these two types is seen in the stress distribution through the thickness of the plate with anticipated cracking. While the stress in Type "a" hot-spots varies substantially through the thickness of the cracked plate (see also Figure 6-5), it is more uniform in Type "b" hot-spots. It follows that a linearization of the stress in Type "a" details should consider the plate thickness as a parameter, while the linearized hot-spot stress in Type "b" details is insensitive to the plate thickness.

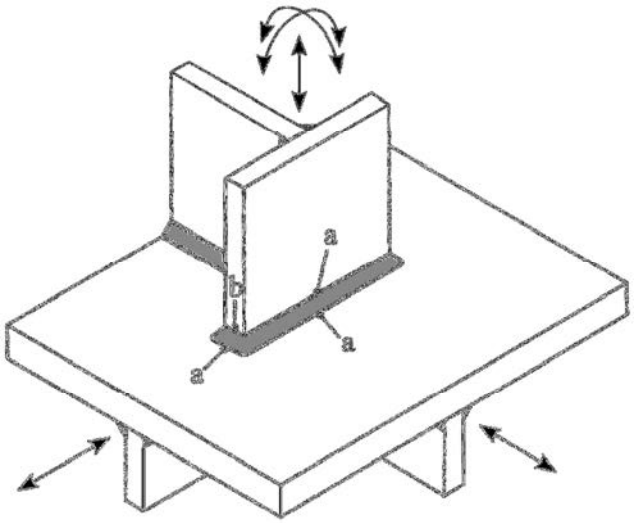

Figure 5-6 Fatigue-critical hot-spot points at weld toes proposed by Fricke [16]

In general, the design value of stress range for fatigue verification with the structural hot-spot stress method can be obtained using one of the following methods:

1. Analytically, using stress concentration formulas for specific details
2. Numerically, using FEM or other numerical methods
3. Experimentally, by measuring the strains in specific reference points.

In all three cases, some kind of stress linearization is needed to exclude the non-linear peak stress, as was mentioned before.

The main disadvantage of analytical formulas is their limited applicability. Even though stress concentration formulas for calculating the structural hot-spot stress are wide spread in the literature, these are usually applicable to the particular detail in hand within specific geometrical and dimensional limits.

Determination of the structural hot-spot stress from testing was the main technique used when the method evolved some decades ago. Today, with the wide spread of the finite element method for analysis and design of structures, numerical calculations of the stresses in welded details is by far the most common way of performing fatigue design and analysis using the finite element method. Therefore, while analytical determination of the stress concentration factors for fatigue evaluation with the structural hot-spot stress method is omitted from this document, the main effort is devoted to numerical procedures based on the finite element method. Determination of the structural hot-spot stress from experiments is presented shortly in Section 5.3.2.

5.3.1 The determination of the structural hot-spot stress using FEM

The most conventional procedure to determine the structural hot-spot stress in welded steel structures is using a finite element analysis.

FE models can be constructed with thin/thick shell elements or alternatively solid elements. Models composed with shell elements are fairly simple to construct. The elements should be positioned in the mid-plane of the plates in the structural elements, see Figure 5-7 (a). The welds are usually not modelled except for special cases where the results are affected by high local bending, e.g. due to an offset between plates or due to a small free plate length between adjacent welds such as at lug (or collar) plates, see Section 6.6.2 for more details.

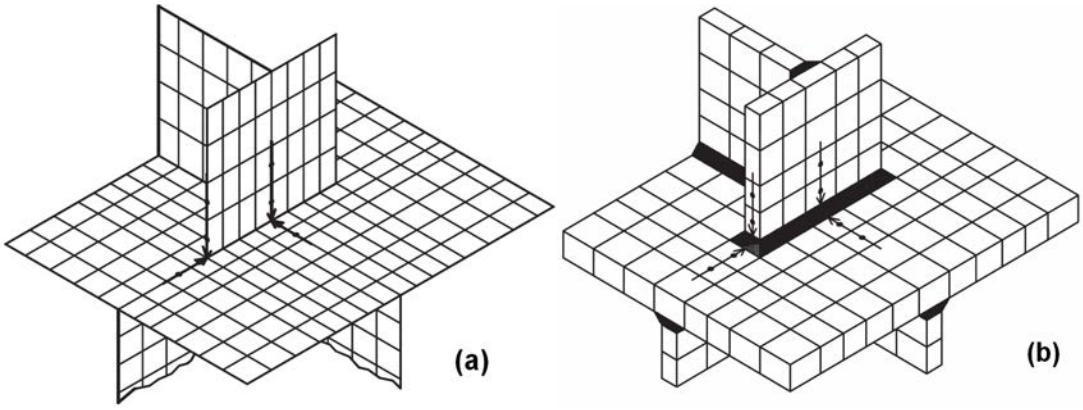

Figure 5-7 Three-dimensional FE modelling (a) Shell model (b) Solid model including weld

Solid elements are particularly recommended for modelling complex details. FE models with solid elements can be created using isoparametric 20-node solid element. In this case, only one element is needed over the plate thickness. Since the modelling of the welds with solid modelling is easily incorporated, it is generally recommended to include the welds in FE models with solid elements, see Figure 5-7 (b).

For the purpose of fatigue verification with the hot-spot stress method, FE models are generally created assuming ideal geometry of the structural detail. Possible unintended misalignments and other type of imperfections are indirectly covered on the resistance side, i.e. in the S-N curves. S-N curves for the hot-spot method are derived from statistical analysis of test data where imperfections – within specific limits – exist in the test specimens. Other geometrical imperfections or misalignments outside the range of what is covered by the S-N curves should be accounted for, either directly in the model, or by employing a relevant stress concentration factor.

The use of the finite element method for determining hot-spot stresses requires good understanding of the principles of the FEM and the philosophy behind the structural hot-spot stress method. The result from FEA can be highly mesh sensitive, since the structural hot-spot stresses are often in an area of high strain gradients, i.e. stress singularities. The stress values obtained from FE programs may also differ depending on element size and type and whether or not the welds are represented in the model. It is therefore necessary to establish ***consistent procedures*** for the determination of the structural hot-spot stress in welded details, so that a correct correlation is obtained between calculated stresses and fatigue lives for these details. This modelling and mesh dependency is the main disadvantage of the structural hot-spot stress approach.

The recommendations provided by the International Institute of Welding, IIW [17] supplies the most comprehensive rules for the application of structural hot-spot stress method. *EN 1993-1-9:2005* [18] also allows the application of this method for fatigue verification of welded structures. However, apart from a list of structural details with the corresponding fatigue design curves, *EN 1993-1-9.2005* provides no recommendations or instructions, regarding the application of the method, i.e. modelling and extrapolation techniques and type of hot-spots points.

One major feature which is always needed in the calculation of the structural hot-spot stress from FE model (irrespective of the details of the FE model) is the process of ***stress linearization***. This process is necessary in order to separate the membrane and bending stress components in the detail from the non-linear stress peak generated by the local weld geometry (See Section 5.2).

Commonly stress linearization is performed by means of ***stress extrapolation*** from specific points at some distance away from the region affected by high local stress gradients. Usually ***surface stress extrapolation*** is employed. In some special cases, a linearization of stress through the thickness might be needed to obtain more accurate results. To start with, stress extrapolation techniques will be presented in the following sub-sections. Some alternative stress determination methods are then presented and discussed in Section 6.5.

5.3.1.1 Linear stress extrapolation

The linear surface stress extrapolation technique involves reading out the nodal stresses at two reference points and then using these stress values to extrapolate a value for the structural hot-spot stress at the weld toe. This is the most common procedure[4] to derive the hot-spot stress from FE analysis. The notch stress (nonlinear stress) due to the weld itself is excluded through the linear extrapolation of surface stress from the two reference points, which should be located outside the region affected by the local weld geometry. Extensive strain measurements and FE analysis of welded details show that the non-linear notch stress effects usually diminish a small distance away from the weld toe. This distance was seen to be a function of the plate thickness, around 0,3t[5].

Linear surface stress extrapolation can be used for welded details with type “a” or type “b” hot-spots. The location of the two reference points for stress extrapolation is however different for these two types. The location of stress extrapolation points is also dependent on the mesh density in FE models. More details regarding the

[4] Recommended by most design codes and regulations; IIW, DNV, ABS, GL, AWS
[5] Haibach measured the stress at this point by assuming that the stress at his point is free from the notch stress

discretization of FE models, selection of mesh density and element types will be given in Section 5.6 "*Recommendations for finite element modelling*"

Figure 5-8 shows the position of stress extrapolation points for type "a" hot-spots s in FE-models with "fine" respectively "coarse" mesh. The two reference points on the stress curve are located normal to the weld toe. The first reference point closest to the weld toe is positioned at 0,4t or 0,5t in models with fine respectively coarse mesh. These values are selected in order to include the effect of detail geometry, but exclude the effect of the notch stress due to the weld profile as mention before. The second point is positioned at 1,0t or 1,5t from the weld toe, which is accepted as the point where the effect of geometric features of the detail will diminish.

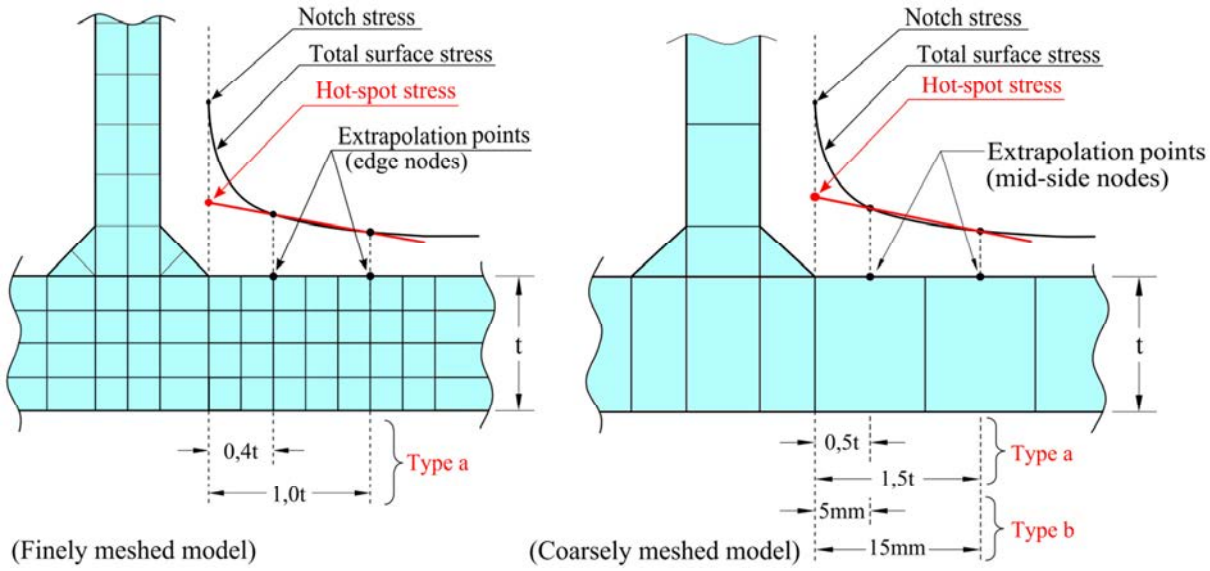

Figure 5-8 Linear extrapolation of the hot-spot stress from fine and coarse mesh model

For fatigue critical points located at the plate edges (type b), the same surface stress extrapolation procedure can be used, but with different locations for the reference points. Here, the stress is uniform through the thickness of the plate and therefore the location of the extrapolation points is no longer a function of plate thickness. For linear extrapolation, it is recommended to use the reference points located at 5 respectively 15mm in front of the weld toe for coarsely meshed models. For structural details with type "b" hot-spots, the extrapolation recommended for FE models with fine mesh is the quadratic extrapolation, which is treated in the next section.

It should be observed that the properties of the finite element model (i.e. element size and element type) usually influence the derived stresses in the hot-spot region. Therefore, the mesh – whether coarse or fine – should comply with the rules of stress extrapolation. For example, FE models with coarse mesh will usually have one quadratic FE element through the thickness of the plate. The stress extrapolation points are thus found at the element intermediate nodes as shown in Figure 5-8 (b). Recommendations regarding meshing techniques and selection of suitable element types will be given in Section 5.6 "*Recommendations for finite element modelling*"

5.3.1.2 Quadratic (non-linear) stress extrapolation

In some specific cases, linear extrapolation may lead to non-conservative results and the more accurate method with quadratic (non-linear) surface stress extrapolation

procedure is recommended. A typical example is found in welded details where the stress distribution is strongly non-linear near the weld toe due to geometric complexities or/and local loading conditions. Further examples of details for which quadratic stress extrapolation is recommended will be presented in Section 5.6 "*Recommendations for finite element modelling*"

Three reference points are required for obtaining the structural hot-spot stress with quadratic extrapolation. As for linear extrapolation, the locations of these reference points is different for type "a" and type "b" hot-spots, see Figure 6-10. For "type a" hot-spots, the reference points should be located at 0,4t, 0,9t and 1,5t from the weld toe, again being dependent on the thickness of the cracked plate. For details with "type b" hot-spots, the reference points have constant distances; 4, 8, 12mm from the weld toe. Apparently, the above mentioned reference points require finely meshed FE models. In order to obtain sufficiently accurate stresses at the extrapolation points the element mesh close to the weld toe must be sufficiently fine and the reference points must be coincident with element edge nodes. The stress values at the reference points are the surface stresses at the nodes, i.e. nodal stress (nodal stress values are the averaged values of stress at each element edge nodes).

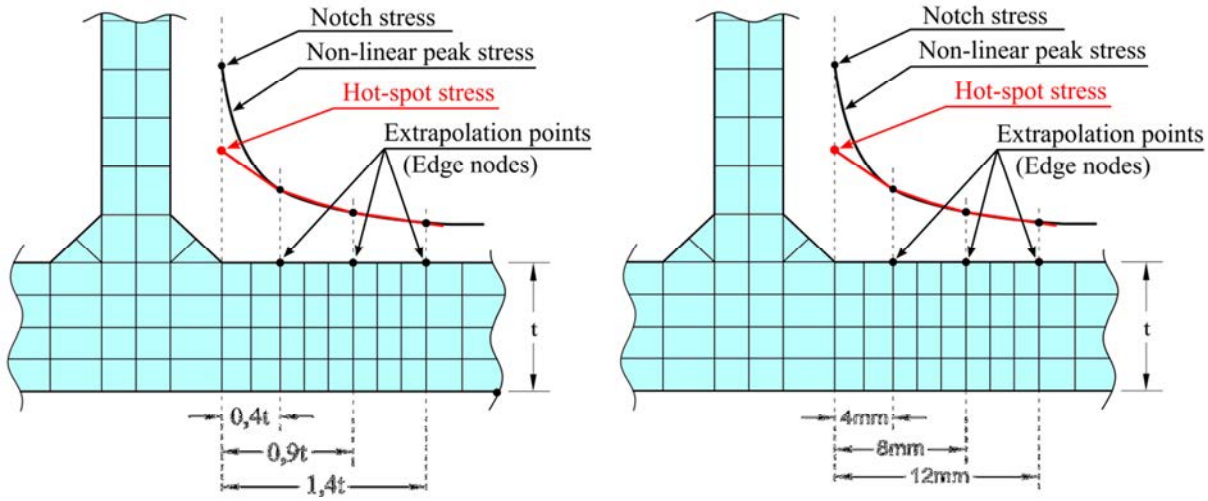

Figure 5-9 Quadratic stress extrapolation of structural hot-spot stress acc. to IIW

To summarize, Table 5-1 below presents the linear and quadratic surface stress extrapolation rules for "type a" and "type b" hot-spot points and for FE models with fine and coarse mesh. The values in Table 6-1 are consistent with those given in the IIW recommendations [17].

Table 5-1 Surface stress extrapolation at the weld toe recommended by IIW

Type of hot-spots point	***Linear extrapolation***		***Quadratic extrapolation***	
	Fine mesh	***coarse mesh***	***Fine mesh***	***coarse mesh****
Type a	0,4t and 1,0t	0,5t and 1,5t	0,4t, 0,9t and 1,4t	0,5t, 1,5t and 2,5t
	$1{,}67\sigma_{0{,}4t} - 0{,}67\sigma_{1{,}0t}$	$1{,}5\sigma_{0{,}5t} - 0{,}5\sigma_{1.5t}$	$2{,}52\sigma_{0{,}4t} - 2{,}24\sigma_{0{,}9t} + 0{,}72\sigma_{1{,}4t}$	$1{,}875\sigma_{0{,}5t} - 1{,}25\sigma_{1{,}5t} + 0{,}375\sigma_{2{,}5t}$

Type b	--	5mm and 15mm	4, 8 and 12mm	--
	--	$1{,}5\sigma_{5mm} - 0{,}5\sigma_{15mm}$	$3\sigma_{4mm} - 3\sigma_{8mm} + \sigma_{12mm}$	--

** This recommendation is given in another IIW document, see reference [19].*

5.3.1.3 One point stress determination

Besides the two common stress extrapolation techniques, a simpler approach has been suggested by Fricke [20]. Here the value of the structural hot-spot stress is directly read from one point, 0,5t away from the weld toe. Neither extrapolation nor integration (as in other techniques covered in Section 6.5) is needed. Previous studies have shown promising results when the one point stress method was used to evaluate available fatigue test results. For example a smaller scatter was observed in test results when the stress in these tests was calculated with this method in [20] and [21]. It is however shown that, in order to get a good fit to fatigue test results, the structural hot-spot stress obtained from the one-point stress determination method should be magnified with a factor of 1,12. This is equivalent to one S-N curve reduction (i.e. from 90 to 80 or from 100 to 90).

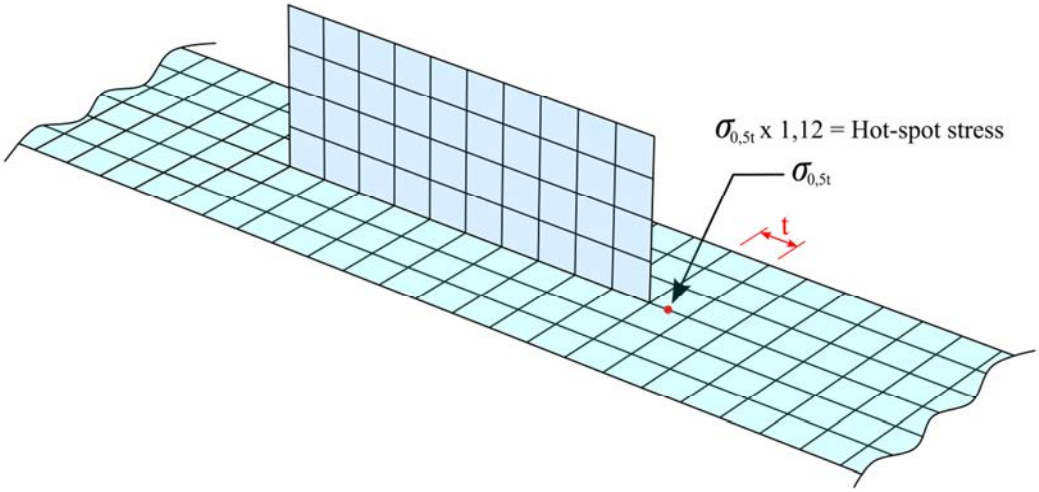

Figure 5-10 One point structural hot-spot stress determination

When a finite element analysis is performed using a model with element size of $t \times t$ *(t=plate thickness)*, which is normally practical for structure analysis, the point at a distance of *0,5t* from weld toe is a useful validation. The stress at this point located in the mid-element side of a second order element can be directly read out from the FE-model.

5.3.2 Determination of the structural hot-spot stress from measurements

Fatigue design and analysis with the structural hot-spot stress method was originally developed to be applied in conjunction with strain measurements. These strain measurements can be performed either in field to verify the fatigue strength of existing steel structures, or in laboratory on fatigue test specimens to verify the fatigue strength of steel details. In both cases, it is usually rather hard to determine proper locations for the strain gauges so that the measured strains are “pure” nominal strains,

i.e. excluding the effect of geometric discontinuities in the detail. The concept of the structural hot-spot stress evolved to solve this particular problem

Analogous with the procedures described before for the determination of the structural hot-spot stress from FE models, the hot-spot stress can be obtained from measurements using either linear or quadratic extrapolation of the measured strain. The distances at which the strain gauges are positioned obey the same rules presented in ~~Table 6-1~~ Table 5-1 above; see also Figure 5-11~~Figure 6-11~~.

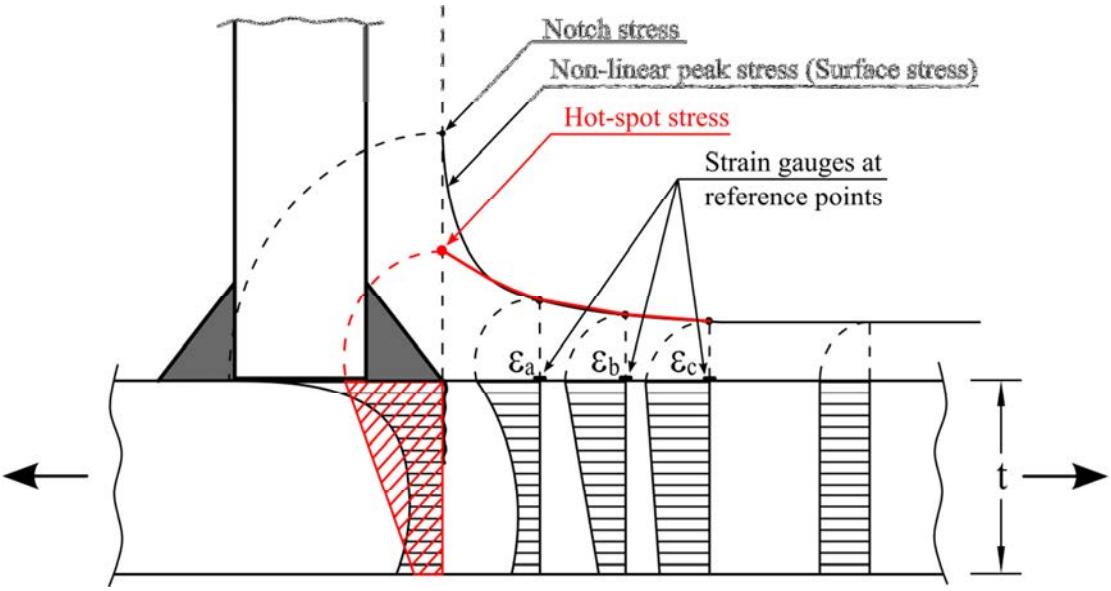

Figure 5-11 Experimental structural hot-spot stress determination using strain gauges

The IIW recommends using quadratic strain extrapolation in certain cases where the stress in the extrapolation region can be strongly non-linear, such as a plate resting on a relatively stiff elastic foundation. In these cases the strain gauges should be placed at 0,4t, 0,9t and 1,4t from the weld toe for "type a" hot-spots s and 4mm, 8mm and 12mm from the weld toe for "type b" hot-spots.

It is worth pointing out here that when the structural hot-spot stress is to be determined from strain measurements, the type and orientation of the strain gauges should be considered thoroughly. While single grid strain gauges give sufficient accuracy in many details, rosettes will usually be needed in details with biaxial state of stress. Here, both the value and the direction of the maximum principle stress (in relation to the weld toe) need to be determined from the measurements.

5.3.3 Determination of the structural hot-spot stress in biaxial stress state

In case of biaxial stress state in a fatigue critical region, The IIW recommends using the maximum principal stress if the stress direction is not changing significantly over the loading cycle (i.e. proportional loading) and only if the stress acts within ±60° with reference to the normal on the weld [17]. In other cases, the stress perpendicular to the weld toe line (normal stress) should be used, see Figure 5-12.

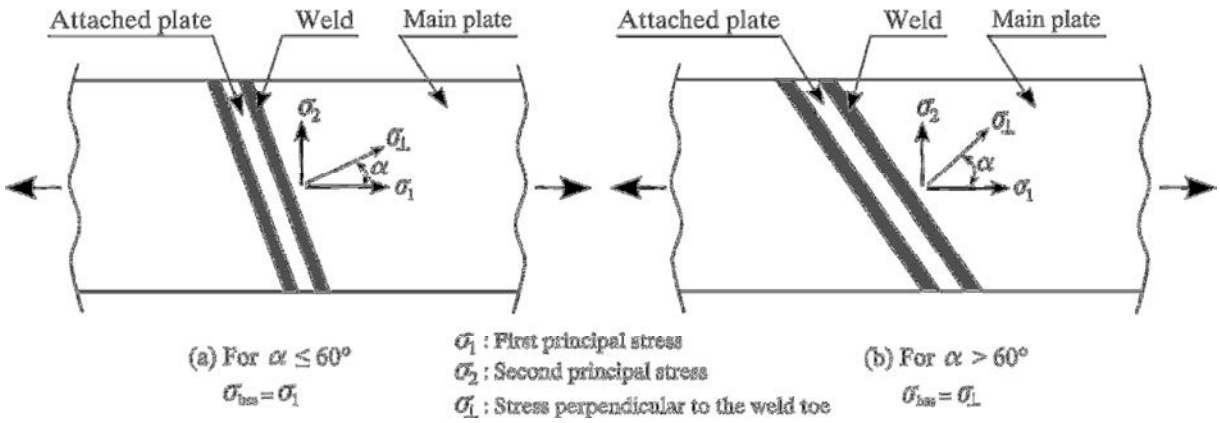

Figure 5-12 Structural hot-spot stress at the weld toe for biaxial stress state

5.4 Fatigue verification with the structural hot-spot stress method

Fatigue verification of welded details using the structural hot-spot stress method follows the same procedure applied in the nominal stress method. Of course, following the fact that the fatigue load effects are different in these two methods, different S-N curves have also to be used when the hot-spot method is applied. A fatigue strength class is a logarithmic relationship between stress range, $\Delta\sigma$, and number of stress cycles, N, to failure. The fatigue classes given in *EN 1993-1-9:2005* for the use with the structural hot-spot stress method are similar to the nominal stress based S-N curves, with the same slope and limit for constant amplitude fatigue loading (CAFL), i.e. a line with constant slope of 3.0 in logarithmic scale and a CAFL at 5 million cycles. Figure 5-13 shows the three S-N curves to be used in fatigue verification with the structural hot-spot stress method, with fatigue strengths of 90, 100 and 112MPa.

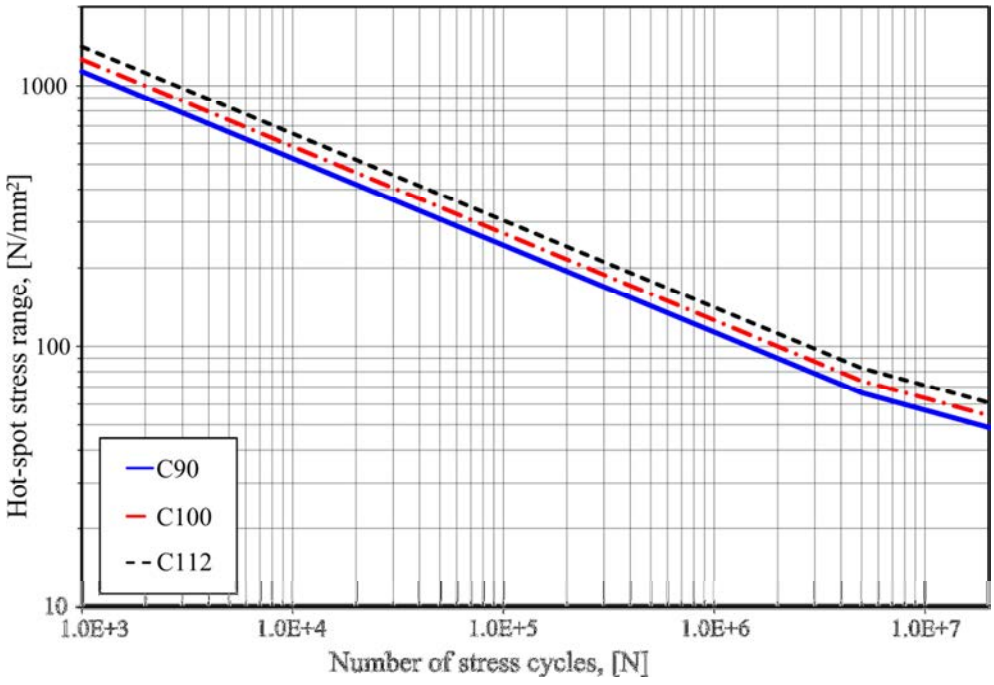

Figure 5-13 Structural hot-spot stress based S-N curves recommended by EN 1993-1-9:2005

The structural hot-spot stress is defined by *EN 1993-1-9:2005* [18] as the maximum principal stress in the plate where toe cracking is anticipated, taking into account the stress concentration effects due to the overall geometry of a particular constructional detail. Besides the detail categories for the structural hot-spot stress method, which are reproduced in ~~Table 6-2~~ Table 5-2, Eurocode provides no information or recommendations as to how the structural hot-spot stress in welded details should or can be determined. In that respect, a detailed – and widely used – set of rules and recommendations is provided by the IIW document "*Recommendation for fatigue design of welded joints and components*" [17].

Table 5-2 Detail categories for the structural hot-spot stress method according to EN 1993-1-9:2005 [18]

Detail category	Constructional detail	Description	Requirements
112	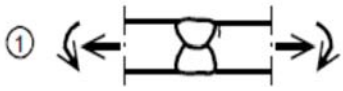	1) Full penetration butt joint.	1) - All welds ground flush to plate surface parallel to direction of the arrow. - Weld run-on and run-off pieces to be used and subsequently removed, plate edges to be ground flush in direction of stress. - Welded from both sides, checked by NDT. - For misalignment see NOTE 1.
100	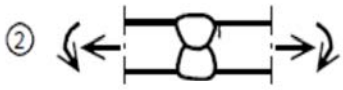	2) Full penetration butt joint.	2) - Weld not ground flush - Weld run-on and run-off pieces to be used and subsequently removed, plate edges to be ground flush in direction of stress. - Welded from both sides. - For misalignment see NOTE 1.
100	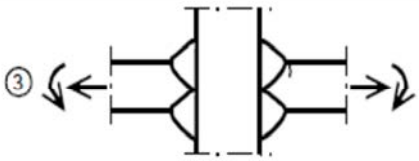	3) Cruciform joint with full penetration K-butt welds.	3) - Weld toe angle ≤60°. - For misalignment see NOTE 1.
100	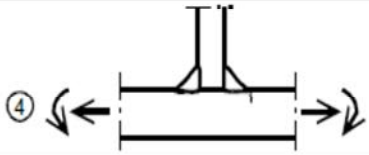	4) Non load-carrying fillet welds.	4) - Weld toe angle ≤60°. - See also NOTE 2.
100	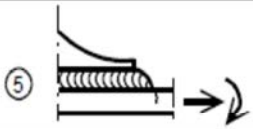	5) Bracket ends, ends of longitudinal stiffeners.	5) - Weld toe angle ≤60°. - See also NOTE 2.
100	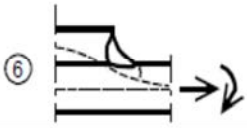	6) Cover plate ends and similar joints.	6) - Weld toe angle ≤60°. - See also NOTE 2.
90	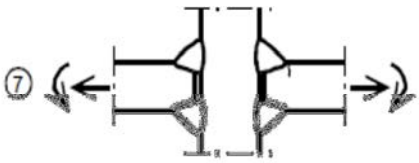	7) Cruciform joints with load-carrying fillet welds.	7) - Weld toe angle ≤60°. - For misalignment see NOTE 1. - See also NOTE 2.

It should be mentioned again that the fatigue classes given in Table 6-2 already cover the effect of unintended small misalignment and imperfections in welded joints. Guidance on allowable misalignments, depending on the type of welded detail, can be found in *EN 1090-2:2002* [22] and *ISO 5817* [23]. However, significant misalignments which reduce fatigue strength due to secondary bending stress must be considered explicitly during the stress determination stage. The correlation of the structural hot-spot stress due to the misalignments is described in more detail in Chapter 5.4.2.

According to EN 1993-1-9:2005, the fatigue life of a welded joint can be estimated by following the fatigue life calculation procedure shown Figure 5-14:

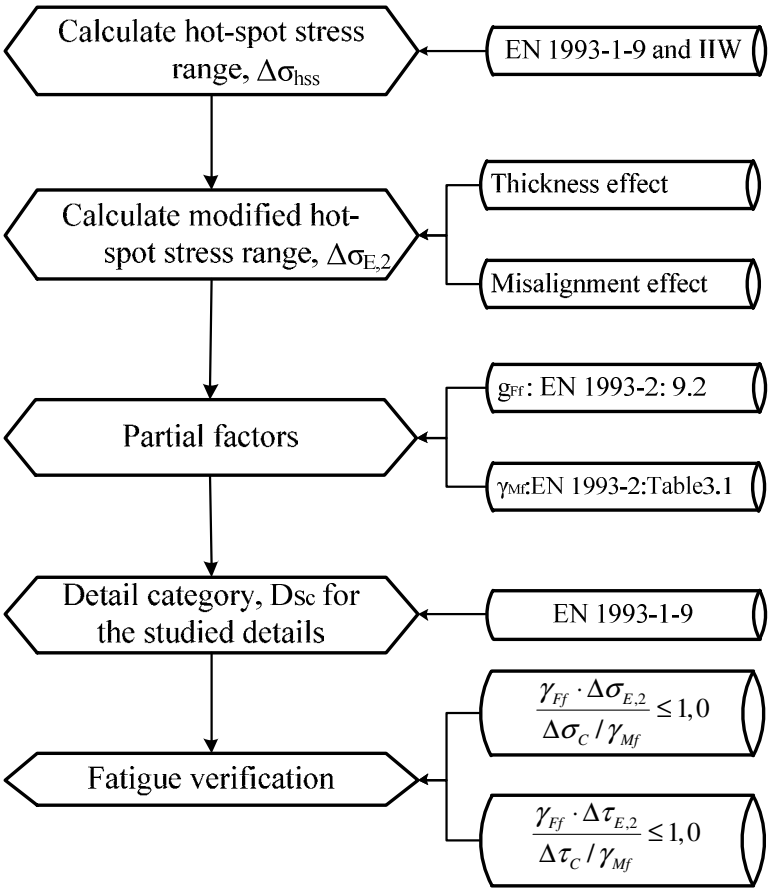

Figure 5-14 Flow chart for fatigue life estimation using the structural hot-spot stress method

According to EN 1993-1-9:2005, the following criteria should be verified when using the structural hot-spot stress method:

$$\frac{\gamma_{Ff}\cdot\Delta\sigma_{E,2}}{\Delta\sigma_C/\gamma_{Mf}}\le 1{,}0 \qquad \text{for structural hot-spot stress ranges} \qquad \textit{Eq. 5-1}$$

and

$$\frac{\gamma_{Ff}\cdot\Delta\tau_{E,2}}{\Delta\tau_C/\gamma_{Mf}}\le 1{,}0 \qquad \text{for shear stress ranges} \qquad \textit{Eq. 5-2}$$

For biaxial stress states, EN 1993-1-9:2005 requires that the fatigue life should be verified by the following criteria, *Eq. 5-3*:

$$\left(\frac{\gamma_{Ff}\cdot\Delta\sigma_{E,2}}{\Delta\sigma_C/\gamma_{Mf}}\right)^3+\left(\frac{\gamma_{Ff}\cdot\Delta\tau_{E,2}}{\Delta\tau_C/\gamma_{Mf}}\right)^5\le 1{,}0 \qquad \textit{Eq. 5-3}$$

5.4.1 Thickness correlation factor

Another effect that must be considered when using the S-N curves during the fatigue design process is the effect of plate thicknesses. As mentioned earlier, in thicker plates the stress distribution below the weld toe is less steep than it in thinner plates. According to the definition of the structural hot-spot stress approach, the stress through the thickness has a linear distribution (the sum of membrane and bending stresses), which implies that the hot-spot stress method cannot directly capture thickness effect. Therefore, a reduction factor (thickness correction factor, k_s) is generally needed if the thickness of the main plate exceeds the reference thickness when determining the fatigue design stress based on either the nominal stress or the structural hot-spot stress. *EN 1993-1-9.2005* recommends using following formulas to take into account the thickness effect:

$$\Delta\sigma_{hss,red} = k_s \cdot \Delta\sigma_{hss} \qquad \textit{Eq. 5-4}$$

$$k_s = \left(\frac{t_{ref}}{t}\right)^n \qquad \textit{Eq. 5-5}$$

where, t_{ref} is 25mm and the exponent n varies from 0.1 to 0.3 depending on the welded detail.

5.4.2 Misalignment correlation factor

S-N curves are generally derived from fatigue test results obtained from a large number of specimens which likely include some misalignments and imperfections. In *EN 1090-2:2002* [22] and *ISO 5817* [23], the limitations for axial and angular misalignments are given for various structural details and weld classes. Unintended misalignments within the standard tolerances do not need to be covered. However, for larger misalignments exceeding the allowable tolerances, the design stress should be either multiplied by a misalignment correlation factor or the misalignment should be considered in the FE model in order to take into account the stress raising effects in the design process. Stress concentration formulas for different kinds of misalignment and eccentricity can be found in many text books. Figure 5-15 and Figure 5-16 give two examples with two common cases of eccentricity and angular misalignment.

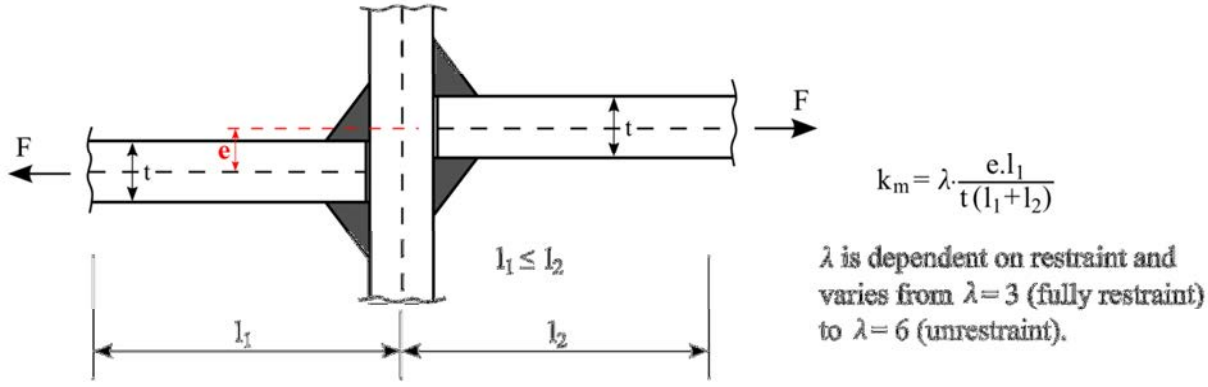

Figure 5-15 Angular misalignment of cruciform joints and correlation factor for toe cracks

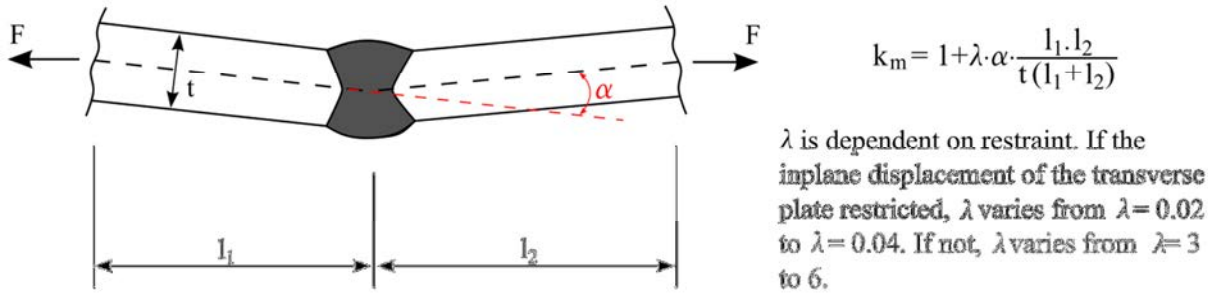

Figure 5-16 Angular misalignment of cruciform joints and correlation factor for toe cracks

5.5 Alternative structural stress approaches

The structural hot-spot stress approach is in generally a procedure of transferring the fatigue strength calculations of welded details to a semi-local analysis level where the effect of detail geometry is included in the calculation of load effects.

As stated previously, the stress distribution close to the weld toe (whether surface stress or through thickness stress) is generally highly non-linear. This stress nonlinearity has to be excluded when load effects for fatigue verification are calculated. This can be achieved either through stress extrapolation (as discussed before), or by a linearization of the stress into a combination of membrane and bending stress, see Figure 6-13. Stress linearization also means – at least in principle – that the derived structural stress becomes "mesh-insensitive" (equilibrium of forces has to be fulfilled at any section in the detail).

The concept of a linearized structural stress over the plate thickness was firstly developed by Radaj [13] and later modified by Dong at the Battelle Institute [24-26] Another, relatively new, concept for determining the structural stress has been proposed by Xiao and Yamada [27] where the computed stress value at a depth of 1mm below the surface at the weld toe is assumed to give a good representation. These alternative methods are briefly reviewed in the following sections.

5.5.1 Through-thickness structural stress approach

The through-thickness structural stress approach is based on a linearization of the stress distribution over the thickness of the plate with anticipated cracking at the location of the crack, i.e. weld toe. The stress linearization is performed utilizing the equilibrium conditions at the section of consideration, such that the integration of the nonlinear stress over the plate thickness is balanced by the membrane and bending stresses at the same section see Figure 5-17.

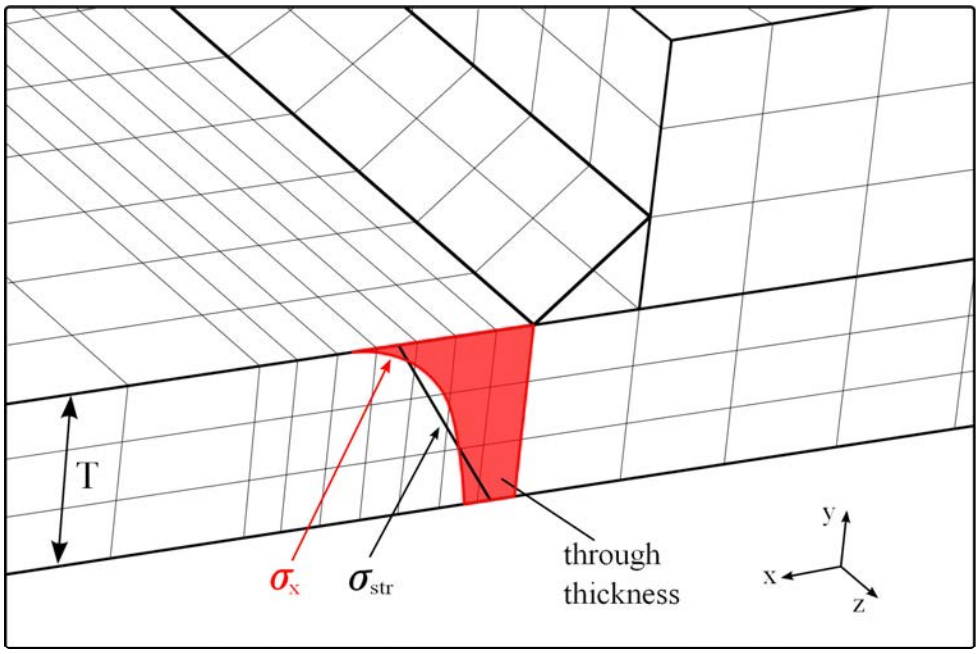

Figure 5-17 Determination of the structural hot-spot stress at the weld toe using the through thickness structural stress approach [28]

For a two-dimensional problem, equilibrium gives:

$$\Delta\sigma_{str} = \frac{1}{T}\int_0^T \sigma_x(y)dy + \frac{6}{T^2}\int_0^T \sigma_x(y)(\frac{T}{2} - y)dy \qquad \text{Eq. } 5\text{-}6$$

It is apparent that – at least for simple 2D-problems – the hot-spot stress computed with through-thickness stress linearization would be mesh-insensitive. This needs however to be verified, especially when FE models with coarse mesh are used. Mesh sensitivity might in such case results from the post processing of the stress result where stress averaging over the nodes shared by neighbouring elements is usually performed by FE software. Therefore, when using the through thickness structural stress method, it is important to pay attention to the nodal averaging, so that the calculated stress at the nodes is not reduced due to the adjacent elements. For more details on this problem, see Section 5.6.

5.5.2 Battelle structural stress approach

The concept of a linearized structural stress distribution over the plate thickness has been modified by P. Dong at Battelle Institute [24-26] in order to better fit to fatigue test results from different connection types and sizes. For determining of the structural stress from finite element analysis, a special stress determination procedure is proposed. This procedure considers the equilibrium conditions with normal and shear stress on two reference plane, at the weld toe and at a distance δ from the weld toe, see Figure 5-18. Considering the equivalent stress conditions on these two reference planes (section A-A and section B-B in Figure 5-18), the structural stress can be defined at section B-B which will be equal to the structural stress at the weld toe.

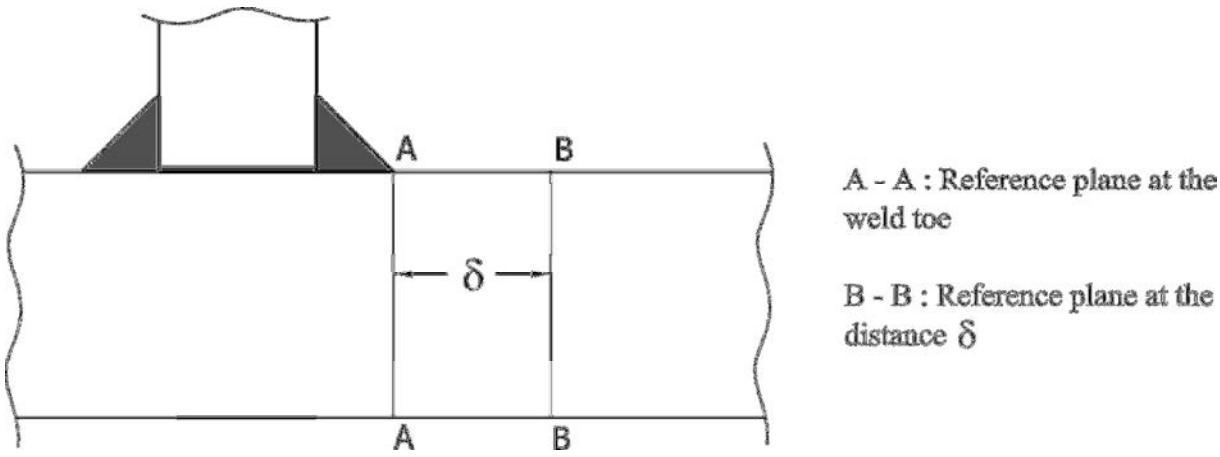

Figure 5-18 Structural stress determination according to the Battelle structural stress method [29]

According to the method the normal and shear stress in section A-A should be in equilibrium on section B-B, see Figure 5-19. Following the definition of the hot-spot stress, the stress sought stress distribution in section B-B should be linear and is defined as the sum of membrane and bending stress:

$$\sigma_{str} = \sigma_m + \sigma_b \qquad \textit{Eq. 5-7}$$

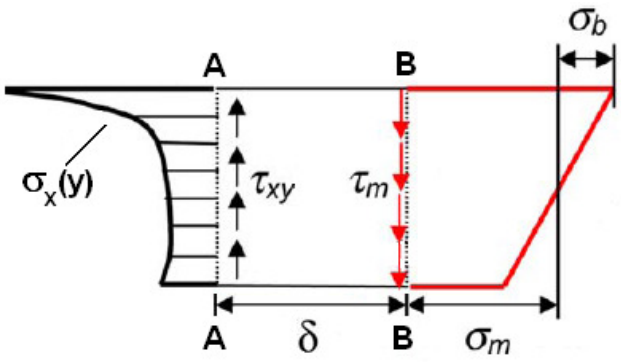

Figure 5-19 Linearization of the stress distribution at the weld toe according to Battelle structural stress method

Calculating the stress a small distance from the weld toe (where singularity exists) is supposed to give a structural stress that is not mesh-sensitive. However, recent research work has shown that the success of the method can be highly dependent on the selection of the distance δ. It should also be mentioned here, that the application of the Battelle approach on FE-models with solid elements may be very complicated and time-consuming, as the number of stress components which need to be considered in the equilibrium conditions becomes substantial.

5.5.3 1mm structural stress method

Another – relatively new and fairly simple – concept for the determination of structural stress utilizes the stress 1 mm below the surface at the weld toe for fatigue verification of welded details with toe cracks. The method, which was proposed by Xiao and Yamada [27], is theoretically based on a generalized crack propagation analysis for weld toe cracking. The 1-mm subsurface stress is assumed to represent

the stress gradient over the plate thickness, excluding the non-linear stress gradient caused by the weld. The approach was verified by Xiao and Yamada for longitudinal and transversal non-load-carrying attachments. Later Noh et al. [30] have shown that the concept is also valid in fatigue assessment of cruciform joints with partial and full penetration welds.

The 1mm structural stress method can be utilized in two different ways; using a reference detail or finely meshed FE models.

In the first case, a non-load carrying cruciform joint with a plate thickness of 10mm is chosen as the reference detail. The stress at the depth of 1mm correlates the crack propagation life or the fatigue strength of the welded component with the corresponding values of the reference details. As shown in Figure 5-20 (a) and Figure 5-20 (b), the stress at the depth of 1mm in the reference detail corresponds approximately to the nominal stress σ_n in the main plate. This stress value in a welded joint can be used as the parameter expressing the fatigue life or strength considering a corresponding stress concentration factor K_s, see Figure 5-20 (c).

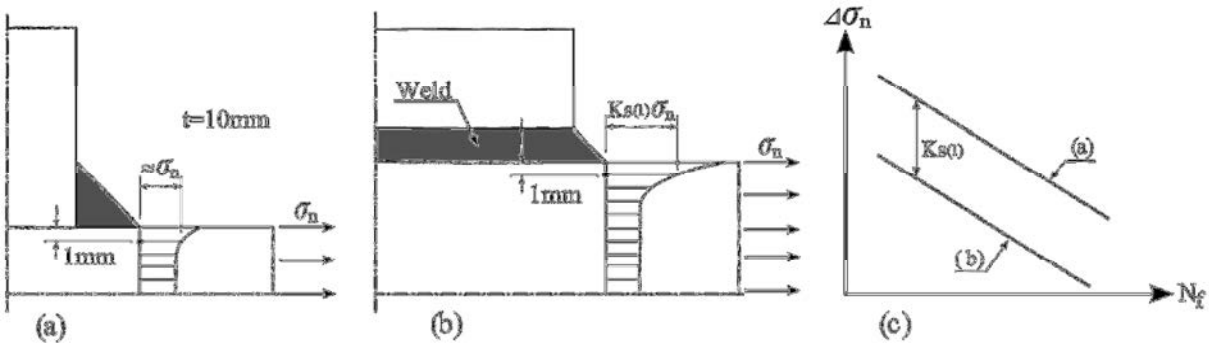

Figure 5-20 Structural stress determination proposed by Xiao and Yamada; (a) reference detail with plate thickness t=10 mm, (b) object detail and (c) corresponding S–N curve in logarithmic scales

The 1mm stress can also be obtained from FE analyses. The element size and orientation[6] around the weld toe region should be modelled in a way that it is possible to read out the stress in the reference point, which may give FE models with very fine mesh. As in other hot-spot stress approaches, the 1 mm structural stress approach is not applicable for root failures.

5.5.4 Structural stress for evaluating weld root cracking

As stated before, the structural hot-spot stress method is applicable for the evaluation of weld toe cracking. When fatigue assessment of fillet welds with respect to root cracking is required, alternative methods, such as the nominal stress method or the effective notch stress method should – in general – be used. To address this limitation, Fricke et al. [31] proposed an approach for evaluating the fatigue strength of fillet welds with the structural hot-spot stress method. The proposed approach, which follows the principles of the structural hot-spot stress method, has especially intended to assess the fatigue strength of fillet welds mainly subjected to weld through bending such as axially loaded one-sided fillet welded joints. This approach has also applied to

[6] An element node, either mid-side or edge node, must be located at 1mm from the surface.

fillet welded cruciform joints and joints with partial-penetration welds. Fricke's proposal for the linearization of the stress in the weld is shown in Figure 5-21. The resulting structural hot-spot stress in the weld is calculated using Eq. 5-8, Eq. 5-9 and Eq. 5-10. A linearized weld stress in the weld leg plane, as shown in Figure 5-21, is used to derive the membrane and bending stresses in the weld. It should be noted that for calculating the structural stress in the weld, the weld leg plane is chosen instead of the weld throat section due to the fact that the fatigue crack path is usually closer to the weld leg plane than to the weld throat section in fillet welds subjected to throat bending.

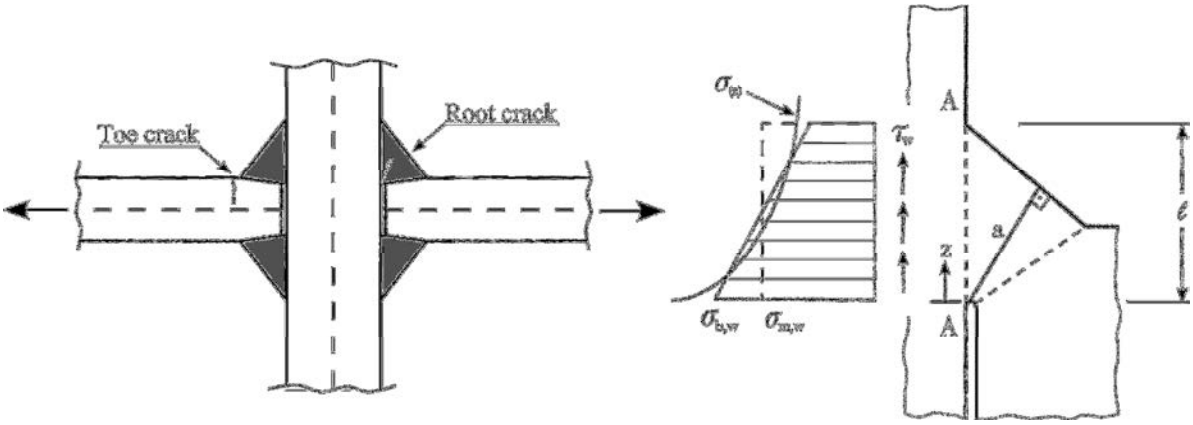

Figure 5-21 Possible fatigue cracks in cruciform joint with partial-penetration welds and linearization of the weld stress in the weld leg section [31]

$$\sigma_{m,w} = \frac{1}{l}\int_0^l \sigma(z)dz \qquad \text{Eq. 5-8}$$

$$\sigma_{b,w} = \frac{6}{l^2}\int_0^l \sigma(z)(\frac{l}{2} - z)dz \qquad \text{Eq. 5-9}$$

$$\sigma_{s,w} = \sigma_{m,w} + \sigma_{b,w} \qquad \text{Eq. 5-10}$$

Where:

z the coordinate along the weld leg,

σ(z) the stress normal to the leg section,

$\sigma_{m,w}$ the membrane portion

$\sigma_{b,w}$ the bending portion of the stress in the weld

$\sigma_{s,w}$ structural stress in the weld section

The authors recommend using detail category 80 for welds not subjected to longitudinal shear stress, $\tau_{//}$.

5.6 Recommendations for finite element modelling

5.6.1 General recommendations for finite element modelling

This section will cover – in more details – aspects of appropriate modelling techniques that can be applied in conjunction with FE analysis of welded steel details for fatigue verification with the hot-spot stress method. To start with, some general guidelines and recommendations are given below. These are applicable in most general cases. The subject of weld modelling is treated in the proceeding section, along with guidelines and examples on when and how the welds in structural details should be modelled. In the last two sections, detailed examples are presented on FE modelling for the purpose of fatigue verification on both "simple details" and more complex bridge details.

With respect to the finite element method, there is a number of general "rules" that should be respected when performing fatigue verification using the hot-spot method. Some of these rules that apply irrespective of the type of detail and the FE elements used are:

- ***The size of the FE-elements*** within the region of stress extrapolation in the detail should be chosen with regard to the reference stress extrapolation points. The latter should coincide with the elements' mid-side or edge nodes.
- Select ***element type*** and ***number of elements*** so as to produce a linear stress distribution through the thickness of the cracked plate in the detail. This can be achieved by using at least one quadratic or two linear FE-elements through the thickness.
- To avoid inaccuracy, the maximum ***aspect ratio*** of FE elements (i.e. the ratio of the longest dimension to the shortest dimension in the FE element) should be kept below 1:3. A ratio between 1:1 and 1:2 is recommended.
- ***Mesh transitions***, from fine meshed to coarse meshed region should be gradual and smooth, especially when this transition is taking place close to the reference stress extrapolation points.
- ***Stress averaging*** over element boundaries (nodal averaging) has not any effect for the structural hot-spot stresses determined by surface stress extrapolation procedure. On the contrary, ***stress averaging*** should be used for the through-thickness structural stress approach while ***stress averaging*** should be avoided for the Battelle structural stress approach.

In many cases, especially in modelling large welded structures, such as complex bridge details and details in ships and offshore structures, it is more practical to use shell elements in fatigue design with the structural hot-spot stress method. In these cases the designer should consider the following recommendations when constructing the FE models:

Modelling with shell elements:

- ***Higher order shell elements***: 8-node (second order) should be used in the following cases:
    1. In models with coarse mesh; in order to read out the stress in mid-side node
    2. To capture the high stress gradient in fatigue critical areas, especially in the vicinity of welds in complex details
- ***Mid-plane orientation***: shell elements should be arranged in the mid-plane of the plate. In case of eccentricity between the plates, the plates may be

modelled considering the mid-plane or by using the offset function which is available in most FE software.

- ***Modelling of the welds:*** In shell element models, the welds are usually not modelled except in cases where the results are affected by high local bending (due to an offset between plates for example) or in case of eccentric weld arrangement (e.g. cover plate joints and welded joints with cut-out holes).

Shell elements should be avoided when fatigue verification of the following details is performed with the structural hot-spot stress method: 1) cruciform joints; 2) simple T-joints in plated structures and 3) simple butt joints that are welded from one side only. Analysis of these details with shell elements will in general give a structural hot-spot stress that is equal to the nominal stress in the loaded plate. The principle is illustrated in Figure 5-22. It is obvious that for the load in the transverse direction (direction I) there will be no stress flow into the transverse plate which is represented in the model by a single plane of shell elements only. On the contrary, for loads in longitudinal direction (direction II) the stiffness of the longitudinal plate is correctly represented.

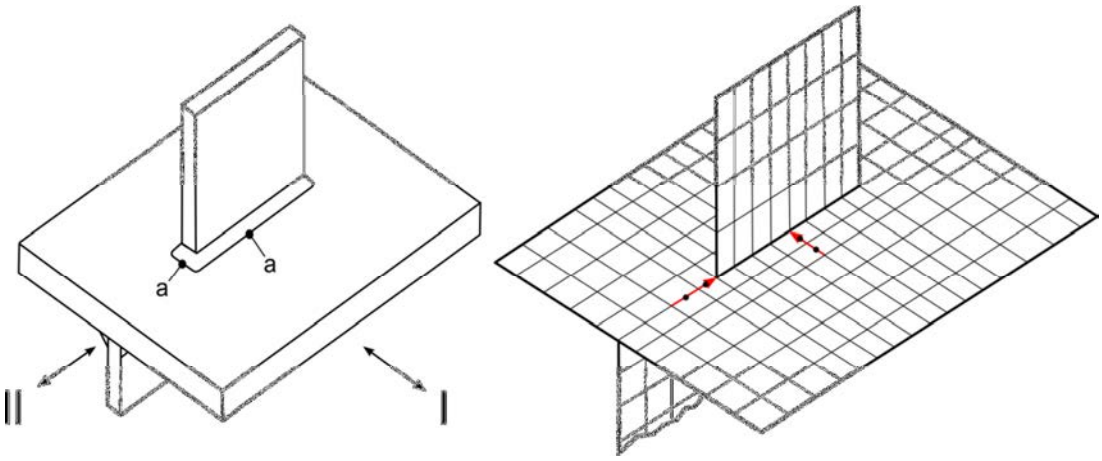

Figure 5-22 Illustration of the structural hot-spot stress method's limitation for simple joints

Another problem that should be pointed out here is the effect of nodal stress averaging which is usually performed by FE-software. Figure 5-23 is used to highlight this problem. During post processing the stress along the intersection plane is usually computed as an average value of the stress in the element nodes. For instance, stresses in the elements on the left side of the weld toe section as shown in Figure 5-23 can be substantially different than the stresses in the elements on the right side, which the stresses are lowered due to the weld itself. Nodal stress averaging over element boundaries (at the weld toe) has not any effect for the structural hot-spot stresses determined by surface stress extrapolation procedure since the stresses used in the extrapolation are taken from the reference points away from the averaged stresses. On the contrary, nodal averaging is highly important for the through-thickness structural stress and Battelle structural stress approach if coarsely meshed models are used. Stress averaging should be used for the through-thickness structural stress approach and the weld elements should be excluded while stress averaging should be avoided for the Battelle structural stress approach when determining the structural stress.

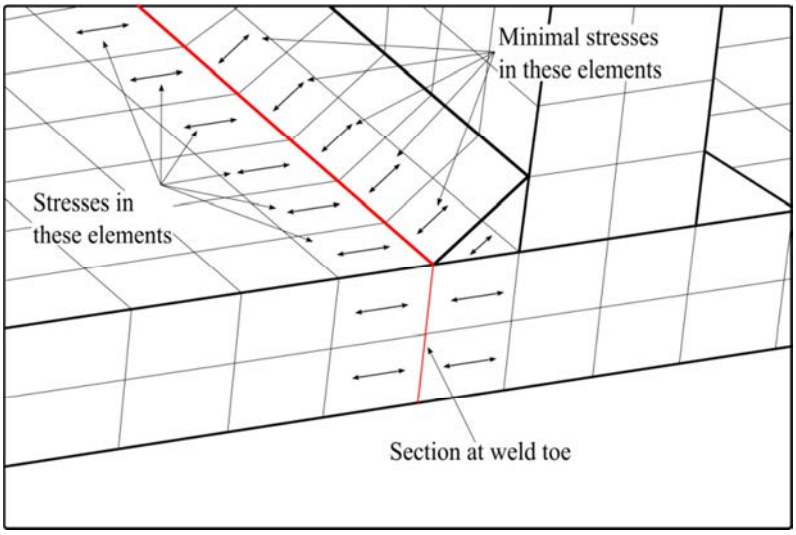

Figure 5-23 Nodal stress averaging during post processing

Modelling with solid elements:

- ***Higher order solid elements***: 20-node (second order) solid elements should be used in the following cases:
    1. For coarsely meshed solid element models; in order to read out the stress in mid-side node, since linear extrapolation requires the stresses at the mid-side nodes
    2. To capture high stress gradient in fatigue critical areas, especially in the vicinity of welds in complex details
- The ***Displacement function*** of the FE element should allow steep stress gradients as well as plate bending giving linear stress distribution in the plate thickness direction
- For hot-spot stresses obtained with surface stress extrapolation, only one[7] 20-nodes element is required through the thickness of the plate in hand.
- The welds should usually be incorporated in models constructed with solid elements.

5.6.2 Modelling of welds

In shell element models the welds are usually not modelled except for special cases where the results are affected by high local bending, e.g. due to an offset between plates or due to a small free plate length between adjacent welds such as at lug (or collar) plates and in details with complex geometries resulting in complex stress distribution. In these cases the *stiffness of the weld* should be represented in the model correctly. Various techniques exist for modelling the welds depending on the detail and the type of FE elements used. In solid element models the welds are usually easy to incorporate, while modelling of the welds in shell elements models require some additional effort. In shell element models the stress results can be highly dependent on the weld modelling technique. In the following sections, the most common weld modelling techniques are presented for different types of details and FE models.

[7] For the case one layer solid element in the thickness direction the surface stress extrapolation is recommended. When using multi-layer (two or more) elements in the thickness direction, the non-linearity is considered well and also the accuracy of the stress, but a stress linearization is still possible.

These techniques are also demonstrated in the proceeding sections, Section 5.6.3 and Section 5.6.4.

5.6.2.1 Weld modelling using oblique shell elements

In shell element models the welds in a welded joint can be represented by oblique shell elements. Both the stiffness and geometry of the weld can be correctly represented by means of this method.

Figure 5-24 shows two simple joints with orthogonal plates connected using fillet welds. The plates are modelled with shell elements located in the mid-thickness planes of the plates. The welds are modelled with oblique shell elements oriented at 45 degrees with reference to the connected plates. Generally, the oblique shell elements should have a thickness equal to the weld throat thickness. The same technique is used in the connection between a longitudinal rib and a transversal cross-beam in an orthotropic bridge deck, see Figure 5-25.

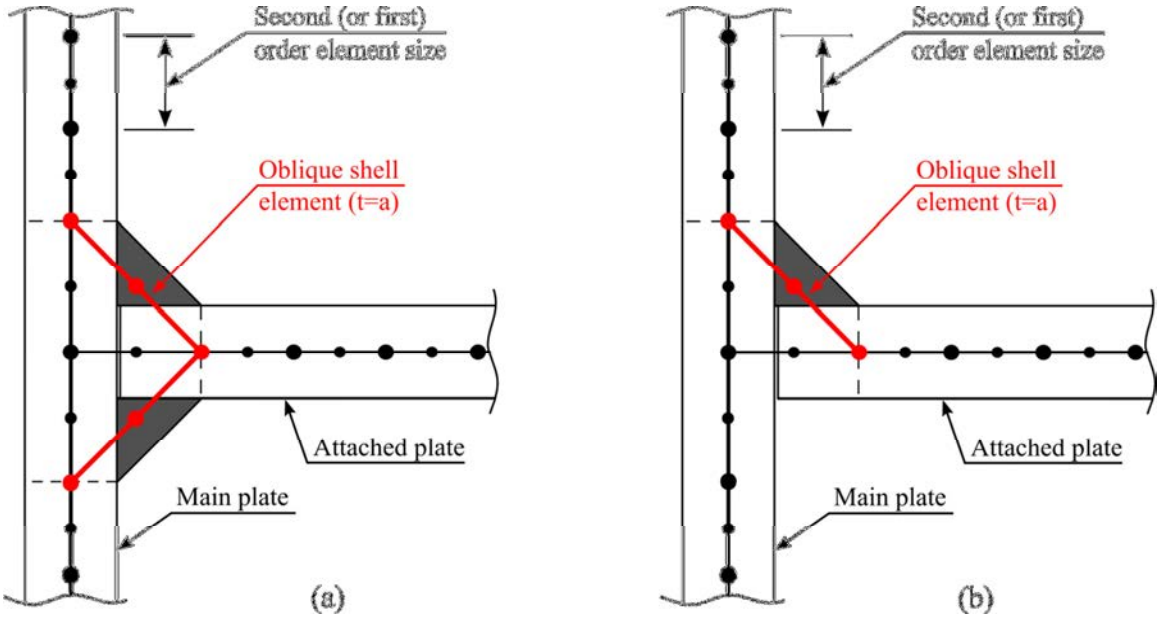

Figure 5-24 Weld modelling using oblique shell elements; a)two-side fillet weld, b) one-sided fillet weld

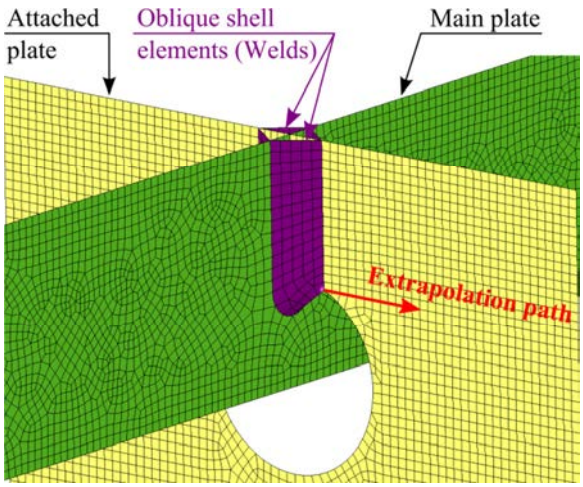

Figure 5-25 Weld modelling using oblique shell elements and extrapolation path

It should be pointed out here, that the use of oblique shell elements in fatigue assessment of welded details with the hot-spot stress method aims at representing the effect of the weld stiffness and geometry on the stresses in the connected plates, i.e. with reference to toe cracking. These elements should not be used to assess the load effects in the welds themselves, for example to perform fatigue verification with reference to root cracking.

5.6.2.2 Weld modelling using increased thickness

Another weld modelling technique to represent the stiffness of welds is to use shell elements with increased thickness in the intersection region of welded joints. This method has two important geometrical properties; the increased thickness and the length of the elements. The definition of these two parameters is shown in Figure 5-26 (a).

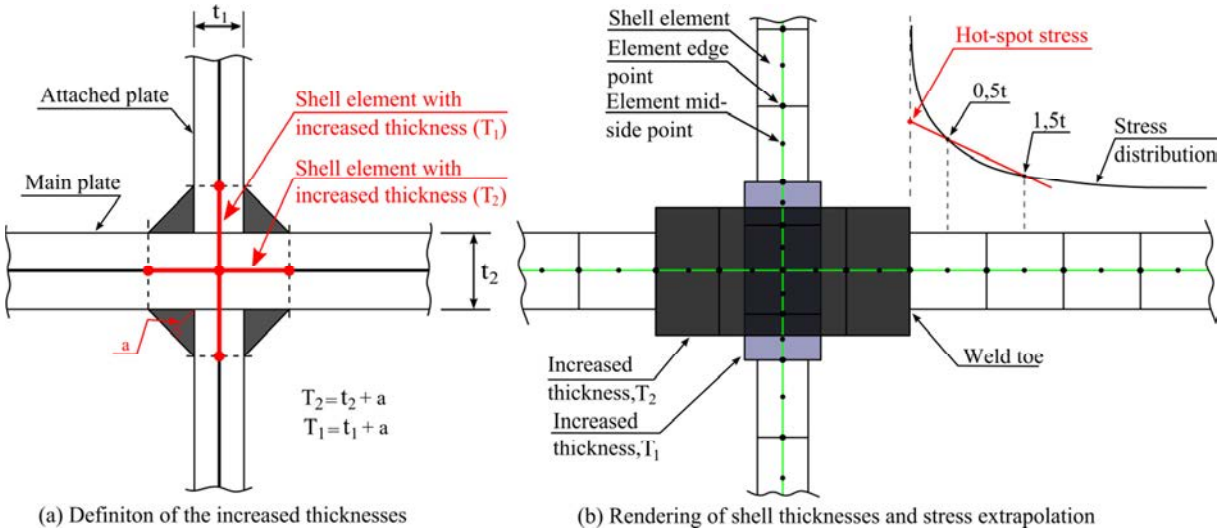

Figure 5-26 Modelling welds with shell elements with increased thickness and surface stress extrapolation path

In order to represent the stiffness properties of the welds correctly, two rows of shell elements with increased thickness are used, i.e. both for the attached plate and the main plate for the detail in Figure 5-26. The size of the weld zone that should have shell elements with increased thickness and the extrapolation of the structural hot-spot stress to weld toe is shown in Figure 5-26 (b). Figure 5-27 shows another detail (a cover plate connection) in which increased shell thickness is applied, along with rigid links to include the effect of the eccentricity between the connected plates. The increased thickness (T_2) that should be used in the weld zone is shown in this figure *[32]*. Observe that, in this example, an increased shell element thickness is only needed in the main plate due to the configuration of the joint.

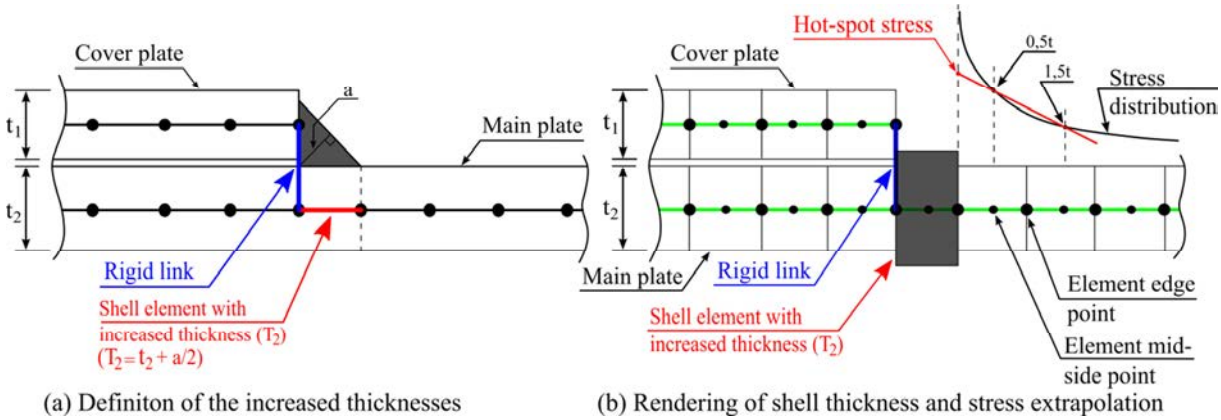

(a) Definiton of the increased thicknesses (b) Rendering of shell thickness and stress extrapolation

Figure 5-27 Modelling cover plate welds using shell elements with increased thickness and rigid links

5.6.2.3 Weld modelling using solid elements

Modelling welds with deformable solid elements both in solid and shell element models is widely used because of the simplicity in modelling work and the accuracy in results. The stiffness of welds can be modelled accurately. When this technique is used in models with solid elements, prismatic solid elements should be used in order to read out the stresses in the extrapolation points, see Figure 5-28.

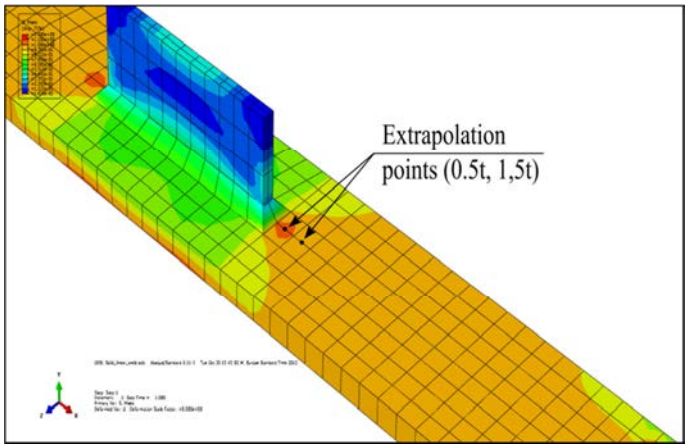

Figure 5-28 Modelling welds in solid model

When modelling the welds with solid elements in FE models otherwise constructed with shell elements, a special technique is necessary to connect these two different element types as shown in Figure 5-29 (solid elements have three degrees of freedom per node while shell elements have six degrees of freedom). The bending moments from shell elements need to be transferred to the solid elements. There are a couple techniques available to achieve this. The most common way is to use Multi Point Constraint (MPC) equations. This method requires generating MPC equations to transfer rotation from shell elements to the solid elements, a procedure which is usually implemented in commercial FE softwares.

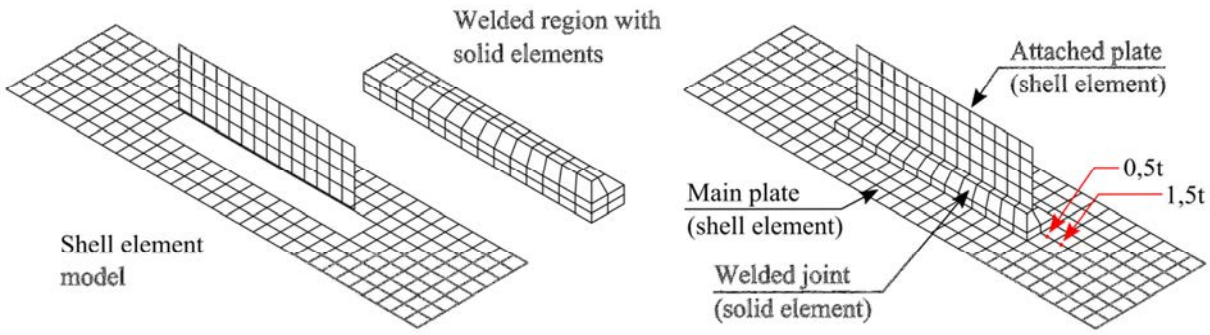

Figure 5-29 Modelling welds in solid elements only in welded region

5.6.2.4 Weld end modelling

In some cases the geometry of welds in a joint may have larger influence than their stiffness. One example is fatigue cracking from weld toes at weld ends. In such case it might be necessary to model the weld end only so that a more accurate representation of the stress distribution in the region of interest is obtained. Shell elements can be used for this purpose keeping the thickness of the weld elements the same as the thickness of the welded plate [33]. An example is shown in Figure 5-30.

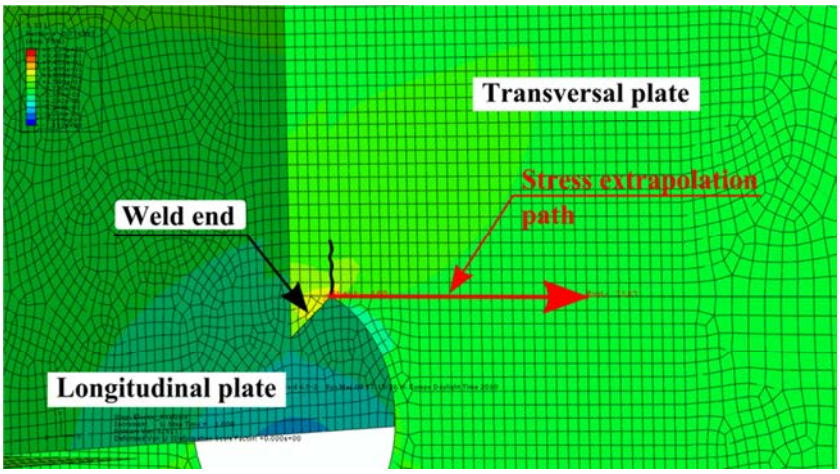

Figure 5-30 Weld ends modelling using shell elements

In this example the fatigue crack initiates at the weld toe in the transversal plate which is welded to a longitudinal plate. Since there is a cut-out hole at the end of the weld, the stress distribution is affected by both the hole and weld end so that the shape of the weld end should be considered, here by introducing the weld end profile with shell elements. The weld end gives a smooth transition from the cut-out hole to the longitudinal plate in the intersection region. A comparison work for various welds modelling technique can be found in [34].

5.6.2.5 Weld modelling using rigid links

Weld modelling technique using rigid links was firstly suggested by Fayard et al. [35]. Here, it is proposed that the stress at the weld toe can be directly read out at the elements' centre of gravity. This means that there is no need for any extrapolation when determining the hot-spot stress at weld toe.

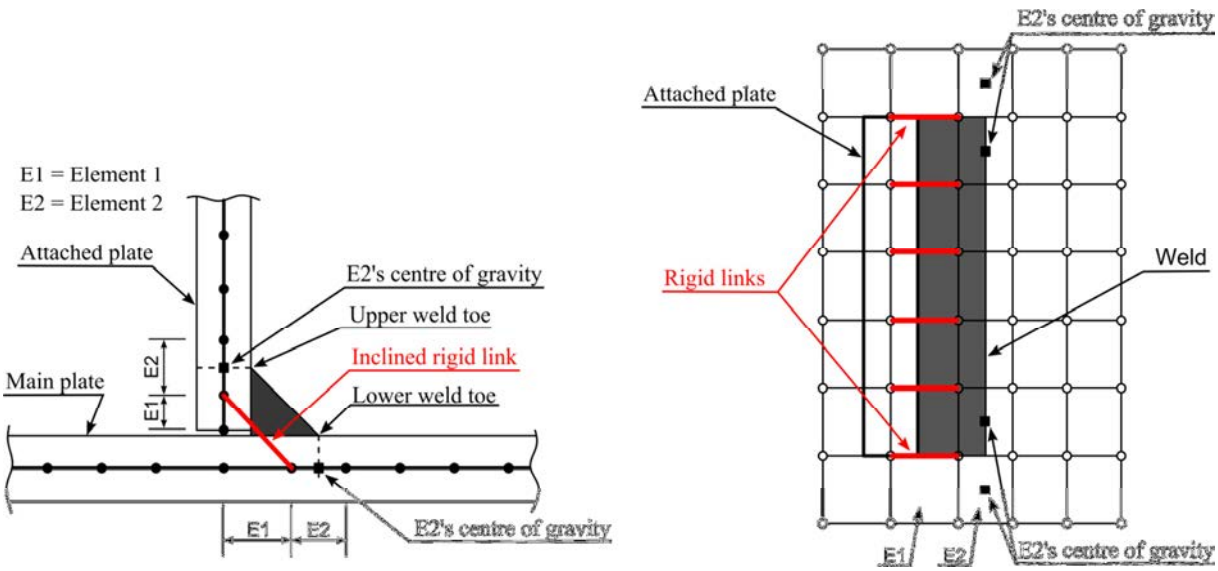

Figure 5-31 Single-side weld modelling with rigid links according to Fayard et al. [35]

The basis of this technique is to model the local rigidity of a joint resulting from the weld stiffness. This rigidity can be modelled by connecting the two adjacent shell elements using rigid links each connecting a pairs of nodes located along the whole weld length. The lengths of elements, E1 and E2 as shown in Figure 5-31, should be chosen correctly in order to represent the local stiffness of the welds. The common node in elements E1 and E2 is then used to link these elements by rigid links. It is important to notice that the FE elements at the intersection are not connected, i.e. don't share common nodes. Also the use of 4-node shell elements is recommended for this technique. An example of using rigid links to represent the welds between a rib and a cross-beam in an orthotropic deck is shown in Figure 5-32.

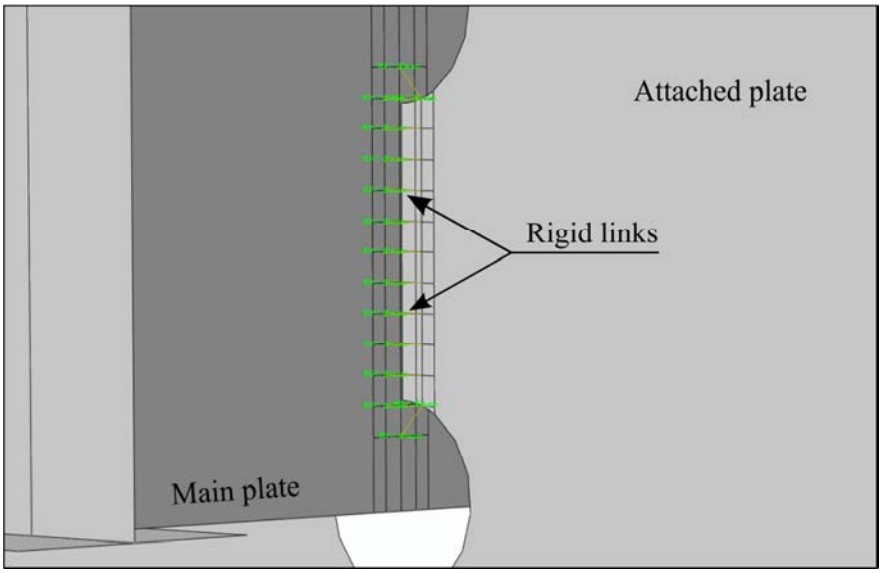

Figure 5-32 Weld modelling using rigid links[33]

5.6.3 Modelling of some common fatigue-prone details

In this Section, the application of the hot-spot method is demonstrated on a number of common welded details. Recommendations for FE modelling and stress extrapolation are also given in each case. The work follows the scheme presented in *Figure 5-33*.

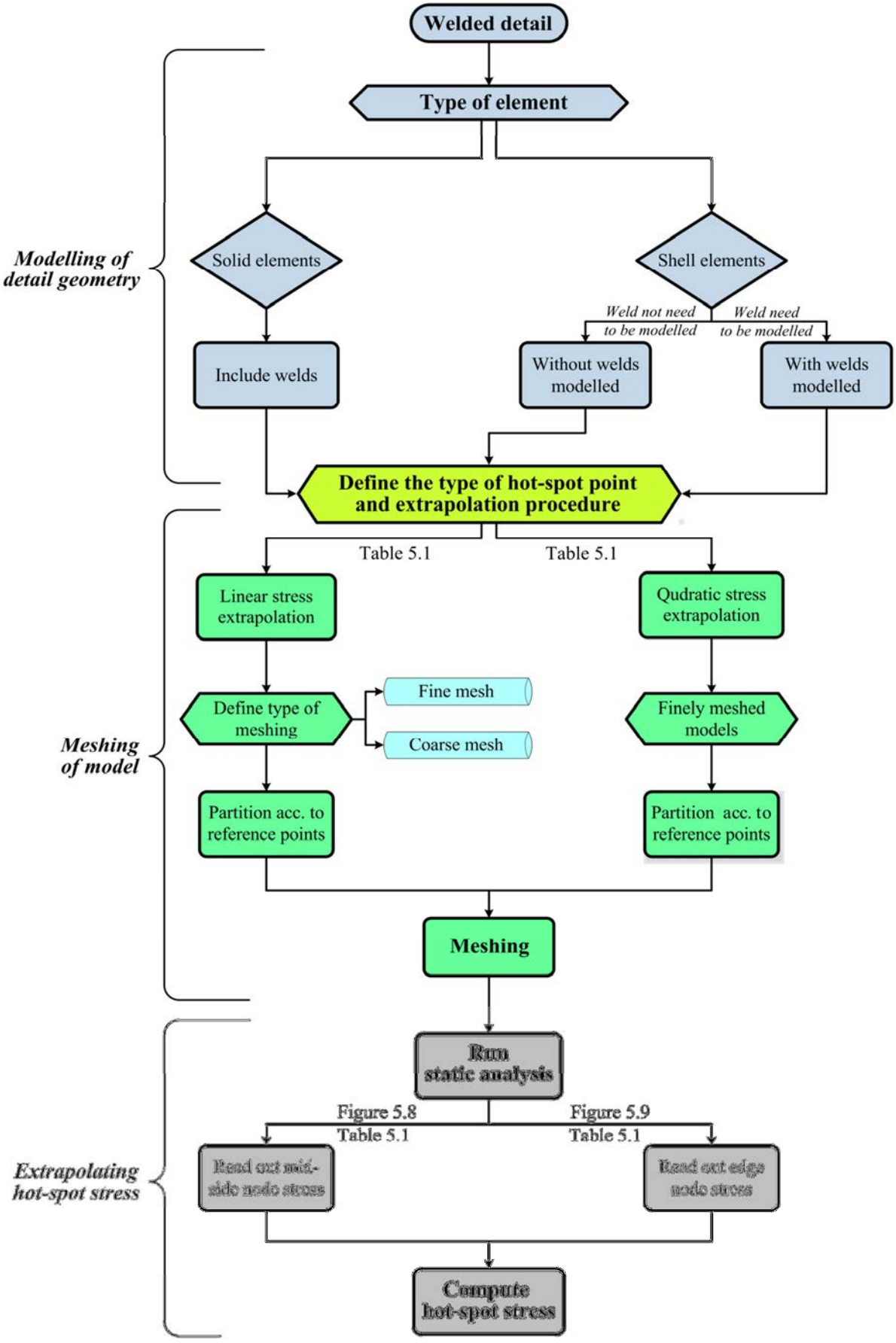

Figure 5-33 Scheme for the determination of structural hot-spot stress

5.6.3.1 Transverse butt welds

EN 1993-1-9:2005 specifies detail categories C112 and C100 for the fatigue assessment of transverse full-penetration butt weld joints with the structural hot-spot stress method. The higher fatigue strength is assigned to transverse butt welds welded from both sides, ground flush and verified by NDT. This is of course the same detail category used for similar butt welds when assessed by the nominal stress method (as the structural hot-spot stress for such detail is equal to the nominal stress). If the weld is not ground flush, detail category C100 applies. The effect of weld convexity on the stress concentration – and thus the fatigue strength – should, when the structural hot-spot stress method is applied, be captured by modelling the weld profile, which can be easily done in solid element models and in 2D models with plane strain elements, see Figure 5-34.

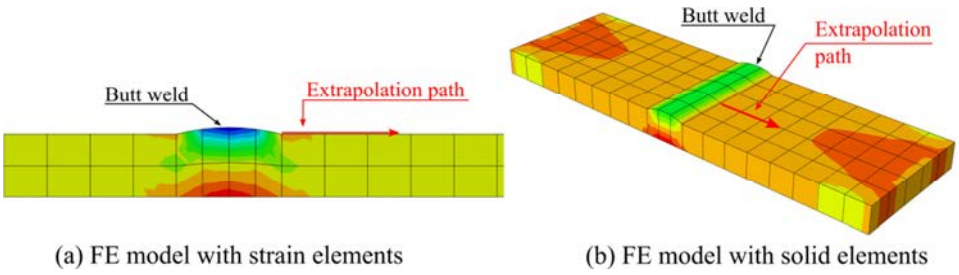

Figure 5-34 FE models of transverse butt welds using 2D plane strain and 3D solid elements

5.6.3.2 Transverse attachments

EN 1993-1-9:2005 specifies detail category C100 for transverse non load-carrying attachments when using the structural hot-spot stress method. The fatigue critical point in this type of joints is located at the weld toe in the main plate, see Figure 5-35. Thus, the hot-spots point is defined as "type a" (see Section 5.2)

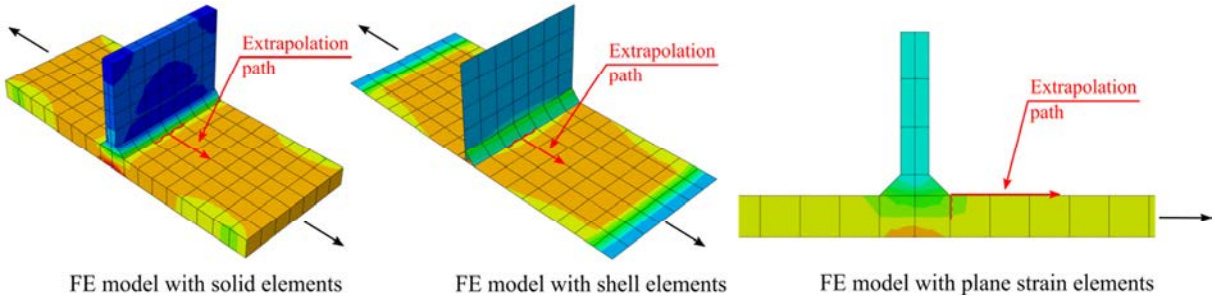

Figure 5-35 FE models of transverse attachments using various finite elements

Transverse welded attachments can be modelled with 3D shell and solid elements as well as 2D plane strain elements. The reader may find the following recommendations helpful to obtain a reliable result from FE models of details with transverse attachments.

Models with solid elements:

- For coarsely meshed models and linear stress extrapolation, 20-node solid elements should be used
- For finely meshed models and quadratic stress extrapolation, linear or quadratic (first or second order) solid elements should be used

- For this detail, in order to obtain reliable results (hot-spot stress) the welds should be included in the model
- When the welds are included in the FE model, the attached plate may be connected to the main plate in order to facilitate meshing works (i.e. the plates share nodes along the contact surface)
- Straight stress extrapolation path, perpendicular to the weld as shown in Figure 5-35 should be used
- One point stress determination technique can be used

Models with shell elements:

Special care is needed when shell elements are used in FE models of transverse attachments. As mentioned in Section 5.6.1, when analysing these details with shell elements without representing the welds the structural hot-spot stress calculated at the weld toe will be equal the nominal stress. Modelling the welds cannot therefore be omitted in these details when using shell element. The following recommendations are useful for obtaining reliable stress values from FE models with shell elements.

- For coarsely meshed shell element models with linear stress extrapolation, 8-node shell elements should be used
- For finely meshed models and quadratic stress extrapolation, linear or quadratic (first or second order) shell elements should be used
- The welds should be included in transverse attachments either using oblique shell elements (Section 5.6.2.1) or rigid links (Section 5.6.2.5)
- Straight stress extrapolation path perpendicular to the weld as shown in Figure 5-36 should be used
- One point stress determination technique can be used

5.6.3.3 Longitudinal attachments

In *EN 1993-1-9:2005*, longitudinal non-load-carrying attachments are classified according to the nominal stress method as C56 to C80 depending on the shape and length of the attached plate, see Figure 5-1. In a FE model, the stress concentration caused by both parameters can be easily captured and thus only one S-N curve (i.e. fatigue category) is needed to evaluate the fatigue strength of these details with the structural hot-spot stress method. Therefore, Eurocode specifies detail category C100 for these details irrespective of the geometrical parameters.

The fatigue critical point in this type of joints is located at the weld toe in the main plate, see Figure 5-36. Thus, the hot-spots point is defined as “type a”, as described in Section 5.2.

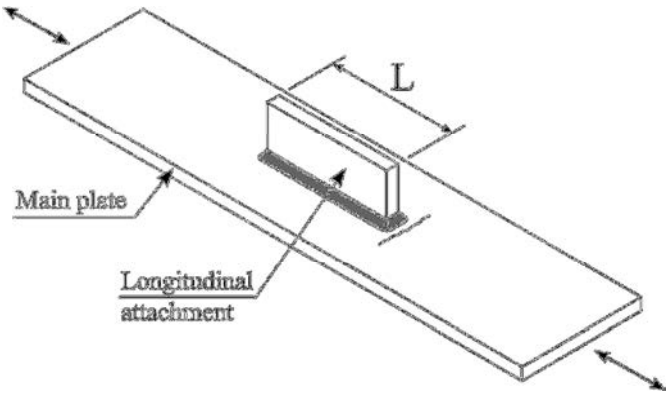

Figure 5-36 Fatigue crack location and stress direction of longitudinal welded attachments

FE modelling for structural hot-spot stress application

As stated earlier, longitudinal welded attachments can be modelled with 3D shell and solid elements. The reader may find the following recommendations helpful to obtain a reliable result from FE models of details with longitudinal attachments.

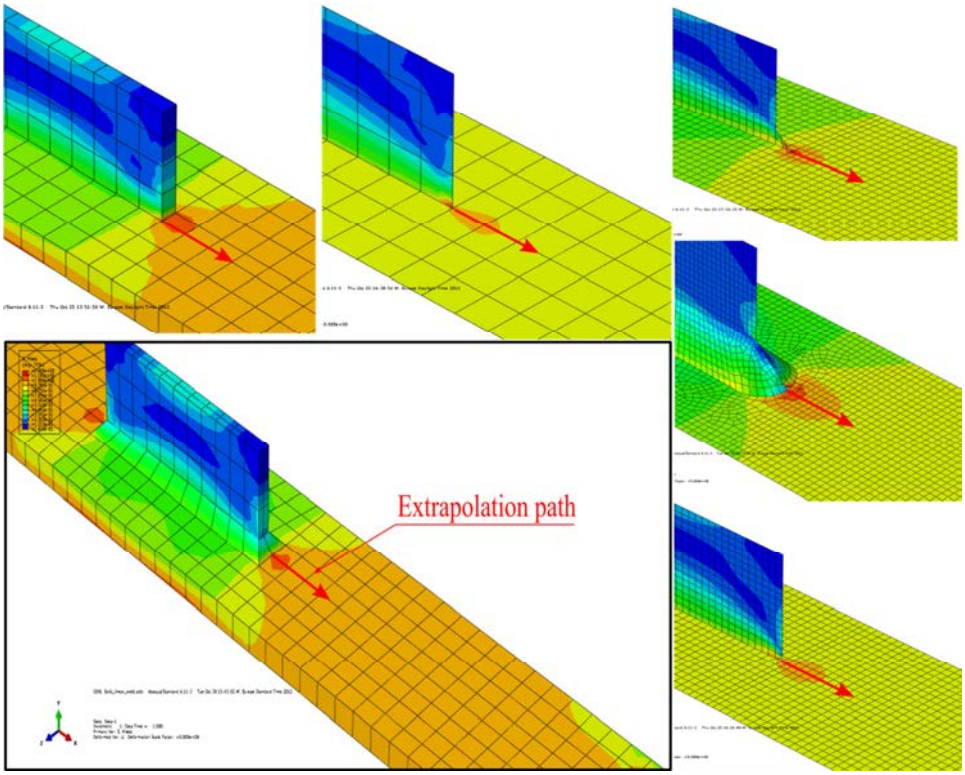

Figure 5-37 FE Modelling of longitudinal attachments and stress extrapolation path

Models with solid elements:

- For coarsely meshed models with linear stress extrapolation, 20-node solid elements should be used
- For finely meshed models and quadratic stress extrapolation, linear or quadratic (first or second order) solid elements should be used
- For this detail, reliable results (hot-spot stresses) are usually obtained even when the welds are not included in the model
- When the welds are included in the FE model, the attached plate may be connected to the main plate in order to facilitate meshing works (i.e. the plates share nodes along the contact surface)
- Straight stress extrapolation path perpendicular to the weld toe as shown in Figure 5-37 should be used
- One point stress determination technique can also be used

Models with shell elements:

Special care is needed when shell elements are used in models of details with longitudinal attachments. One-sided attachments are more sensitive to bending due

the present asymmetry, and thus it is recommended to model the welds in this case to obtain god representation of local stiffness in the region of interest. Modelling the welds can usually be omitted in details with two-sided attachment. The following recommendations are useful for obtaining reliable stress value from FE model with shell elements.

- For coarsely meshed shell element models and linear stress extrapolation, 8-node shell elements should be used
- For finely meshed models and quadratic stress extrapolation, linear or quadratic (first or second order) shell elements should be used
- The welds should be included in one-sided longitudinal attachments, either using oblique shell elements (Section 5.6.2.1) or rigid links (Section 5.6.2.5)
- Straight stress extrapolation path perpendicular to the weld as shown in Figure 5-37 should be used
- One point stress determination technique can be used

5.6.3.4 Plate-edge attachments

Plate-edge details are fairly common in fatigue-loaded structures. A typical example is gusset plates connected to girder flanges in bridge structures. There is a wide range of different geometrical configurations in this category of details, see Figure 5-38.

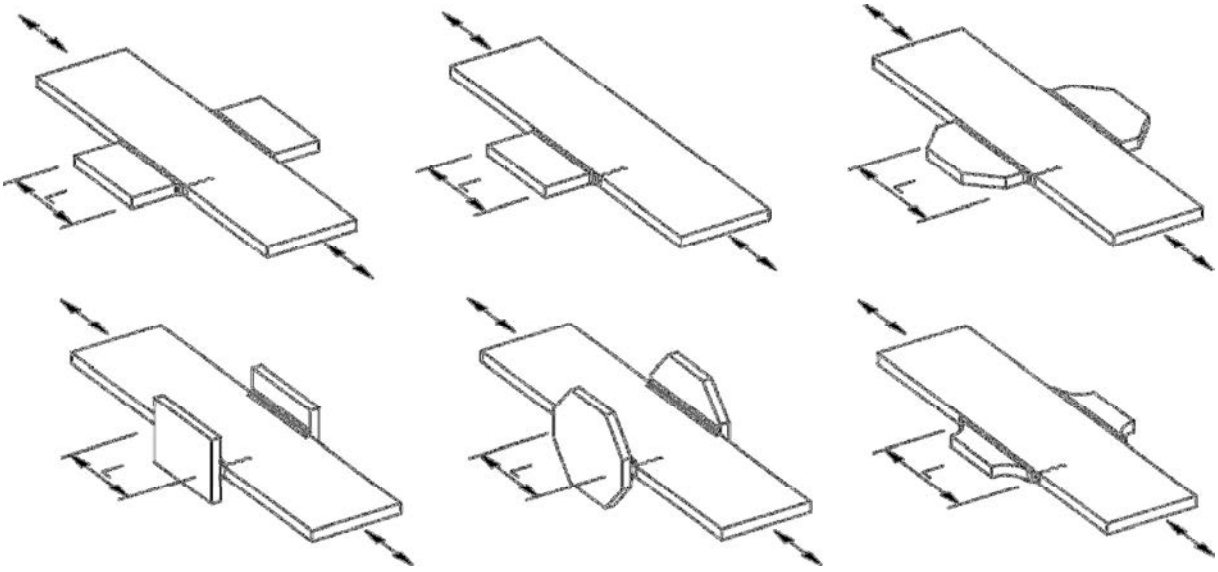

Figure 5-38 Different types of plate-edge welded joints

The most important property of welded plate-edge details in comparison to other welded details is that the stress causing fatigue cracks in the main plate is acting in the same plane as in the main plate, i.e. in-plane joint, as illustrated in Figure 5-39.

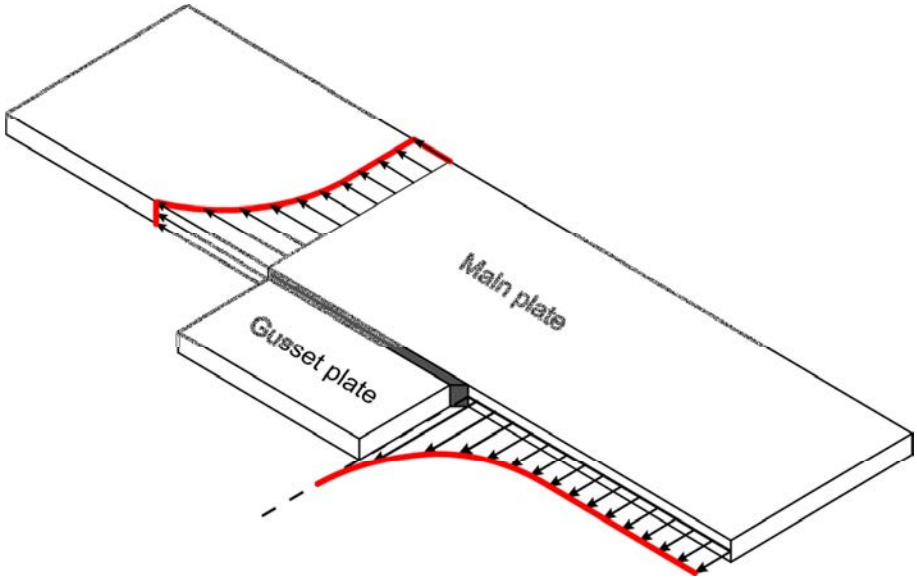

Figure 5-39 Stress distribution at the weld toe in plate edge joint

For this type of details, the length and the geometry of the gusset plate ends have a significant influence on the magnitude of stress concentration at the gusset plate termination; i.e. where fatigue cracks are expected to initiate. It is worth mentioning here that *EN 1993-1-9.2005* disregards the effect of the attached plate length on the fatigue strength of the main plate when using the nominal stress method. Detail category C40 is assigned to this detail (irrespective of the length of the gusset plate) which is conservative. Other standards such as the IIW recommendations assign different fatigue strength classes based on the length of the attachment.

EN 1993-1-9:2005 lacks a statement of the fatigue design curve that should be used in fatigue verification of this detail with the hot-spot stress method. By definition, the effect of all the geometrical parameters of the different configurations is implicitly considered in the hot-spots stress calculation. One S-N curve should be needed to describe the fatigue strength of these welded details. An evaluation study of plate edge details covering a large number of test results was performed in [36]. The results indicate that fatigue category C100 gives a good representation of the fatigue strength of this detail.

FE modelling for structural hot-spot stress application

The fatigue critical point in this type of joints is located at the weld toe, at the edge of the main plate. Therefore, the hot-spot point is defined as a "type b" hot-spot, see Figure 5-6. Welded gusset plates can be modelled with 3D shell and solid elements, see Figure 5-40. In some cases, where the plate thicknesses are equal, this type of joints can also be modelled with 2D plane strain elements. When using the hot-spot stress method, the following recommendations can be followed to obtain a reliable stress value from FE models.

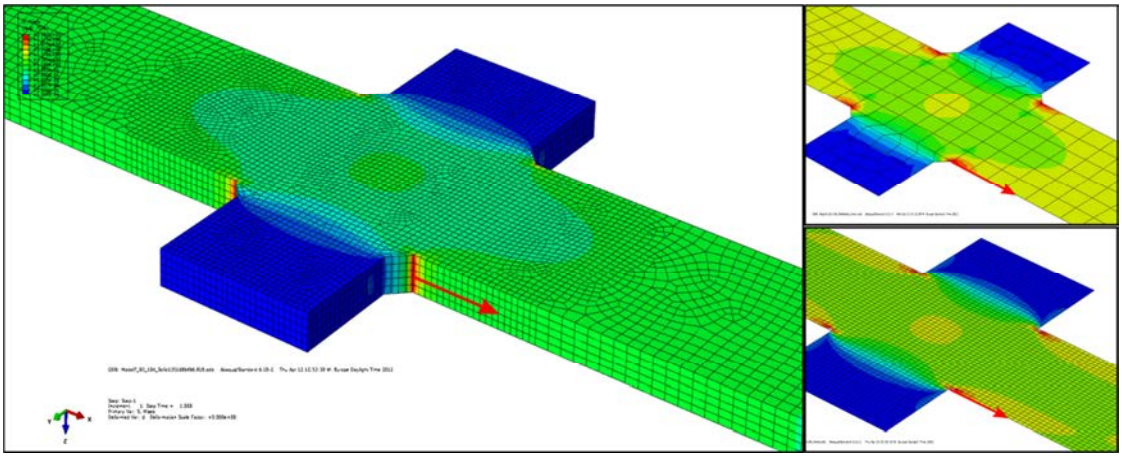

Figure 5-40 FE Modelling of plate-edge details and stress extrapolation path

Models with solid elements:

- For coarsely meshed models and linear stress extrapolation, 20-node solid elements should be used
- For finely meshed models and quadratic stress extrapolation, linear or quadratic (first or second order) solid elements should be used
- Since the weld can be easily modelled it is recommended to include the weld in the model. However, FE models excluding the weld yield accurate hot-spot stress value as well
- In case of including the weld in FE models with solid elements, the gusset plate should be connected to the main plate
- Straight stress extrapolation path perpendicular to the weld toe on the parent plate edge should be used, see Figure 5-40
- One point stress determination technique can also be used

Models with shell elements:

The following recommendations can be followed to obtain a reliable stress value from FE models with shell elements.

- For coarsely meshed models and linear stress extrapolation, 20-node solid elements should be used
- For finely meshed models and quadratic stress extrapolation, linear or quadratic (first or second order) solid elements should be used
- FE models both with and without representing the weld can be used
- The welds can be modelled using weld-end modelling technique (Section 5.6.2.4). However, FE models without modelling weld-end yield as well accurate hot-spot stress values
- Straight stress extrapolation path perpendicular to the weld toe should be used, see Figure 5-40
- One point stress determination technique can be used

5.6.3.5 Overlapped joints

Figure 5-41shows the main geometrical parameters of an overlapped joint along with the two possible cracking modes in these joints (cracking of the fillet welds is not shown). The fatigue strength of welded overlapped joints is higher when cracking takes place in the main plate. This has been recognised by some design codes when

using the nominal stress method, such as *EN 1993-1-9:2005*. In case of using the structural hot-spot stress method, *EN 1993-1-9:2005* recommends detail category C90 for both cracking modes.

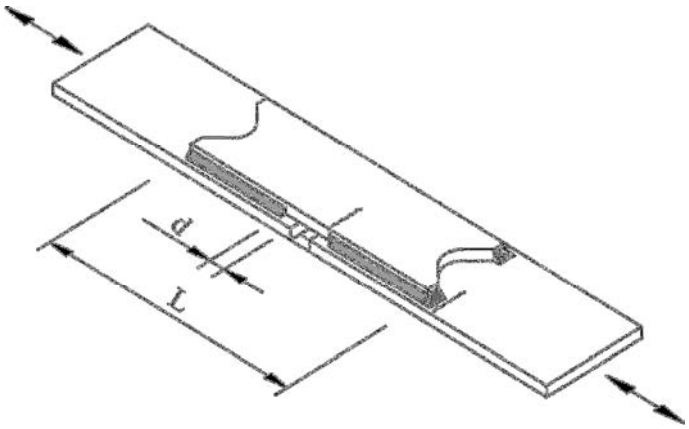

Figure 5-41 Geometrical parameters and failure modes in a overlapped joint

FE modelling for structural hot-spot stress application

The fatigue critical points in this type of joints are located at the weld ends in the main plate and the attached plates. For the crack in the main plate, the hot-spots point is defined as "type a" while cracking in the attached plate is a "type b" hot-spot point. Overlapped joints can be modelled with 3D shell and solid elements. When using the structural hot-spot stress method, the following recommendations can be followed to obtain a reliable stress value from FE models.

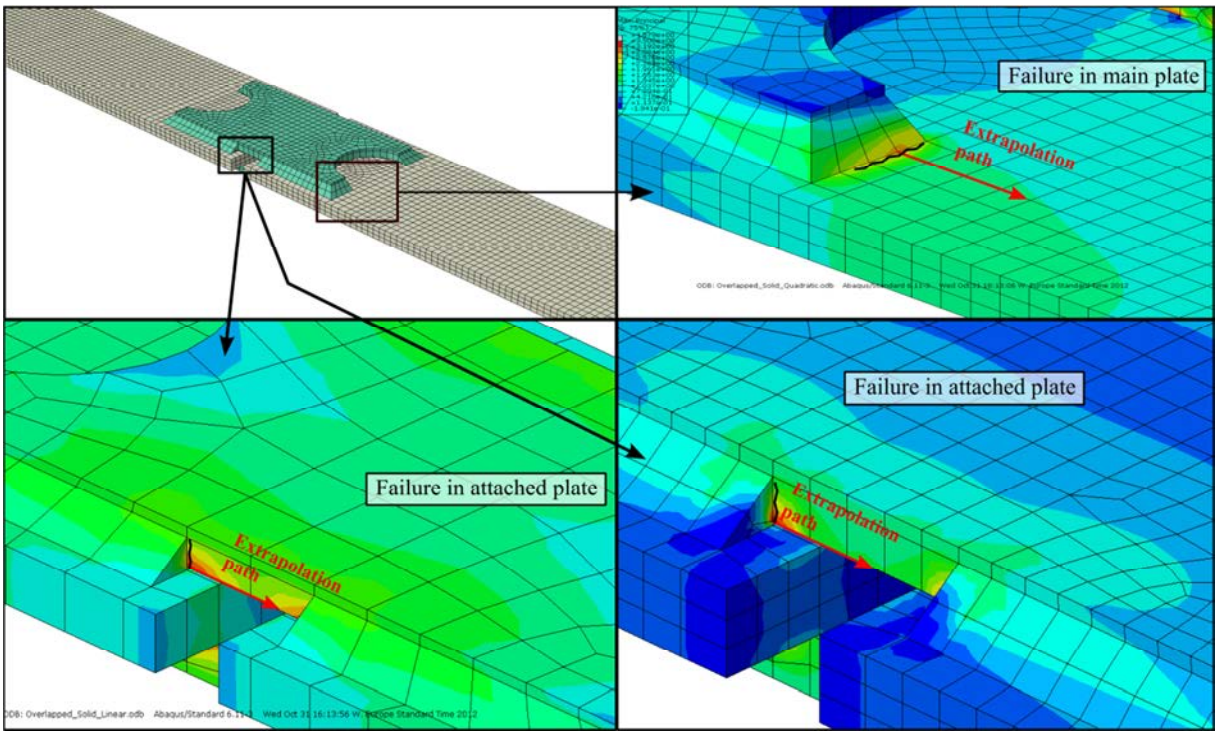

Figure 5-42 FE Modelling of overlapped welded joints and stress extrapolation path

Models with solid elements:

- For coarsely meshed models and linear stress extrapolation, 20-node solid elements should be used

- For finely meshed models and quadratic stress extrapolation, linear or quadratic (first or second order) solid elements should be used
- In overlapped joints, the weld must be included in FE models and the attached plates should be separated from the main plate
- For failure mode in the main plate – the cracks located in the main plate – a stress extrapolation path perpendicular to the weld toe as shown in Figure 5-42 should be used
- For failure mode in the attached plate – the cracks located at the edge of the attached (overlapping) plate – it is also recommended that straight stress extrapolation path perpendicular to the weld toe in the main plate edge should be used
- When the distance between weld ends on each side of the main plates is so short that the stress extrapolation points lay outside this region, the one point stress evaluation method should be used.

Models with shell elements:

The following recommendations can be followed to obtain a reliable stress value from FE model with shell elements.

- For coarsely meshed models and linear stress extrapolation, 8-node shell elements should be used
- For finely meshed models and quadratic stress extrapolation, linear or quadratic (first or second order) shell elements should be used
- The welds must be represented in FE models using one of the weld modelling techniques presented in Section 5.6.2
- Straight stress extrapolation path perpendicular to the weld toe on the main plate should be used for cracking in the main plate, see Figure 5-42
- For failure mode in the overlap plate, it is also recommended that straight stress extrapolation path perpendicular to the weld toe on the edge of the main plate should be used, see Figure 5-42
- In case of small distances (d), where it is not possible to apply the surface stress extrapolation, the one point stress evaluation method can be used.

5.6.3.6 Cover plate details

Partial-length cover plates are usually welded to flanges of steel bridge girders in order to increase the moment capacity and the stiffness of bridge spans, giving better material utilization. Cover plate details may appear in a wide range of geometrical variations, see Figure 5-43. A study comprising a large amount of fatigue test data on this detail [36] shows that the main parameter governing the fatigue strength of this detail is the cover-plate to main plate thickness ratio (t_c/t_m).

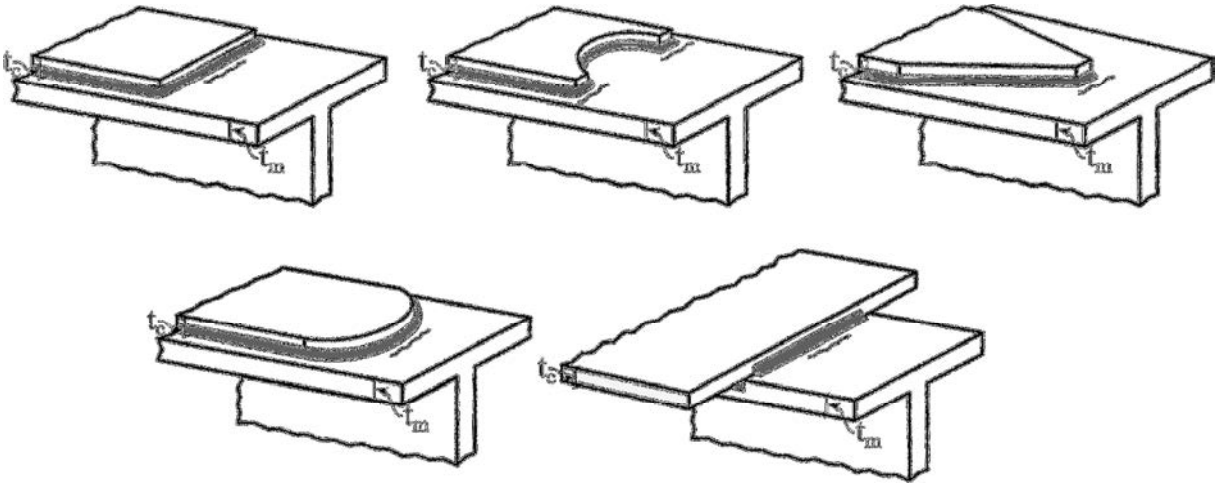

Figure 5-43 various cover plate welded detail configurations

It is known that cover plates with lower t_c/t_m ratio gives higher fatigue strength. However, this effect disappears for details with $t_c/t_m > 1$. These details demonstrate the same fatigue strength. Moreover, investigations of the fatigue strength of cover-plate details [36] show that changing the shape of the cover plate end does not have a pronounced effect on the fatigue strength of these details. When the hot-spot stress method is used for fatigue verification of welded cover-plate details, the effects of different geometrical configurations are directly accounted for in the stress calculation. One S-N curve is thus needed to describe the fatigue performance of these details. Fatigue category C100 is recommended in both Eurocode and IIW.

FE modelling for structural hot-spot stress application

The fatigue critical point in this type of joints is located at the weld toe in the main plate (generally a girder flange). Thus, the hot-spot point is defined as "type a" hot-spot. The cover plate may also be modelled with 3D shell and solid elements, see Figure 5-44. 2D plane strain elements may also be used under specific conditions. When using the structural hot-spot stress method, the following recommendations can be followed to obtain reliable stress values from FE models.

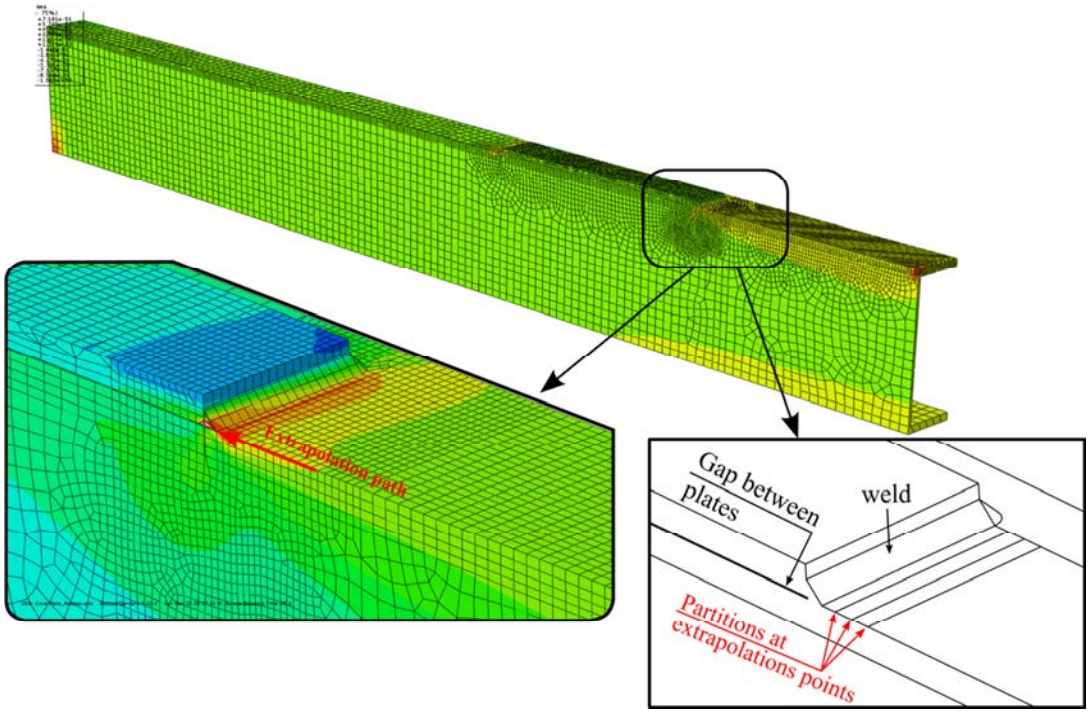

Figure 5-44 FE Modelling of cover plates and stress extrapolation path

Models with solid elements:

- For coarsely meshed models and thus linear stress extrapolation, 20-node solid elements should be used
- For finely meshed models and quadratic stress extrapolation, linear or quadratic (first or second order) solid elements should be used
- In FE models of cover plate joints the eccentricity between the mid-thickness planes of the main plate and the cover plate should be correctly introduced along with the welds connecting these plates
- Straight stress extrapolation path perpendicular to the weld toe on the main plate should be used, see Figure 5-44
- One point stress determination technique can be used

Models with shell elements:

- For coarsely meshed models and linear stress extrapolation, 8-node shell elements should be used
- For finely meshed models and quadratic stress extrapolation, linear or quadratic (first or second order) shell elements should be used
- The welds must be represented in the FE model using oblique shell element (Section 5.6.2.1), rigid links (Section 5.6.2.5) or increased thickness (Section 5.6.2.2)
- Straight stress extrapolation path perpendicular to the weld toe on the main plate should be used, see Figure 5-44
- One point stress determination technique can be used

5.6.4 Modelling of complex fatigue details

The benefits of employing more refined methods in fatigue design are of particular interest in complex details where an accurate determination of nominal stress is

obstructed by the complexity of the detail geometry or the force transfer in the detail. Two examples are treated in this section in order to demonstrate the application of the hot-spots method in such cases. Recommendations for FE modelling, stress determination and fatigue verification are given. These are based on extensive studies performed in conjunction with strain measurements in laboratory tests and bridges in service.

5.6.4.1 Orthotropic bridge deck with open ribs

An orthotropic bridge deck is a multifaceted structural system which is composed of several intersecting elements that interact in a complex manner to provide the required stiffness and strength of the deck. Typically, an orthotropic bridge deck is built up of a deck plate welded to longitudinal ribs (open or closed) and transversal cross beams, see Figure 5-45. The intersection of these elements results in a number of complex welded joints, which have shown to be very sensitive to fatigue cracking.

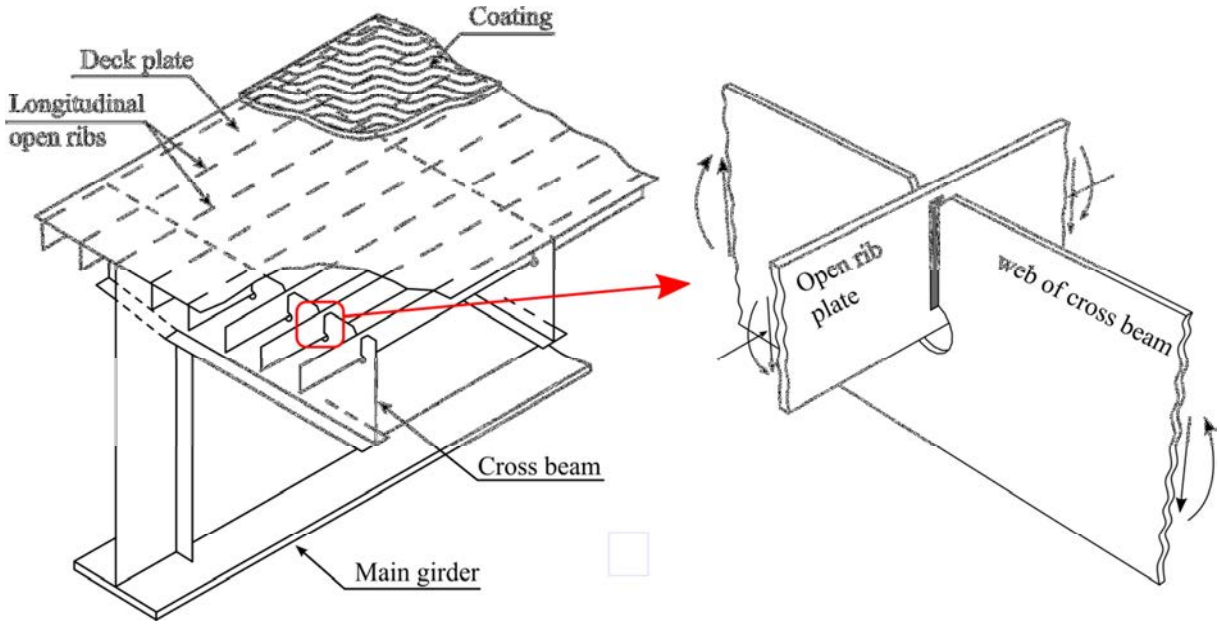

Figure 5-45 Orthotropic bridge deck and sectional forces in an orthotropic bridge deck with open rib

The potential fatigue-critical points in the detail are shown in Figure 5-46. These include:

Crack A: Fatigue crack at the weld toe in the web of the cross beam. This crack usually starts from the edge of the cut-out hole and propagates along the weld. The governing load-effect is a combination of bending and shear stresses. For this type of cracking, the detail is defined as a "type b" hot-spot point

Crack B: Root cracking of the fillet weld connecting the rib to the cross beam

Crack C: Fatigue cracking in the open rib plate starting from the weld toe

Cracks D and E: Fatigue cracking in the deck plate starting, either from the weld end (E) or along the fillet weld between the rib and the deck plate. These cracks are derived by the normal stresses in the deck plate (transversal bending) and both points are defined as "type a" hot-spot points

Crack F: Fatigue crack in the web plate of the cross beam starting from the edge of the cut-out hole and generated by the multi-axial stress condition at this location

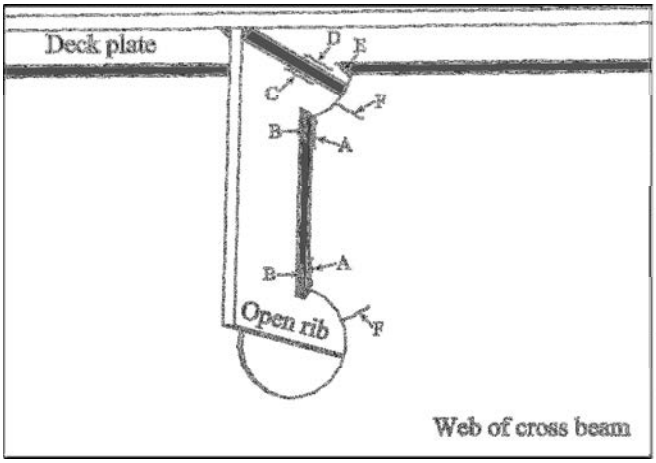

Crack location	Type of hot spot point	Detail category
A	b	90
B	N/A	N/A
C	a	90
D	a	100
E	a	100
F	N/A	N/A

Figure 5-46 Fatigue critical points in a orthotropic bridge deck with open ribs and fatigue classes based on the structural hot-spot stress method

FE modelling and determination of the hot-spot stresses

Orthotropic bridge deck details should be modelled with 3D shell or solid elements. Because of the structure's complexity 2D modelling is not possible. When using the structural hot-spot stress approach, the importance of a correct representation of the welds is essential in welded joints with cut-out holes. One problem, considering "Crack A", is the path along which stress extrapolation should be made. A comparative study was performed in [33] on this type of details, the results show that an extrapolation path perpendicular to the crack direction – see Figure 5-47 – yields results that comply very well with those obtained from testing.

As to the FE modelling of the detail, the following recommendations can be followed to obtain reliable stress value.

Models with solid elements:

- For coarsely meshed models and thus linear stress extrapolation, 20-node solid elements should be used
- For finely meshed models and quadratic stress extrapolation, linear or quadratic (first or second order) solid elements should be used
- The welds should be included in FE models. For models incorporating shell elements, it is important to represent the welds in such complex welded joints, not only in the form of stiffness (thickness) but also geometry. This can be achieved in the best way, for this detail, by using oblique shell elements (section 5.6.2.1).
- Straight stress extrapolation path perpendicular to the weld should be used (for Crack A, see Figure 5-47 (a))
- One point stress determination technique can also be utilized to obtain the structural hot-spot stress at the weld toe

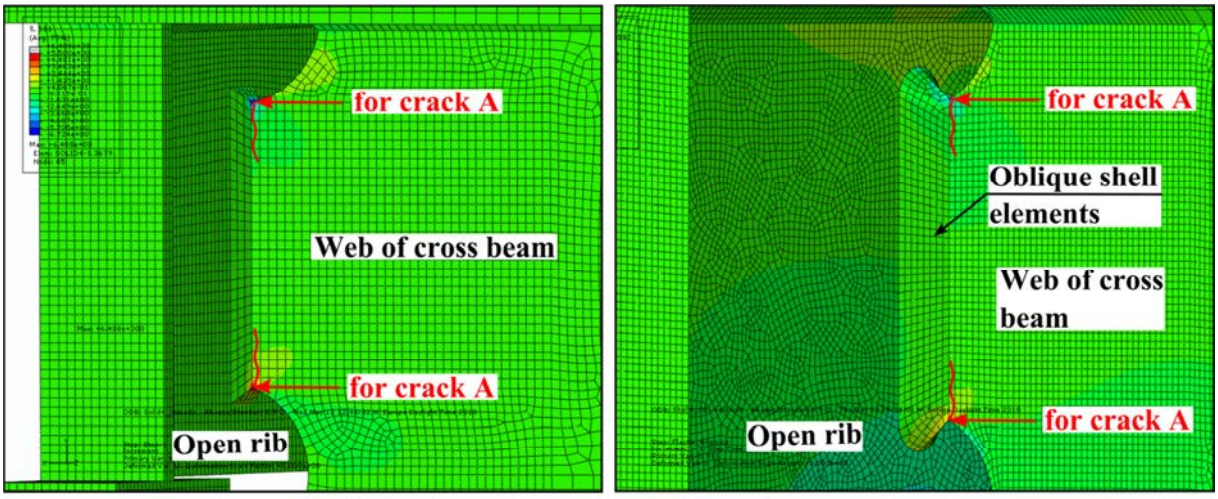

(a) FE model with solid elements (b) FE model with shell elements

Figure 5-47 Stress extrapolation path for Crack A in an orthotropic bridge deck with open ribs

Models with shell elements:

- For coarsely meshed models quadratic 8-node elements should be used
- For finely meshed models quadratic/linear shell elements should be used
- The welds must be included using oblique shell elements (see section 5.6.2.1). The web plate should be joined to the rib plate at the intersection
- Straight stress extrapolation path perpendicular to the weld should be used (for Crack A see Figure 5-47 (b))
- One point stress determination technique can also be utilized to obtain the structural hot-spot stress at the weld toe

In order to demonstrate the application of the structural hot-spot stress method, the welded joint on "Crack A" is chosen. The geometrical configurations of the model and the fatigue test result can be found in [33]. Three different FE models; 1) with solid elements including the welds, 2) with shell elements without representing the welds, 3) with shell elements representing the welds by oblique shell elements, are created. To derive the design stress at the weld toe, quadratic stress extrapolation stress determination procedure is used for all models. In the case of shell element modelling, the most important and crucial question is including the welds in the studied section even though the method - according to its definition - takes into account the effect of the geometrical configurations, not the effect of the weld itself in the stress calculations.

The result from the FE models and the measured stress distribution in the fatigue test specimen is shown in Figure 5-48. It is in this figure obvious that the FE model with solid elements and with shell elements representing the welds using oblique shell elements yields an accurate estimation of the stress at the weld toe in comparison to the test result. However, the FE model with shell elements without modelling weld overestimates the stress at the weld toe and thereby underestimates the fatigue life of the welded joint.

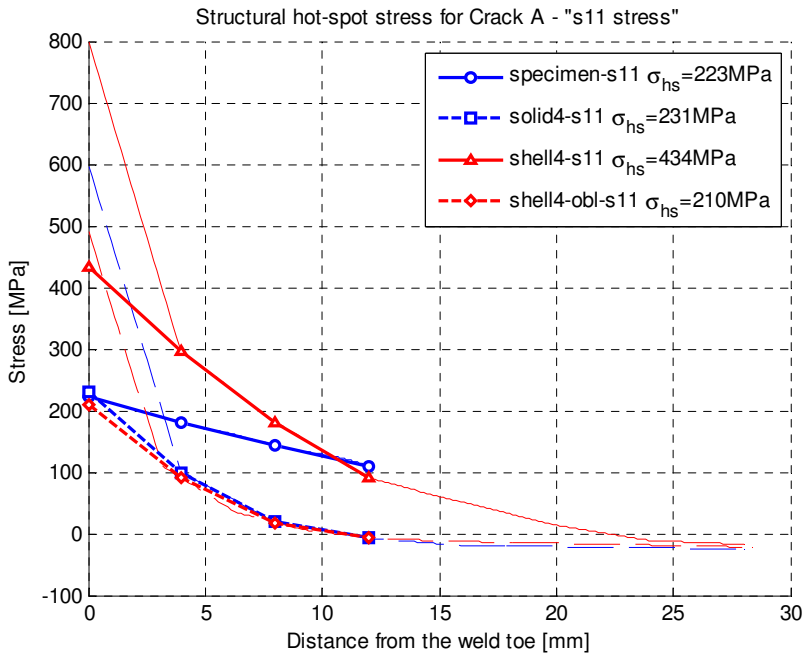

Figure 5-48 Stress distribution in front of the weld toe and the hot spot stresses determined by quadratic surface stress extrapolation

The computed structural hot-spot stress at the weld toe using various modelling technique and the estimated fatigue life is presented in Table 5-3. For estimating the fatigue life of the studied joint, the following formula is used:

$$N = N_C \left(\frac{\Delta\sigma_C / \gamma_{Mf}}{\gamma_{Ff} \cdot \Delta\sigma_{hss}} \right)^3 \qquad \textit{Eq. 5-11}$$

$$N = 2 \cdot 10^6 \left(\frac{\Delta\sigma_{90} / 1{,}35}{1{,}0 \cdot \Delta\sigma_{hss}} \right)^3$$

Table 5-3 Comparison of fatigue life for Crack A in the orthotropic bridge deck

FE model	***Detail category***	***Stress [MPa]***	***N (stress cycles)***
FE model with solid elements	90	$\Delta\sigma_{hss}$ = 231	48 075
FE model with shell elements including welds	90	$\Delta\sigma_{hss}$ = 210	63 988

FE model with shell elements without including welds	90	$\Delta\sigma_{hss} = 434$	7 249
Fatigue test specimen	90	$\Delta\sigma_{hss} = 223$	53 437

As shown in Table 5-3, the FE model with solid elements and with shell elements representing the welds with oblique shell elements yields a rather accurate estimation of the fatigue life of the joint. The model with shell elements without representing the welds underestimates the fatigue life of the welded joint since an accurate stress distribution in front of the weld toe could not be obtained due to the complex geometry, e.g. the presence of cut-out hole and loading conditions (see Figure 5-45).

5.6.4.2 Details prone to distortion-induced cracking

Distortion-induced fatigue damage is generally generated by out-of-plane deformation in local flexible regions such as web gaps at the connection between different members. Even though the deformation of the connected members at the location of cracking is in general very small, the concentration of this deformation in local flexible regions might result in high local stresses that eventually will generate fatigue cracking. Many bridge types have a system of cross beams connected to longitudinal main girders to form a floor system. Especially in old bridges, the flanges of the connected members are cut short to avoid transverse welds in the flange. This way of detailing results in local flexible web "gaps" that is prone to distortion-induced fatigue cracking, see Figure 5-49.

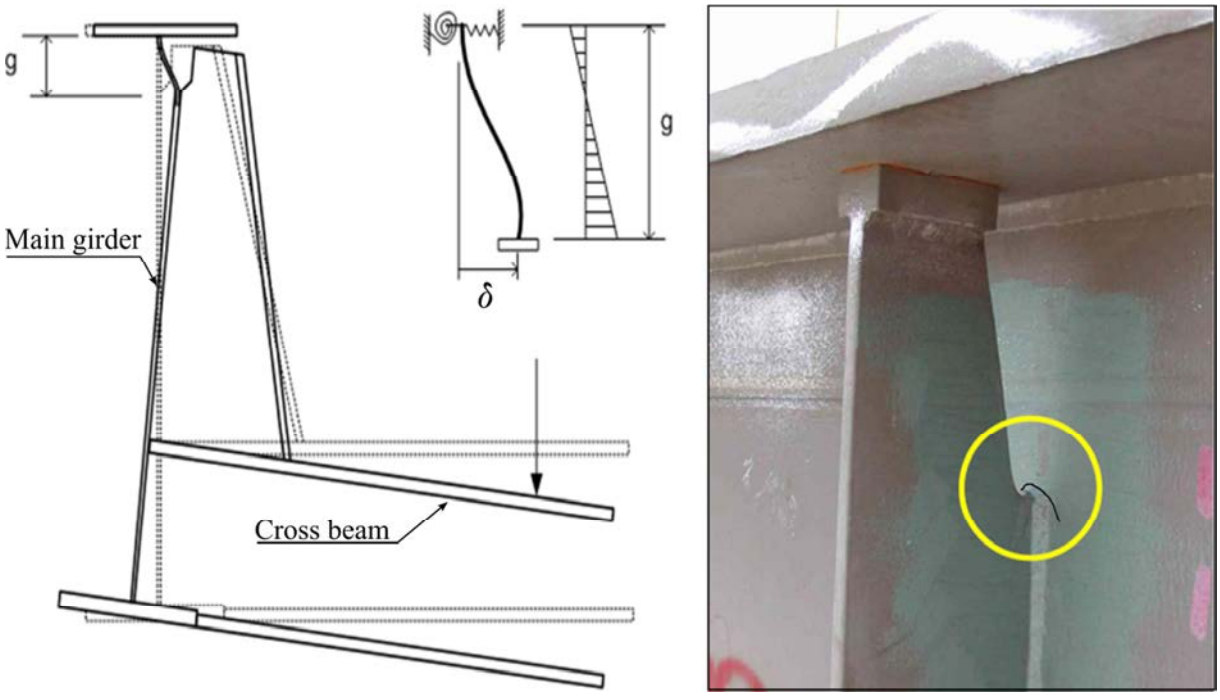

Figure 5-49 Distortion-induced fatigue crack located in the web plate of the main girder

FE modelling for determination of the hot-spot stresses

Distortion-induced fatigue cracking at web gap details is a very complex problem. The stresses acting in the web gap are difficult to determine without a detailed finite

element analysis of the structure. This, in addition to the highly localized nature of the problem, makes an application of the conventional nominal stress method for fatigue verification of such details unfeasible. A more "local" approach which can be used in conjunction with FE analysis is, therefore, to prefer.

Another important aspect of the fatigue verification of details prone to distortional cracking is the need to correctly represent the stiffness of all structural elements that affect the magnitude of local deformation and stresses. This calls to some kind of multi-level modelling to connect the global behaviour of the bridge to the local response of the detail for which the fatigue verification is to be performed, i.e. sub-modelling.

The sub-modelling technique consists of a two-step analysis, see Figure 5-50. A global model of a whole bridge or bridge span is needed along with a local model of the detail of interest. Usually, it is sufficient to use simple beam or shell elements for the global model, while more refined FE models are needed for the local details. Sub-modelling can be made in several steps, i.e. global, local, sub-local, and so on. The boundary conditions for each local model are obtained from the "parent" FE model and applied as deformation and/or sectional forces. This technique is implemented in some commercial finite element analysis packages, such as ABAQUS and ANSYS.

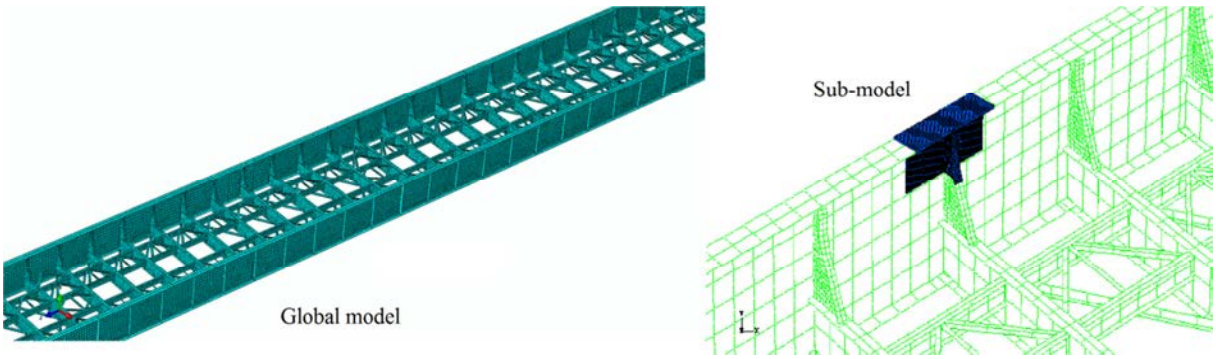

Figure 5-50 Sub-modelling technique on a bridge span; global and sub-model

Figure 5-51 shows two sub-models created with shell and solid finite elements and used in connection with the global model shown in Figure 5-50. The stress path that should be used to extrapolate the structural hot-spot stress at the weld toe is also shown in the same figure.

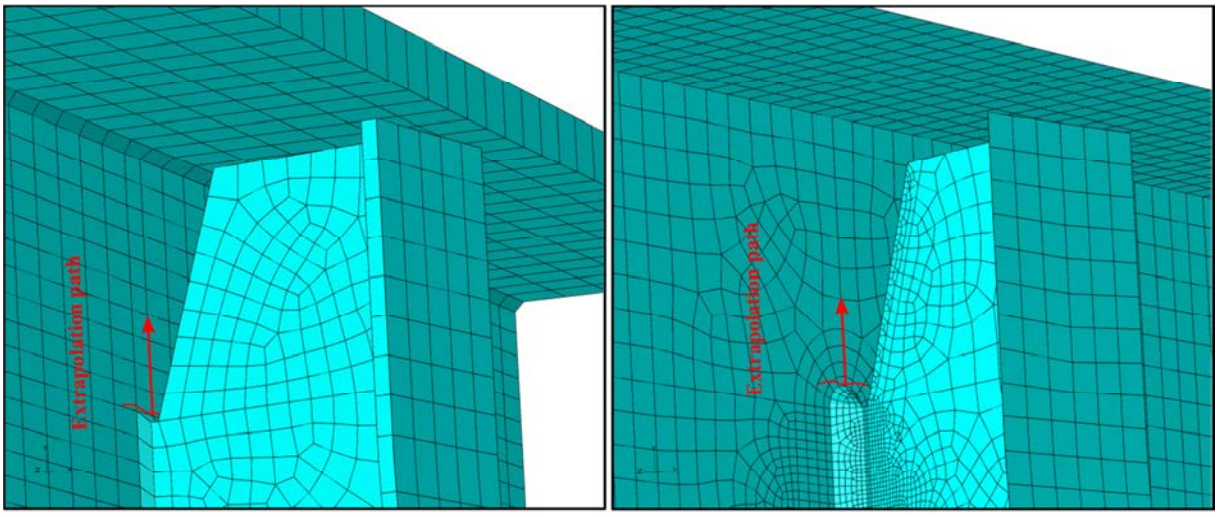

(a) FE sub-model with solid elements (b) FE sub-model with shell elements

Figure 5-51 Coarsely meshed sub-model using (a) solid and (b) shell elements representing the weld

As mentioned before, this welded joint has complex loading conditions and geometrical configurations which result in bending with rather high local stress gradient around the crack location. In order to capture the effect of bending stress at the weld toe, quadratic stress extrapolation is preferred in this case. In addition, the structural hot-spot stress at the weld toe is also determined by through thickness stress determination method since by this procedure, the bending effect in the thickness direction will be captured and the results from the two procedures will be compared. According to the definition of the structural hot-spot stress method, the fatigue design stress should be consisted of the sum of membrane and bending stress. Applying through thickness stress determination method, the non-linear stress at the weld toe caused by the weld itself can be linearized easily and by that the structural hot-spot stress can be determined by summing up the membrane and bending stress which can capture the bending effect more accurately. The stress distribution in the front of the weld toe and the linearized stress are shown in Figure 5-52.

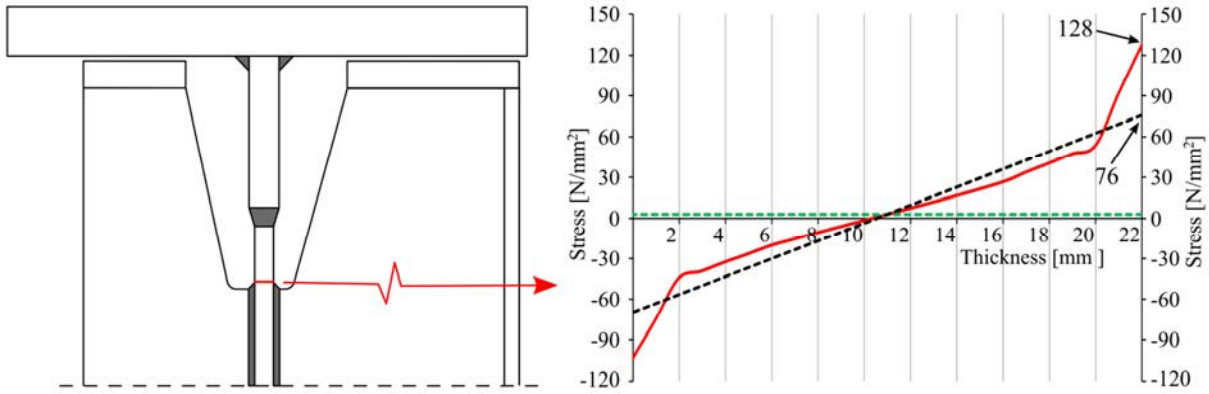

Figure 5-52 Determination of the structural hot-spot stress at the weld toe by through thickness stress linearization

The computed structural hot-spot stress at the weld toe using these two techniques and the estimated fatigue life is presented in Table 5-4. For estimating the fatigue life of the studied joint, the following formula is used:

$$N = N_C \left(\frac{\Delta\sigma_C / \gamma_{Mf}}{\gamma_{Ff} \cdot \Delta\sigma_{hss}} \right)^3 \qquad \text{Eq. 5-12}$$

$$N = 2 \cdot 10^6 \left(\frac{90/1{,}35}{1{,}0 \cdot 70} \right)^3 = 1727675$$

$$N = 2 \cdot 10^6 \left(\frac{90/1{,}35}{1{,}0 \cdot 76} \right)^3 = 1349943$$

Table 5-4 Comparison of fatigue life for distortion-induced fatigue crack

Method	***Detail category***	***Stress [MPa]***	***N (stress cycles)***

	[MPa]		
Structural hot-spot stress (Quadratic extrapolation)	90	70	1 727 675
Structural hot-spot stress (Through-thickness)	90	76	1 349 943

The results presented in Table 5-4 indicate that the fatigue life of the welded joint is overestimated for the use of the structural hot-spot stress determined by the quadratic stress extrapolation even though the difference is not remarkable high. As stated earlier, a possible reason for this is the presence of the highly located bending at the weld toe region. Since the stress at the weld toe is linearized when using the through thickness stress determination procedure, the effect of the local bending is more accurately included in the design stress.

5.6.4.3 Welded details with cope-hole

Welded joints with cope-holes are usually used as field-welded joints in bridge girders to facilitate the transversal butt welds in the flanges and avoid weld crossing when creating build-up girders, see Figure 5-53. The size of the cope-hole is usually chosen to provide access for the NDT of the butt welds (Non-Destructive Testing). The fatigue strength of welded details with cope-holes is generally uninfluenced by the geometrical variations such as the size of cope-holes. Instead the ratio of shear stress to normal stress in the details (τ_a/σ_m) affects the fatigue strength of this kind of joints. It is stated [37, 38] that the higher presence of shear stress at the anticipated crack location, i.e. weld toe in the cope-hole section, can cause lower fatigue strength.

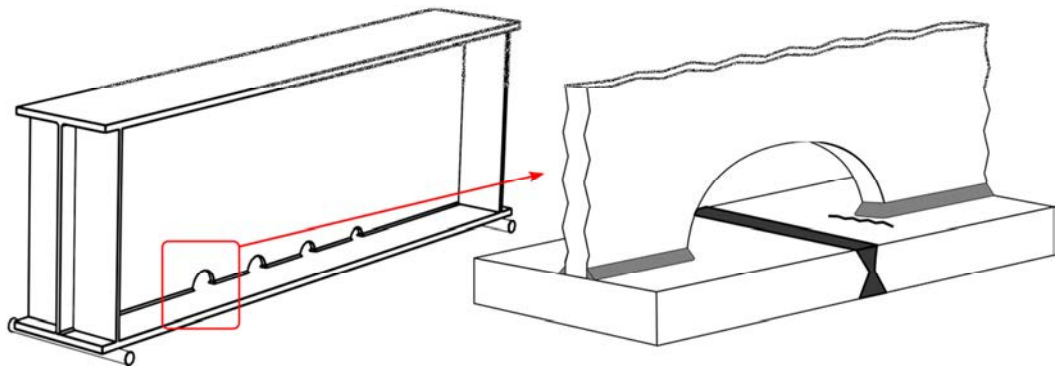

Figure 5-53 Welded detail with cope hole and fatigue crack location

As stated earlier, according to the definition of the structural hot-spot stress method, the effect of the geometrical configurations and loading conditions is already included in the computed stress. However, the structural hot-spot stress method can always not be used for this kind of joints due to two reasons; 1) the thickness of the flanges in bridge girders are usually large and cope holes have smaller radius so that there is not enough distance to locate the reference points for the use of conventional surface stress determination procedure, 2) the stress distribution inside the cope hole as illustrated Figure 5-54. For these reason, the structural hot-spot stress can yield unrealistic design stress to be used in fatigue life calculations. Instead another method,

the effective notch stress method which will be discussed in the next section may be used.

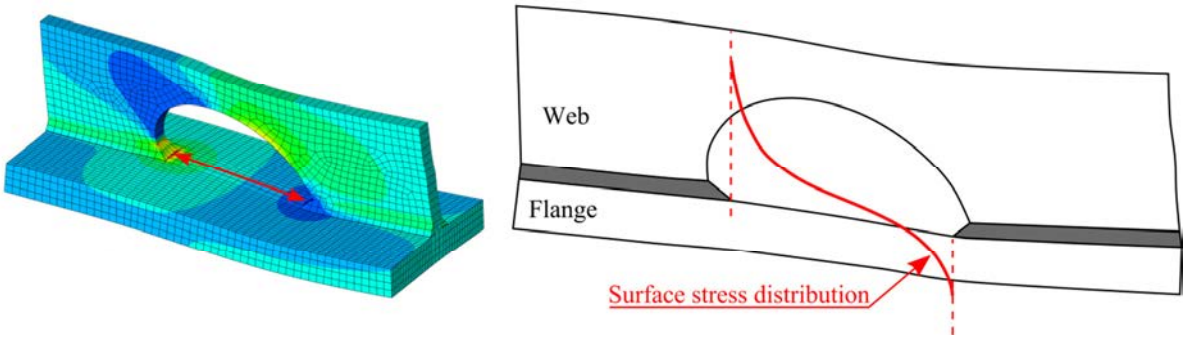

Figure 5-54 Deformed shape and stress distribution inside the cope-hole

6 Fatigue design using the effective notch stress method

6.1 Background and concept

It is well-known that stress raisers or notches emanating from geometrical discontinuities such as holes, sharp local changes in geometry and other geometric discontinuities are rather common and cannot be avoided in welded steel structures. These highly localized stress raisers have a significant influence on the fatigue strength of welded details. The stress at such localized stress raisers is often referred to as the "notch stress". ***The notch stress in welded joints is the total local stress caused by both the component geometry and the local stress raiser, e.g. the shape and local geometry of the weld itself and the local surrounding region***. A notch stress at the weld toe or root in a welded joint can attain very high levels depending on the notch "sharpness" or what is more often referred to as the "notch radius". For very sharp notches (radius approaching zero), the theoretical elastic notch stress tends to infinity. In this case, the stress is referred to as being "singular". Singular (infinite) stresses cannot – of course – be used for fatigue evaluation. To overcome this problem, the effective notch stress was defined as the averaged stresses over a certain distance (2D) or volume (3D).

The basic concept of the effective notch stress method states that if the local stress at the point of crack initiation in a welded detail is calculated – assuming a predefined reference notch radius – then the fatigue strength of this detail can be related to a single fatigue strength curve, a general S-N curve. The term "local stress" implies that the welded detail in hand should be modelled in details, including the welds, weld shape and any significant local geometric discontinuities in the region of anticipated crack initiation. The effective notch stress method was first proposed by Radaj [13] who took account of stress averaging in the micro-support theory according to Neuber Rule with a fictitious radius of 1mm for plate thicknesses of 5 mm and above [17]. The reference notch radius, as illustrated in Figure 6-1, is calculated assuming the worst case conditions[8] (ρ=0) for welded joints in order to conservatively account for the variation in local discontinuities at the weld toe or root, where the notch radius in real welded joints varies widely. When the micro-support length (ρ^*) is taken to 0,4 mm with the constraint factor (s) of 2,5 for steel members, the final rounding radius of notches becomes 1mm in the calculation of the reference radius. The reason for considering a small region (ρ^*) to average the notch stress according to Neuber's micro-support theory is that the crack initiation in this small area is controlled by the averaged notch stress.

[8] The reason for considering the worst case conditions is that the notch radius which is a primary effect on the stress concentration factor in welded joints are widely scattered.

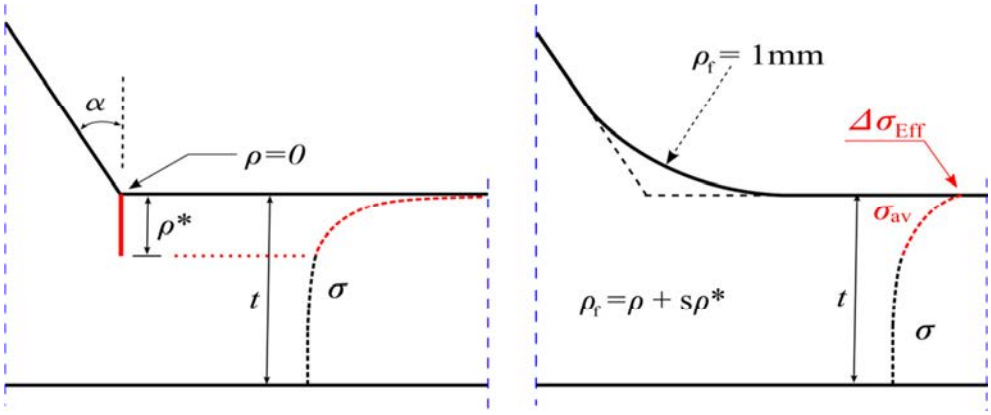

Figure 6-1 Utilizing Neuber's micro-support concept in welded joint

6.2 Principals of the method and determination of the effective notch stress

Fatigue life assessment of welded joints using the effective notch stress method requires rather accurate definition of the detail geometry in and around the region of stress concentration, with a sufficient density of FE elements in order to capture the maximum stress at the point of stress concentration. The sharp notches in regions of anticipated crack initiations (the notches) are modelled rounded with the reference notch radius to avoid stress singularities and arrive at a convergent stress value usable for fatigue calculations, see Figure 6-2. Finite element models for the use in conjunction with the effective notch stress method are usually created with 3D solid element models. 2D plane strain element models can however also be used for cases when the loading and geometry allow such an idealization. Two-dimensional models usually reduce the modelling efforts significantly.

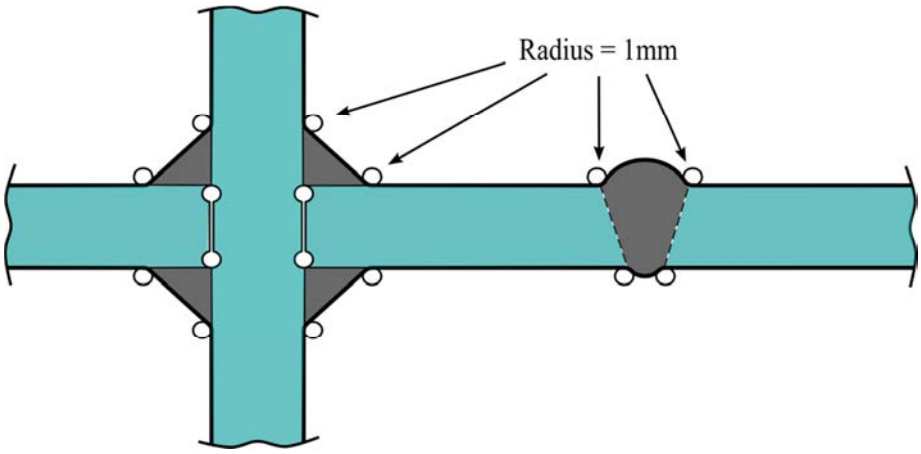

Figure 6-2 Rounding of weld toes and roots

The effective notch stress approach has been included in several fatigue design regulations and codes of standards such as the IIW recommendations and the DNV as an alternative fatigue life assessment method. Recommendations for finite element modelling and the fatigue S-N curve to be used [17, 39] are also given. Unlike the hot-spot stress method, the effective notch stress method can be applied in fatigue design with respect to toe cracking as well as for root cracking of fillet welds. As a result of many years extensive research, the effective notch stress method has been today well established for applying the method on to welded details. Research work is

currently going on to extend the applicability of the method to post-weld treated details as well.

6.2.1 Determination of effective notch stress

The effective notch stress in a welded joint can be determined in two different ways; numerically or analytically. The former is by far more common and general. Since it is not possible to measure "effective notch strains" at weld toes or roots, the effective notch stress cannot be determined experimentally using strain gauges as it is the case in the hot spot stress method.

The most conventional procedure to determine effective notch stress at weld toes or roots is through finite element analysis. FE models with 2D plane or 3D solid elements can be used for this purpose. For complex welded details, 3D models with solid element are generally preferred while FE models with 2D plane stress or strain elements are to be preferred in special simple details.

As mentioned earlier, sharp notches at crack initiation sites (weld toe or root) should be rounded in order to avoid stress singularity. At weld toes, a radius of 1mm (r = 1mm) should be used for plates with thicknesses of 5mm and above, see Figure 6-2. For smaller plate thicknesses, Zhang [40] has proposed the use of a fictitious radius of 0.05mm, which is based on the relationship between the stress-intensity factor and the notch stress [41-43]. Fillet welds can be modelled in two different ways; assuming an idealize weld profile or considering the actual weld profile. For an idealized weld profile, the recommendations for rounding at the weld toe and root to use a flank angle of 45° for fillet welds and 30° for butt welds as shown in Figure 6-3. Where the actual weld profile is to be used in the FE model, the radius between the weld and plate should be fictitiously enlarged in order to consider micro-support effects of the material. In addition to the rounding of sharp notches, the geometry of the studied detail should be modelled as accurately as possible. For fillet welded joints, un-welded regions should be modelled with a certain gap at plate intersections, i.e. the connected plates should not share nodes in the FE model. This requirement increases the effort for modelling and leads often to difficulties in modelling and meshing.

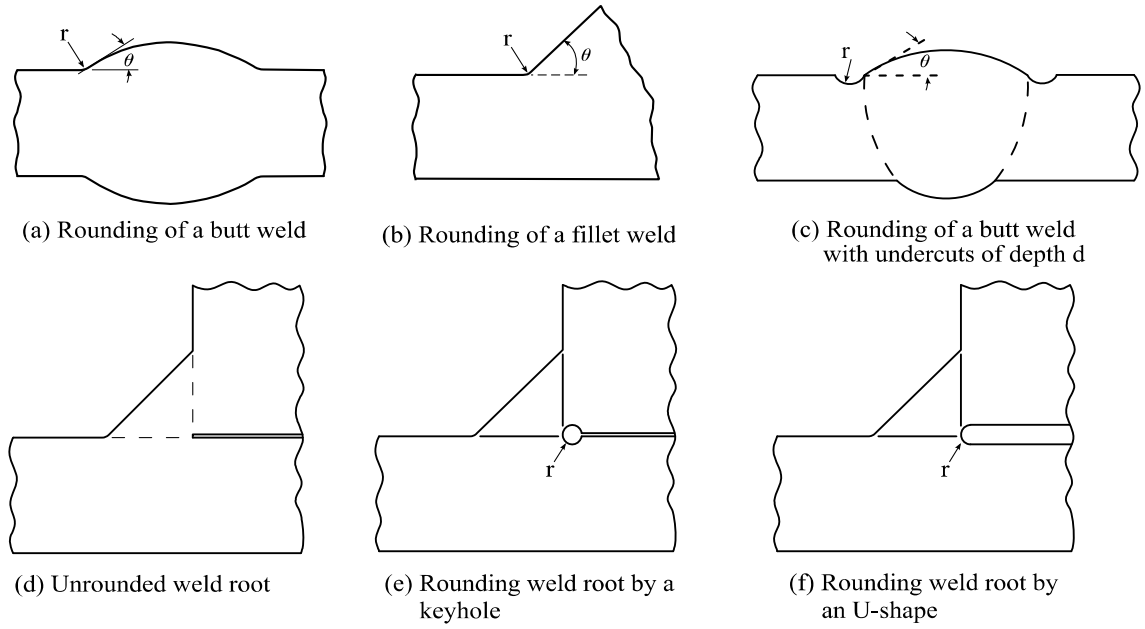

Figure 6-3 Rounding of weld toe and weld root

As shown in Figure 6-3, modelling of the weld root can be performed in two different ways; the so called keyhole and U-shape. The choice of root shape is more or less controlled by the type of weld. In load-carrying welds, both root shapes yield usually the same effective notch stress while in non-load-carrying welds, the effective stress range is lower with the U-shape weld root than with the keyhole weld root. This means that the fatigue strength can be underestimated with U-shape root configuration whereas the fatigue strength can be overestimated with keyhole configuration in non-load-carrying welds. The IIW recommendations suggests therefore using U-shape root configuration when determining the effective notch stress with reference to root cracking in details with load-carrying welds [44].

As to the type and size of FE-elements in the notch region, the recommendations given by the IIW are reproduced in Table 6-1 and illustrated in Figure 6-4.

Table 6-1 IIW Recommendations for FE models when using the effective notch stress [44]

Element type		***Element size***		
		Relative size	***r = 1mm (t ≥ 5mm)***	***r = 0.05mm (t < 5mm)***
Hexahedral	Quadratic	≤ r / 4	0.25mm	0.012mm
	Linear	≤ r / 6	0.15mm	0.008mm
Tetrahedral	Quadratic	≤ r / 6	0.15mm	0.008mm

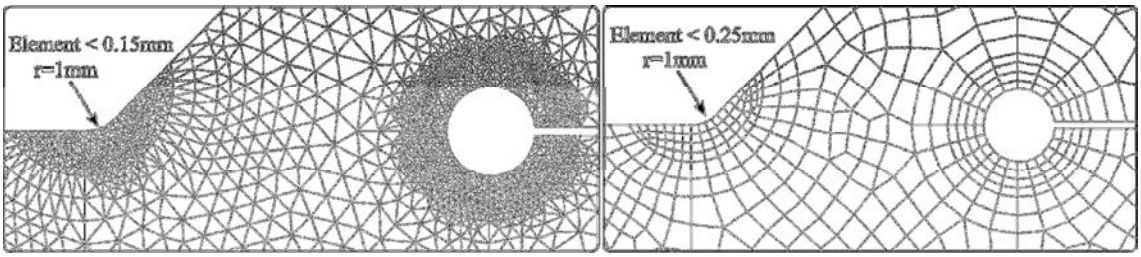

Figure 6-4 Recommended mesh density using tetrahedral and hexahedral elements for an effective notch analysis

6.2.2 Fatigue life evaluation using the effective notch stress

As the effective notch stress covers the global stress concentration effects as well as the effect of local geometry, a single S-N curve should be sufficient to represent the fatigue strength of any welded detail. Eurocode lacks any recommendations with reference to the effective notch stress method.

The recommendations in this Chapter are based on the state-of-the-art research on the application of the effective notch stress in fatigue verification of welded joints.

Reference is made in several locations to the IIW recommendations in this respect, being one of the most complete set of rules which is updated regularly.

The IIW recommendations propose two different S-N curves to be used for fatigue verification of welded details with the effective notch stress method, based on the type of stress considered in the calculations. For plates thicker than 5 mm, an S-N curve with C225 is recommended when the fatigue verification is performed based on the maximum principal stress. Detail category C200 should be applied if the von Mises stress is used. Both S-N curves have a constant slope of 3 before the knee point which is placed at 10 million cycles. Thereafter a slope of 22 is used to replace the cut-off limit, see Figure 6-5. The application of these two S-N curves along with the notch radius recommended can be found in Table 6-2.

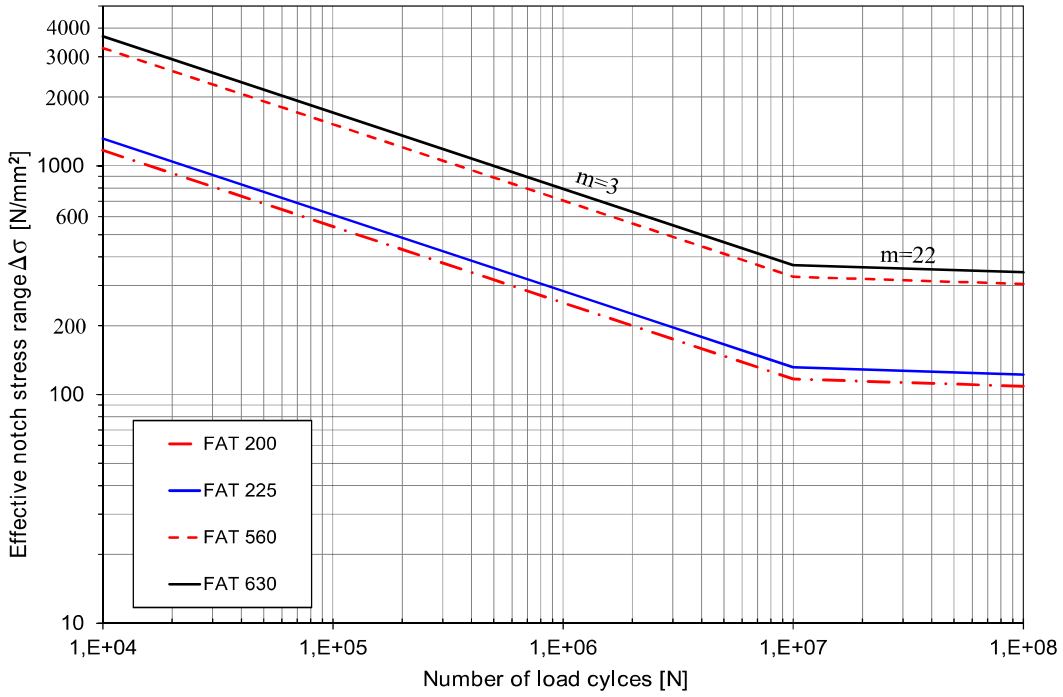

Figure 6-5 Effective notch stress based fatigue S-N curves recommended by IIW [44]

Table 6-2 IIW recommendations for fatigue life evaluating based on the effective notch stress

Reference radius	***Principal stress***	***von Mises stress***
r = 1,0mm	FAT225	FAT200
r = 0.05mm	FAT630	FAT560

As mentioned earlier, the effective notch stress is defined as the maximum elastic stress at a notch, computed by taking into account all stress raising sources and assuming linear elastic material behaviour. The effective notch stress can be obtained either directly by reading out the nodal stress on the notch surface or derived by considering the tangential and normal stress in different sections.

In a detail that experiences a uniaxial state of stress at the location of crack initiation, the maximum principal stress gives a good representation of the fatigue deriving stress range at this location. If stress multiaxiality exists, however, the direction of the principal stress might be constant (proportional loading) or will vary - to both magnitude and direction - over the loading cycle. In both cases, another (scalar) stress is needed to relate the load effects to the fatigue life in a more representative way.

Fatigue verification with the effective notch stress method under stress multiaxiality is still a subject for on-going research. Therefore, complex loading situations with non-proportional loading are left outside this handbook. For details experiencing proportional multiaxial stress at the location of crack initiation, the following recommendations apply:

1. If the first and second principal stresses have the same sign, the first (maximum) principal stress should be used in the fatigue verification,
2. Otherwise, the equivalent von Mises stress using the range of stress components should be used.

It should also be mentioned here that the effective notch stress method is not applicable if there is a significant stress component parallel to the weld. In such cases, fatigue evaluation is more appropriately performed with the nominal stress method.

6.2.2.1 Thickness and misalignment correlation factor

Unlike the nominal and the hot-spot stress methods, the thickness effects do not need to be considered (by a reduction of the fatigue strength) when the fatigue verification is performed with the effective notch stress method. These effects are already "accounted for" on the load effect side (i.e. in the calculated notch stress) as the stress in the thickness direction increases with increased thickness on account of r/t ratio [44]. There is therefore no need for any thickness correction factor in this method. In the presence of significant misalignments, the effect of these can also be easily considered in the stress calculations by modelling the actual misalignment. Of course, it is also possible to apply a correction factor to take into account misalignment effect without including it into FE models.

6.3 Recommendations for finite element modelling

As stated earlier, the effective notch stress method is applicable for 2D plane and 3D solid finite element models and requires an accurately defined FE model. This means that FE models to be used for determining the effective notch stress should reproduce the "exact" geometry of the studied detail, including welds. Gaps between plates in fillet welded joints and any major misalignments not covered by the S-N curve should also be accounted for. FE models with shell elements should not be used in fatigue verification with the effective notch stress method. For simple loading conditions in which the stresses in the transverse direction is negligible, 2D plane-stress elements can be used. Welded steel structures contain rarely simple details or simple loading conditions so 3D solid element models are usually preferred. Building finite element models with solid elements in large structures can, however, easily lead to large FE models that require very long computation time and heavy data to handle. To overcome this problem, sub-modelling can be used to analyse smaller parts of the structure.

6.3.1 Sub-modelling

The purpose of using sub-modelling technique is commonly to obtain a more detailed result (stresses and deformation) in local regions which are of special interest for design. Therefore, sub-models are constructed with more details and equipped with much finer mesh than the global model to which they belong.

A Sub-modelling technique includes, thus, a two-step analysis: an analysis of the global structure; and a refined analysis of a detail in that structure. The global model and the sub-model are usually two distinct finite element models. The global model is usually a simplified representation of the whole structure with minimum detailing and with a fairly coarse mesh. The sub-model, on the other hand, is usually constructed of a smaller part of the structure with a sufficiently detailed representation of local details that are judged to affect the load effects in the region of interest. Being as such, sub-models usually require fine meshing and more modelling efforts. It is important to notice that in a sub-model, the coordinates at the cut-regions should be same as those in the global model. The boundary conditions along the ”cutting edges” in a sub-model are obtained from the global model, either as displacements or sectional forces/stresses.

The procedure for determining the effective notch stress using the sub-modelling technique is given in Figure 6-6.

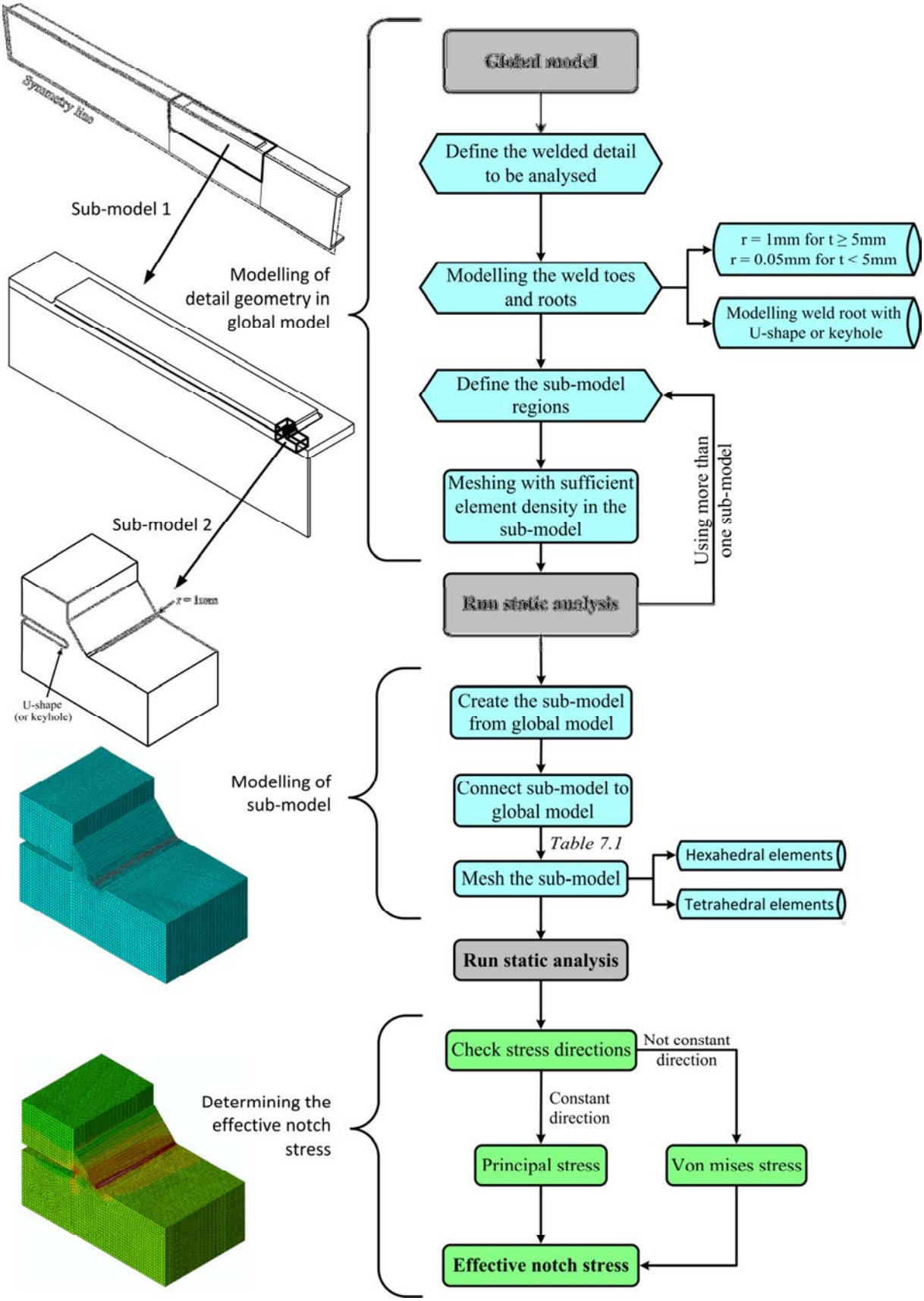

Figure 6-6 Flow chart for determining the effective notch stress

6.3.2 Modelling of common fatigue details

In this chapter, the recommendations for FE modelling of some common fatigue critical details for the purpose of determining the effective notch stress are given. With respect to the finite element method, there is a number of common "rules" that should be respected when performing fatigue verification using the effective notch stress method. Some of these rules that apply irrespective of the type of detail and FE elements used are:

- Prismatic ***solid elements*** can be used. Different element sizes should be used depending on the element type adopted, see Table 7-1.
- ***Rounding the weld toes and roots***. A 1mm fictitious radius should be used for plates with a thickness of 5mm and above. For thicknesses less than 5mm a 0.05mm radius should be used.
- The ***shape of the weld toe and root***. When evaluating weld toe failure, the notch at weld root side can be modelled as U-shape which facilitates the meshing work.
- The maximum elastic stress can be read out from the nodal output, considering the ***maximum principal or the von-Mises stress***.
- ***Mesh transition***, from fine meshed to coarse meshed region should be gradual and smooth, especially when this transition is taking place close to the studied region.
- ***Stress averaging*** over element boundaries (nodal averaging) should be used when applying the effective notch stress method.

6.3.2.1 Transverse butt welds

For butt welded joints, the effective notch stress should be determined by modelling the actual weld profile if it is known. Otherwise it is recommended to model the butt weld with flank angles of 30° and rounding the weld toe with a radius of 1mm or 0.05mm depending on the thickness of welded plates, see Figure 6-7. Transverse butt welded joints can be modelled either by using solid elements or 2D plane strain elements.

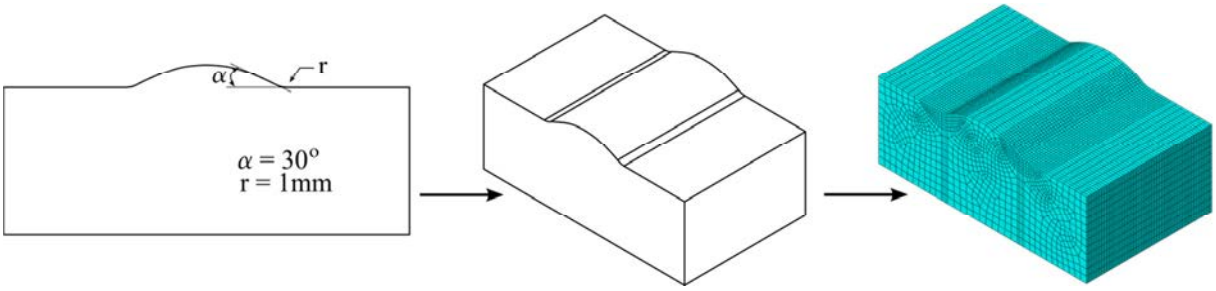

Figure 6-7 FE modelling for determining the effective notch stress for transverse butt welds

6.3.2.2 Transverse attachments

For the determination of the effective notch stress at the weld toe or root in welded joints with transversal attachments, the common "rules" given in Section 6.3.2 can be followed. In addition to FE models with solid elements (Figure 6-8), welded transverse attachments can also be modelled with 2D plane strain elements.

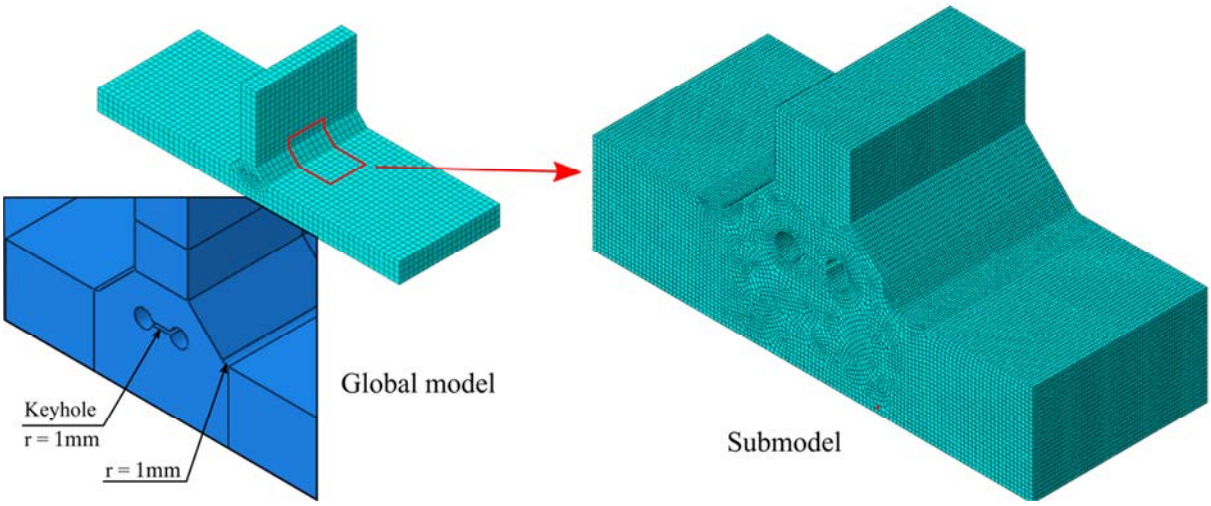

Figure 6-8 FE modelling for determining the effective notch stress for transverse attachments

6.3.2.3 Longitudinal attachments

The fatigue critical point in welded joints with longitudinal attachments is usually located at the weld toe in the main plate at the end of the attachment. Assessing the fatigue resistance of this type of welded joints can be easily made using the effective notch stress method. FE models with 3D solid elements can be used for this purpose see Figure 6-9. In order to obtain a reliable stress value at the weld toe or root, the common "rules" given in Section 6.3.2 can be followed.

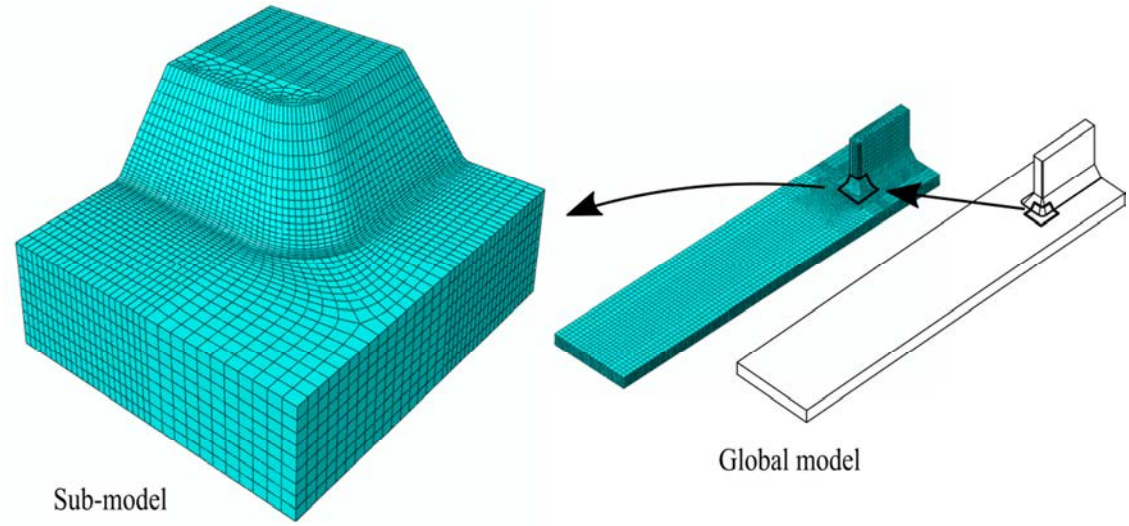

Figure 6-9 FE modelling for determining the effective notch stress for longitudinal attachments

6.3.2.4 Plate-edge attachments

Fatigue cracks in plate-edge welded joints are usually located at the weld toe in the main plate. As mentioned in Section 6.6.3.4, welded plate edge joints can be found in a wide range of different geometrical configurations (see Figure 5-38in Section 5.6.3.4). For the most common joints, FE models with solid and 2D plane strain elements can be implemented to determine the maximum elastic stress. The gusset plates are usually attached to the main plate with butt weld so that the plates are

joined along the connection line. In this case, the modelling effort is quite low and only the weld toe needs to be considered (i.e. rounded) as shown in Figure 6-10.

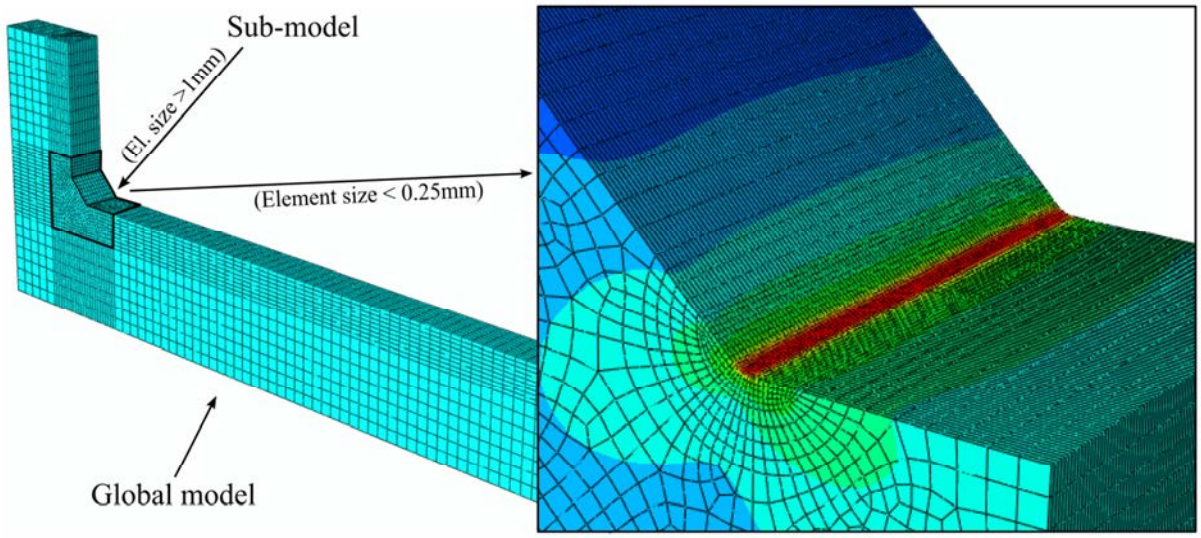

Figure 6-10 FE model for determining the effective notch stress at the weld toe – butt welded

Similar details with fillet welds can be much more demanding in term of modelling effort. A typical example is shown in Figure 6-11 (see also Figure 5-38 in Section 5.6.3.4). Here, the rounded edges with a reference radius of 1mm must continue along the entire weld line to avoid singular stress at possible fatigue critical points. Also the root gap[9] (lack of penetration) between the two connected plates needs to be correctly represented, if the possibility of root cracking is to be considered.

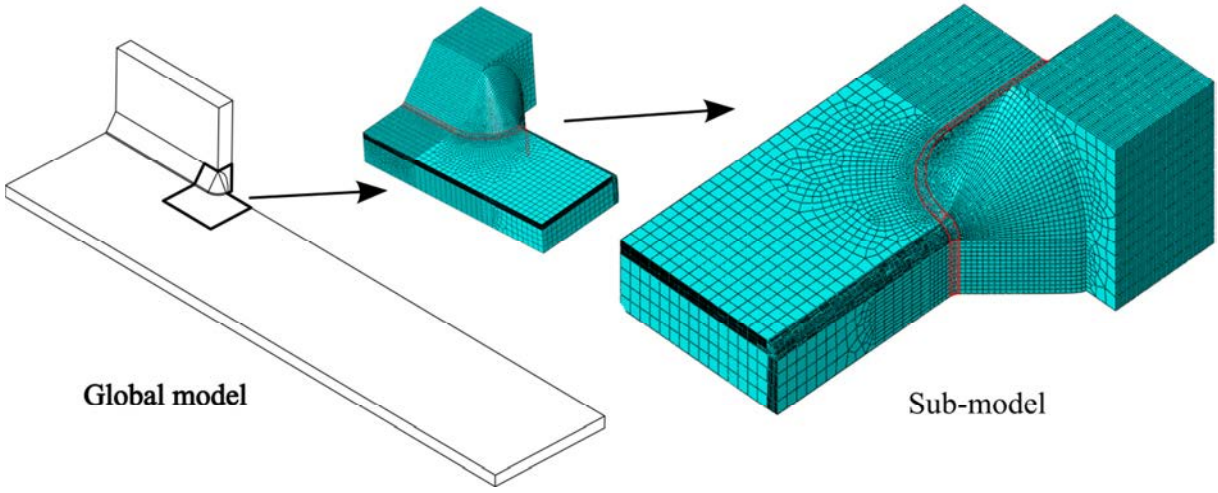

Figure 6-11 FE model for determining the effective notch stress at the weld toe – fillet welded

6.3.2.5 Overlapped joints

As stated in Section 6.3.2.4, overlapped joints have two fatigue critical points; weld toe cracking in the main plate and weld toe cracking in the cover plates. Both regions around the fatigue critical points can be modelled and evaluated with the effective

[9] Except for fully penetrated butt welded joints.

notch stress approach. FE models with 3D solid elements should be used. However, modelling overlapped joints for fatigue evaluation with the effective notch stress method (i.e. creating the joint geometry by rounding sharp edges) is quite time and effort consuming. This is particularly the case since in overlapped joints the weld toe meets a weld root at the end of weld which causes difficulty in modelling. A typical example of fatigue cracking at the weld toe in the main plate is shown in Figure 6-12. The rounded weld toe is here assembled with the rounded weld root at the end of weld. This is necessary to avoid sharp edges (and thus singularity) at fatigue critical points. The meshing work can however be simplified by using tetrahedral elements as shown Figure 6-12.

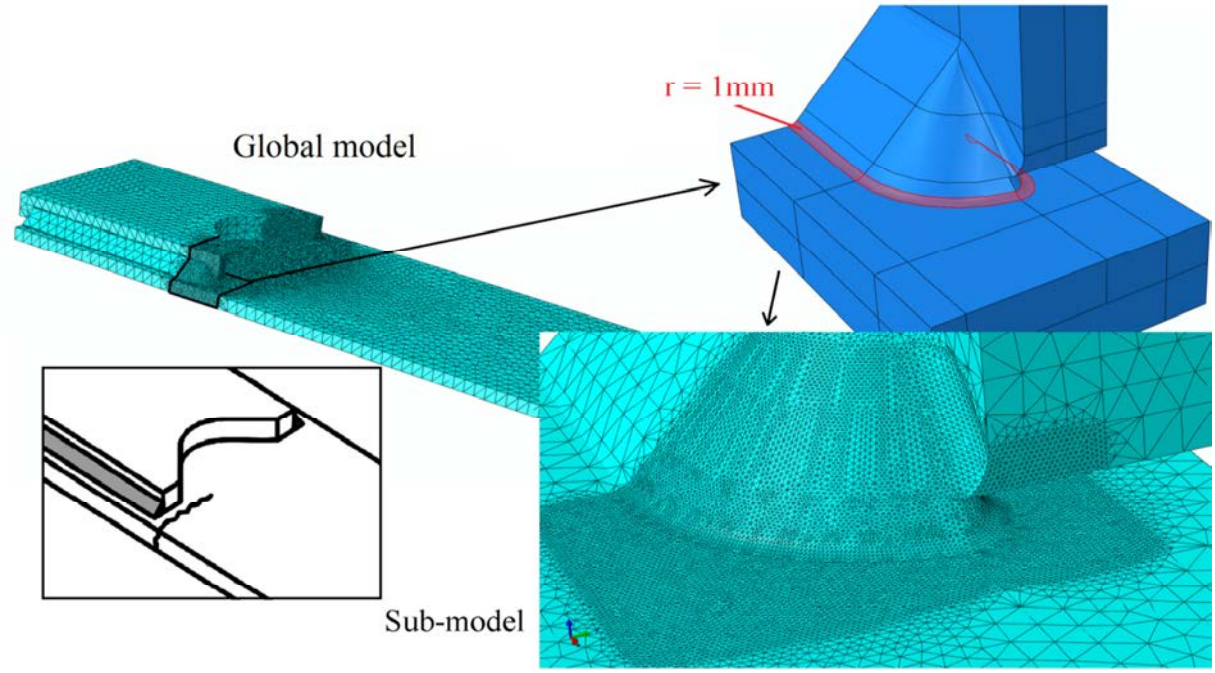

Figure 6-12 FE model for determining the effective notch stress –failure in the main plate

Modelling of the region close to the weld toe in the overlap plate requires more effort due to the fact that the crack is located at the edge of the cover plate. This means that the weld toe on the plate edge and the weld toe in the main plate as well as the weld root between the main plate and the cover plate meet at a fatigue critical point which should be rounded in order to fulfil the method's requirement as shown in Figure 6-13.

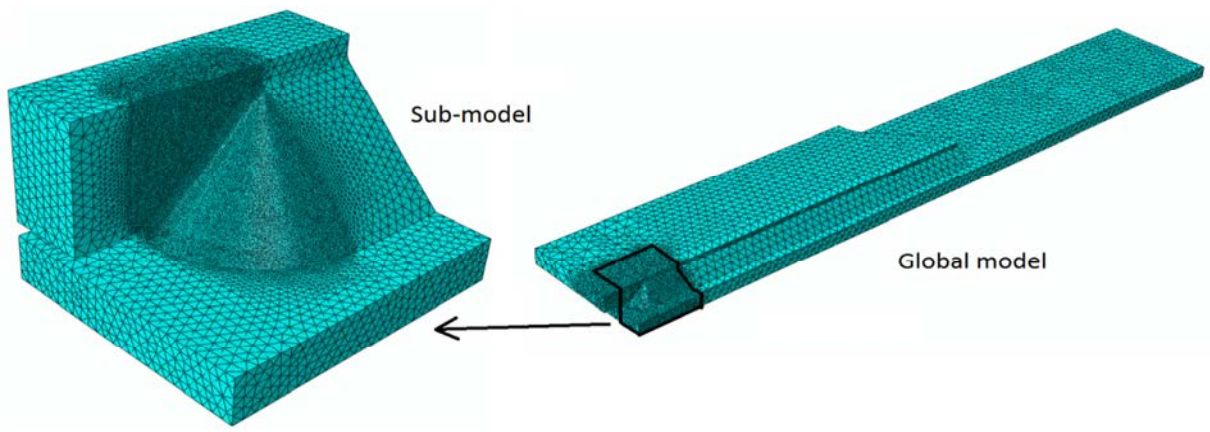

Figure 6-13 FE model for determining the effective notch stress –failure in the overlap plate

Once the modelling and analysis is performed, the maximum elastic stress can be read out from the nodal output, again considering the maximum principal or von Mises stress. Since the geometry is very complex, it is recommended to verify the stress direction before using the maximum principal stress.

6.3.2.6 Cover plate details

Although welded cover plate details exist in a wide range of geometrical configurations, modelling this kind of joints is more convenient than overlap joints. Since fatigue cracks are usually located at the weld toe on the main plate (e.g. a beam flange), the focus in modelling this type of details is directed towards the weld toe region at the cover-plate termination. A typical example is shown in Figure 6-14.

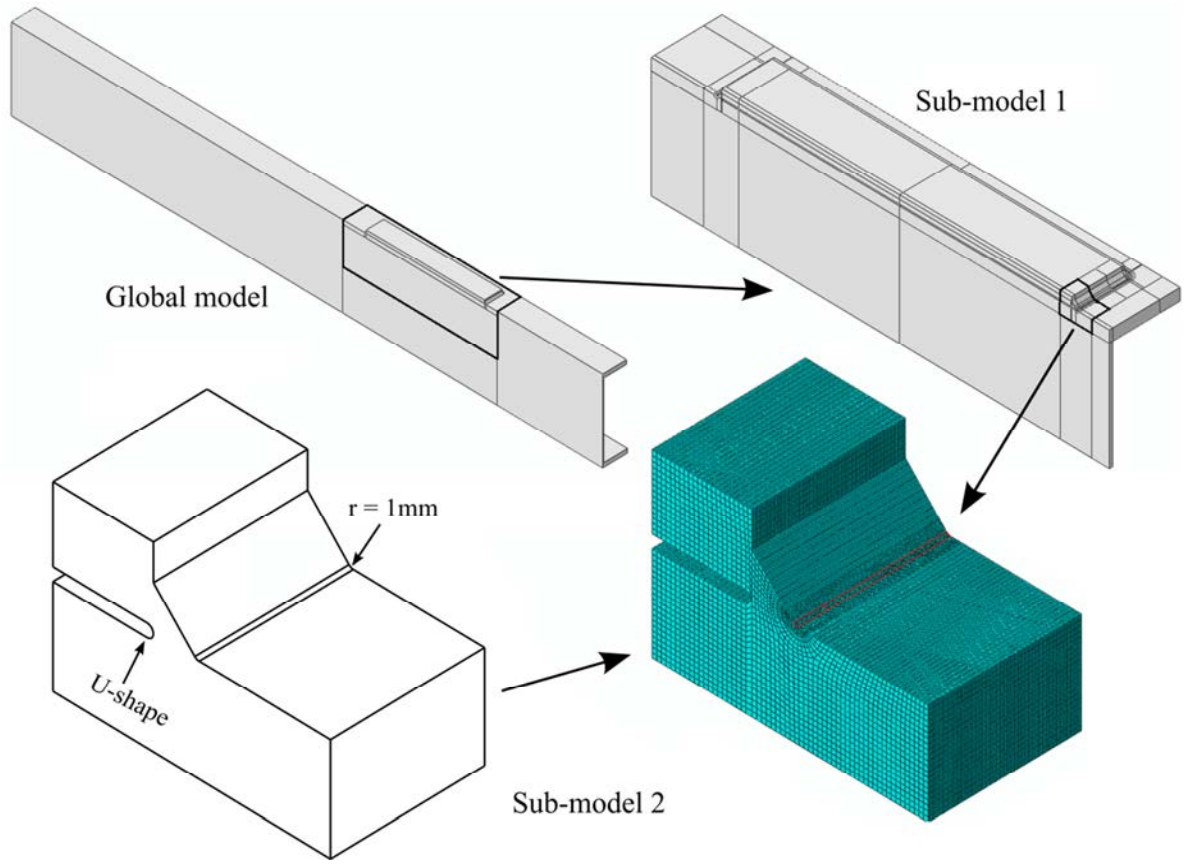

Figure 6-14 FE model of cover plate joint for determining the effective notch stress

To obtain a reliable effective notch stress value at the weld toe or weld root, the common "rules" given in Section 6.3.2 should be used along with the following recommendations:

- Usually, 3D solid elements are required to model cover-plate details. In specific cases, where the geometry allows for that, 2D plane strain elements can also be employed to evaluate the fatigue strength of these details.
- The maximum elastic stress to be used in fatigue evaluation can be read out from the nodal output, using the maximum principal or von-Mises stress. Cover plate details are generally used on steel bridge girders, welded to upper/lower flanges in order to increase the moment capacity. This means that

the stress distribution in the main plate is often uniform without changing its direction considerably in the region of the connections. The maximum principal stress can thus be used for these details.

6.3.3 Modelling of complex fatigue details

The benefits of employing more refined methods in fatigue design are of particular interest for complex details where an accurate determination of the nominal or hot-spot stress is obstructed by the complexity of the detail geometry or the force transfer in the detail. The two examples treated in Chapter 6 are used in this section in order to demonstrate the application of the effective notch stress method in such cases. The results obtained from these two fatigue assessment methods are also compared and discussed. Recommendations for FE modelling, stress determination and fatigue verification are also given.

6.3.3.1 Orthotropic bridge deck with open ribs

This example was already introduced in Section 6.6.4.1 to demonstrate the application of the structural hot-spot stress method. The fatigue critical details for which fatigue verification is needed and in which the effective notch stress method can be applied are listed in Figure 6-15. These include:

Crack A: Fatigue crack at the weld toe in the web of the cross beam. This crack usually starts from the edge of the cut-out hole and propagate along the weld. The governing load effects are a combination of bending and shear stresses.

Crack B: Root cracking of the fillet weld connecting the rib to the cross beam

Crack C: Fatigue cracking in the open rib plate starting from the weld toe

Cracks D and E: Fatigue cracking in the deck plate starting, either from the weld end (E) or along the fillet weld between the rib and the deck plate. These cracks are derived by the normal stresses in the deck plate (transversal bending).

Crack F: Fatigue crack in the web plate of the cross beam starting from the edge of the cut-out hole because of the multi-axial stress condition at this location. This mode of cracking cannot be evaluated with the effective notch stress method.

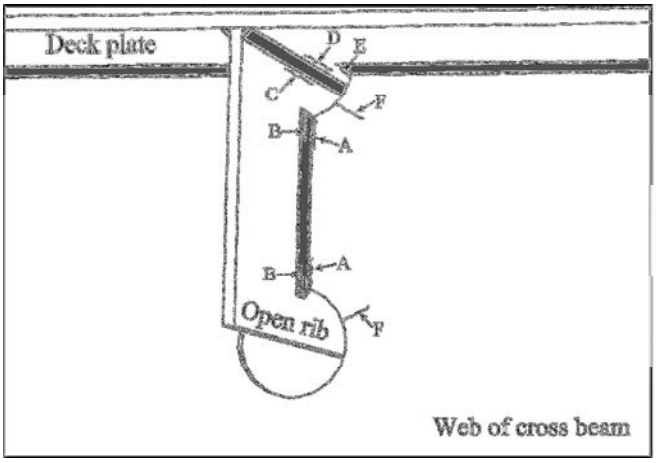

Crack location	Type of crack	Detail category
A	Weld toe	225
B	Weld root	
C	Weld toe	
D	Weld toe	
E	Weld toe	
F	Plate edge	N/A

Figure 6-15 Fatigue critical points in a orthotropic bridge deck with open ribs and fatigue classes based on the effective notch stress method

The effective notch stresses at the investigated fatigue critical points can be computed using the sub-modelling technique, since models with very fine mesh around the

critical points are needed. Since orthotropic bridge decks have very complex geometry, 2D element modelling is usually not suitable and only 3D models with solid elements can be used. In order to correctly simulate the loading and geometrical effects in welded orthotropic bridge decks, sub-modelling can be used to facilitate the modelling work and to reduce the computation time. A coarsely meshed global model with one or more fine-meshed sub-models can be employed to compute the effective notch stresses at local fatigue-critical points. Figure 6-16 shows a part of the orthotropic bridge deck with a global model and two smaller parts are defined as sub-models.

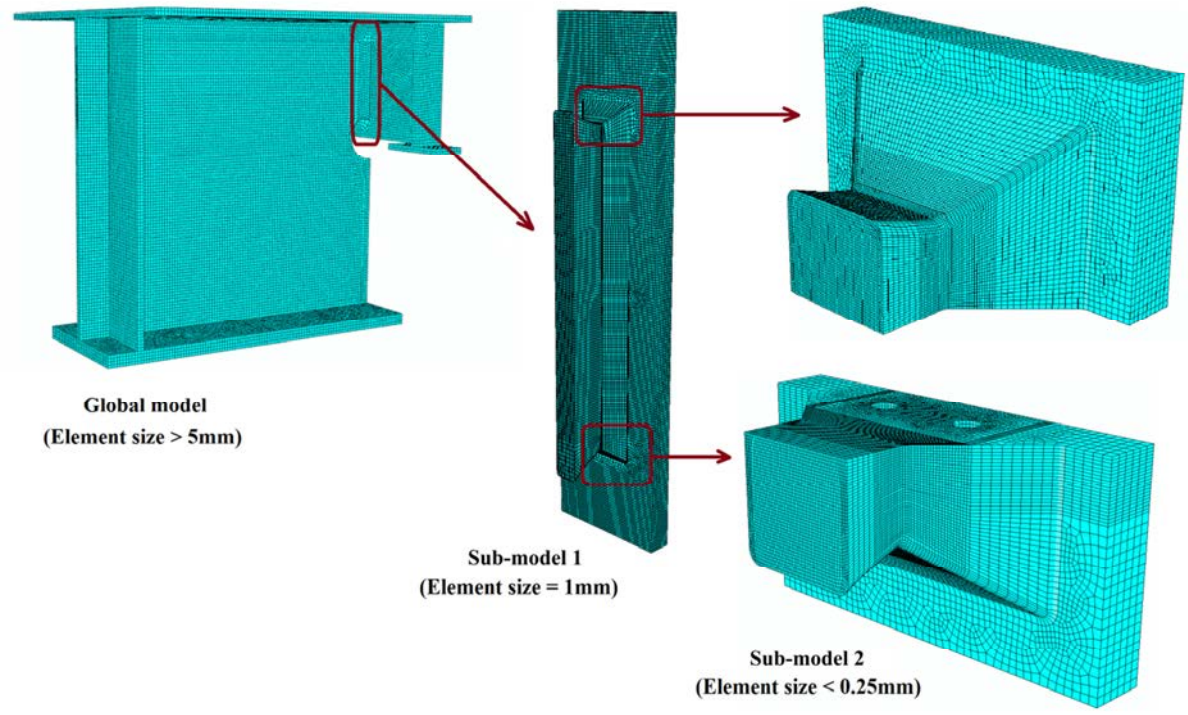

Figure 6-16 Global model and sub-models of a part of an orthotropic bridge deck

As stated earlier, the type of elements used in FE models can be linear and quadratic solid elements (first and second order solid elements). The size of the FE elements in the notch region depends on the type and order of the FE-elements used. As to the former, different types of solid elements, such as tetrahedral[10] and hexahedral, can be used for meshing the models, as shown in Figure 6-17. In general, linear tetrahedral elements should be avoided. If second-order tetrahedral elements are used – to facilitate the meshing work – the density of the mesh should be relatively high, since tetrahedral elements with their 10 nodes usually produce stiffer behaviour than hexahedral elements. Therefore, a finer mesh is required in comparison with hexahedral elements.

[10] Tetrahedral solid elements are often preferable for meshing of complex geometries. These elements are easy to treat in finite element models.

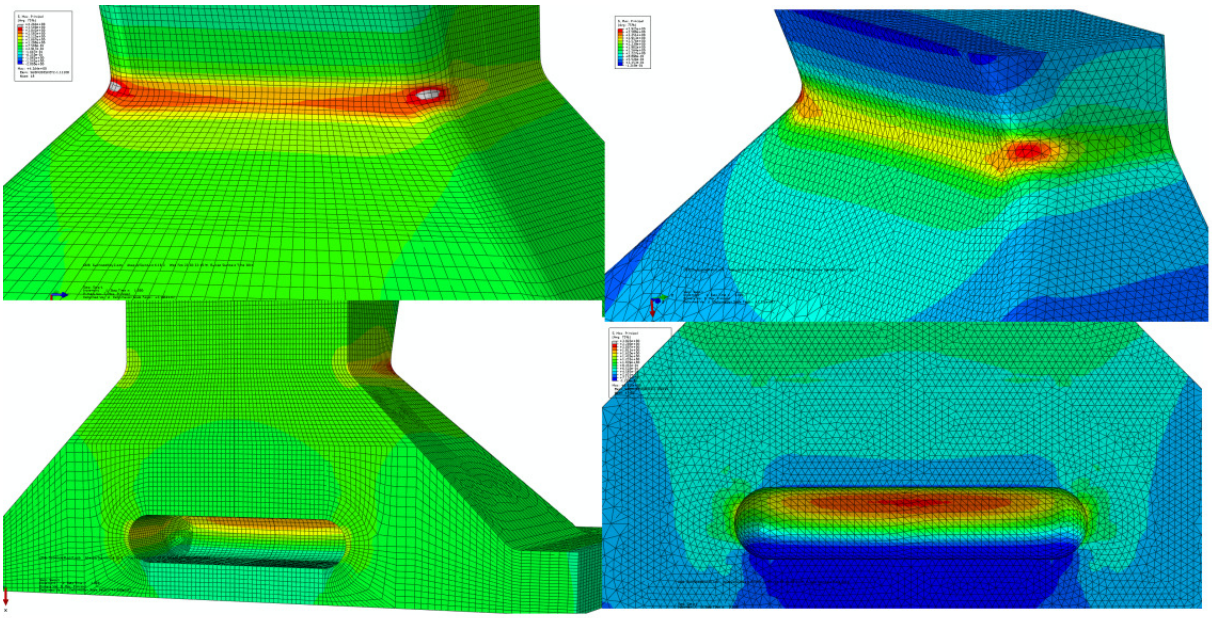

Figure 6-17 Sub-models with hexahedral respectively tetrahedral solid elements

One requirement for modelling the geometry of welds in the effective notch stress method is related to the shape of the weld root. Fricke [45] showed two different techniques for modelling the weld root shape; keyhole and U-shape. These two recommended shapes, which are described in Section 6.2.1, affect the value of effective notch stress obtained at the weld root. A study performed on orthotropic bridge decks with open ribs [33] showed that when evaluating the fatigue strength of weld toes (Crack A in Figure 6-15), the weld root can be modelled using either of keyhole or U-shape configuration. In both cases, the root side of the weld does not need to be "rounded" if root cracking can be excluded, see Figure 6-18.

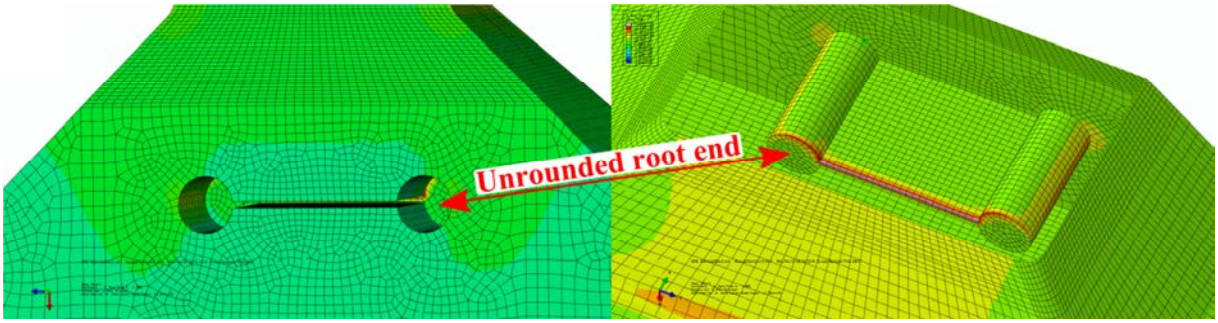

Figure 6-18 Unrounded keyhole shape at the weld root in FE models

Otherwise, the weld root needs to be rounded with the correct notch radii in order to avoid singularity and obtain reliable notch stress values. The U-shaped notch is usually to be preferred in this case, because of its easy handling in modelling and meshing, see Figure 6-19.

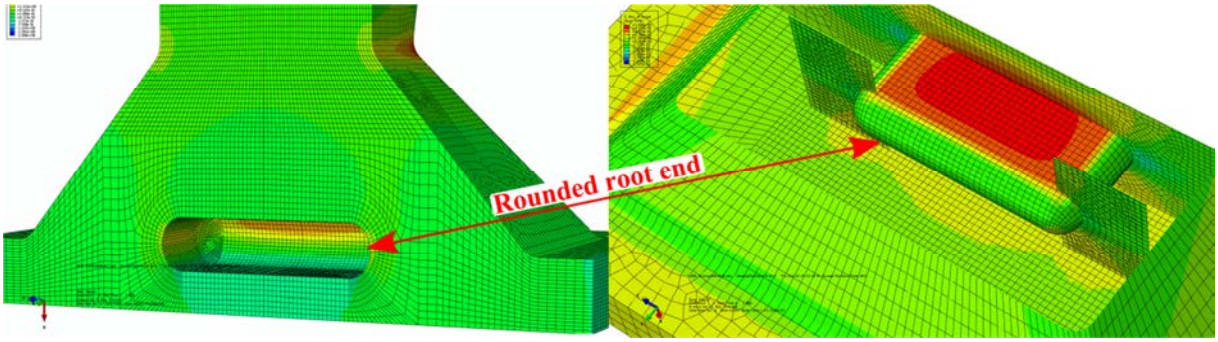

Figure 6-19 Rounded U-shape at the weld root in FE models

The effective notch stresses[11] at both the weld toes and roots as computed from the finite element analyses are summarised in Table 6-3. As can be seen, the shape of weld-root geometry has very little effect on the effective notch stress at the weld toe. Likewise, the way the weld ends are modelled has no significant effect on the computed stress. The differences between the calculated maximum and minimum notch stress are around 5%, which should be within the acceptable limit.

Table 6-3 Finite element model details and analysis results (in MPa) for reference load 1kN

Model type		***Element type***	***Crack A (lower side)***		***Crack A (upper side)***	
			Weld toe	***Weld root***	***Weld toe***	***Weld root***
U-hole	Concave	Hexahedral	4.051	2.158	-4.681	-2.202
		Tetrahedral	3.925	2.044	-4.514	-2.207
	Upright	Hexahedral	4.020	3.320*	-4.647	-3.494*
		Tetrahedral	3.944	4.103*	-4.554	-4.231*
Keyhole	Concave	Hexahedral	4.025	2.197	-4.620	-2.355
		Tetrahedral	3.882	2.310	-4.468	-2.358
	Upright	Hexahedral	3.993	4.264*	-4.550	-3.924*
		Tetrahedral	3.844	11.911*	-4.508	-4.674*

**Singular stress*

The estimated fatigue life of the welded joint on the studied orthotropic bridge deck by considering the three fatigue life assessment methods; the nominal, structural hot-spot and effective notch stress method is presented in Table 6-4. All three methods estimate the fatigue life of the welded joint more or less correctly. It can also be seen in this table that the effective notch stress method yields a fatigue life on the safe side.

[11] The principal stresses were used to calculate the effective notch stresses.

Table 6-4 Comparison of fatigue life of the studied detail in an orthotropic bridge deck

Method	*Detail category*	*Stress [MPa]*	*N (stress cycles)*
Nominal stress (equivalent stress range)	C56	155	38 335
Structural hot-spot stress (Quadratic extrapolation)	C90	231	48 075
Effective notch stress	C225	764	20 763

6.3.3.2 Details susceptible to distortion-induced fatigue

Distortion-induced fatigue damage – as was presented in Section 6.6.4 – is caused by local out-of-plane distortions of flexible regions in various elements, mostly at the connection to other elements or parts of the bridge. A typical example is fatigue cracking in bridge girder webs at the termination of vertical stiffeners, which are used to connect transvers members (cross-beams, cross-bracing, etc.).

The example treated in this section is obtained from an existing railway bridge in which fatigue cracking was detected in the web of the main girders at the connection of vertical stiffeners; see Figure 5-49 in Section 5.6.4.2.

FE modelling for the application of the effective notch stress method

According to the definition of the effective notch stress method, the computed notch stress covers all stress raising effects including the weld itself. In order to compute the effective notch stress for the evaluation of the fatigue life of the welded joint in the current example, the region around the welded joint should be modelled as correctly as possible; including the welds and the gap between the plates when using fillet weld.

Problems similar to the one treated here require multi-level sub-modelling in order to, on one hand, represent the overall behaviour of the entire bridge span in an accurate way and, on the other hand, represent the local region of the critical connection in a model detailed enough to yield accurate results at the notch. Therefore, the fatigue analysis in this example is performed with one global model comprising 4 bridge spans (the bridge is continuous on 7 spans) and 4 different sub-models to arrive at the local region where cracking is anticipated see Figure 6-21. The four sub-models have different sizes and detailing levels. Shell elements are used for the global model. Second order tetrahedral and hexahedral solid elements are used for 2 sub-models and only second order hexahedral elements are used in the third and fourth sub-model. The displacement or force transitions from the global shell element model to the first sub-model are automatically executed by the FE software.

It is worth mentioning here that nature of the fatigue damage in the studied detail necessitates the use of a large global model and several sub-models. The fatigue damage is generated by the deformation of all connected elements, so that the stiffness (deformation) around the studied region should be simulated in the FE model as accurately as possible.

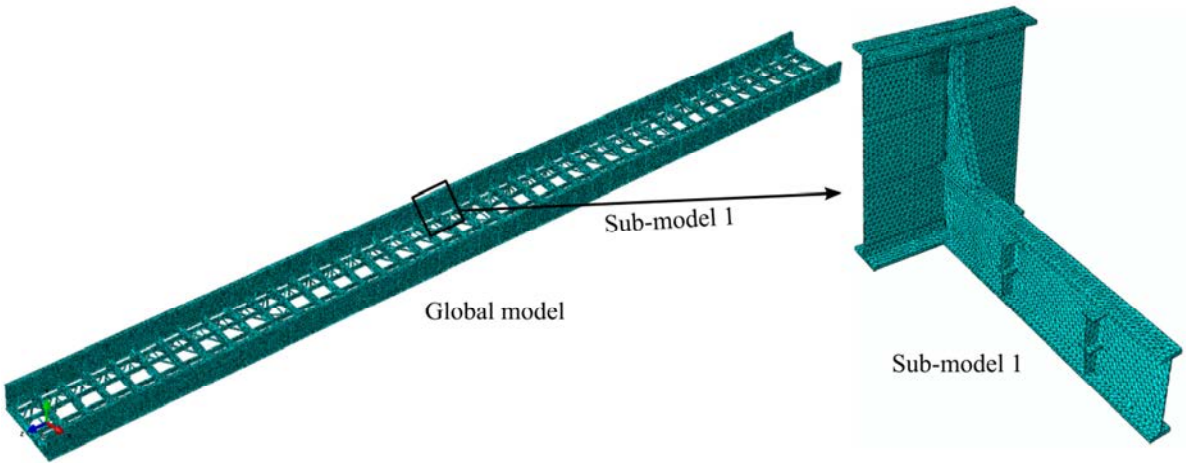

Figure 6-20 Sub-modelling technique on a bridge span; Global and Sub-model 1

The second and the third sub-models were created in order to obtain models with smaller FE elements. To obtain a smooth transition between the regions with larger and smaller elements and to avoid element distortions in sub-models, the FE elements should be downsized gradually.

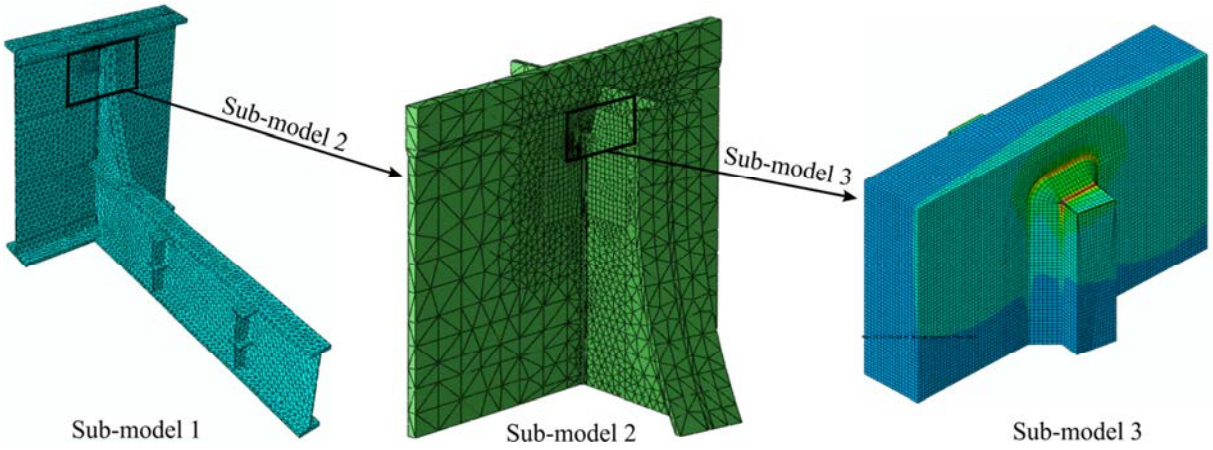

Figure 6-21 Sub-modelling technique on a bridge span; sub-modelling of the bridge part

Sub-model 4 as shown in Figure 6-22 is created by following the recommendations for the element density presented in Section 6.2.1. It is worth pointing out here that the fillet welds in all sub-models are modelled (as recommended) by using idealized weld geometry. Round of the weld toe – with reference radius of 1mm – is only needed in the 4th sub-model, which is used to derive the effective notch stress at the point of interest. The web plate and the transverse stiffener are joined only through the fillet welds.

The state of stress in the detail at the point of crack initiation (the top of the vertical stiffener) is multi-axial to some degree. Normal stresses from global bending of the main girder and local bending of the web gap co-act with the local shear stresses in the girder web at the connection of the stiffener. However, an examination of different stress components reveal that the maximum principal stress should be used in this particular case. The value of the maximum principal stress at the weld toe is 224,5 MPa, with a minimum principal stress of 24 MPa. The von Mises stress is 196 MPa, which is lower than the maximum principal stress (see Section 6.2.2).

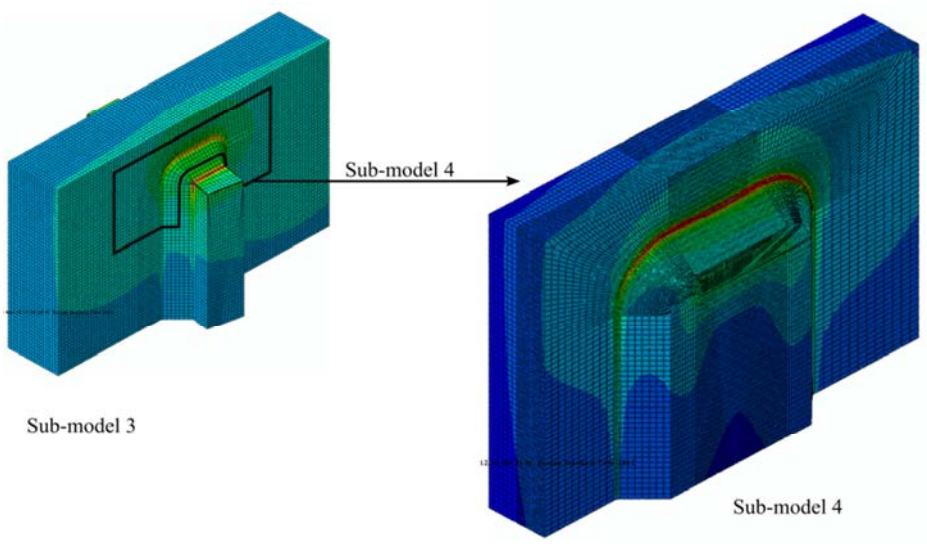

Figure 6-22 Sub-modelling technique on a bridge span; larger sub-model and final sub-model

The fatigue life of the welded joint based on the effective notch stress can be estimated as:

$$N = N_C \left(\frac{\Delta\sigma_{225} / \gamma_{Mf}}{\Delta\sigma_{ens} \cdot \gamma_{Ff}} \right)^3 \qquad \text{Eq. 6-1}$$

$$N = 2 \cdot 10^6 \left(\frac{225/1{,}35}{224{,}5 \cdot 1{,}0} \right)^3 = 818\ 327$$

$$N = 2 \cdot 10^6 \left(\frac{90/1{,}35}{76 \cdot 1{,}0} \right)^3 = 1\ 349\ 943$$

A comparison of the result obtained from the effective notch method and those produced by the hot-spot stress method is made in Table 5-4. The results indicate that the structural hot-spot stress method overestimates the fatigue life when the fatigue life of the studied joint is evaluated using the structural hot-spot stress. Observe that quadratic extrapolation is employed here as the problem is dominated by bending with rather high local stress gradient, see also Figure 7-20. For the same reason, the through-thickness stress linearization yields a result which is much closer to those of the effective notch stress method. Nevertheless, considering the complex nature of the problem and the fact that an evaluation of this type of fatigue damage cannot be made with conventional nominal-stress based methods, it is judged that both the hot-spot stress method and the effective notch stress method yield useful results for the purpose of fatigue assessment of details prone to distortional cracking.

Table 6-5 Comparison of the fatigue life for distortion-induced fatigue crack

Method	***Detail category***	***Stress [MPa]***	***N (stress cycles)***
Structural hot-spot stress (Quadratic extrapolation)	90	70	1 727 675
Structural hot-spot stress (Through-thickness)	90	76	1 349 943
Effective notch stress	225	224,5	818 327

According to the definition of the structural hot-spot stress method, the design stress should be composed of the sum of membrane and bending stress. Applying the through thickness stress as a method of stress linearization, the non-linear stress at the weld toe caused by the weld itself can be separated and the hot-spot stress can be determined by summing up the membrane and bending stress. The local, bending-dominated nature of the problem can thus be captured more accurately. The stress distribution in front of the weld toe and the through-thickness linearized stress are shown in Figure 5-52 in Chapter 5.

7 References

1. Schijve, J., *Fatigue of structures and materials*. 2009: Springer Netherlands. 456.
2. Croce, P., *Background to fatigue load models for Eurocode 1: Part 2 Traffic Loads.* Progress in Structural Engineering and Materials, 2001. **3**(4): p. 335-345.
3. Sedlacek, G., et al., *Background document to EN 1991- Part 2 - Traffic loads for road bridges - and consequences for the design*, in *JRC Scientific and Technical Reports*. 2008, JRC European commission.
4. Kühn, B., et al., *Assessment of Existing Steel Structures: Recommmendations for Estimation of Remaining Fatigue Life*, G. Sedlacek, et al., Editors. 2008.
5. Nussbaumer, A., L. Borges, and L. Davaine, *Fatigue Design of Steel and Composite Structures*. ECCS Eurocode Design Manuals. 2011, ECCS: ECCS – European Convention for Constructional Steelwork. 311.
6. Croce, P., et al., *Guidebook 2 - Design of Bridges*, ed. P. Croce. 2010, Praque: Czech Technical University.
7. Sanpaolesi, L. and P. Croce, eds. *Handbook 4 - Design of bridges*. Leonardo Da Vinci Pilot Project CZ/02/B/F/pp-134007. 2005: Pisa, Italy.
8. Calgaro, J.A., M. Tschumi, and H. Gulvanessian, *Designers' Guide to Eurocode 1: Action on bridges*, ed. H. Gulvanessian. 2010, Chippenham, UK.: Antony Rowe Limited.
9. 1993-2, E., *Eurocode 3: Design of Steel Structures - Part 2: Steel Bridges* 2006, European committee for Standardization: Brussels.
10. Nussbaumer, A., *European standard for fatigue design of steel structures and perspectives*, in *International Conference on Fatigue and Fracture in the Infrastructure*. 2006.
11. *EN 1993-2 Eurocode 3: Design of Steel Structures - Part 2: Steel Bridges* 2006, European committee for Standardization: Brussels.
12. Marshall, P.W. and J. Wardenier. *Tubular versus Non-Tubular Hot Spot Stress Methods*. in *Proceedings of The Fifteenth (2005) International Offshore and Polar Engineering Conference*. 2005. Seoul, Korea: The International Society of Offshore and Polar Engineers.
13. Radaj, D., C.M. Sonsino, and W. Fricke, *Fatigue Assessment of Welded Joints by Local Approaches. 2. Ed*. 2006: Woodhead Publishing, Cambridge.
14. Niemi, E., *Stress determination for Fatigue Analysis of Welded Components*, in *IIW doc. IIS/IIW-1221-93*. 1995, The International Institute of Welding: Cambridge, England.
15. Al-Emrani, M., *Fatigue-critical details in steel bridges (in Swedish)*. 2006, Department of Structural Engineering, Chalmers University of Technology: Report 2006:7

16. Fricke, W., et al., *Comparative fatigue strength assessment of a structural detail in a containership using various approaches of classification societies.* Marine structures, 2002. **Vol. 15**(1): p. pp.1-13.

17. Hobbacher, A., *Recommendation for fatigue design of welded joints and components*, in *IIW-1823-07 ex. XIII-2151r4-07/XV-1254r4-07*. 2008, The international Institute of Welding: Cambridge, England.

18. *EN 1993-1-9. Eurocode 3: Design of Steel Structures - Part 1-9: Fatigue*. 2005: CEN, Brussels.

19. Wernicke, R., *Fatigue strength assessment of cruciform joints with misalignment*, in *Doc. IIW-1872-01*. 2001, The international Institute of Welding: Cambridge, England.

20. Fricke, W., *Recommended Hot Spot Analysis Procedure for Structural Details of FPSO's and Ships Based on Round-Robin FE Analyses.* International Journal of Offshore and Polar Engineering, 2001. **Vol. 12**(No. 1): p. pp.1-8.

21. Storsul, R., E. Landet, and I. Lotsberg, *Convergence Analysis for Welded Details in Ship Shaped Structures*, in *Proceedings of OMAE-FPSO 2004 OMAE Specialty Symposium on FPSO Integrity*, OMAE-FPSO'04-0016, Editor. 2004: Houston, USA.

22. *EN 1090-2. Execution of steel structures and aluminium structures - Part 2:Technical requirement for steel structures*. 2008: CEN, Brussels.

23. *ISO 5817, Welding — Fusion-welded joints in steel, nickel, titanium and their alloys (beam welding excluded) — Quality levels for imperfections*. 2005, International Organization for Standardization: Geneva, Switzerland.

24. Dong, P., *A structural stress definition and numerical implementation for fatigue analysis of welded joints.* International Journal of Fatigue, 2001. **23**(10): p. 865-876.

25. Dong, P. and J.K. Hong, *Analysis of hot spot stress and alternative structural stress methods.* The 22nd international conference on offshore mechanics and artic engineering, 2003. **3**: p. 213-224.

26. Dong, P., J.K. Hong, and Z. Cao, *Structural stress based master S-N curve for welded joints*, in *IIW Doc. XIII -1930-02/XV-1119-02*. 2002, 55th Annual Assembly of International Institute of Welding: Copenhagen, Denmark. p. pp. 24.

27. Xiao, Z.-G. and K. Yamada, *A method of determining geometric stress for fatigue strength evaluation of steel welded joints.* International Journal of Fatigue, 2004. **26**(12): p. 1277-1293.

28. Radaj, D., *Assessment of fatigue strength of welded structures based on local parameters.* VTT symposium 157 fatigue design, 1995. **3**: p. 349-366.

29. Kyuba, H. and P. Dong, *Equilibrium-equivalent structural stress approach to fatigue analysis of a rectangular hollow section joint.* International Journal of Fatigue, 2005. **27**(1): p. 85-94.

30. Noh, B., J. Song, and S. Bae, *Fatigue Strength evaluation of the Load-Carrying Cruciform Fillet Welded Joints Using Hot-Spot Stress.* Key Engineering Materials, 2006. **Vols.324-325**: p. pp. 1281-1284.

31. Fricke, W., A. Kahl, and H. Paetzold, *Fatigue Assessment of Root Cracking of Fillet Welds Subjected to Throat bending Using the Structural Stress Approach*, in *IIW document XIII-2072-05/XV-1198-05*. 2005, The International Institute of Welding: Germany.

32. Eriksson, Å., et al., *Weld evaluation using FEM - A guide to fatigue-loaded structures*. 2003, Gothenburg, Sweden: Industrilitteratur AB.

33. Aygül, M., M. Al-Emrani, and S. Urushadze, *Modelling and fatigue life assessment of orthotropic bridge deck details using FEM.* International Journal of Fatigue, 2012. **40**(0): p. 129-142.

34. Aygül, M., et al., *Evaluation of the fatigue strength of an orthotropic bridge deck detail using hot spot stress approach*, in *63rd Annual Assembly & International Conference of the International Institute of Welding*. 2010, AWST-10/63: Istanbul, Turkey. p. 261-268.

35. Fayard, J., A. Bignonnet, and K. Dang Van, *Fatigue Design Criterion For Welded Structures.* Fatigue & Fracture of Engineering Materials & Structures, 1996. **19**(6): p. 723-729.

36. Aygül, M., et al., *A comparative study of different fatigue failure assessments of welded bridge details.* International Journal of Fatigue, 2013. **49**(0): p. 62-72.

37. Miki, C. and K. Tateishi, *Fatigue strength of cope hole details in steel bridges.* International Journal of Fatigue, 1997. **19**(6): p. 445-455.

38. Aygül, M., et al., *A comparative study of different fatigue failure assessments of welded bridge details.* International Journal of Fatigue, 2013. **49**(0): p. 62-72.

39. *DNV-RP-203 Fatigue Design of Offshore Steel Structures*. 2011, Det Norske Veritas - Offshore Codes: Norway.

40. Zhang, G. and B. Richter, *New approach to the numerical fatigue-life prediction of spot-welded structures.* Fatigue and Fracture of Engineering Materials and Structures, 2000. **23**(6): p. 499-508.

41. Sonsino, C.M., et al., *Notch stress concepts for the fatigue assessment of welded joints - Background and applications.* International Journal of Fatigue, 2012. **34**(1): p. 2-16.

42. Sonsino, C.M., *A consideration of allowable equivalent stresses for fatigue design of welded joints according to the notch stress concept with the reference radii r_{ref} = 1.00 and 0.05 mm.* Welding in the World, 2009. **53**(3-4).

43. Radaj, D., C.M. Sonsino, and W. Fricke, *Recent developments in local concepts of fatigue assessment of welded joints.* International Journal of Fatigue, 2009. **31**(1): p. 2-11.

44. IIW, *Guideline for the Fatigue Assessment by Notch Stress Analysis for Welded Structures*, W. Fricke, Editor. 2010, IIW Doc. XIII-2240-08/XV-1289-08, International Institute of welding.

45. Fricke, W., *Guideline for the fatigue assessment by notch stress analysis for welded structures.* The International Institute of Welding, 2008. **IIW Doc. XIII-2240-08/XV-1289-08**(IIW Doc. XIII-2240-08/XV-1289-08).